

**ČESKÉ VYSOKÉ UČENÍ TECHNICKÉ V PRAZE**

---

**Fakulta stavební  
Katedra hydrauliky a hydrologie**

**Bioindikace změn hydrologického režimu zalesněného horského  
povodí**

**Bioindication of changes in the hydrological regime of a forested  
mountain catchment**

**DISERTAČNÍ PRÁCE**

**Ing. Eva Pažourková**

Doktorský studijní program: Stavební inženýrství  
Studijní obor: Vodní hospodářství a vodní stavby

Školitel: Doc. Ing. Josef Křeček, CSc.

---

**Praha 2022**





## **PROHLÁŠENÍ**

Jméno doktoranda: Eva Pažourková

Název disertační práce: Bioindikace změn hydrologického režimu zalesněného horského povodí

Prohlašuji, že jsem uvedenou disertační práci vypracoval/a samostatně pod vedením školitele Doc. Ing. Josefa Křečka, CSc.

Použitou literaturu a další materiály uvádím v seznamu použité literatury.

Disertační práce vznikla v souvislosti s řešením projektu:

- Vliv hydrologických extrémů na kvalitu vody a oživení horských toků v podmínkách acidifikace (SGS16/140/OHK1/2T/11), 2016-2017
- Bioindikace změn vodního režimu zalesněného horského povodí (SGS18/120/OHK1/2T/11), 2018-2019
- Vliv globálních změny klimatu na extrémní průtoky a environmentální dopady v zalesněném horském povodí (SGS20/110/OHK1/2T/11), 2018-2019
- Hydrologie lesa v systému horského povodí a vodní nádrže (SGS2022/093/OHK1/2T/11), 2022-2023
- Mountain Waters of Bohemia (Earthwatch Institute), 1991-2012
- The integrated impact of climate change, air quality, and forest management on water ecosystem in headwater catchments (GA ČR 526-09-0567 – CLIMHEAD), 2009-2013

- Climate – smart forestry in mountain regions (COST action project CA15226), 2017-2021
- Ekosystémové služby horských lesů a povodí vodárenských nádrží v podmínkách kyselé atmosférické depozice a změny klimatu (INTER-EXCELLENCE: INTER-COST LTC 17006), 2017-2021

V Praze dne .....

.....  
podpis

# PODĚKOVÁNÍ

Ráda bych poděkoval svému školiteli doc. Ing. Josefu Křečkovi, CSc. za vedení a neocenitelné rady při výzkumu a tvorbě této práce. Dále bych ráda poděkovala zejména doc. Ing. Janě Novákové, CSc., prof. RNDr. Evženu Stuchlíkovi, CSc. a RNDr. Zuzaně Hořické, Ph.D. za odborné rady při botanickém a biologickém průzkumu.

Díky patří i všem organizacím, které svoji podporou (viz výše) umožnili práci na tomto výzkumu.

## Abstrakt

Horská povodí jsou důležitá pro tvorbu a ochranu vodních zdrojů, ale i z hlediska krajinné ekologie a zachování biodiverzity. Chráněná pramenná oblast Jizerských hor byla v minulém století zasažena extrémní kyselou atmosférickou depozicí a následnou acidifikací prostředí a intenzivní lesní těžbou stávajících smrkových porostů. V současné době se snížením depozice síry (a kyselé zátěže) zde probíhá revitalizace půdně-vegetačního pokryvu a povrchových vod, ale současně se projevují vlivy globální klimatické změny, jejíž budoucí projevy závisí na vývoji emisí skleníkových plynů.

Cílem této disertace je příspěvek k objasnění možností bioindikace k detekci změn povodí a jejich dopadu na hydrologické prvky, rutinní staniční observace v uzávěrových profilech povodí, případně stanovení jejich časové prodlevy. Pro popis vodního prostředí je uvažován makrozoobentos jako vhodný ukazatel kvality vody a proudění vody v roku. Stav povodí byl popsán pomocí Ellenbergových indikačních hodnot, vycházejících z životního optima cévnatých rostlin.

Oba indikátory (makrozoobentos i Ellenbergovy indikační hodnoty) se ukázaly jako vhodné pro popis změn v povodí, ale u obou byla zaznamenána časová prodleva oproti měřeným veličinám. V porovnání s vývojem evapotranspirace byl vývoj Ellenbergovy indikační hodnoty vlhkosti zpožděn o zhruba 14 let. U makrozoobentosu byla pozorována časová prodleva zotavení populace oproti zlepšení kyselosti prostředí asi o 5 let. Při použití těchto bioindikačních metod v podmínkách sledovaného povodí je nutné změny sledovat v širším kontextu, jelikož se zde mohou projevovat i jiné změny prostředí (v případě makrozoobentosu například extrémní povodňové situace a v případě vegetačního pokryvu radikální lesnické zásahy).

## Abstract

Mountain catchments are very important for their high biodiversity and water resources recharge. The protected headwater region of the Jizera Mountains has been struggling in the last century with the extreme acid atmospheric deposition, acidification of both terrestrial and aquatic ecosystems and commercial forestry practices (intensive harvest of damaged spruce plantations). Contemporary, this region is affected by the global climate

future with future prognoses related to the expected progress in the emissions of greenhouse gases.

The aim of this study was a contribution to the exploration of bioindication methods in the detection of changes in hydrological characteristics observed in outlets of investigated catchments. Macrozoobenthos was considered as a suitable indicator to describe water quality and the aquatic environment. The soil-vegetation complex of catchments was analysed by the Ellenberg's indicator values based on the life optimum of vascular plants.

Both indicators (macrozoobenthos and Ellenberg's indicator values) proved to be suitable for describing changes in the catchment, but a time delay compared to the measured values was recorded for both. Compared to the evolution of evapotranspiration, the evolution of the Ellenberg moisture indicator value was delayed by about 14 years. For macrozoobenthos, a time delay of about 5 years was observed in the recovery of the population compared to the improvement in environmental acidity. However, the evaluated changes in bioindicators need to be considered in a broader context: for example, in the case of macrozoobenthos, extreme flood events can dramatically change the data, and the vegetation cover can be affected also by the forestry practices.

## Klíčová slova

Bioindikace, horské zalesněné povodí, makrozoobentos, Ellenbergovy indikační hodnoty, acidifikace, kyselá atmosférická depozice, intenzivní lesní hospodářství, změna klimatu.

## Keywords

Bioindication, mountain forested catchment, macrozoobenthos, Ellenberg indicator values, acidification, acidic atmospheric deposition, intensive forestry, climate change.

# Obsah

Abstrakt.....	6
Abstract.....	6
Klíčová slova .....	7
Keywords.....	7
Úvod.....	9
1. Stručný přehled problematiky .....	11
1.1. Bioindikace.....	11
1.2. Bioindikace povrchových vod .....	12
1.3. Makrozoobentos .....	15
1.4. Ellenbergovy indikační hodnoty .....	16
1.5. Kyselá atmosférická depozice .....	21
1.5.1. Vznik a příčiny .....	21
1.5.2. Atmosférická depozice.....	22
1.5.3. Sezónní a epizodická acidifikace .....	23
1.6. Intenzivní lesní hospodářství .....	23
1.7. Globální změna klimatu.....	24
2. Metodika.....	26
2.1. Lokalita .....	26
2.1.1. Povodí Sklářského potoka .....	26
2.1.2. Povodí Holubího potoka .....	28
3. Výsledky a diskuze .....	31
3.1. Možnosti indikace stavu povodí a tvorby vodních zdrojů v horském povodí .....	31
3.2. Indikace kvality vody v lesním povodí ovlivněném kyselou atmosférickou depozicí a těžbou dřeva .....	43
3.3. Vliv extrémních hydrologických jevů na bioindikaci kvality vody.....	71
3.4. Vliv změn klimatu na bioindikaci hydrologických procesů v horském povodí .....	88
Závěr.....	127
Seznam obrázků .....	128
Seznam tabulek .....	128
Seznam použitých zkratek .....	128
Seznam literatury .....	128
Publikace autora .....	134
Významné publikace relevantní k tématu.....	134
Ostatní významné publikace .....	134



# Úvod

Horská povodí jsou významná pro tvorbu a ochranu vodních zdrojů (Messerli et al., 2004). V podmínkách ČR byl k podpoře tvorby a ochrany vodních zdrojů vyhlášen zákonem o vodách 254/2001 Sb. (Tureček et al., 2002) institut CHOPAV (Chráněné oblasti přirozené akumulace vody), který zahrnuje účelovou regulaci hospodaření v horských povodích vybraných pramenných oblastí. V těchto povodích je zakázáno zmenšovat rozsah lesních pozemků, odvodňovat lesní či zemědělské pozemky, provádět lesní těžbu holosečí nad limitním plošným rozsahem, těžit rašelinu, a další (Vládní nařízení 40/1978, Tureček et al., 2002).

Horská povodí se vyznačují značnou prostorovou a výškovou nehomogenitou a s tím spojenou variabilitou meteorologických a hydrologických charakteristik (Shaw, 1994). Prostorová interpolace a extrapolace bodových meteorologických dat v horských povodích je komplikována vlivem proměnlivosti podmínek mezo- a mikro-klimatu (Křeček a Punčochář, 2012). V takových podmínkách je zapotřebí hustá síť pozorování k dosažení věrohodných dat. WMO (1994) doporučuje v horských oblastech hustotu meteorologických stanic 25 km<sup>2</sup> na stanici. Ve skutečnosti je tomu právě naopak, horské oblasti mají poměrně řídkou síť pozorování a to z několika důvodů. Jsou to místa poměrně špatně dostupná, s náročnými podmínkami jak pro pozorovatele, tak pro přístrojovou techniku. Hustá observační síť je z finančního hlediska nákladná. Horské oblasti jsou většinou oblasti málo hustě osídlené, takže ze strany veřejnosti není velká poptávka po měření meteorologických veličin. Navíc měřená data jsou často zatížena chybami nebo řady dat obsahují mezery měření. Proto se jako vhodný nástroj pro zjišťování podmínek povodí jeví bioindikace, která nám je schopná poskytnout informace o stavu a změně stanoviště na základě fauny a flóry vyskytující se v daném místě.

Horské oblasti v poslední době čelí celé řadě změn, ať už se jedná o zatížení kyselou atmosférickou depozicí, intenzivnímu lesnímu hospodářství či změnám klimatických podmínek způsobených oteplováním. Většinou se jedná o lokality se specifickými morfologickými, topografickými i hydrologickými podmínkami a výše pospané změny či zásahy mohou mít dalekosáhlé důsledky. Vzhledem k tomu, že horská povodí jsou velmi

podstatná pro zásobování obyvatelstva pitnou vodou, Messerli et al. (2004) uvádí, že 40-80 % vody z horských oblastí zásobuje níže položené lokality pitnou vodou a jejich význam bude narůstat se zvyšující se populací a změnami klimatu (UNEP, 2007; Viviroli et al., 2007), měla by být těmto oblastem věnována značná pozornost. Ve střední Evropě je většina horských povodí zalesněna (FAO, 2008). Forman (1995) uvádí, že les má schopnost chránit kvalitu půdy a vodních zdrojů, proto je nezbytné dodržování dobrých lesnických zásad.

Cílem této studie je zhodnocení možností popisu horského povodí, jeho hydrologického režimu a především změn způsobených vlivem kyselé atmosférické depozice, lesnické činnosti a klimatické změny pomocí metod bioindikace. Pro popis změn vodního prostředí povrchových vod zájmových povodí v Jizerských horách byla zvolena indikace pomocí makrozoobentosu. Na základě výskytu jednotlivých druhů a jejich citlivosti na jednotlivé faktory se předpokládá možnost posouzení změny kvality vody s ohledem na trvalou, sezónní a episodickou formu zátěže kyselou atmosférickou depozicí (Rashid & Pandit, 2014; Guerold et al., 2000). Bentické organismy jsou v takovémto prostředí vystavovány stresu jednak ze samotné acidifikace prostředí, následně při zlepšení stavu jsou vystavováni nárazovému snížení pH při sezónní a epizodické acidifikaci (v průběhu povodně), která je doprovázena zvýšenými rychlostmi, což je další limitující prvek výskytu (Brookes, 1988).

Pro popsání stavu povodí je uvažováno použití Ellenbergových indikačních hodnot. Jednotlivé indikační hodnoty v sobě zahrnují více faktorů prostředí, například indikátor vlhkosti je kombinací faktorů úrovně hladiny podzemní vody, režimu atmosférických srážek, sluneční radiace, teploty a vlhkosti vzduchu (Ellenberg, 1974, 1988; Ellenberg et al, 1992). Dále se dá usuzovat, že jednotlivé indikační hodnoty mají časovou prodlevu vzhledem k charakteru výskytu vegetace (při výskytu neodpovídajících podmínek pro stávající vegetaci potrvá nějakou dobu, než tyto druhy vymizí a zároveň nějaký čas zabere rozšíření nových druhů).

Studie bude zahrnovat vzájemné vztahy meteorologických a hydrologických veličin, a stav zalesněného horského povodí, které je možné detekovat pomocí metod bioindikace (detekcí makrozoobentosu a Ellenbergových indikátorů travní vegetace).

Práce je členěna do čtyř dílčích kapitol, které popisují možné negativní vlivy ovlivňující stav horských povodí a uvádějí je do souvislostí s možností zapojení bioindikace.

# 1. Stručný přehled problematiky

## 1.1. Bioindikace

Ekosystém je podle české legislativy chápán jako funkční soustava živých a neživých složek životního prostředí, jež jsou navzájem spojeny výměnou látek, tokem energie a předáváním informací a které se vzájemně ovlivňují v určitém prostoru a čase (Zákon o životním prostředí, § 3 zákona č. 17/1992 Sb., 1992). Je tedy tvořen živou složkou, což jsou organismy, a neživou složkou, kterou chápeme jako prostředí nebo stanoviště. Obě tyto složky se vzájemně ovlivňují. Vlastnosti prostředí, ať už chemické či fyzikální, formují živou složku vyskytující se v daném prostředí a naopak organismy nám poskytují informace o prostředí. Pro tento jev se ustálil pojem bioindikace, což je metoda, kdy se na základě vlastností biologických systémů odhadují vlastnosti prostředí, neboli výskyt a stav určitého druhu organismu signalizuje určité podmínky prostředí (Anděl, 2011).

Bioindikátor je organismus či soubor organismů, kterým je sledována daná vlastnost prostředí. Vhodné druhy používané pro bioindikaci mají úzkou ekologickou valenci (rozsah hodnot, které je organismus schopný snášet je malý). Podle přirozeného výskytu organismů můžeme usuzovat, jaké podmínky na stanovišti panují, ale je také možné díky bioindikátorům zaznamenat změny v prostředí. To je využíváno pro detekci znečištění prostředí, kdy dojde k vymizení určitého druhu, který je citlivý na dané znečištění, nebo jsou u něj zaznamenány chemické, fyziologické či behaviorální změny a naopak je možné pozorovat i zotavování habitatu ze znečištění, v současnosti je pro tento proces používán název biomonitoring (Markert et al, 2003).

Rozlišujeme několik druhů indikátorů znečištění (Kulich a kol., 2002):

- Sentinel (strážný) je citlivý druh, který je úmyslně přidán do zkoumaného prostředí a okamžitě reaguje na nepříznivou změnu v prostředí.
- Detektor je druh, vyskytují se přirozeně ve zkoumané oblasti, který měřitelným způsobem reaguje na změny prostředí (mortalitou, věkovým rozvrstvením populace, změnou chování).
- Exploiter (vykořisťovatel) je druh, jehož přítomnost značí narušení prostředí.

- Akumulátor je druh, který přijímá a hromadí chemické látky z prostředí v měřitelných množstvích.
- Biossay organism (organismus pro biologickou kvantitativní zkoušku) je vybraný druh, který se používá v laboratoři ke zjištění přítomnosti nebo koncentrace škodlivých látek.

Pro zájmovou lokalitu je možné také stanovit index druhové pestrosti (diverzity), který vyjadřuje informaci o celkovém počtu nalezených druhů. Jde o váhový vztah absolutního počtu přítomných druhů v lokalitě k velikosti vzorku (počtu kusů), obecně tyto indexy nejsou vhodné, jelikož odráží spíše proces vzorkování společenstva než jeho biodiverzitu (Opařilová & Horký).

Meinhinickův index druhové pestrosti (Menhinick, 1964):

$$D = \frac{S}{\sqrt{N}} \quad (1)$$

Margalefův index druhové pestrosti (Margalef, 1951):

$$D = S - \frac{1}{\log N} \quad (2)$$

*S ... počet taxonů*

*N ... celkový počet jedinců*

Používají se bioindikátory rostlinné i živočišné, například pro vodní prostředí se jako indikační skupina organismů používá fytobentos, makrofyta, pobřežní vegetace, makrozoobentos a ryby, ale tímto způsobem se dá studovat jakýkoli ekosystém.

## 1.2. Bioindikace povrchových vod

U povrchových vod se za pomoci bioindikace stanovuje jakost povrchových vod. Ta pokud jde o organické znečištění povrchových vod, se hodnotí saprobním systémem, který vychází z předpokladu, že v rozdílně znečištěných vodách žijí různé organismy, které se podílejí na rozkladných procesech. Organismy, kteří indikují organické znečištění, se nazývají saprobionty. Pro stanovení stupně znečištění vod je nutné provést biologický rozbor, jelikož různému stupni saprobity odpovídají různé biocenózy tvořené rozlišně odolnými živočichy. V druhové skladbě se organické znečištění obecně projevuje poklesem, tedy nižší

diverzitou biotopu, ale nárůstem počtu organismů (Tagliapietra et al, 2012; Sládeček, 1973; Rödlová, 2012).

U povrchových tekoucích vod se obecně jako indikační skupiny uvažují fytoENTOS, makrofyta, pobřežní vegetace, makrozoobentos a ryby, pro stanovení saprobity je to zejména makrozoobentos a nárosty. Pro stojaté vody jsou indikační skupiny fytoplankton, fytoENTOS, makrofyta, zooplankton, makrozoobentos a ryby, jako saprobieoty se používá nejvíce plankton (Rödlová, 2012).

Základní stupně saporiby stanovili Kolkwitz & Marsson (1909):

- Kataprobity – nejčistší vody, slabé oživení, druhy podzemních vod (prameny, podzemní vody).
- Oligosaprobity – vody pstruhového a lipanového pásma s nepatrným organickým zatížením, nadbytek kyslíku a silně aerobní procesy, druhová diverzita malá.
- $\beta$ -mezosaprobity – střední části vodních toků (dolní části lipanového a dále parmového pásma), které jsou přirozeně zatížené organickými látkami nebo menším sekundárním znečištěním toku, voda je dostatečně okysličená, samočištění probíhá především na úrovni oxidačních pochodů (aerobní procesy), vysoká druhová skladba.
- $\alpha$ -mezosaprobity – střední a dolní části vodních toků (cejnové pásmo a dále se vyskytující už jenom kaprovité ryby), znečištění organickými látkami je vysoké, kyslíku je zde málo, aerobní a anaerobní procesy jsou vyrovnané, nastupuje méně odolnějších druhů, které vytváří silné populace, druhová skladba se snižuje.
- Polysaprobity – silně znečištěné vody, je zde minimum kyslíku, převládají anaerobní procesy, bez rybích populací a většiny dalších organismů, na samočištění se podílí pouze nárostové bakterie, některé řasy, nitěnky a pakomáři, druhová diverzita je velmi nízká, avšak populace těchto druhů dosahují velké hustoty.

System dále rozšířil Sládeček pro stojaté a tekoucí vody (Sládeček, 1973):

- Kataprobity (K) – nejčistší vody se slabým oživením, druhy podzemních vod.

- Limnosaprobity (L) - povrchové i podzemní vody různě znečištěné, odlišná struktura společenstev.
- Eusaprobity (E) - odpadní vody se značně zvýšeným obsahem organických látek.
- Transsaprobity (T) – zvláštní odpadní vody s nehmotnými látkami (nebo faktorem, který je brzdí – ropné, toxické látky, vysoká teplota, radioaktivita).

Saprobni index je metoda umožňující kvantitativní vyjádření a srovnání s jinými ukazateli.

Stanovení podle Pantle & Buck (1955):

$$S = \frac{\sum(h \cdot S_i)}{\sum h} \quad (3)$$

*S ... Saprobni index celého společenstva*

*Si ... Individuální saprobni index druhu*

*h ... abundance (početnost jedinců jednoho druhu na určitém místě – populace, počet organismů na ml)*

Stanovení podle Sládečka (1973):

$$S = \frac{0\sum_{hx} + 1\sum_{ho} + 2\sum_{h\beta} + 3\sum_{h\alpha} + \dots}{\sum h} \quad (4)$$

*S ... Saprobni index celého společenstva*

*$\sum_{hx/\alpha/h\beta}$  ... součet hodnot abundance xenosaprobni/oligotropni/... indikátorů*

*$\sum h$  ... suma všech bioindikátorů*

Saprobni index má hodnoty od -1 (katarobity – nejčistší vody prakticky bez znečištění, vody podzemní a pramenné) do 8 (ultrasaprobity – koncentrované průmyslové vody, které bez zředění nelze čistit).

Saprobni index se obecně používá k detekci antropogenního znečištění větších vodních toků (Sládeček, 1973), u malých horských toků postižených acidifikací postrádá smysl. V tomto případě je účelné použít Ellenbergovy indikační hodnoty pro stav povodí a analýzu makrozoobentosu pro vodní prostředí.

### 1.3. Makrozoobentos

Jsou to organismy viditelné pouhým okem, které žijí na dně nebo v těsné blízkosti dna. Podle různých klasifikačních systémů je velikost makrozoobentosu větší jak 1 mm nebo 0,5 mm. Výskyt makrozoobentosu ovlivňuje řada faktorů: rychlost proudu, teplota, substrát, vegetace, dostupnost potravy, zastínění, mezidruhová kompetice i náchylnost na vysychání toku a povodně (Brookes, 1988). Bentické organismy se adaptovaly na život v proudící vodě (tvar těla snižující tření, drápky, háčky, přilnavé výrůstky, zatěžování těla pomocí schránek z kamínků atd.), ale makrozoobentos, který žije v pomalu proudící vodě tyto morfologické adaptace k obsazení a pohybu na stanovištích s rychlým proudem nemá (Statzner & Holm, 1982; Hoover & Richardson, 2010). Jelikož žijí v písčném dnu toku, v mezerách dna nebo si přímo tvoří schránky z malých kamínků a jiného materiálu vyskytujícího se na dně je jejich pohyblivost omezená. Způsob jakým se bentos přesouvá na delší vzdálenost, se nazývá drift a může být chtěný či nechtěný. Závisí na velikosti proudu (rychlosti), světelných podmínkách, teplotě, hustotě osídlení, výskytu predátorů a životním cyklu jednotlivých jedinců. Brittain & Eikeland (1988) uvádějí několik druhů driftu: katastrofický drift, behaviorální drift, aktivní drift, distribuční drift a konstantní drift. Katastrofický drift je spojen zejména s povodňovými událostmi, kdy je narušeno dno a makrozoobentos se nedobrovolně dostává do proudu. Behaviorální drift je pohyb, kdy se bentos přesouvá při hledání potravy a dobrovolně nebo nedobrovolně se nechá unášet proudem. Dalším důvodem je únik před predátorem, kdy bentos do proudu vstupuje aktivně, proto je často označován za aktivní drift. Distribuční drift je uvažován při rozptýlení živočichů po vylíhnutí a konstantní drift (nebo drift na pozadí) je považován za náhodný proces, kdy se do proudu dostávají nízké počty živočichů bez ohledu na jakoukoli denní periodicitu.

Do skupiny makrozoobentosu patří například červi, pijavky, mlži, plži, roztoči, korýši a larvální stádia vodního hmyzu. Tito živočichové mají různé požadavky na prostředí i různou citlivost na vnější vlivy. Rashid & Pandit (2014) považují benthos za velmi účinný indikátor stavu vodního prostředí kvůli jejich omezené pohyblivosti, relativně dlouhému životnímu cyklu a různé citlivosti na rozličné druhy znečištění. I z těchto důvodů je makrozoobentos považován jako dobrý bioindikátor vodního prostředí. Fritz et al. (2013) uvádí, že chemismus vody a výskyt makrozoobentosu patří mezi nejdůležitější ukazatele environmentálního stavu horních částí toků. Jestliže má být makrozoobentos použit jako indikátor stavu prostředí

je nutné provádět terénní měření, které určí vyskytující se taxony a jejich počet a mělo by reflektovat stav zájmového úseku toku. Nejprve je nutné stanovit charakteristický úsek toku, který odráží fyzikální a ekologické charakteristiky dané lokality, délka úseku by měla být čtrnáctinásobek šířky toku, maximálně však 100 m. V tomto úseku toku si stanovíme odběrový úsek, který by měl charakterizovat všechny habitaty nacházející se v toku, a je nutné zaznamenat polohu pro možnost opakování odběru v budoucnu. Vytipují se jednotlivé habitaty například místa s různou rychlostí proudu, různě vzdálená od břehu, trsy trav splývající u břehu do vody, větve nebo kmeny ležící po určitou dobu ve vodě, kořeny, různé typy dna (písčité, kamenité, hlinité), vodní rostliny atd. Postupuje se proti proudu, hydrobiologický cedník nebo bentosové síť se umístí spodním okrajem na dno a místo před cedníkem/sítí se rozruší nohou či rukou do hloubky pěti až deseti centimetrů, tím se uvolní organismy do proudu a jsou odneseny do cedníku/sítě. Do cedníku/sítě je také nutné opláchnout ponořené rostliny, kořeny, větve, kameny a jiné předměty, abychom získali i přisedlé organismy. Získaný vzorek je přetříděn do taxonomických skupin a pak dále do co nejnižší druhové úrovně buď v terénu, nebo v laboratoři (Kokeš & Němejcová, 2006).

Jako základní charakteristiky z vyhodnocení vzorku se pak stanovuje počet druhů, počet jedinců daného druhu, počet EPT taxonů (*Ephemeroptera* - jepice, *Plecoptera* - pošvatky a *Trichoptera* - chrostíci) a případně další charakteristiky. Důležitou informací je počet jedinců daného druhů neboli abundance, jelikož popisuje, o jak významnou populaci se jedná.

#### 1.4. Ellenbergovy indikační hodnoty

Stav povodí lze popsat třemi systémy: půda, vegetace, povrchové vody. Mezi těmito složkami probíhá neustálá interakce. Ke zkoumání stavu půdního prostředí je možné využít jako bioindikátory edafon (půdní organismy). Zkoumání půdního prostředí nám dá pouze omezenou informaci o vegetaci (Ellenberg, 1988). Proto naopak je doporučováno (Ellenberg, 1974, 1988) využití bylinné vegetace jako indikátoru, který umožňuje odhadnout i charakteristiky půdy (vlhkostní režim, salinitu, půdní reakci, dostupnost živin aj.).

Myšlenka indikačních hodnot vychází z předpokladu, že jednotlivé druhy rostlin se vyskytují především tam, kde jsou pro ně vyhovující vlastnosti daného stanoviště. Pokud tedy známe nároky jednotlivých druhů rostlin, pak dokážeme odhadnout a popsat vlastnosti stanoviště podle vyskytujících se druhů rostlin.



U druhů cévnatých rostlin byl stanoven soubor hodnot, které vystihují životní optima jednotlivých druhů (2726 pro střední Evropu) na základě terénních pozorování případně experimentem. Pro oblast Německa a přilehlých států soubor indikačních hodnot stanovil Heinz Ellenberg, ale používají se i jiné indikační hodnoty například Borhidioho pro oblast Maďarska (využitelná i pro území Moravy vzhledem k podobnosti druhů) či Zarzyckiho stanovené pro území Polska (Zelený, 2012).

Ellenbergův soubor indikačních hodnot je sestaven pro světlo (L) viz Tab. 1, teplotu (T) viz Tab. 2, kontinentalitu (K), vlhkost (F) viz Tab. 3, živiny (obsah dusíku N) viz Tab. 5, půdní reakci neboli pH (R) viz Tab. 4 a salinitu. Faktory světla, tepla a kontinentalita popisují klima stanoviště, faktory vlhkosti, půdní reakce a zásobení stanoviště dusíkem zase popisují půdní podmínky stanoviště. Výše jmenovaným vlastnostem stanoviště jsou přisouzeny hodnoty od jedné do devíti na ordinální škále, výjimkou je vlhkost, která má škálu od jedné do dvanácti, přičemž poslední tři stupně jsou pro druhy nějakou měrou žijící ve vodním prostředí (Zelený, 2012; Ellenberg, 1974, 1988; Ellenberg et al, 1992).

Tab. 1: Škála Ellenbergových indikačních hodnot pro světlo (Ellenberg, 1974, 1988).

Hodnota	Indikované prostředí	Tolerance relativních
1	rostliny hlubokého stínu	stále se vyskytující při <1%, zřídka >10%
2	mezi 1 a 3	
3	rostliny stínomilné	většinou <5%
4	mezi 3 a 5	
5	rostliny polostínu	většinou při >10%, výjimečně v plném
6	mezi 5 a 7	
7	rostliny částečně světlomilné	
8	mezi 7 a 9	výjimečně při <40%
9	rostliny zcela světlomilné	zřídka při <50%

Tab. 2: Škála Ellenbergových indikačních hodnot pro teplotu (Zelený, 2012, Ellenberg, 1974, 1988).

Hodnota	Indikované prostředí
1	rostliny indikující nízké teploty, rostoucí pouze ve vysokých horských oblastech, v alpínském nebo v boreálně-arktických oblastech
2	mezi 1 a 3, vysokohorské druhy často sestupující na úroveň subalpínského stupně
3	rostliny chladného podnebí, většinou subalpínského stupně
4	mezi 3 a 5, zejména na chladných místech
5	rostliny poměrně teplého podnebí, vyskytující se od nížin do hor, především v submontánním stupni
6	mezi 5 a 7
7	rostliny teplého podnebí v nížinách a kolinním stupni
8	mezi 7 a 9
9	rostliny extrémně teplého podnebí, z Mediteránu zasahuje jen do nejteplejších oblastí horního Porýní

Tab. 3: Škála Ellenbergových indikačních hodnot pro vlhkost (Ellenberg, 1974, 1988).

Hodnota	Indikované prostředí
1	rostliny indikující extrémní sucho, omezeno na půdy, které často na nějakou dobu vyschnou
2	mezi 1 a 3
3	rostliny indikující suché místo, častěji se vyskytují na suchých místech než na vlhkých
4	mezi 3 a 5
5	rostliny indikující vlhká místa, zejména na čerstvých půdách průměrné vlhkosti
6	mezi 5 a 7
7	rostliny indikující vlhkost, vyskytující se na vlhkých nikoli mokřích půdách
8	mezi 7 a 9

<b>9</b>	rostliny indikující velmi vlhké půdy, často saturované a špatně provzdušněné půdy
<b>10</b>	rostliny indikující místa s mělkou vodou, které po delší dobu mohou být bez stojaté vody
<b>11</b>	zakořeněné rostliny pod vodou, ale alespoň po nějakou dobu nad ní, nebo rostliny plovoucí na povrchu
<b>12</b>	ponořené rostliny, trvale nebo téměř trvale pod vodou

Tab. 4: Škála Ellenbergových indikačních hodnot pro reakci půdy (Ellenberg, 1974, 1988).

<b>Hodnota</b>	<b>Indikované prostředí</b>
<b>1</b>	rostliny indikující extrémní kyselost, nevyskytující se na slabě kyselých nebo zásaditých půdách
<b>2</b>	mezi 1 a 3
<b>3</b>	rostliny indikující kyselost, vyskytující se zejména na kyselých půdách, výjimečně také na téměř neutrálních půdách
<b>4</b>	mezi 3 a 5
<b>5</b>	rostliny indikující mírně kyselé půdy, jen příležitostně se vyskytují na velmi kyselých nebo neutrálních až zásaditých půdách
<b>6</b>	mezi 5 a 7
<b>7</b>	rostliny indikující slabě kyselé až slabě zásadité půdy, nikdy se nevyskytují na velmi kyselých půdách
<b>8</b>	mezi 7 a 9
<b>9</b>	rostliny indikující bazické prostředí, vždy nalezeny na vápenatých půdách nebo jiných půdách s vysokým pH

Tab. 5: Škála Ellenbergových indikačních hodnot pro obsah dusíku (Ellenberg, 1974, 1988).

<b>Hodnota</b>	<b>Indikované prostředí</b>
<b>1</b>	indikátor extrémně neplodných míst
<b>2</b>	mezi 1 a 3
<b>3</b>	indikátor více či méně neplodných míst

4	mezi 3 a 5
5	indikátor míst střední plodnosti
6	mezi 5 a 7
7	indikátor bohatě úrodných míst
8	mezi 7 a 9
9	indikátor extrémně úrodných míst, místa odpočinku skotu nebo místa v blízkosti znečištěných řek

Při botanickém průzkumu se u fytosociologických snímků stanovuje pokryvnost, zastoupení jednotlivých druhů a vývojové formy na ploše 4 x 4 m. Hodnota Ellenbergova indexu se stanoví jako vážený průměr zastoupených druhů. Indikační hodnota určitého druhu se stanoví podle rovnice 5:

$$IND_{ij} = A_{ij} \cdot B_{ij} \cdot 100 \quad (5)$$

$$A_{ij} = M_{ij} / M_i \quad (6)$$

$$B_{ij} = N_{ij} / N_i \quad (7)$$

*IND<sub>ij</sub> ... indikační hodnota určitého druhu*

*M<sub>ij</sub> ... průměrné zastoupení druhu i v zóně j (abundance – velikost populace)*

*M<sub>i</sub> ... průměrné zastoupení druhu i ve všech zónách*

*N<sub>ij</sub> ... počet stanovišť v zóně j, kde se druh i vyskytuje (frekvence)*

*N<sub>i</sub> ... počet stanovišť v zóně j.*

Indikační hodnoty neodrážejí okamžitý stav prostředí, ale jeho integraci v čase. Jednotlivé indikační hodnoty odrážejí komplex faktorů prostředí, například vlhkost v sobě zahrnuje kombinaci úrovně hladiny podzemní vody, režim atmosférických srážek, sluneční radiaci, teplotu a vlhkost vzduchu. Schmidtlein (2005) uvádí, že se pomocí Ellenbergových indexů dá odhadovat doplňování zásob podzemních vod.

## 1.5. Kyselá atmosférická depozice

Acidifikace je jedním z výrazných problémů ovlivňující životní prostředí, jak v minulosti, tak i v současnosti a její vliv na ekosystémy se dá předpokládat i v budoucnosti, proto je potřeba zkoumat vliv kyselé atmosférické depozice na suchozemské a vodní ekosystémy (Reuss & Johnson, 1986).

### 1.5.1. Vznik a příčiny

Obecně je kyselá atmosférická depozice (acidifikace) proces, při kterém dochází k okyselování prostředí. Příčin vzniku je hned několik, v minulosti se na acidifikaci prostředí nejvíce podílel oxid siřičitý ( $\text{SO}_2$ ), který se na Zemi sice vyskytuje přirozeně (produkován sopečnou činností a oxidací sulfanu při rozkladu odumřelé biomasy), ale antropogenní činností se v minulém století koncentrace síry v atmosféře výrazně zvýšila. Přispělo k tomu spalování fosilních paliv (obsah síry v černém uhlí je přibližně 1%, v ropě 1-3%, v palivovém dřevu 0,1% a v hnědém uhlí 1-8%) a sirný průmysl. Znečištění oxidem siřičitým se projevuje na velké vzdálenosti od zdroje, jelikož přenos látky ovzduším může být v řádech stovek kilometrů za den a v atmosféře setrvá i několik dní. Od největšího znečištění v 80. letech minulého století se koncentrace síry snižují díky odsiřovacím zařízením a spalováním uhlí s redukováným obsahem síry (Hruška & Kopáček, 2005, 2009; Reuss & Johnson, 1986). Prechtel et al. (2001) uvádí, že i přes snížený přísunu depozice síry některé lokality reagují na toto snížení opožděně a dá se u nich očekávat, že acidifikace povodí bude pokračovat úbytkem bazických kationtů z půdy a okyselováním půdy i vodního prostředí.

V současnosti emise síry nahrazují zejména oxidy dusíku, které se rovněž vyskytují přirozeně (vznikají při lesních a stepních požárech, při mikrobiálních pochodech a při elektrických výbojích v atmosféře), ale antropogenní činností se jejich koncentrace mnohonásobně zvýšila. Mohou za to spalovací procesy, přičemž znečišťovatelem není dusík obsažený ve spalované látce, ale vzdušný dusík ( $\text{N}_2$ ) oxidovaný za vysokých teplot. Takto vzniklé emise záleží na množství spotřebovaného paliva, způsobu jeho spálení (teplotě a přebytku vzduchu) a typu zdroje, jestli se jedná o stacionární zdroj (pálení uhlí v běžném stacionárním zdroji vyprodukuje 2-4 g emisí dusíku na jeden kilogram paliva) nebo mobilní zdroj (při jízdě v osobním automobilu vzniká zhruba 10-25 g emisí dusíku na kilogram paliva). U stacionárních zdrojů se znečištění daří snižovat, ale vzhledem ke vzrůstající automobilové

doprově celkové znečištění dusíkem neklesá (Hruška & Kopáček, 2005, 2009; Reuss & Johnson, 1986; Schöpp et al., 2003).

Z atmosféry se na zemský povrch dostávají i soli síry a dusíky (zejména síran a dusičnan amonný), vznikající reakcí kyselin s plynným amoniakem ( $\text{NH}_3$ ), který v atmosféře snižuje kyselost srážek, jelikož na sebe váže  $\text{H}^+$ , čímž vzniká amonný iont ( $\text{HN}_4^+$ ). Po dopadu na zemský povrch amonný iont výrazně zvyšuje acidifikaci půdy, jelikož se zúčastní procesu nitrifikace (rostliny odebírají z půdy amonné ionty, které biochemickou přeměnou nahradí za  $\text{H}^+$ ). Tudiž dalšími zdroji způsobujícími okyselování prostředí je nadměrné používání dusíkatých hnojiv a zvýšené množství amoniaku vyprodukované v důsledku chovu skotu (Hruška & Kopáček, 2005, 2009; Reuss & Johnson, 1986; Schöpp et al., 2003).

Acidifikace prostředí působí na půdu, vodu i na faunu a flóru. V půdě se kyseliny neutralizují s bazickými kationty až do vyčerpání pufrční kapacity, pak se půdní prostředí stává kyselým, což může vést k úhynu vegetace a nahrazení stávající vegetace jinými méně sensitivními druhy (Prechtel et al., 2001). Následně se okyselují i povrchové vody a dochází k mobilizaci toxických forem hliníku, což může vést k úhynu vodní fauny (Bache, 1985). Acidifikace vod je limitující pro mnoho druhů vodních organismů (NIVA, 2013), kteří vymizí a mohou být nahrazeny méně citlivými druhy. Guerold et al. (2000) doporučuje bezobratlé vodní organismy jako nejlepší indikátor negativního vlivu acidifikace na životní prostředí.

### 1.5.2. Atmosférická depozice

Atmosférická depozice je proces, při kterém se látky z ovzduší přenášejí k zemskému povrchu (hmotnost sledované látky na jednotku plochy za určité časové období). Jedná se o proces samočištění atmosféry, ovšem sloučeniny, prach a jiné částice se tímto způsobem dostávají na zemský povrch, do půdy a vody a do přímého kontaktu s faunou a flórou a tím může docházet k jejich znečištění jako je tomu i u kyselé atmosférické depozice.

Podle charakteru dělíme depozici na suchou a mokrou. Mokrú depozice je způsobena vertikálními a horizontálními srážkami, kdy dochází k tzv. vymývání atmosféry. Hruška & Kopáček (2005, 2009) uvádějí, že atmosférické srážky bez antropogenních vlivů jsou velmi slabě kyselé s hodnotou pH 5-6, hodnota kyselých dešťů se pohybuje v rozmezí pH 3,5-4,5, jelikož je pH logaritmická veličina, pak pokles o dvě jednotky znamená zvýšení kyselosti asi stonásobně. Navíc horizontální srážky vyskytující se zejména v horských oblastech

působí na vegetaci a prostředí po delší dobu a s vyššími koncentracemi, tudíž mohou prostředí značně ovlivnit (Křeček et al., 2019).

Suchá depozice je proces, kdy se plyny a aerosol z atmosféry zachycují na povrchu rostlin a ty jsou následně opláchnuty deštěm do půdy tzv. podkorunová depozice. Při tomto ději záleží na typu vegetace, jelikož jehličnaté stromy mají větší specifický povrch oproti listnatým stromům a mají jehličí po celý rok (až na výjimky), lépe zachytávají emisní znečištění (Křeček & Hořická, 2006; Hruška & Kopáček 2005, 2009).

### 1.5.3. Sezónní a epizodická acidifikace

V regionech zasažených kyselou atmosférickou depozicí může hodnota pH ve vodním prostředí klesat v důsledku sezónní a epizodické acidifikace. Epizodická acidifikace vzniká v důsledku srážkových událostí a sezónní acidifikace je způsobena jarním táním sněhu (Falkenmark & Allard, 2015). Při obou typech událostí dochází k dočasnému, někdy i výraznému snížení hodnoty pH vodního prostředí, což může negativně ovlivnit vodní organismy a způsobit mobilizaci toxických forem hliníku (Bache, 1985). Růžičková a kol. (2004) uvádějí, že sezónní acidifikaci lze považovat za hlavní faktor determinující výskyt bioty v tocích. Stejně tak je tomu u epizodické. Horecký a kol. (2005, 2013) tvrdí, že již relativně malý rozdíl v pH, stejně jako silně acidifikovaný tok, mohou ovlivnit biologické společenstvo. U kyselých toků je patrný pokles v biodiverzitě zejména vymizením jepic, měkkýšů a korýšů a nižšími počty pošvatek, chrostíků a jiných bezobratlých.

## 1.6. Intenzivní lesní hospodářství

Intenzivní lesní hospodářství chápe funkci lesa pouze jako produkční (výroba dřevní hmoty). Funkce lesa ovšem může být při správném hospodaření i mimoprodukční (krajinná, půdo ochranná, úprava vodního režimu, vytváření cenných ekosystémů, klimatická, atd.). Hospodaření v lesích způsobem, které vyžaduje intenzivní technologie, může zapříčinit podstatné změny v biologické rozmanitosti, struktuře a funkci ekosystémů, nevratně poškozovat půdní povrch, používáním chemických látek či rozsáhlými mechanickými zásahy narušovat ekologickou rovnováhu a měnit vodní režim území (Moucha & Pelc, 2008; FAO 2010; Čížek a kol., 2007).

Les obhospodařovaný intenzivním způsobem má často jedno-druhový neboli monokulturní charakter a stromy jsou stejné věkové kategorie, vysazované do čtvercové sítě s různým

rozpětím vzdálenosti podle druhu. Po uplynutí doby obmytí je les vykácen za pomoci těžké techniky a celý koloběh se opakuje. Negativní účinky této praktiky jsou náchylnost ke škůdcům (snadné šíření) a k přírodním pohromám kvůli jedno-druhové skladbě a stejnověkosti porostu. V takovýchto lesích chybí rozmanitost typů prostředí, tudíž se snižuje celková biodiverzita ekosystému. Obhospodařování těžkou technikou způsobí udusání půdy, jenž vede k poklesu infiltrace, k zvýšení povrchového odtoku a tím zintenzivnění eroze, která je navíc podpořena ztrátou ochrany korun stromů před přímým působením mechanického rozrušování povrchu srážkami (Moucha & Pelc, 2008; Hédl a kol., 2011)

Dalším problémem intenzivního způsobu lesního hospodaření je výběr druhu pro danou lokaci. Lesníci od nedávné minulosti do současnosti dávali přednost poměrně rychle a rovně rostoucímu smrku před listnatými stromy, které do doby obmytí rostou podstatně déle. Takže se smrkové (případně borovicové) monokultury staly dominantní na celém našem území i na místech, která pro smrk nejsou vůbec vhodná (Moucha & Pelc, 2008).

## 1.7. Globální změna klimatu

Globální změna klimatu je v poslední době velmi diskutované téma, které sebou přináší mnoho otázek. V průběhu historie docházelo vždy ke změnám klimatu a neexistoval žádný vyvážený stav (Arnell, 1999). Ovšem změny klimatu, které pozorujeme v dnešní době, jsou podle mnohých vědců velmi rychlé a jejich dopad je velice rozsáhlý. IPCC (2014) uvádí, že mezi hlavními indikátory klimatických změn patří rostoucí teplota, která koresponduje s rostoucí koncentrací skleníkových plynů v atmosféře, tyto plyny jsou často označovány za jeden z hlavních činitelů změn klimatu. Mezi nejdůležitější skleníkové plyny emitované vlivem činnosti člověka jsou oxid uhličitý (CO<sub>2</sub>), metan (CH<sub>4</sub>), oxid dusný (N<sub>2</sub>O) a fluorované uhlovodíky (obsahující brom, fluor a chlor).

Změna klimatu se promítne vzrůstající teplotou vzduchu, která souvisí s klimatickými, hydrologickými a meteorologickými procesy (evapotranspirace, tání sněhu, zahřívání oceánů, atd.), redistribucí srážek a nárůstem extrémů. Důsledky změn klimatu nejsou rovnoměrně distribuované ani v prostoru ani v čase, což znamená, že na některých místech bude změna výraznější než na jiných. Pro Evropu se klimatické modely víceméně shodují, že k poklesu srážek dojde ve středomoří a v letních měsících, nárůst srážek by pak měl být na severu a v zimním období. Hranice mezi nárůstem a poklesem srážkových úhrnů



je pro letní sezónu mezi 45 a 50 rovnoběžkou severní šířky, pro zimní období se posouvá na jih středomoří (Rajczak & Schär, 2017; Knist et al, 2018; IPCC 2013; Blöschl et al, 2019).

K predikci slouží globální a regionální klimatické modely, které jsou schopny popsat matematický popis dějů probíhajících v klimatickém systému Země podle různých scénářů vývoje koncentrací skleníkových plynů. Globální klimatické modely (GCM) v sobě zahrnují kombinaci modelu atmosféry, oceánu, kryosféry a zemského povrchu. Jsou schopny zachytit základní charakteristiky klimatu na velkých územích (rozlišení bývá většinou několik stovek km horizontálně, vertikálně je rozčleněn na několik desítek vrstev). Regionální klimatické modely (RCM) se používají pro podrobnější přiblížení a je do nich možné promítnout okolnosti ovlivňující klima na regionální úrovni (Hanel et al, 2011).

Vývoj obsahu skleníkových plynů v atmosféře je ovlivněn socio-ekonomickým vlivy a je těžké určit přesné množství, proto jsou vytvářeny emisní scénáře. V minulosti se používaly 4 emisní scénáře SRES (A1, A2, B1 a B2) zohledňující pouze ekonomický vývoj nebo lokální vývoj společnosti zohledňující ekologickou udržitelnost a jejich kombinace. Nyní se přechází k RCP (representative concentration pathways) scénářům, jež popisují pouze reprezentativní směry vývoje koncentrací (Hanel et al, 2011; IPCC, 2014).

Predikce klimatických modelů jsou zatíženy velkou nejistotou, která se ještě zvyšuje v horských oblastech, vzhledem k rozlišení modelů a prostorové a výškové nehomogenitě horských povodí.

V horských povodích se jako nejcitelnější jeví změny ve vodním režimu, kdy v letních měsících může dojít k poklesu srážkového úhrnu a tím snížení vodnosti toků i pod hranici minimálního zůstatkového (ekologického) průtoku, což se může promítnout do biodiverzity flóry (například vysychání rašelinišť) i fauny (pokles druhů ve vodním prostředí). Naopak v zimním období se srážkový úhrn může zvýšit a to zejména ve formě deště na úkor sněhu. Doba výskytu sněhové pokrývky se zkrátí kvůli vyšší teplotě. I v horských oblastech se dá očekávat nárůst extrémních událostí a to po celý rok například období sucha, povodní z příválových dešťů a s tím související sesuvy půdy atd. (Trnka a kol., IPCC, 2013).

## 2. Metodika

### 2.1. Lokalita

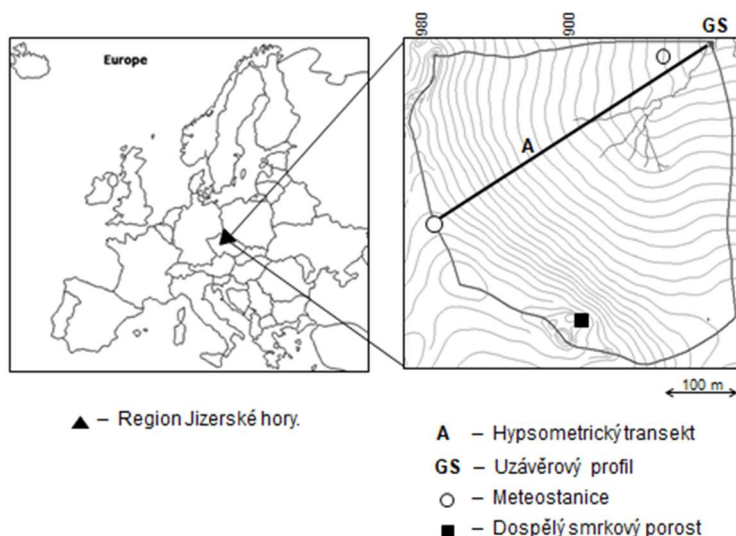
V rámci studie byly zkoumány dvě experimentální povodí v Jizerských horách.

#### 2.1.1. Povodí Sklářského potoka

Experimentální povodí Sklářského potoka (Jizerka, 50°48'21" - 50°48'59"N, 15°19'34" 15°20'48" E, číslo hydrologického pořadí: 1-05-01-004) reprezentuje náhorní plochu Jizerských hor, charakterizovanou podnebím Severního mírného pásu a subartického okrsku Dfc Köppenovy klasifikace. Na základě údajů klimatického normálu (1961 – 1990) vyplývají pro toto povodí: dlouhodobý průměrný roční úhrnem srážek 1400 mm, dlouhodobá průměrná roční teplotou vzduchu 4 °C, průměrné roční maximum sněhové pokrývky 120 cm a průměrné trvání sněhové pokrývky od začátku listopadu do konce dubna (Tolasz, 2007). Morfologické charakteristiky povodí jsou uvedeny v Tab. 6.

Tab. 6: Morfologie povodí Sklářského potoka (Jizerka).

<b>Plocha</b>	(km <sup>2</sup> )	1.03
<b>Nadmořská výška</b>	(m)	927 (862-994)
<b>Sklon</b>	(%)	7.52 (0.02-24.33)
<b>Index tvaru povodí index</b>	(-)	0.69
<b>Celková délka vodotečí</b>	(m)	1 490
<b>Intenzita drenážní sítě</b>	(km/km <sup>2</sup> )	1.45
<b>Délka hlavního toku</b>	(m)	657
<b>Sklon hlavního toku</b>	(%)	5.98
<b>Strahlerovo pořadí toku</b>	(-)	2



Obr. 1: Experimentální povodí Sklářského potoka (Jizerka).

V osmdesátých létech 20. století bylo toto povodí ovlivněno intenzivní kyselou atmosférickou depozicí (zejména spadem síry a dusíku), vedoucí k defoliaci a poškození smrkových porostů (*Picea abies*). V letech 1984 – 1988 byla většina plochy povodí smýcena holou sečí a stávající dospělé smrkové porosty byly nahrazeny společenstvím *Juncus effusi-Calamagrostietum villosae* s dominancí travní vegetace (zejména třtiny chloupkaté *Calamagrostis villosa*), Křeček a Nováková (2009). S obnovou lesa (byly použity převážně jehličnaté dřeviny *Picea abies*, *Picea pungens*, a *Pinus mugo*) se začalo do jednoho roku po těžbě, ale vysoká úmrtnost vysazovaných jedinců (v průměru 60%) vlivem nepříznivého prostředí výrazně prodloužila proces obnovy a výsadba musela být v období 1991 – 2000 několikrát opakována. Výsledkem obnovy lesa je druhové zastoupení dřevin *Pinus mugo* (80%) a *Picea abies* (20%) v dolní části povodí, zatímco v horní části převládá druhově pestřejší porost *Picea pungens* (50%), *Picea mariana* (14%), *Sorbus aucuparia* (7%), *Picea abies* (5%) a *Betula alba* (2%).

Hydrometeorologická observace na povodí Sklářského potoka započala v roce 1981. V uzávěrovém profilu povodí byl vybudován trojúhelníkový (120°) ostrohranný měrný přeliv, kde hladina přepadajícího paprsku je evidována kombinovaným tlakovým čidlem ALA 4020: v desetiminutovém intervalu jsou tak automaticky evidovány průtok a teplota vody. Meteorologická pozorování zahrnují automatickou staniční observaci v nadmořských

výškách 875 a 975 m, 12 manuálních kolektorů mlžné vody podél hypsometrického transektu A a 10 srážkoměrů umístěných pod korunami dospělého smrkového porostu viz Obr. 1.

Depozice atmosférických srážek je evidována v měsíčních intervalech a povrchová voda v uzávěrovém profilu povodí odebírána v týdenních intervalech. In situ monitoring zahrnuje měření teploty, pH, a vodivosti přenosným multimetrem WTW- 350i, vzorky pro laboratorní analýzu jsou filtrovány (40 µm) a analyzovány v akreditované laboratoři Hydrobiologické stanice Velký Pálenec (UK Praha). Chemické analýzy jsou prováděny podle metodiky Stuchlík et al. (2006). Jsou měřeny koncentrace hlavních iontů (Ca<sup>2+</sup>, Mg<sup>2+</sup>, Na<sup>+</sup>, K<sup>+</sup>, NH<sub>4</sub><sup>+</sup>, Cl<sup>-</sup>, NO<sub>3</sub><sup>-</sup>, a SO<sub>4</sub><sup>2-</sup>). V případě vzorků srážkové vody je evidentní, že bakteriální aktivita může ovlivnit chemické složení (hlavně dusík) s dobou uchování, v případě chladné subarktické oblasti předpokládáme, že bakteriální aktivita je kontrolována relativně chladným prostředím, relativně vysokými koncentracemi dusíku a nízkými hodnotami pH i rozpuštěného organického uhlíku (Cape et al., 2001). Současně potenciální nárůst řas je zde redukován používáním tmavých vzorkovacích nádob a ochranné clony u kolektorů srážkových vod. Makrozoobentos je vzorkován v květnu (po jarním tání sněhu), červenci/srpnu (vrcholné léto) a září/říjnu (relativně suché období) s použitím techniky “kick-net sampling” (Rosenberg & Resh, 1993) a síta 500 µm. Nasbíraný materiál je dále prosíván (300 µm) a uchováván v 80% roztoku etanolu. Druhové zastoupení organismů je určováno v laboratoři s použitím binokulárního mikroskopu zvětšení 12-16x. Fytcenologické snímky (relevés 4 x 4 m) byly analyzovány v období vrcholného léta (červenec – srpen) ve 12 bodech transektu A (smýcená část povodí s obnovou lesa) ve vzdálenosti po 100 m a 8 bodech přetrvávajícího dospělého smrkového porostu, Obr. 1.

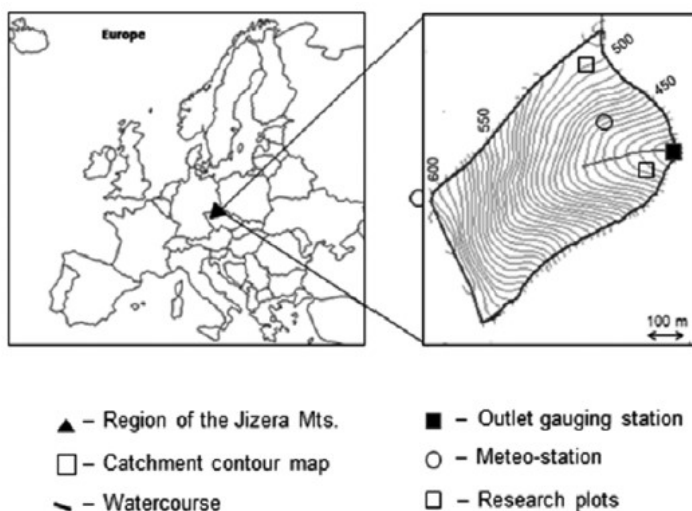
### 2.1.2. Povodí Holubího potoka

Experimentální povodí Holubího potoka (Oldřichov v Hájích, 50°52,45'- 50°52,49'N, 15°6.18' - 15°6.51'E, číslo hydrologického pořadí: 2-04-10-014) reprezentuje oblast Národní přírodní rezervace Jizerskohorské bučiny (součást první zóny Chráněné krajinné oblasti Jizerské hory).

Tab. 7: Morfologie povodí Holubího potoka (Oldřichov).

<b>Plocha</b>	(km <sup>2</sup> )	2.58
<b>Nadmořská výška</b>	(m)	312 - 712

<b>Sklon</b>	(%)	28.11 (0.00-83.60)
<b>Index tvaru povodí index</b>	(-)	0.002
<b>Celková délka vodotečí</b>	(m)	4 979
<b>Intenzita drenážní sítě</b>	(km/km <sup>2</sup> )	1.9
<b>Délka hlavního toku</b>	(m)	2 071
<b>Sklon hlavního toku</b>	(%)	6.50
<b>Strahlerovo pořadí toku</b>	(-)	3



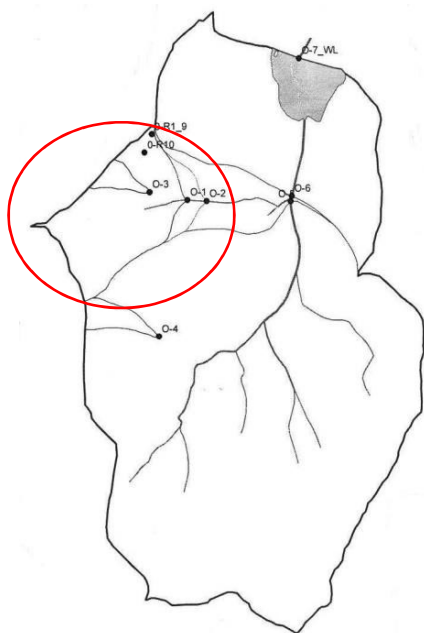
Obr. 2: Experimentální povodí Holubího potoka.

Povodí Holubího potoka se rozkládá v rozsahu nadmořské výšky 312 až 712 m, celková plocha povodí je 2,58 km<sup>2</sup>, průměrný sklon 28 %. Morfologické charakteristiky povodí jsou uvedeny v Tab. 7. Zalesnění je 100 % semi-přirozenými dospělými porosty buku (*Fagus sylvatica*), které nevykazovaly během „imisi kalamity“ v průběhu osmdesátých a devadesátých let 20. století výraznější poškození listového aparátu (Křeček a Hořická, 2006).

Koryto vodního toku je zřetelně vyvinuté s významným stoupáním hladiny při povodních a kamenitým až balvanitým dnem.

V uzávěrovém profilu povodí je instalován měrný objekt s ostrohranným kombinovaným přelivem (Thomson trojúhelníkový přeliv a Poncelet obdelníkový přeliv). Vodní hladina je měřena kombinovaným tlakovým čidlem ALA 4020: v desetiminutovém intervalu jsou automaticky evidovány průtok a teplota vody. Standardní meteorologická observace

(ALA monitorovací systém) je umístěna v nadmořské výšce 498 m a zaznamenává srážkový úhrn, solární radiaci, teplotu a vlhkost vzduchu, rychlost větru, půdní vlhkost každou hodinu. Na povodí jsou vytvořeny 2 experimentální plochy (velikosti 30 x 30 m) v nadmořské výšce 409 a 507 m k pozorování geneze odtoku v mladém a už vzrostlém bukovém lese, viz Obr. 2.



Obr. 3: Širší okolí povodí Holubího potoka (zvýrazněno) s vyznačeným zkoumaným územím O1, O2 a O3.

V zájmovém transektu vodního toku O1, O2, O3, viz Obr. 3, byly indikovány stromy s cílem detekce možného poškození v průběhu povodní. Sledovány byly stromy, které se nacházejí v těsné blízkosti koryta. Sledována byla především viditelná poškození v dolních částech kmene a kořenů, stejně jako různé růstové anomálie, naznačující dřívější poškození. Pro odběr vzorku byly následně vybrány jen ty stromy, u kterých byla zjištěna jizva orientovaná směrem k vodoteči. Stromy, u kterých mohl být původ jizvy způsoben jinou událostí (pád sousedního stromu, lesnická činnost) nebyly do tohoto výběru zahrnuty (Vrtiška a kol., 2016).

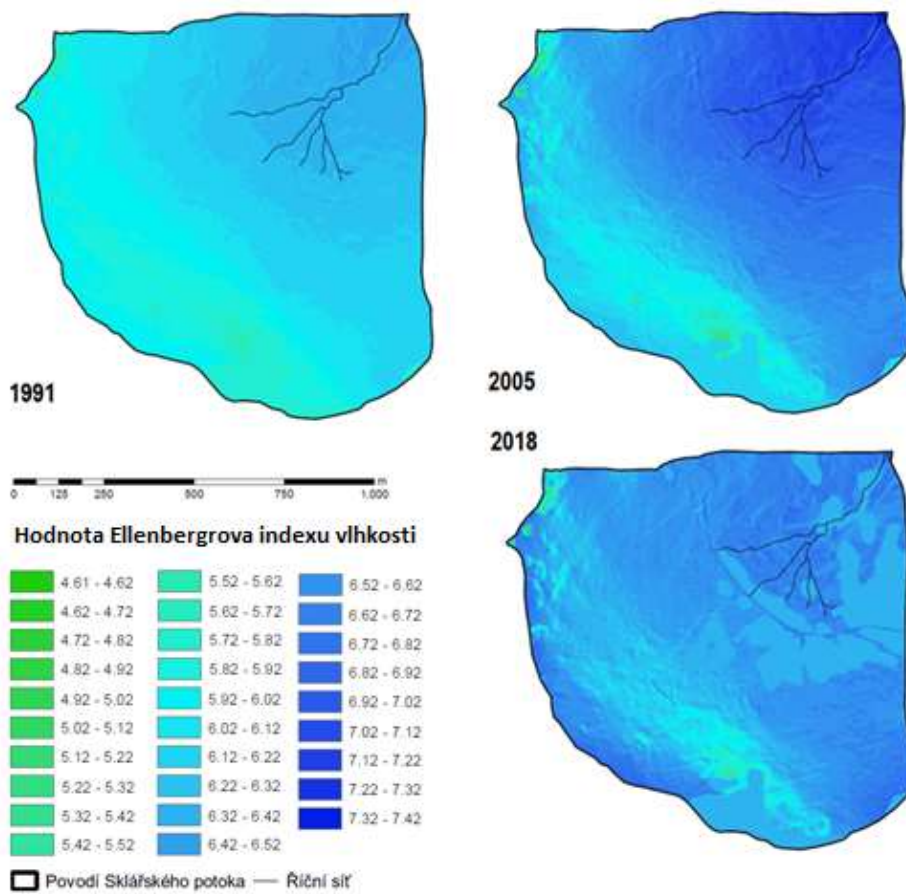
## 3. Výsledky a diskuze

### 3.1. Možnosti indikace stavu povodí a tvorby vodních zdrojů v horském povodí

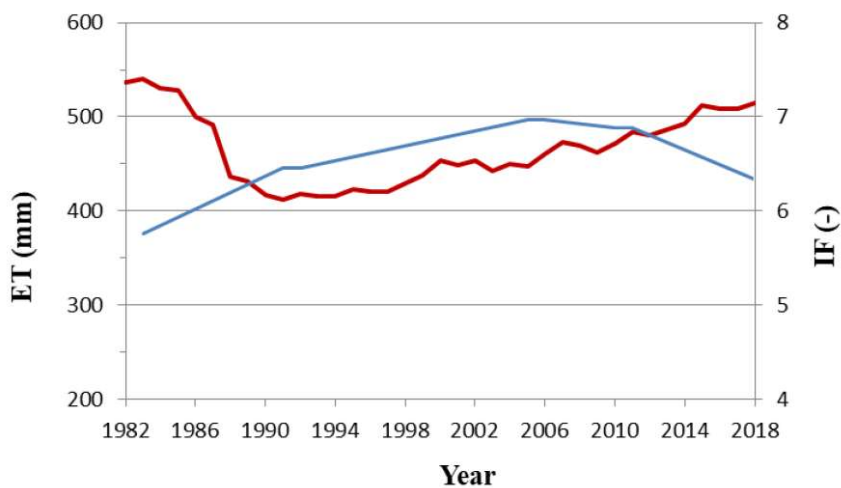
Ellenbergova indikační hodnota pro vlhkost byla použita pro popsání změn povodí Sklářského potoka v Jizerských horách v rozmezí let 1982 – 2018. Oblast Jizerských hor, kde se povodí nachází, byla v 80. létech minulého století silně zasažena kyselou atmosférickou depozicí, což vedlo k poškození smrkového porostu. Po jeho smýcení se hlavní vegetací na povodí stal travní porost (*Junco effusi-Calamagrostietum villosae*).

Pro popsání změn ve vývoji vegetace byl v letech 1991, 2002, 2005 a 2018 proveden na území povodí botanický průzkum. Fytopcenologické snímky o velikosti 4 x 4 m byly určeny na 12 místech transektu A, který charakterizuje smýcenou oblast s hlavním sklonem povodí a dále v 8 bodech transektu B, jenž sousedí s vzrostlým smrkovým porostem. Určená místa na transektu jsou od sebe vzdálená 100 m a v každém snímku byla elektrodou měřena vlhkost půdy v hloubce 15 cm v měsíčním intervalu (v 10 náhodných bodech každého snímku).

Průměrná hodnota Ellenbergovy indikační hodnoty vlhkosti pro povodí Sklářského potoka byla stanovena 6.45 pro rok 1991, 6.97 pro rok 2005 a 6.33 pro rok 2018, Obr. 4. Podle těchto hodnot je možné povodí zařadit jako vlhké. Při porovnání indikačních hodnot s vývojem vegetace a evapotranspirace je možné lépe porozumět vývoji hodnot. Po smýcení poškozeného lesního porostu se stala dominantní vegetací travní společenství, které v roce 1991 zaujímal 62%, v 2005 22% a v roce 2018 zaujímal ještě 13% plochy povodí. Se změnou vegetace se snížila i hodnota evapotranspirace, přičemž nejnižší hodnota evapotranspirace byla v roce 1991. Je patrné, že vývoj indikační hodnoty vlhkosti (maximální hodnota 6.97 byla stanovena v roce 2005) v porovnání s vývojem evapotranspirace je opožděn o zhruba 14 let, viz Obr. 5. Toto zjištění potvrzuje tvrzení, že Ellenbergovy indikační hodnoty indikují zejména dlouhodobé podmínky prostředí (Ter Braak & Gremmen, 1987).



Obr. 4: Ellenbergův index vlhkosti v povodí Sklářského potoka (Jizerka) pro roky 1991, 2005 a 2018.



Obr. 5: Evapotranspirace (červeně) a Ellenbergův index vlhkosti (modrá) v povodí Sklářského potoka v průběhu let 1982-2018.



Blíže je celá problematika popsána v níže přiloženém článku: Bioindication of water resources recharge in a small mountain catchment.

## BIOINDICATION OF WATER RESOURCES RECHARGE IN A SMALL MOUNTAIN CATCHMENT

MSc. Eva Pažourková<sup>1</sup>

Assoc. Prof. Dr. Josef Křeček<sup>1</sup>

Assoc. Prof. Dr. Jana Nováková<sup>2</sup>

<sup>1</sup> Czech Technical University in Prague, Czech Republic

<sup>2</sup> Independent botanist, Prague, Czech Republic

### ABSTRACT

Ellenberg's indicator values (simple ordinal classes of plants with a similar realized ecological niche) were developed to characterize ecological status of the soil-vegetation complex. The indicator of soil moisture (IF) was employed to describe changing environment and water resources recharge in a small forest catchment at the Jizera Mountains (Czech Republic) during the period 1982 – 2018. In the 1980s, the extreme acid atmospheric deposition has led to the decline of spruce plantations (*Picea abies*) particularly in the upper plateau of the Jizera Mountains. After the forest dieback and clear-cut of damaged forests, *Junco effusi-Calamagrostietum villosae* became a new dominant community there. In the investigated catchment of 1.03 km<sup>2</sup>, detailed botanical survey was carried out in vegetation seasons of 1991, 2002, 2005, 2008 and 2018. These data were compared with hydrological parameters: soil water content and evapotranspiration loss. The Ellenberg's indicator of soil moisture IF describes well the plant succession related to microclimate and water balance at clear-cut sites. After the clear-cut (1984-1988), the average IF value has increased from original 5.76 (1982) to 6.45 (1991), reaching maximum 6.97 (2005). With the forest regrowth (reforestation started within one year after the clear-cut), the IF indicator was decreasing back to 6.33 (2018). These data correspond with observed changes in the evapotranspiration loss (and water yield), but, with a lag period of more than ten years.

**Keywords:** Mountain catchment, forestry practices, Ellenberg's indicators, soil moisture, evapotranspiration loss.

### INTRODUCTION

Mountain catchments provide between 40 and 80 % of the water resources available to lowland settlements [1]. In central Europe, mountain regions are predominantly covered by forests; thus, forestry practices are critical for the recharge of water resources there [2]. Unfortunately, hydrological studies in mountain terrains often face problems with the lack of available data and limited density in ground observation networks [3]. For many years, there has been an urgent call for the improvement of climatological inputs (atmospheric precipitation, solar radiation, air temperature, humidity and wind speed) used by catchment hydrological models [4].

Ellenberg [5] summarized environmental characteristics of vascular plants in Central Europe, by assigning to each species indicator values for light regime, soil moisture, nitrogen status, soil reaction, temperature, continentality, and salinity. These indicators have been widely used as indirect metrics of environmental conditions within Europe [6], [7]; and are also considered to identify processes in landscape ecology and catchment hydrology [8], particularly, how can quantitative landscape ecology support predictions in ungauged basins.

The aim of this paper was to assess the effectiveness of the Ellenberg's indicator of soil moisture (IF) to identify changes in the environmental status and water resources recharge at a small forest catchment affected by the acid rain impact, forest dieback, clear-cut harvest and reforestation in the Jizera Mountains (Czech Republic) during the period 1982 – 2018.

#### MATERIAL AND METHODS

The study was performed in the Jizerka experimental catchment (50°48'21" - 50°48'59" N, 15°19'34" - 15°20'48" E, the Elbe river district 1-05-01-004,) operating since 1982. This basin extends in the upper plain of the Jizera Mountains (Northern Bohemia, Czech Republic), Figure 1. This area belongs to the North Temperate Zone; Köppen Dfc - sub-arctic spot, with mean annual precipitation 1,400 mm, and mean air temperature 4 °C, and the average maximum snowpack of 120 cm (the snow cover usually lasts from the beginning of November to the end of April), [9].

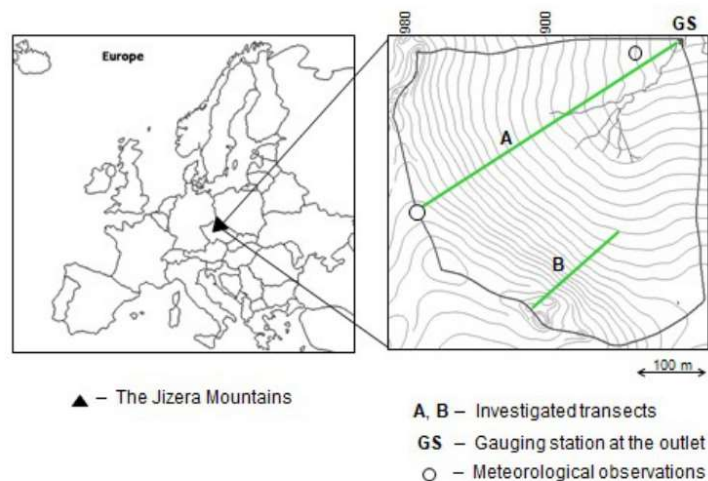


Figure 1. The experimental catchment Jizerka with observation units.

The catchment area is 1.03 km<sup>2</sup>, elevation ranges between 862 and 994 m, and slope between 0.02 and 24.33 %. Low-base-status soils (sandy-loamy Podzols) developed on porphyritic granite reach the depth between 0.5 and 1.2 m. The root system dominates

in the topsoil occurring up to the depth of 15 cm. The topsoil is created by litter (Ol, depth of 0-2 cm), humus layer (Of + Oh, 2-10 cm), and leached horizon (Ah, 10-15 cm). Moor is the most common humus (2-5 cm). In this basin, climax forests include Norway spruce (*Picea abies*) and Common beech (*Fagus sylvatica*), [10], but spruce plantations dominate there since the end of the 18th century. In 1984 – 1988, mature spruce stands (showing ca 30 percent defoliation) were harvested by clear-cutting followed by reforestation with coniferous stands again.

In the 1980s, the Jizera Mountains region was affected by the extreme acid atmospheric deposition, and defoliation and die-back of mature spruce forests (*Picea abies*). After the clear-cut (1984 – 1988), grass dominated *Junco effusi-Calamagrostietum villosae* became a new dominant community there [7]. The reforestation was complicated by the relatively high level of air pollutants (SO<sub>2</sub> and NO<sub>x</sub>), and extreme climate conditions at clear-cut sites.

Detailed botanical investigations were carried out at two parallel transects (A and B) in vegetation seasons of 1991, 2002, 2005, 2008 and 2018. Phytosociological relevés (4 x 4 m) were taken at each of the twelve-point transect A (clear-cut, main slope of the Jizerka basin), and at the eight-point transect B (neighbouring fragments of mature spruce stands); the focused points at both transects are located in step of 100 m. The additional supporting information included both ground and space forest inventory. The standard parameters (tree species, age, basal area, tree height, timber volume, horizontal canopy density, vitality of trees) were estimated on plots 20 x 20 m; and the supervised classification of multiband raster images (Landsat 4,5) was used to classify the images by the image analyst [11]. At each spot of the investigated transects A and B, near surface soil moisture (volumetric water content up to the depth of 15 cm) was measured in situ by a sensitive electrode in monthly intervals (observed at 10 random points at each spot). The catchment outlet (Figure 1) is equipped by the sharp-crested V-notch weir with the automatic water pressure recorder ALA 4020, meteorological observations were made along transect A (established for hypsometric studies) at 875 and 975m elevation.

## THEORY

In a hydrological year (1st November – 31st October), the annual water budget of the investigated catchment can be considered by the equation (1):

$$ET = P - R \quad (1)$$

Where, ET – evapotranspiration loss, P – aerial precipitation calculated from readings of 4 rain-gauges by inverse distance weighting [3], R – run-off observed at the catchment outlet.

Daily fluctuations in water content at the topsoil were approximated by the antecedent precipitation index API [12], (2):

$$API_t = P_t + K_t API_{t-1} \quad (2)$$

Where, API<sub>t</sub> – antecedent precipitation index on the day 't' (mm), API<sub>t-1</sub> – antecedent precipitation index on the day 't-1' (mm), P<sub>t</sub> – precipitation on the day 't' (mm), and K<sub>t</sub> – recession constant given by the equation (3), [13].

$$K_t = \text{EXP}(-\text{PET}_t/\text{AWC}_t) \quad (3)$$

Where,  $\text{PET}_t$  – the Penman evaporation potential of the day ‘t’ (mm), calculated from the observed meteorological data [12], and  $\text{AWC}_t$  – soil water content available to vegetation at the day ‘t’ (mm) according to the equation (4).

$$\text{AWC}_t = \text{SWC}_t - \text{PWP} \quad (4)$$

Where,  $\text{SWC}_t$  – the soil water content at the day ‘t’ (mm), and PWP – the water content adequate to the permanent wilting point (mm).

For each botanical relevè, the Ellenberg’s indicator values of soil moisture (IF) were calculated as the weighted average of all recognized species [5]. To include the impact of all species abundance, the data were transformed from the Braun-Blanquet’s scale to a nine-point scale according to the approach of Van der Maarel [14], Table 1.

Table 1. Classification of species abundance.

Braun-Blanquet’s scale	r	+	1	2	3	4	5
van der Maarel’s transformation	1	2	3	5	7	8	9

## RESULTS

After the harvest of mature spruce stands (1984-1988), the regrowth of the Jizerka catchment is documented in Figure 2. After the harvest of mature spruce forests (1984-1988), the percentage of grass dominating areas was affected by relatively slow

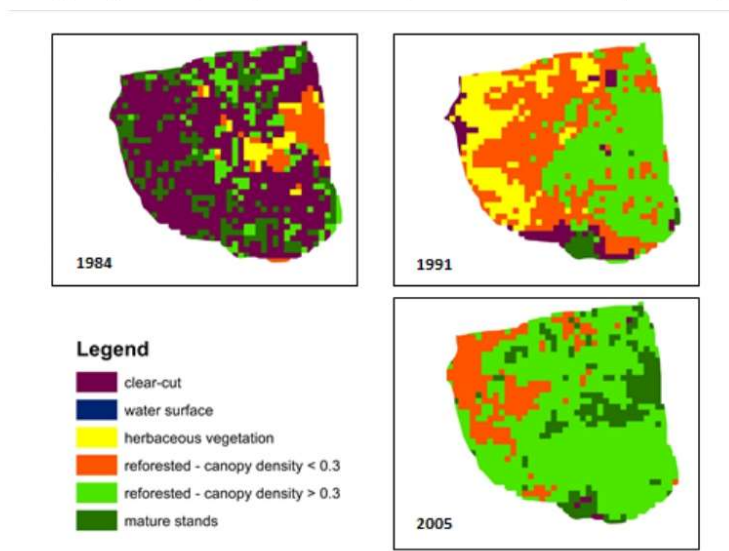


Figure 2. Vegetation canopy at Jizerka in 1984, 1991 and 2005.

regrowth of trees, reaching still 62% in 1991, 22% in 2005, and 13% in 2018. Corresponding values of Ellenberg’s soil moisture indicator IF are shown in Figure 3. In these consecutive years; average IF values within the basin are 6.45, 6.97 and 6.33.

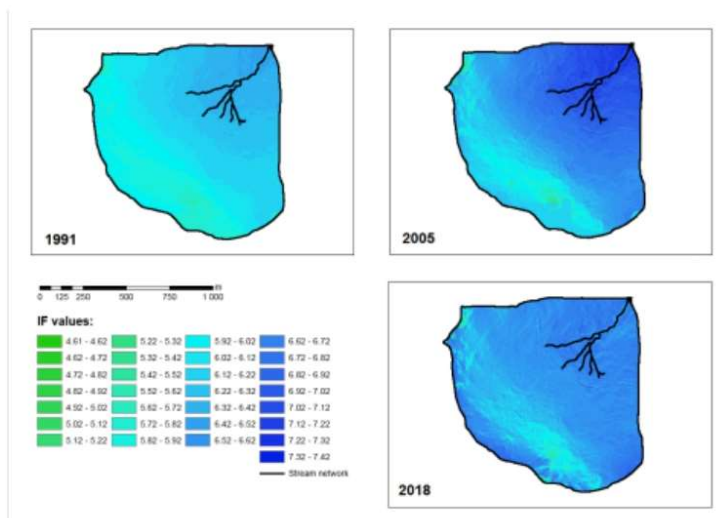


Figure 3. Ellenberg’s soil moisture indicator IF at Jizerka in 1991, 2005 and 2018.

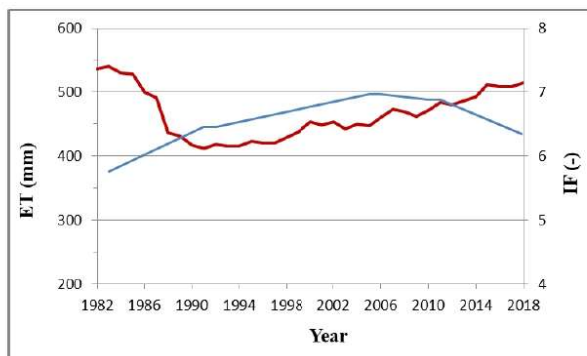


Figure 4. Evapotranspiration loss ET (red) and Ellenberg’s soil moisture indicator IF (blue) in the Jizerka catchment, 1982 – 2018.

After the clear-cut; evapotranspiration loss has been reduced by the lack of trees (tall vegetation), indicated by higher IF values with the delay of 14 years (water yield culminated in 1991 while IF indices in 2005), Figure 4. Consequently, in the vegetation period, daily values of the antecedent precipitation index API increased by 11 – 13 mm at the harvested area (transect A) against the mature stand (transect B), Figure 5.

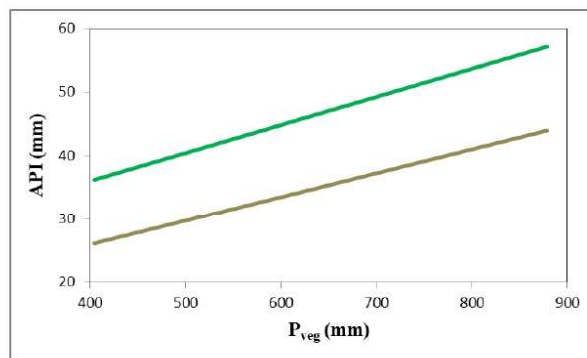


Figure 5. Mean daily API values (grass – green, forest – brown) related to precipitation sums  $P_{veg}$  in summer seasons.

## DISCUSSION AND CONCLUSIONS

In the Jizerka catchment, herbaceous vegetation has developed in mature spruce stands with the defoliation of trees initiated by the ‘acid rain’ impact during the 1980s. After the forest clear-cut; *Calamagrostis* sp. (namely, *C. villosa*) have spread widely with rising soil moisture and light income. Increases in soil moisture corresponded with the drop in evapotranspiration by the removal of trees, [2]. In the mountain landscape, significant correlations between the Ellenberg’s indices for soil moisture (IF) and light (L), and geomorphologic parameters, particularly, the elevation (increasing precipitation incomes and decreasing air temperatures) and the canopy density were already reported by [7]. This study also confirmed the high indication potential of the Ellenberg’s soil moisture indicator in mountain regions.

After the harvest of mature spruce stands (1984-1988), catchment spots with dominating herbaceous cover reached 62% in 1991, 22% in 2005, and 13% in 2018. This situation corresponds to the relatively slow reforestation in rather hard climate and environmental conditions [7], [9], [10]. In the consecutive years; average catchment values of the Ellenberg’s indicator IF were 6.45, 6.97 and 6.33. There is an evident delay between the canopy development and its indication by the Ellenberg’s soil moisture values. Thus, the maximum water yield (by the drop in evapotranspiration) is detected there with the delay of 14 years. This fact confirms the statement that the Ellenberg’s IF values indicate, namely, the long-term environmental conditions, [15].

In the vegetation period, the Ellenberg's soil moisture values indicate also changes in the daily antecedent precipitation index API (related to the soil moisture content): increasing values by 11 – 13 mm on the harvested sites with herbaceous canopy in comparison with the remaining mature spruce stand. These rising API values indicate lower retention capacity of the catchment by a response to rainfall events.

We did not confirm a significant direct correlation between the Ellenberg's soil moisture indicator and annual parameters of the water budget (water yield, evapotranspiration loss) reported by [16]. However, the recognized processes and trends in Ellenberg's IF values follow well the changes in water yield (found by the drop in evaporation loss). Therefore, the Ellenberg's soil moisture indices provide us with valuable information on changing environmental conditions upon the required water resources control, [17].

#### ACKNOWLEDGEMENTS

This research was supported by the Earthwatch Institute (Oxford, UK, Mountain Waters of Bohemia, 1991-2012), Ministry of Education of the Czech Republic (INTER-EXCELLENCE: INTER-COST LTC 17006, 2017-2020) and Czech Technical University in Prague (SGS 18/120/OHK1/2T/11, 2018–2019).

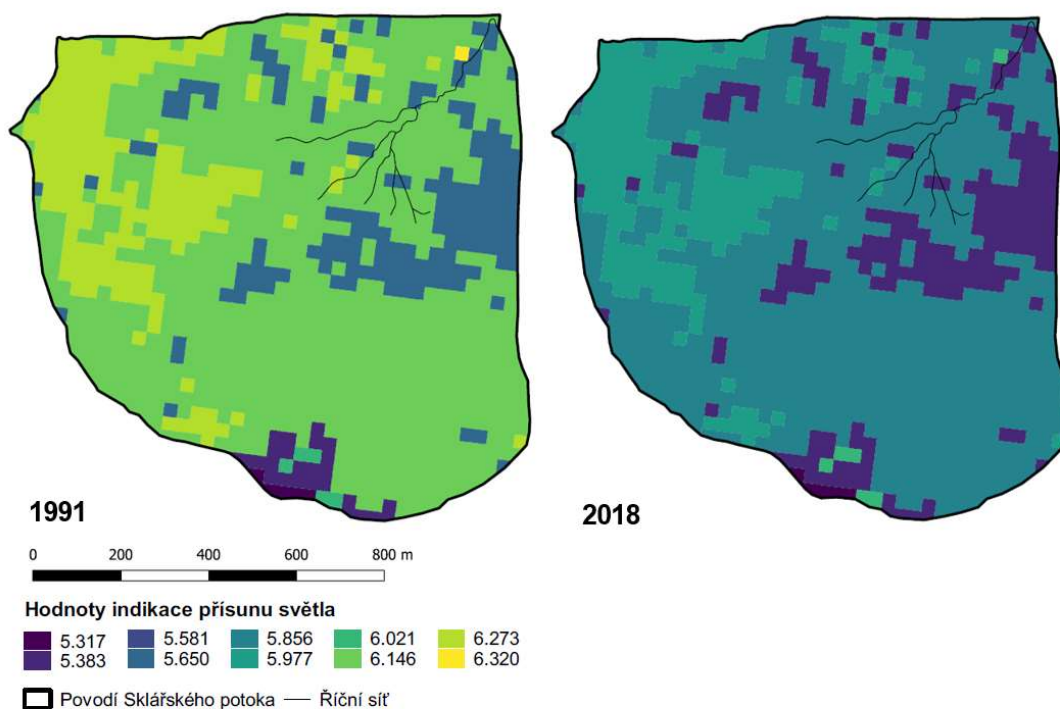
#### REFERENCES

- [1] Viviroli, D., Dürr, H.H., Messerli, B., Meybeck, M., Weingartner, R., Mountains of the world, water towers for humanity: typology, mapping, and global significance. *Water Resources Research*, vol. 43, W07447, 2007.
- [2] FAO, Forests and water. Forestry paper 155, Food and Agriculture Organization of the United Nations, Italy, 2008, pp 78.
- [3] Křeček, J., Punčochář, P., Design of climate station network in mountain catchments. *Hungarian Geographical Bulletin*, vol. 64, pp 19-29, 2012.
- [4] Foy, C., Arabi, M., Yen, H., Asce, A.M., Gironas, J., Bailey, R.T., Multisite assessment of hydrologic processes in snow-dominated mountainous river basins in Colorado using a watershed model. *Journal of Hydrologic Engineering*, vol. 20/10, 04015017, 2015.
- [5] Ellenberg, H., Weber, H.E., Dull, R., Wirth, V., Werner, W., Paulissen, D., Zeigerwerte von Pflanzen in Mitteleuropa. *Scripta Geobotanica*, vol. 18, pp 1-258, 1992.
- [6] Diekmann, M., Use and improvement of Ellenberg's indicator values in deciduous forests of the Boreo-nemoral zone in Sweden. *Ecography*, vol. 18, pp 178–189, 1995.
- [7] Křeček, J., Nováková, J., Hořická, Z., Ellenberg's indicator in water resources control: the Jizera Mountains, Czech Republic. *Ecological Engineering*, vol. 36, pp 1112-1117, 2010.
- [8] Schröder, B., Pattern, process, and function in landscape ecology and catchment hydrology – how can quantitative landscape ecology support predictions in ungauged basins? *Hydrology and Earth System Sciences*, vol. 10, pp 967–979, 2006.



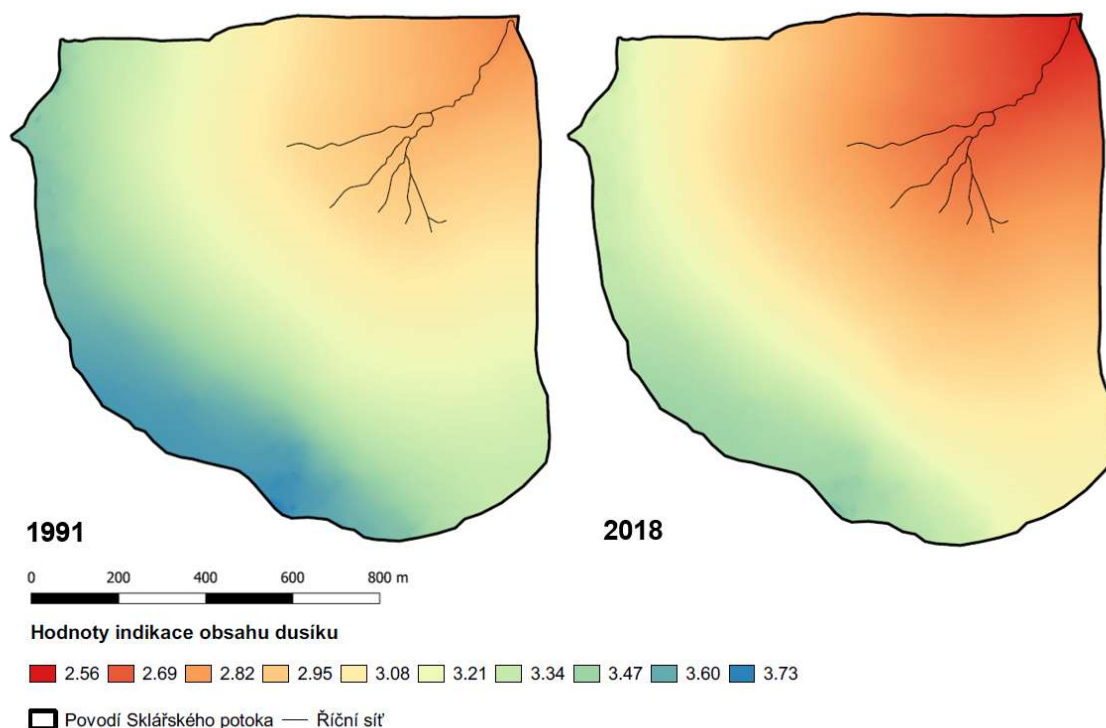
- [9] Tolasz, R. Climate atlas of Czechia. Czech Hydrometeorological Institute, Prague, pp 256, 2007.
- [10] Zlatník, A., Forest phytocenology (In Czech). SZN Prague, 1976, 495 pp.
- [11] Nagi, R., Using the Landsat image services to study land cover change over time. Imagery and Remote Sensing, ArcGIS online, ESRI, 2011, <http://esri.com/esri/arcgis>, accessed on the 24<sup>th</sup> October 2019.
- [12] Shaw, E.M., Hydrology in Practice. Second edition, Chapman and Hall, London, 1991, 539 pp.
- [13] Choudhury, B.J., Passive microwave remote sensing contribution to hydrological variables. Surveys in Geophysics, vol. 12, pp 63-84, 1991.
- [14] Van der Maarel, E., Transformation of cover-abundance values in phytosociology and its effect on community similarity. Vegetatio, vol. 39, pp 97-114, 1979.
- [15] Ter Braak, C.J.F., Gremmen, N.J.M., Ecological amplitudes of plant species and the internal consistency of Ellenberg's indicator values for moisture. Vegetatio, vol. 69, pp 79-87, 1987.
- [16] Ertsen, A.C.D., Alkemade, J.R.M., Wassen, M.J., Calibrating Ellenberg indicator values for moisture, acidity, nutrient availability and salinity in the Netherlands. Plant Ecology, vol. 135, pp 113–124. 1998.
- [17] Gleick, P.H., Water in crisis: path to sustainable water use. Ecological Applications, vol. 8, pp 571–579, 1997.

Pro popsání stavu povodí byly z botanického průzkumu stanoveny i Ellenbergova indikační hodnota přísunu světla a obsahu dusíku pro roky 1991 a 2018.



Obr. 6: Ellenbergův index přísunu světla v povodí Sklářského potoka (Jizerka) pro roky 1991 a 2018.

Pro rok 1991 byla zjištěná průměrná hodnota Ellenbergovy indikace přísunu světla za celé povodí 6.08, minimální hodnota na povodí byla 5.32 a maximální 6.32. Pro rok 2018 byla průměrná hodnota za povodí 5.80, minimální 5.32 a maximální 6.02, viz Obr. 6. Minimální hodnota se nezměnila pro pozorovaná období a byla pozorována v oblasti dospělého lesního porostu, který nebyl smýcen. Kdežto u maximální je zřejmý posun z 6.32 pro rok 1991 na 6.02 pro rok 2018, tento posun je způsobený vývojem vegetace z pouze bylinné (po smýcení lesa) na obnovující se lesní porost. Podle indikační hodnoty lze zařadit vegetaci jako rostliny polostínu, přičemž vyšší hodnota značí více světlomilné rostliny. Na průměrných hodnotách z povodí lze tedy pozorovat vývoj z rostlin vyskytujících se více na světle k rostlinám spíše ve stínu, což indikuje obnovující se les.



Obr. 7: Ellenbergův index obsahu dusíku v povodí Sklářského potoka (Jizerka) pro roky 1991 a 2018.

Průměrná hodnota Ellenbergova indexu obsahu dusíku za rok 1991 byla 3.24, minimální 2.78 a maximální 3.73, pro rok 2018 se průměrná hodnota snížila na 3.04, minimální na 2.58 a maximální na 3.53, viz Obr. 7. Podle indikačních hodnot obsahu dusíku lze prostředí zařadit jako více či méně neplodné. Posun hodnot v průběhu let lze vysvětlit změnou vegetace, kdy vzrůstající stromy mohly část dusíku odčerpat. Křeček et al. (2010) uvádějí obdobná zjištění, že Ellenbergovy indikátory vlhkosti a přísunu světla velmi dobře popisují sukcesi rostlin v souvislosti s mikroklimatem a hydrologií na odlesněných lokalitách, u Ellenbergova indikátoru obsahu dusíku zjistili, že sleduje trend atmosférické depozice, ale s nižší citlivostí.

### 3.2. Indikace kvality vody v lesním povodí ovlivněném kyselou atmosférickou depozicí a těžbou dřeva

Šetření výskytu bentických organismů bylo provedeno v letech 1994 a 2004-2005 v blízkosti uzávěrového profilu v období května (po jarním tání), na přelomu července a srpna (vrchol

léta) a v období září/října (charakterizující suché podzimní období). Pro vzorkování organismů byla použita metoda kick-net (Rosenberg and Resh 1993).

Z šetření vyplývá, že oproti roku 1994 se výskyt makrozoobentosu v roce 2005 zvýšil z 36 jedinců na 68. V roce 1994 byl počet taxonomických druhů 7 s nejvyšší abundancí u taxy *Plecoptera* (12 jedinců) následovanou *Diptera excl. Chironomidae* (11 jedinců). V roce 2005 bylo pozorováno 10 taxonomických druhů s nejvyšším zastoupením u *Plecoptera* (20 jedinců) a druhou v pořadí *Trichoptera* (17 jedinců). Z nárustu počtu tříd i jedinců lze usuzovat zlepšení kvality prostředí a tento vývoj dokládá i provedený výzkum chemismu povrchové vody.

V osmdesátých letech minulého století bylo v blízkosti uzávěrového profilu naměřena průměrná roční hodnota pH 4.0 (1982-1985), která značí silně acidifikované prostředí (pH < 4.2, Veselý a Majer 1996), což je v souladu s pozorovaným výskytem bentických organismů. Také Hall, Likens & Hendrey (1980) pozorovaly obdobný stav, kdy v povodí Hubbard Brook v sedmdesátých letech minulého století experimentálně okyselovali průtok, po snížení pH v toku na hodnotu 4, byla významně snižena biodiverzita a to již po prvním týdnu pozorování. V devadesátých letech minulého století se při šetření na povodí průměrná roční hodnota pH zvýšila na 5.3 (1990-1994), což umožnilo dlouhodobý vývoj přirozené revitalizace toku. Tento fakt dokládá i provedený průzkum bentických organismů v roce 2005, kdy počet jedinců a zastoupených tříd odpovídá spíše středně acidifikovanému prostředí (pH = 5.0-6.3, Horecký et al. 2013), navíc se objevili i druhy citlivé na kyselé prostředí (*Crustacea*, *Ephemeroptera*). Zlepšení chemismu vody (zvýšení pH) bylo pozorováno již zhruba po 5 letech, v důsledku kombinace snižování emisí SO<sub>2</sub> a redukcí smrkových lesních porostů na rozsáhlém území. Ovšem obnovení vodního společenstva lze pozorovat až s delším časovým odstupem.

Vodní organismy jsou i nadále stresovány dočasným snížením pH při epizodické acidifikaci (jarní tání sněhové pokrývky), kdy hodnoty pH klesají pod 5.3, pod touto hodnotou navíc začne docházet k mobilizaci toxických forem hliníku (Bache 1985; Veselý a Majer 1996).

Hodnota pH se v podmínkách lokalit zatížených atmosférickou depozicí jeví jako velice vhodná pro separaci přímého odtoku. Vykazuje nejvyšší hodnotu závislosti s velikostí

průtoku. Koeficient korelace (R) mezi průtokem a pH je 0.91, konduktivitou 0.78, Ca -0.24, Mg -0.19, Na -0.21, SO<sub>4</sub> 0.35 a NO<sub>3</sub> -0.29 (kritická hodnota R<sub>k</sub> je 0.361 při n = 50 a α = 0.01).

Více je celá problematika popsána v níže přiloženém článku: Water-quality genesis in a mountain catchment affected by acidification and forestry practices.

# Water-quality genesis in a mountain catchment affected by acidification and forestry practices

Josef Křeček<sup>1,3</sup>, Ladislav Palán<sup>1,4</sup>, Eva Pažourková<sup>1,5</sup>, and Evžen Stuchlík<sup>2,6</sup>

<sup>1</sup>Department of Hydrology, Czech Technical University in Prague, Thákurova 7, CZ-166 29 Prague

<sup>2</sup>Institute of Hydrobiology, Biology Centre CAS, Na Sádkách 7, CZ-37005 České Budějovice

**Abstract:** Effects of changes in air pollution and forest cover on the acid atmospheric deposition and runoff were studied in the Jizerka experimental catchment (Czech Republic), a sensitive mountain environment of low buffering capacity. From 1982 to 2015, resident scientists and volunteers measured water quality of precipitation, fog, and stream samples at the watershed level. Archived LANDSAT imagery was used to reconstruct changes in forest composition in the watershed based on a detailed ground inventory done in 2010 to 2012. Spatial interpolation was used to approximate atmospheric deposition of water and  $\text{SO}_4^{2-}$ ,  $\text{NO}_3^-$ , and  $\text{NH}_4^+$  over the watershed area. The open-field load of S peaked in 1987 to 1988 and dropped substantially in the 1990s, but inorganic N did not show a significant trend. The N : S deposition ratio increased from 0.37 to 2.83. Mean annual stream-water pH increased from 4.2 to 5.9, and concentrations of  $\text{SO}_4^{2-}$  and  $\text{NO}_3^-$  decreased by 55 and 53%, respectively. Seasonal acidification of stream water was observed during snowmelt (March, April) and episodic summer rainstorms. The relatively rapid response of stream-water quality to reduced deposition corresponded with subsurface runoff generated in a shallow podzolic soil. Relatively high leaching of  $\text{NO}_3^-$  in the 1980s followed limited N uptake in damaged spruce stands and clear-cut areas. Recovery of stream-water chemistry followed the drop in the acid atmospheric deposition by ~5 y, and stream biota revived after 10 to 15 y. Removal of spruce forest and reduced air pollution caused faster recovery from acidification than expected from pure air-quality improvement. Reduced atmospheric deposition and fog-drip interactions caused by lower canopy area suggest that modified forestry practices can affect deposition rates and stream-water quality. Deciduous or mixed forests could decrease the acidic atmospheric load by reducing leaf area and surface roughness.

**Key words:** mountain catchment, acid atmospheric deposition, forestry practices, runoff genesis, citizen science

Mountainous parts of many river basins provide 40 to 80% of the water that is available to lowland users (Messerli et al. 2004). The importance of mountain catchments as water resources will increase with population pressure (UNEP 2007, Viviroli et al. 2007) and effects of expected climate change (Christensen 2005). Leopold (2006) emphasized the role of headwater mountain streams in river system development, and Körner and Ohsawa (2005) considered the recharge of water resources as the most important environmental benefit of mountain regions. Mountain watersheds in central Europe are mostly forested, and their sustainable environmental benefits are guaranteed by forestry practices (FAO 2008).

Biswas et al. (2014) suggested that water-quality deterioration at the global scale is attributable mainly to poor

management of water resources. The European Commission (2012) recommended application of a multidisciplinary approach to watershed management and revision of stream water-quality regulations. In populated regions, the quality of natural fresh waters is degraded mostly by point-source pollution, whereas distant mountain catchments are particularly affected by large-scale air pollution (emissions of  $\text{SO}_2$ ,  $\text{NO}_x$ ,  $\text{NH}_4^+$ ) and atmospheric acid deposition (Reuss and Johnson 1986, Baldigo and Lawrence 2001, Schöpp et al. 2003, Kopáček et al. 2016).

Anthropogenic emissions of acidic precursors have been increasing since the industrial revolution and peaked in the late 1980s. International cooperation to reduce atmospheric emissions (the 1985 Helsinki Protocol on the Reduction of Sulphur Emissions or their Transboundary Fluxes by  $\geq 30\%$ )

E-mail addresses: <sup>3</sup>josef.krecek@fsv.cvut.cz; <sup>4</sup>ladislav.palan@fsv.cvut.cz; <sup>5</sup>eva.pazourkova@fsv.cvut.cz; <sup>6</sup>evzen.stuchlik@yandex.com

DOI: 10.1086/698533. Received 14 June 2017; Accepted 28 February 2018; Published online 18 June 2018.  
Freshwater Science. 2019. 38(2):257–269. © 2018 by The Society for Freshwater Science.

257

has led to signs of recovery in acidified European headwater regions (Křeček and Hořícká 2001, Holen et al. 2013). Falkenmark and Allard (2015) called for a detailed analysis of natural waters from a dynamic perspective, but too many studies in headwater catchments have investigated only base-flow conditions. Thus, studies are needed of water movement through the surface and subsurface environments combined with chemical reactions taking place along their pathways (Bolstad and Swank 1997, Takagi 2015).

Lumb et al. (2011) reviewed methods of indexing with a numerical value based on physical, chemical, and biological indicators, including especially pH and  $\text{NO}_x$  loading. For larger-scale investigations, Rapport et al. (1998) emphasized the important role of citizens in monitoring indicators to assess water quality, and the USEPA (1997) developed detailed methods of volunteer water monitoring. Since the 1970s, several nonprofit organizations have been founded to promote participation of lay volunteers in environmentally sound field research (Hand 2010). Irwin (1995) and Silvertown (2009) see involvement of volunteers in collecting and processing the field data as an important part of scientific inquiry and environmental education.

Czech Republic was graded above average relative to 147 countries based on the Water Poverty Index (Lawrence et al. 2002). However, the Czech Republic received lower values for environmental indicators associated with the risk of water pollution. In the headwaters of the Jizera

Mountains (northern Bohemia, Czech Republic), water acidification began to be visible in the 1950s and peaked in the mid-1980s (Křeček and Hořícká 2006). Its consequences were a large-scale (40–80%) die-back of spruce stands and their subsequent removal particularly in headwater catchments, a decrease in water pH, and degradation of life in streams and water reservoirs (Stuchlik et al. 1997). The number of species in planktonic and benthic communities was significantly reduced, and fish became extinct in the late 1950s.

Our objective was to analyze long-term (1982–2015) changes in water quality in the Jizerka experimental catchment and link these data to changes in atmospheric acid deposition and forest cover. We hypothesized that on a catchment scale, the acid atmospheric load and streamwater quality in mountain regions could be ameliorated by forestry practices.

## METHODS

### Study site

The study was performed in the upper plain of the Jizera Mountains (Fig. 1). In the 1980s, this area was strongly affected by acidic atmospheric deposition and die-back of spruce plantations (*Picea abies*). After the clear-cut of damaged spruce stands, grass-dominated *Juncus effusus*–*Calamagrostietum villosae* became a new dominant commu-

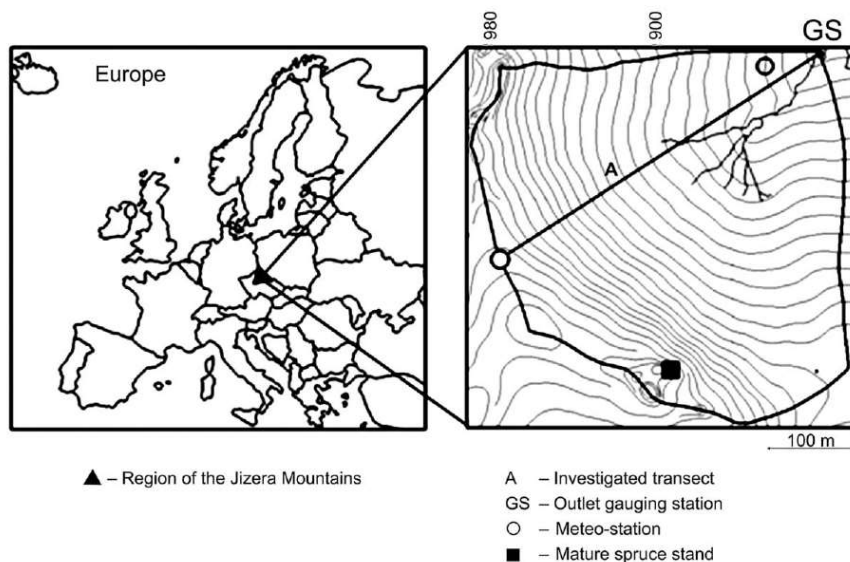


Figure 1. The Jizerka experimental basin in Europe.

nity (Křeček et al. 2010). The Jizerka experimental catchment (lat 50°48'21"–50°48'59"N, long 15°19'34"–15°20'48"E, Elbe river district 1-05-01-004; Table 1) has operated since 1981. Characteristics of the recent climate (1961–1990) are: north temperate zone, Köppen Dfc subarctic region, mean annual precipitation = 1400 mm, air temperature = 4°C, average maximum snowpack = 120 cm (snow cover usually lasts from the beginning of November to the end of April; Tolasz 2007). Here, low-base-status soils (sandy-loamy podzols) between 0.5- and 1.2-m depth have developed above porphyritic granite bedrock. Topsoils are dominated by grass root systems to depths of 15 cm. The topsoil is composed of litter ( $O_l$ , depth = 0–2 cm), humus layer ( $O_f + O_h$  = 2–10 cm), and leached horizon ( $A_h$  = 10–15 cm). Mor is the most common humus (2–5 cm). The area is characterized by rapid subsurface runoff where the ground is restricted to shallow, weathered rock formations. In this basin, climax forests include Norway spruce (*Picea abies*) and common beech (*Fagus sylvatica*), but, since the end of the 18<sup>th</sup> century, spruce plantations have dominated the landscape. In 1984–1988, mature spruce stands (showing ~30% defoliation) were harvested by clear-cutting followed by reforestation with coniferous stands.

#### Instrumented catchment

The experimental basin (Fig. 1) was instrumented in 1982. The outlet is equipped with a sharp-crested v-notch weir with an automatic water pressure and temperature recorder ALA 4020 (ALA, Bučovice, Czech Republic) logging every 10 min. In situ monitoring of stream waters, including temperature, pH, and conductivity, was done with the field multimeter WTW-350i (WTW, Weilheim, Germany). Meteorological observations were made along transect A (established for hypsometric studies) at 875 and 975 m asl. Two Czech Hydrometeorological Institute climate stations (Košenov-Jizerka and Desná-Souš, elevation = 772 and 850 m asl) are ~2500 and 300 m from the catchment boundary.

Table 1. Geomorphology of the Jizerka catchment.

Variable	Value (range)
Area (km <sup>2</sup> )	1.03
Elevation (m)	927 (862–994)
Slope (%)	7.52 (0.02–24.33)
Shape index	0.69
Length of streams (m)	1490
Drainage density (km/km <sup>2</sup> )	1.45
Length of the main stream (m)	657
Slope of the main stream (%)	5.98
Strahler stream order	2

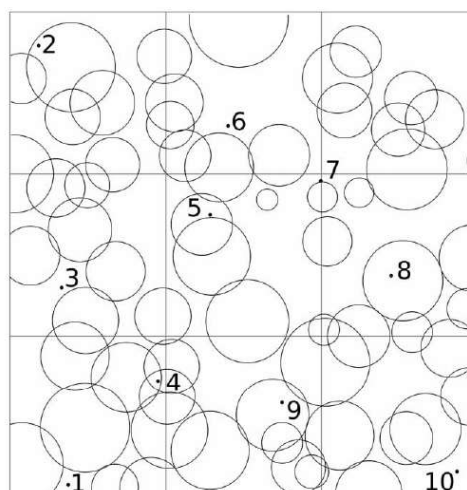


Figure 2. Locations of rainfall collectors (1–10) and the horizontal canopy projection of the mature spruce stand.

Along the vertical transect A (harvested in 1984), an additional 3 modified Hellmann rain gauges (area = 200 cm<sup>2</sup>, plastic collectors with a shield against bird contamination, 1-L sampling bottles) were placed at elevations of 862, 899, and 975 m asl in 1991. In the mature spruce stand (plot area = 30 × 30 m, elevation = 975 m), through-fall under the canopy (Fig. 2) was sampled with 10 rainfall storage gauges (200 cm<sup>2</sup>), and stemflow was collected at 2 average trees. This method of through-fall observation is recommended as the most appropriate approach to identify fog and cloud water deposition (Lovett 1988). Sets of modified storage gauges (200 cm<sup>2</sup>) were installed in the soil to collect through-fall under the ground vegetation in 2 harvested (and reforested) sites at elevations of 862 and 975 m asl. To identify the evidence of fog drip, 12 passive fog collectors were installed along transect A (862–994 m). At each collector, the fog drip was generated by 400 m of Teflon line (diameter = 0.25 mm, surface area index [SAI] = 5) exposed at the height of 1.7 m above the ground. Sample bottles were protected against direct rainfall access by a wide-brimmed cover that overlapped the fog collector at an angle of 34°.

#### Water and biota sampling, analytical methods

Stream waters at the catchment outlet were sampled weekly with more frequent sampling during flood events, and deposited rain/fog drip was sampled monthly with more frequent sampling (weekly or after individual rain events) during the field expeditions. Samples (rain/fog drip, through-fall, stemflow, stream water) were filtered through



40- $\mu\text{m}$  inert mesh, stored in the refrigerator, and analyzed in the laboratory at the Hydrobiological Station Velký Pálenec (Charles University, Prague). Concentrations of all ions were determined by ion chromatography with conductometric detection; pH was measured with radiometer combination electrodes, and conductivity determined by radiometer conductometric sensor (Stuchlík et al. 2006).

The chemical composition (especially N) of the rain/fog drip samples can be altered by bacterial activity at the time of collection. However, in our study area, bacterial activity is greatly reduced by a combination of the relatively cold mountain climate (subarctic region), relatively high concentrations of N, and low values of pH and dissolved organic C (Cape et al. 2001). The potential growth of algae was reduced by the dark sampling bottles and shelters.

Benthic macroinvertebrates were sampled near the outlet of the Jizerka catchment (a low-gradient stream channel with only sand and gravel substrate types, depth < 0.5 m) in May (after snowmelt), July/August (high summer), and in September/October (a relatively dry period). In 2004–2005, this sampling was done in the framework of a Czech regional campaign (Horecký et al. 2013). A kick-net sampling technique was used (Rosenberg and Resh 1993). The invertebrates were collected with a hand-net (mesh size = 500  $\mu\text{m}$ ) then sieved through a 300- $\mu\text{m}$  net and preserved with an 80% ethanol solution. Accurate counts of each taxon were undertaken in the laboratory (by eye and under a binocular microscope at 12–16  $\times$  magnification) by trained professional staff.

#### Catchment inventory

The archive of LANDSAT imagery (NASA 2014) was used to detect development of the vegetative cover (1984, 1992, and 2010). This imagery has a resolution of 30 m. Only data from clear-sky summer seasons (June–August) were used. The normalized difference vegetation index (NDVI) was calculated for the spectral reflectance registered in the visible (red) and near-infrared bands according to Weier and Herring (2000):

$$\text{NDVI} = (\text{NIR} - \text{VIS}) / (\text{NIR} + \text{VIS}), \quad (\text{Eq. 1})$$

where NIR is near-infrared radiation (0.7–1.1  $\mu\text{m}$ ), and VIS is visible radiation (0.4–0.7  $\mu\text{m}$ ).

Supervised classifications of multiband raster images (Landsat 4 and 5) were used simultaneously, and images representing distinct sampling areas of the different canopies were classified with the image analyst tool in ArcGIS (version 10.2; Environmental Systems Research Institute, Redlands, California; Nagi 2011).

Since 1991, detailed forest inventories have been conducted during field surveys of 12 (20  $\times$  20-m) fixed quadrats situated at 100-m incremental altitudinal steps along transect A. Basic forestry variables (tree species, age, basal

area, tree height, timber volume, and horizontal canopy density) were evaluated by standard techniques (Watts and Tolland 2005). Complementary detailed botanical investigations included phytosociological relevés (4  $\times$  4 m) and seasonal development of herbaceous canopy (height, canopy area). The assimilating area of grass was measured with a portable leaf area meter LI-3100C (LI-COR, Lincoln, Nebraska). In 2012, the leaf area of spruce stands was estimated by direct ground-based measurements (Breda 2003). The definition of leaf area index (LAI) was interpreted as  $\frac{1}{2}$ (total green leaf/needle area per unit surface area), as recommended by Chen and Black (1992).

Five canopy classes were identified from the multiband raster images in the years 1983, 1985, 1992, 2002, and 2010. These 5 classes were: 1) mature spruce forests, 2) stands with crown closure >0.3, 3) reforested plots with crown closure < 0.3, 4) areas covered by herbaceous communities only, and 5) clear-cut (Křeček and Krčmář 2015). These classes correspond with definitions of forest used by the United Nations Framework Convention on Climate Change (crown closure > 0.3, height >2–5 m at maturity; Sasaki and Putz 2009).

#### Atmospheric deposition and runoff genesis

According to the findings of Krečmer et al. (1979), Wrzesinsky and Klemm (2000), and Křeček et al. (2017), atmospheric precipitation is affected by both elevation and vegetative canopy. The hypsometric method was used to assess the effect of elevation on precipitation, canopy throughfall, and deposition of  $\text{SO}_4^{2-}$ ,  $\text{NO}_3^-$ , and  $\text{NH}_4^+$  under the canopy (Křeček et al. 2017) using the same 5 canopy classes used by Křeček and Krčmář (2015). Seasonal atmospheric loads were estimated as (Křeček et al. 2017):

$$m = (bE + b_0)F_c/A_{er}, \quad (\text{Eq. 2})$$

where  $m$  = seasonal load (summer and winter),  $b$  and  $b_0$  = empirical hypsometric coefficients,  $E$  = elevation,  $A_{er}$  = effective receptor area, and  $F_c$  = fog-drip coefficient.

Methods of spatial interpolation (ArcGIS) were used to approximate the catchment deposition of water and acidifying substances ( $\text{SO}_4^{2-}$ ,  $\text{NO}_3^-$ , and  $\text{NH}_4^+$ ), and their runoff was estimated from concentrations and discharge ( $Q$ ) measured at the catchment outlet. Mean annual concentrations were calculated by weighted averages, and mean pH values were recalculated from converted values of  $\text{H}^+$ . The method of local minima in the hydrograph separation was applied to detect fast (direct) runoff in the catchment (Sloto and Crouse 1996).

Standard descriptive statistics and 1-way analysis of variance (ANOVA) was applied to analyze the data sets and to identify relationships between the groups of data (Motulsky and Searle 1998). Trends in the time series data (and a change in trends) were detected by the Change and Trend Problem Analysis (CTPA) programme (WMO 2001).

### Participation of citizen scientists

From 1991 to 2012, voluntary citizen scientists participated in ground observations. This participation made possible extra and time-sensitive sample collection during critical hydrological events. Each year, 4 to 5 teams each involving 4 to 8 volunteer participants spent 2 wk engaged in supervised field surveys organized by the Earthwatch environmental program (Earthwatch Institute 2012). After the standard preliminary selection done by Earthwatch, volunteers were instructed and trained in the field. The accuracy of their results was assessed daily. This project also was focused on the environmental education of volunteers, so after the 2-wk field activities and thematic discussions, their knowledge and skills were evaluated by specific tests.

According to findings of Robson et al. (1993) or Hodgson and Evans (1997), stream-water observations in upland watersheds require sampling at hourly or shorter intervals to provide good temporal resolution. Therefore, volunteers also gathered more detailed information on stream-water characteristics (temperature, pH, and conductivity) and collected water samples during some snowmelt and rain events. Data measured by volunteers in situ were controlled under laboratory conditions.

## RESULTS

### Changes of the canopy

The Jizerka catchment was covered by mature spruce stands. In 1984, 62% of the catchment area was harvested by clear-cutting, and ~88% was harvested by the end of the 1980s. Reforestation was complicated by establishment of invasive grass communities (*Calamagrostis* sp., predominantly *Calamagrostis villosae*) that spread over the basin area. Characteristics of the monitored reforested stands along transect A (A1–A12) and the mature stand (Fig. 1)

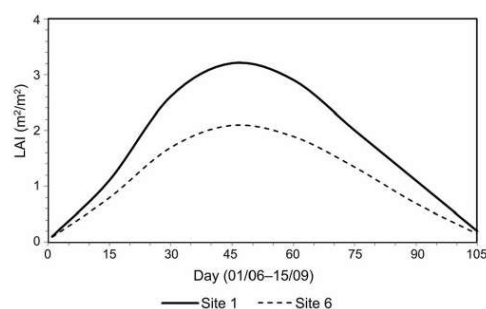


Figure 3. Seasonal changes in the living canopy of grass as leaf area index (LAI) along the A transect in 2012. Days are formatted dd/mm.

are presented in Table 2. In the reforested area (2012 inventory), blue spruce (*Picea pungens*) and Norway spruce (*Picea abies*) predominated with areal coverage of 48 and 32%, whereas the areal percentage of deciduous species, mountain-ash (*Sorbus aucuparia*) and silver birch (*Betula pendula*), was only 10%.

In 2012, 25 y after the clear-cut, LAI of reintroduced trees was 0.11 to 2.76 (mean =  $1.31 \pm 0.26$ ). In addition, the seasonal assimilating surface of the herbaceous canopy (Fig. 3) reached maximum LAI values between 2.1 and 3.2 in high summer. The corresponding values of NDVI varied from 0.66 to 0.76 (mean of  $0.72 \pm 0.1$ ) and were relatively insensitive to changes in the canopy when LAI was >2. Thus, the supervised classification of multiband raster images (Landsat 4, 5) was a more efficient indicator of canopy classes according to the crown closure of trees. In 1982 to

Table 2. Characteristics of the monitored stands in 2012.  $N_t$  = number of trees, CD = canopy density (crown closure), H = average tree height, LAI = leaf area index of trees, NDVI = normalized difference vegetation index.

Stand	Elevation (m)	$N_t$	CD ( $m^2/m^2$ )	H (m)	LAI ( $m^2/m^2$ )	NDVI
A1	862	107	0.38	3.62	1.9	0.68
A2	870	416	0.62	2.33	2.63	0.66
A3	878	317	0.55	2.61	2.07	0.69
A4	885	192	0.28	2.74	1.28	0.68
A5	891	324	0.59	3.96	2.76	0.70
A6	899	99	0.31	5.42	1.56	0.71
A7	907	72	0.06	0.50	0.11	0.75
A8	918	56	0.16	1.48	0.37	0.76
A9	930	102	0.21	2.61	1.06	0.75
A10	942	49	0.20	3.86	1.08	0.75
A11	961	146	0.15	2.39	0.5	0.75
A12	975	90	0.17	2.41	0.42	0.75
Mature stand	975	68	0.78	23.0	6.7	0.90

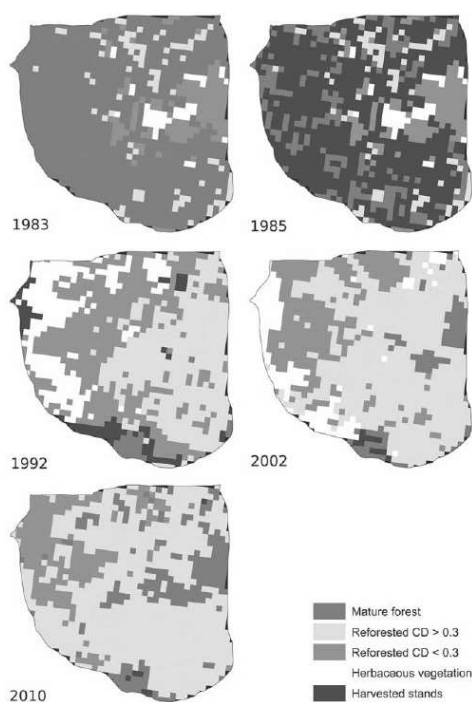


Figure 4. Canopy crown closure of trees (CD) in the Jizerka catchment from 1983 to 2010.

2015, canopy changes were reconstructed from the multi-band imagery (Fig. 4). The areal percentage of the 5 canopy classes is presented in Table 3.

#### Acidic atmospheric deposition

In 1982 to 2015, open-field deposition of  $\text{SO}_4^{2-}$ -S and N ( $\text{NO}_3^-$ -N and  $\text{NH}_4^+$ -N) recorded in most of the Jizerka catchment correspond with content of  $\text{SO}_2$  and  $\text{NO}_x$  in the air ( $r = 0.87$  and  $r = 0.48$ , respectively;  $r_{\text{crit}} = 0.32$ ,  $n = 34$ ,  $p = 0.05$ ; moving averages of order 3 are presented

Table 3. Areal percentage of the canopy classes in the Jizerka basin (1982–2010). CD = canopy density (crown closure).

Stands	1983	1985	1992	2002	2010
Mature forests	71	9	2	7	16
Reforested CD > 0.3	14	14	38	58	65
Reforested CD < 0.3	11	11	38	22	18
Grass	4	4	16	11	0
Clear-cut	0	62	6	2	1

in Fig. 5). Atmospheric concentrations of  $\text{SO}_2$  and  $\text{NO}_x$  were retrieved from the standard observation network of CHMI (2016): AIM (Ambient Ion Monitor) stations Desná-Souš (LSOU-1022) and Kořenov-Jizerka (LJIZ-1047).  $\text{SO}_2$  was measured by UV fluorescence over 10 min, and  $\text{NO}_x$  was measured by chemiluminescence in hourly intervals.

In 1982 to 1992, mean annual concentrations of  $\text{SO}_2$  exceeded the threshold for forests ( $20 \mu\text{g SO}_2/\text{m}^3$ ; Posch et al. 2001), whereas concentrations of  $\text{NO}_x$  were below the critical value ( $30 \mu\text{g NO}_x/\text{m}^3$ ). The deposition of S showed a decreasing trend with gradient of  $-0.12$  ( $t = 20.3$ ,  $t_{\text{crit}} = 2.1$ ,  $p = 0.05$ ; WMO 2001). However, the trend in the deposition of N was not quite significant ( $t = 0.69$ ). In 1982 to 2015, mean annual pH of precipitation increased from 4.2 to 5.3, and a pH-relevant annual open-field flux of  $\text{H}^+$  in precipitation decreased from  $90$  to  $5 \text{ mg m}^{-2} \text{ y}^{-1}$ . However, based on the deposition of  $\text{SO}_4^{2-}$ ,  $\text{NO}_3^-$ , and  $\text{Cl}^-$  (Yang et al. 2010), the open-field  $\text{H}^+$  flux decreased from  $265$  to  $86 \text{ mg m}^{-2} \text{ y}^{-1}$ , and the total  $\text{H}^+$  flux in the Jizerka catchment decreased from  $325$  to  $93 \text{ mg m}^{-2} \text{ y}^{-1}$ . The annual open-field flux of buffering basic cations ( $\text{Ca}^{2+}$ ,  $\text{Mg}^{2+}$ ,  $\text{K}^+$ , and  $\text{Na}^+$ ) fluctuated between  $1.67$  and  $3.35$  (mean =  $2.86$ )  $\text{g m}^{-2} \text{ y}^{-1}$ , and did not show any significant trend.

Interception loss of spruce stands was modified by the deposition of fog water on the canopy. The observed canopy storage capacity in the  $975\text{-m}^2$  study stand (Figs 1, 2) was  $2.3 \text{ mm}$ . Given a seasonal rainfall of  $683 \text{ mm}$  and  $\sim 100$  rainy days saturating the storage capacity, the total interception loss of the spruce canopy (not affected by fog) was  $\sim 230 \text{ mm}$  (34% of the gross precipitation). Therefore, the interception loss of  $112 \text{ mm}$  (16% of gross precipitation) was evidently caused by additional deposition of

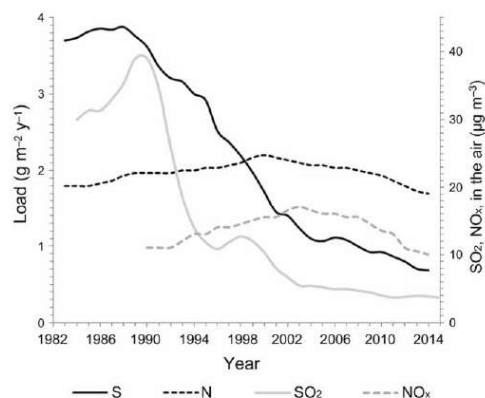


Figure 5. Concentrations of  $\text{SO}_2$  and  $\text{NO}_x$  in the air and the open-field load of S ( $\text{SO}_4^{2-}$ -S) and inorganic N ( $\text{NO}_3^-$ -N and  $\text{NH}_4^+$ -N); moving averages of order 3 in the Jizerka catchment from 1982 to 2015.

Table 4. Seasonal coefficients  $b$  and  $b_0$  for summer (May–October) and winter (November–April) loads of acidifying substances.

Chemicals	Summer		Winter	
	$b$	$b_0$	$b$	$b_0$
$\text{SO}_4^{2-}\text{-S}$	0.0766	-56.1069	0.1126	-81.7721
$\text{NO}_3^-\text{-N}$	0.0270	-19.8859	0.0362	-26.2902
$\text{NH}_4^+\text{-N}$	0.0754	-55.5671	0.0940	-68.6638

fog water. The volume of stem-flow was negligible. Along transect A (Fig. 1), measurable volumes of fog water were collected by passive collectors at elevations >900 m (collectors 7–12). Mean monthly fog drip and elevation were significantly correlated in summer (May–October) and winter (November–April) ( $r = 0.93$  and  $0.98$ , respectively;  $r_{\text{crit}} = 0.75$ ,  $n = 5$ ,  $p = 0.05$ ). These relationships have slopes significantly different from 0 ( $p = 0.0082$  and  $0.0033$ , respectively) and no significant departure from linearity ( $F = 39.3$  and  $73.75$ , respectively;  $F_{\text{crit}} = 9.78$ ). The load of fog drip was greater in winter than in summer by 23 to 50%.

The empirical coefficients  $b$  and  $b_0$  (Eq. 2) based on field observations in 2010 to 2012 are given in Table 4. Fog-drip coefficients  $F_c$  were calculated as 1 (dense mature stand), 0.33 (stand of crown closure >0.3), and 0.18 (area overgrown by grass).

The atmospheric load of water and acidifying substances ( $\text{SO}_4^{2-}$ ,  $\text{NO}_3^-$ , and  $\text{NH}_4^+$ ) in the Jizerka catchment was estimated by spatial interpolation based on the canopy classes and elevation (Eq. 2) in 1982 to 2015. Annual values of fog drip, open-field deposition, and an additional canopy load (total loads are sums of the open-field and the extra canopy values) are shown in Fig. 6A–C. These data reconstruct the atmospheric load at a catchment scale. In 1982 to 2015 (34 y), the mean annual runoff of S ( $2.96 \text{ g m}^{-2} \text{ y}^{-1}$ ) exceeded the open-field deposition ( $2.14 \text{ g m}^{-2} \text{ y}^{-1}$ ) by 38%, but not the total deposition ( $3.31 \text{ g m}^{-2} \text{ y}^{-1}$ , 89%) (Fig. 6B). The mean annual runoff of N ( $0.95 \text{ g m}^{-2} \text{ y}^{-1}$ ) was less than the total ( $2.43 \text{ g m}^{-2} \text{ y}^{-1}$ , 39%) and the open-field ( $1.68 \text{ g m}^{-2} \text{ y}^{-1}$ , 56%) loads (Fig. 6C).

The decreasing trends in the output (runoff) of S and N (slopes =  $-0.163$  and  $-0.025$ , respectively;  $t = 22.49$  and  $11.2$ ,  $t_{\text{crit}} = 2.1$ ,  $p = 0.05$ ) exceeded that found in the open-field deposition ( $-0.12$  and  $0.002$ ; Fig. 5). Comparing data from 1982 to 1984 (before the forest clear-cut) with 2001–2015 (after the drop in emissions and forest regrowth), mean total annual deposition of S decreased from  $8.7$  to  $1.6 \text{ g m}^{-2} \text{ y}^{-1}$  (the extra loading on the canopy decreased from 60 to 40%, Fig. 6B), whereas N did not change significantly (from  $2.62$  to  $2.74 \text{ g m}^{-2} \text{ y}^{-1}$  with decreasing canopy effect from 45 to 27%; Fig. 6C). Annual fog-drip amounts corresponded to the % forest area covered by stands with crown closure >0.3 ( $r = 0.79$ ,  $r_{\text{crit}} = 0.32$ ,

$n = 34$ ,  $p = 0.05$ ; Fig. 6A). From 1982 to 2015, atmospheric N deposition consisted of 72%  $\text{NH}_4\text{-N}$  and 28%  $\text{NO}_3\text{-N}$ . The ratio between the total N and S loads increased from 0.35 (1982–1988) to 2.0 (2011–2015).

### Runoff genesis

Significant correlations were found between mean annual stream-water characteristics (pH, contents of  $\text{SO}_4^{2-}$ , and  $\text{NO}_3^-$ ) and the air pollution (AP; concentrations of  $\text{SO}_2$  and  $\text{NO}_x$  combined) and mean canopy density (CD) of the Jizerka catchment (Table 5). These characteristics

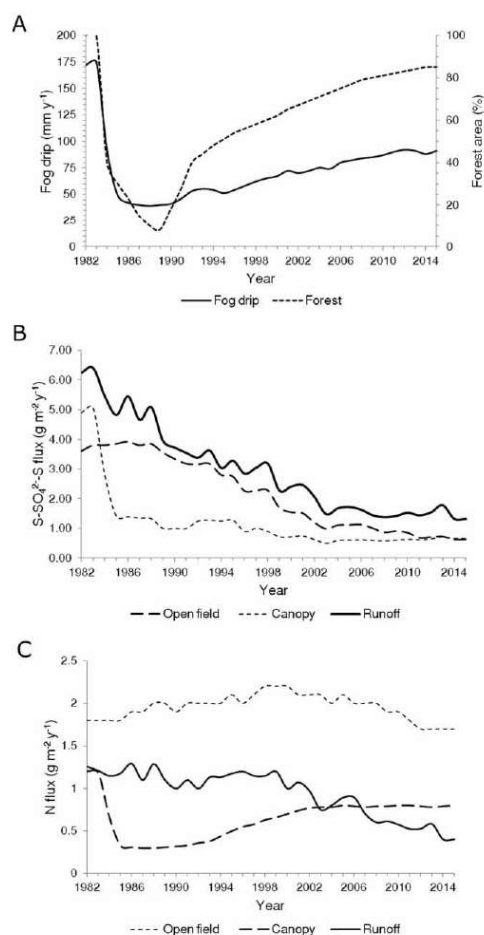


Figure 6. Fog drip (A), the balance of S (B), and the balance of N (C) in the Jizerka catchment (1982–2015).

Table 5. The correlation matrix between mean annual stream-water pH,  $\text{SO}_4^{2-}$ , and  $\text{NO}_3^-$ , air pollution (AP;  $\text{SO}_2$  and  $\text{NO}_x$  combined), and canopy density (CD) in 1982–2015 ( $r_{\text{crit}} = 0.28$ ,  $n = 33$ ,  $p = 0.05$ ).

Variable	CD	AP	$\text{SO}_4^{2-}$	$\text{NO}_3^-$	pH
CD	1	0.55	0.62	0.38	-0.49
AP	0.55	1	0.84	0.23	-0.61
$\text{SO}_4^{2-}$	0.62	0.84	1	0.53	-0.94
$\text{NO}_3^-$	0.38	0.23	0.53	1	-0.63
pH	-0.49	-0.61	-0.94	-0.63	1

were not well correlated with annual precipitation or runoff ( $r = 0.04$ – $0.06$ ) because of high annual precipitation (mean  $\pm$  SD,  $1398 \pm 143$  mm). Thus, in the 1990s, the recovery of stream waters from acidification resulted from a synergy of the drop in  $\text{SO}_2$  emissions and reduction of the surface area of spruce forests. Later, open-field deposition rates for both elements stabilized, and their atmospheric loads and stream-water chemistry were controlled by regrowth of forest stands (Fig. 7, Table 3).

Fast (direct) flow, estimated from observed hydrographs by local minimum separation (Sloto and Crouse 1996) ranged between 54 and 61% of the annual runoff. Differences in the hydrograph formation are determined by annual snow water volume and frequency of rainstorms and are not affected by changes in forest canopy (Křeček and Hořická 2001). Relationships between stream-water variables (pH, electrical conductivity, concentrations of  $\text{SO}_4^{2-}$ ,  $\text{NO}_3^-$ ) and instantaneous discharge are shown in Table 6. pH was the most effective single variable distinguishing the occurrence of fast direct runoff at the Jizerka catchment outlet.

The recovery of stream-water chemistry (Fig. 8) followed the drop in the atmospheric acid deposition by  $\sim 5$  y, but a revival of stream biota reflects these changes with a lag period of 10–15 y (Table 7). In 1994, the number of taxa of benthic organisms (36) corresponded to a strongly acidified environment (pH < 4.2; Veselý and Majer 1996), whereas by 2005, the number of taxa had increased to 68, which is more typical of a moderately acidified environment (pH = 5.0–6.3; Horecký et al. 2013). By 2005, several acid-sensitive taxa either had reappeared (Crustacea, Ephemeroptera) or increased significantly in the number of species present (Plecoptera, Trichoptera). The stream investigated at Jizerka was devoid of fish in the 1980s and remained without fish in 1990–2015.

#### Seasonal and episodic acidification

Annual distributions of mean monthly pH in 1982 (before the forest harvest), 1992, 2002, and 2012 (progressed forest regrowth) are shown in Fig. 8. Monthly pH increased, but seasonal pH minima continued to drop < 5.3, which is

considered a threshold for the rapid mobilization of toxic Al (Křeček and Hořická 2001). Streamflow Al content decreased from 1 to 2 (1980s) to 0.2 to 0.5 (1990s) and 0.1 to 0.2 mg/L (2010s). Seasonal acidification was driven mainly by direct (fast) runoff from spring snowmelt (Fig. 9A). In summer, stream-water pH decreased during rainstorms (Fig. 9B).

#### DISCUSSION

In the Jizerka catchment, the open-field deposition of  $\text{SO}_4^{2-}$ -S peaked in the late 1980s and showed a decreasing trend with the drop in atmospheric emissions of  $\text{SO}_2$  during the 1990s (Fig. 5) in response to the 1985 Helsinki Sulphur Protocol (Holen et al. 2013). However, the open-field load of  $\text{NO}_3^-$ -N and  $\text{NH}_4^+$ -N did not change significantly. Between 1982 and 2015, the N : S deposition ratio increased from 0.37 to 2.83.  $\text{NH}_4^+$  and  $\text{NO}_3^-$  presented 72 and 28% of the long-term load of inorganic N, respectively. Ground observations confirmed linear hypsometric relationships between precipitation, the number of foggy days, and fog drip with atmospheric deposition. Rapidly decreasing trends in catchment runoff of both S and N (Fig. 6B, C) correspond with clear-cutting of spruce stands (1984–1988) and reduction of canopy area. Reforestation (mainly with spruce stands) of the Jizerka basin started only a year after the harvest, but regrowth of forests was relatively slow. Field surveys in 1992, 2002, and 2010 showed that the area dominated by grass (crown closure < 0.3) was 62, 37, and 19%, respectively. The invasive grass community (*Calamagrostis* sp.) spread across the catchment with the defoliation of mature spruce stands (Křeček et al. 2010).

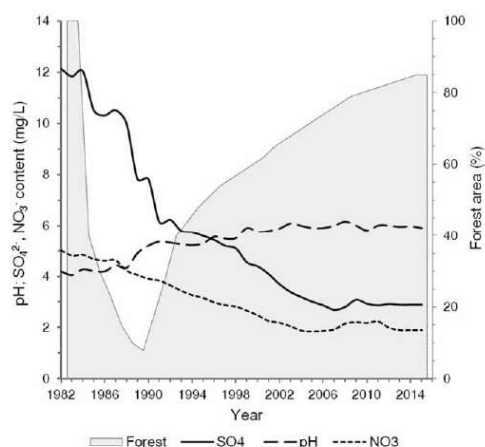


Figure 7. Changes of mean annual pH,  $\text{SO}_4^{2-}$ , and  $\text{NO}_3^-$  in stream water as the forest regrew in the Jizerka catchment (1982–2015).

Table 6. The correlation matrix between stream-water discharge (Q), pH, electrical conductivity (EC), and concentrations of  $\text{SO}_4^{2-}$  and  $\text{NO}_3^-$  in 2010–2012 ( $r_{\text{crit}} = 0.20$ ,  $n = 102$ ,  $p = 0.05$ ).

Variable	Q	pH	EC	$\text{SO}_4^{2-}$	$\text{NO}_3^-$
Q	1	-0.67	-0.46	0.35	-0.29
pH	-0.67	1	0.51	-0.40	-0.33
EC	-0.46	0.51	1	0.31	0.24
$\text{SO}_4^{2-}$	0.35	-0.40	0.31	1	0.30
$\text{NO}_3^-$	-0.29	-0.33	0.24	0.30	1

The Landsat imagery analysis was an effective tool for identifying changes in the canopy and atmospheric depositions in the Jizerka catchment. However, NDVI values were relatively insensitive when canopy LAI was  $>2$ , as found previously by Křeček and Krčmář (2015). In contrast, supervised classification of multiband raster images (Landsat 4, 5) was more efficient in detecting differences in crown closure of trees (Fig. 4).

Prošková and Hůnová (2006) regarded an elevation of 800 m as the threshold for significant fog/cloud occurrence in the Czech Republic. In the upper plain of the Jizerka Mountains, Křeček et al. (2017) reported significantly modified interception processes by fog deposition at elevations  $>700$  m. In our study stand (elevation = 975 m), interception storage not affected by fog (34% of the gross precipitation) corresponded with the interception loss (30–40%) found in similar spruce forests by Krečmer et al. (1979). The observed interception loss (112 mm; 16% of gross precipitation) was affected by the additional deposition of fog water. The volume of stem-flow was negligible, consistent with findings by Krečmer et al. (1979) and Lovett and Reiners (1986). Compared to an open-field load, the reconstructed estimates of fog drip and additional canopy deposition (Fig. 6A–C) provided more realistic information on the atmospheric load within a mountain catchment and a better view of where this deposition exceeded critical levels of S and inorganic N. In the Jizerka catchment, the critical load of S ( $75 \text{ meq m}^{-2} \text{ y}^{-1}$ , according to the regional mapping; Schwarz et al. 2009) was exceeded from 1982 (beginning of the study) until 2002 ( $75\text{--}247 \text{ meq m}^{-2} \text{ y}^{-1}$ ) in the open-field (herbaceous vegetation), and continues to be exceeded in forest stands ( $79\text{--}553 \text{ meq m}^{-2} \text{ y}^{-1}$ ). The critical load of N ( $55 \text{ meq m}^{-2} \text{ y}^{-1}$ ) also continues to be exceeded in both (99–149  $\text{meq m}^{-2} \text{ y}^{-1}$ ) and spruce stands (142–206  $\text{meq m}^{-2} \text{ y}^{-1}$ ). Bobbink and Roelofs (1995) consider  $1 \text{ g m}^{-2} \text{ y}^{-1}$  ( $71 \text{ meq m}^{-2} \text{ y}^{-1}$ ) as an empirical critical deposition of N in forests of central Europe. This threshold has been exceeded by a factor of 2 to 3 throughout the period from 1982 to 2015 in the Jizerka catchment. This greater deposition of nutrient N is particularly important considering the evidence of increased

environmental sensitivity and changes in biodiversity (Matzner and Murach 1995).

Prechtel et al. (2001) reported a significant decline of  $\text{SO}_4^{2-}$  concentrations in European headwater streams in the 1990s (relative to in the 1980s), but less than the decline in input fluxes. The response in runoff increases as soil storage capacity decreases. In the Jizerka catchment, the fast response of  $\text{SO}_4^{2-}$  runoff relative to the drop in the deposition during the 1990s, reflects the clear-cut of spruce forests (1984–1988) and prevailing fast subsurface runoff generated by relatively shallow podzolic soils of a low  $\text{SO}_4^{2-}$  storage capacity. The open-field load of N did not change significantly in 1982–2015, but  $\text{NO}_3^-$  concentrations in stream water decreased by 12% in the 1990s and by 53% after 2010 (relative to in the 1980s). The relatively high leaching of  $\text{NO}_3^-$  before the forest harvest (1982–1984) corresponds with high atmospheric loads of N and limited N uptake by already damaged spruce stands (defoliation of 30%). Grenon et al. (2004) reported higher  $\text{NO}_3^-$  leaching from forest floor with forest decline caused by the decreased uptake of N by vegetation and increased microbial release of N. Decreased N uptake by spruce trees contributes to increasing availability of mineral N in the summer, whereas enhanced microbial N release takes place over the whole year. Tahovská et al. (2010) reported increased in situ availability of  $\text{NO}_3^-$  before the defoliation peaked, and Huber (2005) found a positive correlation between herbaceous ground vegetation and  $\text{NO}_3^-$  concentration in soil water during the first 2 to 5 y after forest die-back.

Low pH (Figs 7, 8), low hardness ( $\leq 10 \text{ mg/L Ca}^{2+}$  and  $\text{Mg}^{2+}$ ), and high Al contents ( $>0.2 \text{ mg/L}$ ) were observed in surface waters of the Jizerka Mountains in the 1980s (Křeček and Hořická 2006). With the recovery of the water environment in the 1990s, pH values increased from 3.3–

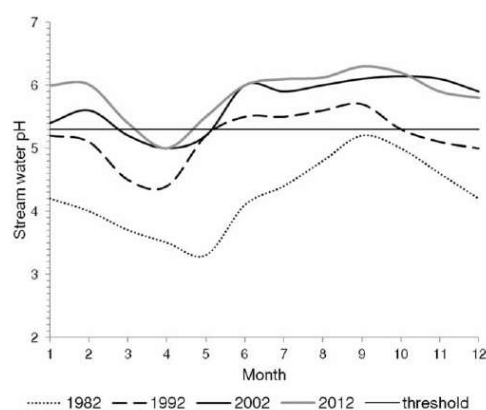


Figure 8. Mean monthly pH of stream water at the outflow of the Jizerka catchment.

Table 7. The number of identified taxa of benthic organisms at the Jizerka outlet.

Taxa	1994	2005
Nematoda	–	1
Oligochaeta	2	4
Hydracarina	–	1
Crustacea	–	1
Ephemeroptera	–	3
Plecoptera	12	20
Megaloptera	1	–
Trichoptera	4	17
Diptera excl. Chironomidae	11	10
Chironomidae	4	5
Coleoptera	2	6
Total	36	68

5.2 to 4.4–5.7, Al content dropped to 0.1–0.2 mg/L and fish (Brook Char and Brown Trout extinct since the 1980s) were reintroduced in selected streams (Křeček and Hořícká 2001). No health-based guideline value has been proposed for pH of water, but pH is one of the most important operational water-quality variables (WHO 2004). Without pollution or acidic rain, most lakes and streams would have a pH level near 6.5 (Merilehto et al. 1988). Decreased pH is particularly associated with increased mobility of Al and heavy metals in the podzolic soil layer and has a negative impact on the drinking-water supply and survival of aquatic biota (Křeček and Hořícká 2006, Horecký et al. 2013). Mean annual pH at the Jizerka outlet increased from 4.0 (1982–1985) to 5.3 (1990–1994), but repetitive episodic acidification still affects the recovery of the biota, particularly acid-sensitive species. Seasonal pH minima during snowmelt (Fig. 8) are <5.3, a threshold associated with a rapid mobilization of toxic Al (Bache 1985, Veselý and Majer 1996). Water pH seems to be an effective variable of the hydrograph separation (Fig. 9A, B, Table 6) and is more powerful than conductivity recommended by Caissie et al. (1996).

Guerold et al. (2000) considered aquatic invertebrate communities as the best indicator for assessing the negative environmental effect of acidification. Skjelkvåle et al. (2003) found large-scale evidence of chemical recovery from surface-water acidification in Europe, but little evidence of biological recovery. Recovery of stream-water chemistry at the Jizerka outlet (Fig. 7) occurred ~5 y after drop in the acid atmospheric deposition, but recovery of stream biota appeared after a lag of 10–15 y (Table 7).

Acidification of sensitive ecosystems has been a serious environmental problem in Europe in recent decades. Schöpp et al. (2003) estimated the amounts of SO<sub>2</sub>, NO<sub>x</sub>, and NH<sub>3</sub> emissions in Europe from 1880 to 2030, and Kopáček et al. (2016) modeled the chemistry of precipita-

tion affected by industrial dust in Central Europe since the 1850s. Spruce forests contributed to acidification of headwater catchments in Central Europe by increasing acidic atmospheric deposition. Data from the Jizerka catchment (1982–2015) document that the acidic atmospheric deposition and stream-water quality can be modified at the catchment scale by forestry practices. In comparison with mature spruce stands, the herbaceous canopy that developed on harvested areas decreased the atmospheric acid load by ~40% and mitigated acidification of surface waters. Deciduous or mixed forests could decrease the acidic atmospheric load because of their lower leaf area and surface roughness (Lovett and Reiners 1986), particularly in the dormant season. In the Jizera Mountains, mixed forests of near-native composition can increase the soil buffering capacity (Matzner and Murach 1995) and support ecological stability (Rappport et al. 1998) by a deeper root system

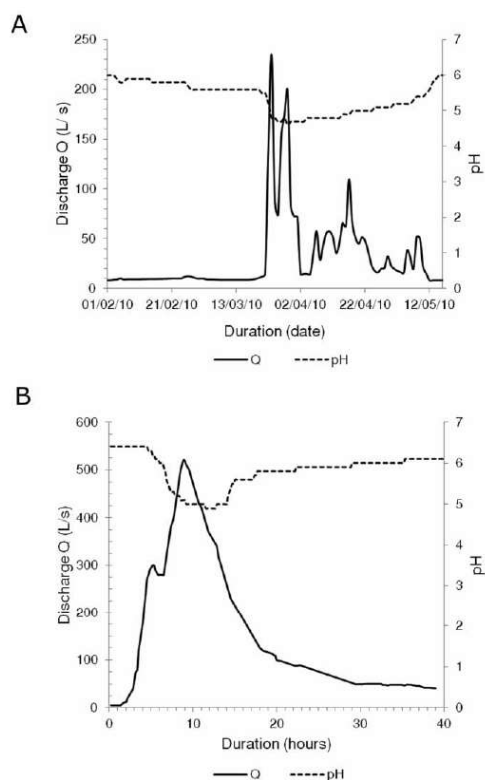


Figure 9. pH and discharge ( $Q$ ) of snowmelt runoff in the Jizerka basin from March–May 2010 (A) and of summer runoff episode of a frequency > 1 (B) in the Jizerka basin from June 8–9 2010. Dates are formatted dd/mm/yy.

and a higher resistance to air pollution. UNEP (2007) calls for a reduction of the acidic atmospheric deposition in headwater catchments to mitigate the progressive downstream acidification of rivers and the ocean. However, the regrowth of coniferous stands following a reduction in atmospheric emissions could slow the recovery of surface waters (Fig. 7). Uncertainties in predictions of the future of recovery from acidification still depend on rates of production of atmospheric emissions, global climate change, and the long-term behavior of N in forest ecosystems.

### Citizen scientists

Citizen scientists of the Earthwatch Institute played an important role in gathering extensive field data. Hodgson and Evans (1997) warned of reduced accuracy and increased response time when measuring pH in waters with naturally low ionic strength. The in situ data (pH, conductivity) collected by volunteers showed a relatively good agreement with values obtained under the laboratory conditions (20 readings tested/expedition,  $r = 0.79\text{--}0.93$  ( $r_{\text{crit}} = 0.16$ ,  $n = 100$ ,  $p = 0.05$ ) in the years of field expeditions. Rosenberg and Resh (1993) considered the primary role of nonspecialist volunteers to be sampling benthic macroinvertebrates, but their participation in water monitoring and the forest inventory were controlled by the professional project staff in our study. In addition, the volunteers enabled greater temporal resolution in the sampling campaigns and were a source of essential data. The motivation of citizen participants played an important role in their education as evaluated by the Earthwatch Institute (2012).

### ACKNOWLEDGEMENTS

Author contributions: JK contributed to the design of this study, analyzed the data, and wrote the initial version of the manuscript, LP and EP contributed to the data processing, and ES to the laboratory analyses and their interpretations.

This research was supported by the Earthwatch Institute (Oxford, UK, Mountain Waters of Bohemia, 1991–2012), Grant Agency of the Czech Republic (GA ČR 526-09-0567 CLIMHEAD, 2009–2013), Czech Technical University in Prague (SGS 16/140/OHK1/2T/11, 2016–2017), and the Ministry of Education (INTER-EXCELLENCE: INTER-COST LTC 17006, 2017). We are grateful to Zuzana Hořická (co-PI of the Earthwatch project in 1994–2008) for her field logistic assistance and helpful comments.

### LITERATURE CITED

Bache, B. W. 1985. Aluminium mobilization in soils and waters. *Journal of the Geological Society* 143:699–706.

Baldigo, B. P., and G. B. Lawrence. 2001. Effects of stream acidification and habitat on fish populations of a North American river. *Aquatic Sciences* 63:196–222.

Biswas, A. K., C. Tortajada, and R. Izquierdo. 2014. *Water quality management: present situations, challenges and future perspectives*. Routledge, London, UK.

Bobbink, R., and J. G. M. Roelofs. 1995. Nitrogen critical loads for natural and semi-natural ecosystems: the empirical approach. *Water, Air, and Soil Pollution* 85:2413–2418.

Bolstad, P. V., and W. T. Swank. 1997. Cumulative impacts of landuse on water quality in a southern Appalachian watershed. *Journal of the American Water Resources Association* 33:519–533.

Breda, N. 2003. Ground-based measurements of leaf area index: a review of methods, instruments and current controversies. *Journal of Experimental Botany* 54:2403–2417.

Caissie, D., T. L. Pollock, and R. A. Cunjak. 1996. Variation in stream water chemistry and hydrograph separation in a small drainage basin. *Journal of Hydrology* 178:137–157.

Cape, J. N., A. Kirika, A. P. Rowland, D. R. Wilson, T. D. Jickells, and S. Cornell. 2001. Organic nitrogen in precipitation: real problem or sampling artefact? *TheScientificWorld* 1:230–237.

Chen, J. M., and T. A. Black. 1992. Defining leaf area index for non-flat leaves. *Plant, Cell and Environment* 15:421–429.

CHMI (Czech Hydrometeorological Institute). 2016. Air pollution in the Czech Republic. Czech Hydrometeorological Institute, Prague, Czech Republic. (Available from: <http://portal.chmi.cz/historicka-data/ovzdusi>)

Christensen, J. H. 2005. Prediction of regional scenarios and uncertainties for defining European climate change risks and effects (PRUDENCE). Final Report. Danish Meteorological Institute, Copenhagen, Denmark. (Available from: <http://prudence.dmi.dk>)

Earthwatch Institute. 2012. *Earthwatch annual report*. Earthwatch Europe, Oxford, UK.

European Commission. 2012. Report on the implementation of the Water Framework Directive: river basin management plans. Commission Staff Working Document COM 670. European Commission, Brussels, Belgium. (Available from: <http://ec.europa.eu/environment/water/water-framework>)

Falkenmark, M., and B. Allard. 2015. Water quality genesis and disturbances of natural freshwaters. *Water Pollution* 5:45–78.

FAO (Food and Agriculture Organization). 2008. *Forests and water*. FAO Forestry paper 155. Food and Agriculture Organization of the United Nations, Rome, Italy. (Available from: <http://www.fao.org/docrep/011/i0410e/i0410e01.pdf>)

Grenon, F., R. L. Bradley, G. Joannisse, B. D. Titus, and C. E. Prescott. 2004. Mineral N availability for conifer growth following clear cutting: responsive versus non-responsive ecosystems. *Forest Ecology and Management* 188:305–316.

Guerold, F., J. P. Boudot, G. Jacquemin, D. Vein, D. Merlet, and J. Rouiller. 2000. Macroinvertebrate community loss as a result of headwater stream acidification in the Vosges Mountains (NE France). *Biodiversity and Conservation* 9:767–783.

Hand, E. 2010. Citizen science: people power. *Nature* 466:685–687.

Hodgson, P., and J. G. Evans. 1997. Continuous pH, electrical conductivity and temperature measurement at Plynlimon: towards an integrated, reliable and low maintenance instrument system. *Hydrology and Earth System Sciences* 1:653–660.

Holen, S., R. F. Wright, and I. Seifert. 2013. Effects of long range transported air pollution (LRTAP) on freshwater ecosystem services. ICP-Waters report 115/2013, SNO 6561-2013, Norwegian Institute for Water Research (NIVA), Oslo, Norway.



- Horecký, J., J. Rucki, P. Krám, J. Křeček, P. Bitušík, J. Špaček, and E. Stuchlík. 2013. Benthic macroinvertebrates of headwater streams with extreme hydrochemistry. *Biologia* 68:1–11.
- Huber, C. 2005. Long lasting nitrate leaching after bark beetle attack in the highlands of the Bavarian Forest National Park. *Journal of Environmental Quality* 34:1772–1779.
- Irwin, A. 1995. *Citizen science: a study of people, expertise, and sustainable development*. Rutledge, London, UK.
- Kopáček, J., J. Hejzlar, P. Krám, F. Oulehle, and M. Posch. 2016. Effect of industrial dust on precipitation chemistry in the Czech Republic (Central Europe) from 1850 to 2013. *Water Research* 103:30–37.
- Körner, C., and M. Ohsawa. 2005. Mountain systems. Pages 683–716 in R. Hassan, R. Scholes, and N. Ash (editors). *Ecosystems and human well-being: current state and trends*. Island Press, London, UK.
- Křeček, J., and Z. Hořícká. 2001. Degradation and recovery of mountain watersheds: the Jizera Mountains, Czech Republic. *Unasylva* 52:43–49.
- Křeček, J., and Z. Hořícká. 2006. Forests, air pollution and water quality: influencing health in the headwaters of Central Europe's "Black Triangle". *Unasylva* 57:46–49.
- Křeček, J., and V. Krčmář. 2015. Landsat imagery applications to identify vegetation recovery from acidification in mountain catchments. *Hungarian Geographical Bulletin* 64:121–126.
- Křeček, J., J. Nováková, and Z. Hořícká. 2010. Ellenberg's indicator in water resources control: the Jizera Mountains, Czech Republic. *Ecological Engineering* 36:1112–1117.
- Křeček, J., L. Palán, and E. Stuchlík. 2017. Acid atmospheric deposition in a forested mountain catchment. *iForest* 10:680–686.
- Křečmer, V., V. Fojt, and J. Křeček. 1979. Fog precipitation and fog drip in forests as an item of water balance in a mountain region. *Meteorological Bulletin* 32:78–81.
- Lawrence, P., J. Meigh, and C. Sullivan. 2002. The water poverty index: an international comparison. *Keele Economics Research Papers*, Keele University, Keele, UK.
- Leopold, L. B. 2006. *A view of the river*. Harvard University Press, Cambridge, Massachusetts.
- Lovett, G. M. 1988. A comparison of methods for estimating cloud water deposition to a New Hampshire (U.S.A.) subalpine forest. Pages 309–320 in D. Fowler and M. H. Unsworth (editors). *Acid deposition at high elevation sites*. Springer, Dordrecht, The Netherlands.
- Lovett, G. M., and W. A. Reiners. 1986. Canopy structure and cloud water deposition in subalpine coniferous forests. *Tellus* 38:319–327.
- Lumb, A., T. C. Sharma, and J. F. Bibeault. 2011. A review of genesis and evolution of water quality index (WQI) and some future directions. *Water Quality, Exposure and Health* 3:11–24.
- Matzner, E., and D. Murach. 1995. Soil changes induced by air pollutant deposition and their implication for forests in central Europe. *Water, Air, and Soil Pollution* 85:63–76.
- Merilehto, K., K. Kenttämies, and J. Kämäri. 1988. Surface water acidification in the ECE region. *The Nordic Council of Ministers (NORD)*, Copenhagen, Denmark.
- Messerli, B., D. Viviroli, and R. Weingartner. 2004. Mountains of the world: vulnerable water towers for the 21st century. *AMBIO* 13:29–34.
- Motulsky, H. J., and P. Searle. 1998. *InStat guide to choosing and interpreting statistical tests*. GraphPad Software, Inc., San Diego, California.
- Nagi, R. 2011. *Classifying Landsat image services to make a land cover map*. ArcGIS Resources, Environmental Systems Research Institute, Redlands, California (Available from: <http://esri.com/esri/arcgis>).
- NASA (National Aeronautics and Space Administration). 2014. *Landsat science*. National Aeronautics and Space Administration, Washington, DC. (Available from: <http://landsat.usgs.gov>)
- Posch, M., P. A. M. de Smet, J. P. Hettelingh, and R. J. Downing. 2001. Modelling and mapping of critical thresholds in Europe. RIVM Report No. 259101010. National Institute for Public Health and the Environment, Bilthoven, The Netherlands. (Available from: <https://www.rivm.nl/bibliotheek/rapporten/259101010.pdf>)
- Prechtel, A., C. Alewell, M. Armbruster, J. Bittersohl, J. M. Cullen, C. D. Evans, R. Helliwell, J. Kopáček, A. Marchetto, E. Matzner, H. Meessenburg, F. Moldan, K. Moritz, J. Veselý, and R. F. Wright. 2001. Response of sulphur dynamics in European catchments to decreasing sulphate deposition. *Hydrology and Earth System Sciences* 5:311–325.
- Prošková, J., and I. Hůnová. 2006. Assessment methods of fog and low cloud deposition. *Meteorological Bulletin* 59:151–157.
- Rapport, D. J., R. Constanza, P. R. Epstein, C. Gaudet, and R. Levins. 1998. *Ecosystem health: principles and practice*. Blackwell Science, Oxford, UK.
- Reuss, J. O., and D. W. Johnson. 1986. *Acid deposition and the acidification of soils and waters*. Ecological Studies 59. Springer, New York.
- Robson, A. J., C. Neal, S. Hill, and C. J. Smith. 1993. Linking variations in short- and medium-term stream chemistry to rainfall inputs—some observations at Plynlimon, Mid-Wales. *Journal of Hydrology* 144:291–310.
- Rosenberg, D. M., and V. H. Resh. 1993. Introduction to freshwater biomonitoring and benthic macroinvertebrates. Pages 1–9 in D. M. Rosenberg and V. H. Resh (editors). *Freshwater biomonitoring and benthic macroinvertebrates*. Chapman and Hall, New York.
- Sasaki, N., and F. E. Putz. 2009. Critical need for new definitions of "forest" and "forest degradation" in global climate change agreements. *Conservation Letters* 2:1–7.
- Schöpp, W., M. Posch, S. Mylona, and M. Johansson. 2003. Long-term development of acid deposition (1880–2030) in sensitive freshwater regions in Europe. *Hydrology and Earth System Sciences* 7:436–446.
- Schwarz, O., J. Hošek, P. Anděl, J. Hruška, J. Hofmeister, T. Svoboda, and L. Petržílka. 2009. Maps of critical atmospheric loads of sulphur and nitrogen in forest ecosystems of the Giant Mountains National Park and the Jizera Mountains (in Czech). *Lesnická práce, Kostelec nad Černými lesy (Czech Republic)*. (Available on CD-ROM from: *Lesnická práce s.r.o., náměstí Smičických 1, 281 63 Kostelec nad Černými lesy, Czech Republic*)
- Silvertown, J. 2009. A new dawn for citizen science. *Trends in Ecology and Evolution* 24:467–471.
- Skjelkvåle, B. L., C. Evans, T. Larssen, A. Hindar, and G. Raddum. 2003. Recovery from acidification in European surface waters: a view to the future. *AMBIO: A Journal of the Human Environment* 32:170–175.

- Sloto, R. A., and M. Y. Crouse. 1996. HYSEP: a computer program for streamflow hydrograph separation and analysis. U.S. Geological Survey, Water Resources Investigations Report 96-4040. US Geological Survey, Lemoyne, Pennsylvania.
- Stuchlík, E., Z. Hořícká, M. Prchalová, J. Křeček, and J. Barica. 1997. Hydrobiological investigation of three acidified reservoirs in the Jizera Mountains, the Czech Republic, during the summer stratification. *Canadian Technical Report of Fisheries and Aquatic Sciences* 2155:56–64.
- Stuchlík, E., J. Kopáček, J. Fott, and Z. Hořícká. 2006. Chemical composition of the Tatra Mountain lakes: response to acidification. *Biologia, Bratislava* 61/Supplement 18:S11–S20.
- Tahovská, K., J. Kopáček, and H. Šantrůčková. 2010. Nitrogen availability in Norway spruce forest floor: the effect of forest defoliation induced by bark beetle infestation. *Boreal Environment Research* 15:553–564.
- Takagi, M. 2015. Water chemistry of headwater streams under stormflow conditions in catchments covered by evergreen broadleaved forest and by coniferous plantation. *Landscape and Ecological Engineering* 11:293–302.
- Tolasz, R. 2007. Climate atlas of the Czech Republic. Czech Hydrometeorological Institute, Prague, Czech Republic.
- UNEP (United Nations Environmental Programme). 2007. Global environmental outlook 4. United Nations Environmental Programme, Progress Press, Valetta, Malta.
- USEPA (US Environmental Protection Agency). 1997. Volunteer stream monitoring: a methods manual. EPA 841/B97003. US Environmental Protection Agency, Washington, DC.
- Veselý, J., and V. Majer. 1996. The effect of pH and atmospheric deposition on concentrations of trace elements in acidified freshwaters: a statistical approach. *Water, Air, and Soil Pollution* 88:227–246.
- Viviroli, D., H. H. Dürr, B. Messerli, M. Meybeck, and R. Weingartner. 2007. Mountains of the world, water towers for humanity: typology, mapping, and global significance. *Water Resources Research* 43:W07447.
- Watts, S. B., and L. Tolland. 2005. *Forestry handbook for British Columbia*. 5<sup>th</sup> edition. University of British Columbia, Vancouver, British Columbia.
- Weier, J., and D. Herring. 2000. Measuring vegetation (NDVI & EVI). Earth Observatory, National Aeronautics and Space Administration, Washington, DC. (Available from: <https://earthobservatory.nasa.gov>)
- WHO (World Health Organization). 2004. Guidelines for drinking-water quality. 3<sup>rd</sup> edition. World Health Organization, Geneva, Switzerland.
- WMO (World Meteorological Organization). 2001. Technology for detecting trends and changes in time series of hydrological and meteorological variables. Hydrological Operational Multipurpose System, World Meteorological Organization, Geneva, Switzerland.
- Wrzesinsky, T., and O. Klemm. 2000. Summertime fog chemistry at a mountainous site in central Europe. *Atmospheric Environment* 34:1487–1496.
- Yang, J. L., L. M. Huang, and G. L. Zhang. 2010. Source and consumption of proton and its impacts on cation flux and soil acidification in a forested watershed of subtropical China. Pages 108–111 *in* Proceedings of the 19<sup>th</sup> World Congress of Soil Science, Soil Solutions for a Changing World, 1–6 August 2010, Brisbane (Australia). International Union of Soil Sciences, Crawley, Australia.

Přirozená druhová skladba lesního porostu povodí Sklářského potoka je kombinace smrku (*Picea abies*) a buku (*Fagus sylvatica*), ovšem od poloviny 18. století převládá smrková monokultura, která pokrývala většinu území povodí. Rozsáhlý úhyn smrkové monokultury, způsobený kyselou atmosférickou depozicí, defoliací a následným napadením hmyzu, vedl k lesní kalamitě. V roce 1984 bylo vykáceno 62% plochy povodí metodou holoseče a do konce osmdesátých let bylo vykáceno 88% plochy. Pohyb těžařské techniky způsobil vytvoření 10.3 km erozních rýh, přičemž 6.1 km rýh hlubších než 25 cm se napojilo na existující říční síť. Hustota říční sítě vzrostla z 1.45 km<sup>-1</sup> (před těžbou) na 7.55 km<sup>-1</sup> (po těžbě). Změny na povodí zapříčiněné lesní těžbou zvýšily erozi půdy 19 krát. Po přirozené obnově bylo v roce 2003 stále aktivních 1.5 km hlubších rýh spojených s říční sítí a 1 km mělkých rýh a tato situace se nezměnila do roku 2015.

Pro analýzu vývoje bylinného patra po smýcení lesa bylo vybráno 156 fytosociologických snímků (velikosti 4 x 4m), které zahrnovaly hluboké erozní rýhy (53 snímků), střední erozní rýhy (33 snímků), mělké erozní rýhy (38 snímků), plochy s mrtvým smrkovým porostem (15 snímků) a vytěžená stanoviště (17 snímků). Pro každý snímek byly určeny všechny druhy i s jejich početním zastoupením.

Poměrně nízká rozmanitost byla pozorována v bylinném pásmu při botanickém průzkumu, přičemž poměrně dominantní roli po smýcení převzalo travní společenství, konkrétně *Calamagrostis villosa*. Ve zkoumaných fytosociologických snímcích bylo nalezeno pouze 48 druhů. Ve zkoumaných oblastech s mrtvým lesním porostem byla pokryvnost bylinným patrem 100%, ale maximální množství druhů na snímek byl 6. V oblastech po smýcení byla pokryvnost 95-100% a pozorovaný počet druhů byl v rozmezí 5 – 10. V oblastech se středními rýhami (hloubka rýhy 25-50 cm) rostliny pokrývaly 20-75% plochy, druhové zastoupení 4-9, zatímco v hlubokých rýhách (hloubka větší jak 50 cm) byla pokryvnost pouze 1-30% a pozorované druhové zastoupení bylo 1-9 druhů. Bylo zaznamenáno, že některé druhy se vyskytovaly velmi zřídka ve středních a hlubokých rýhách oproti ostatním stanovištím (např. *Calamagrostis villosa*, *Galium hircynicum*, *Vaccinium myrtillus*). Poměrně rychlá obnova byla pozorována u mělkých rýh, 15% jejich povrchu bylo pokryto za tři roky a po 10 letech od těžby to již bylo 80%. Ve srovnání s mělkými rýhami bylo v hlubokých rýhách nalezeno více stres tolerujících rostlin (zhruba 45%), což souvisí s pozorovanou erozí vrchní vrstvy půdy a tím sníženým přísunem živin.

Podrobněji je celá problematika popsána v níže přiloženém článku: Soil conservation in a forested mountain catchment.

## SOIL CONSERVATION IN A FORESTED MOUNTAIN CATCHMENT

Josef Křeček<sup>(1)\*</sup>, Jana Nováková<sup>(2)</sup>, Ladislav Palán<sup>(1)</sup>, Eva Pažourková<sup>(1)</sup>

<sup>(1)</sup>Department of Hydrology, Czech Technical University, Prague, Czech Republic

<sup>(2)</sup>Independent botanist, Prague, Czech Republic

\* Corresponding author E.mail: josef.kreck@fsv.cvut.cz

### Abstract

In 1982–2015, environmental impacts of commercial forestry practices were studied in the Jizerka experimental catchment (the Jizera Mountains, Czech Republic). Skidding the timber by wheeled tractors caused 10.3 km<sup>-1</sup> of skid trails and the drainage density increased from 1.45 to 7.55 km<sup>-1</sup>. On the harvested runoff plots, not affected by skid trails, the loss of soil 0.007 - 0.014 mm year<sup>-1</sup> was comparable with undisturbed forests. But, the eroded soil in skid trails reached 6.17 mm (61.73 m<sup>3</sup> ha<sup>-1</sup>) by harvesting 23,882 m<sup>3</sup> of timber (i.e. 0.25 m<sup>3</sup> per 1 m<sup>3</sup> of harvested timber). At the catchment outlet, sediment yield reached 25% of the soil eroded. Natural regeneration of erosion rills was supported particularly by the development of herbaceous vegetation. In 2003, twelve years after the logging, only 1.5 km (15 %) of active deeper rills were still identified.

**Keywords:** *mountain catchment, acid rain, forestry practices, soil erosion, natural recovery.*

### Introduction

Topsoil erosion has been supposed as the most ultimately destructive process of soil degradation (Hillel, 2008). It results in the loss of soil productivity and off-site effects by mobilisation of agricultural chemicals and deposition of sediments. In the landscape-scale, Forman (1995) articulated the role of forests as benefits on reducing drainage network connectivity, stabilisation of slopes, and protection of soil and water quality. In Europe, approx. 70 percent of forests are controlled by management plans, and 25 percent are registered as forests of non-wood services with priorities in soil and water conservation (FOREST EUROPE, 2015). Effects of commercial forest practices on soil erosion are reported by O'Loughlin and Pearce (1984), Akbarimehr and Naghdi (2012), but, there are still uncertainties in their broader environmental consequences. In the 1980s, in central Europe, the acid rain calamity led to large-scale forest dieback and extensive timber harvest. The aim of this study is to analyze effects of forest clear cutting on drainage connectivity, soil erosion and sedimentation, and the natural recovery of a small headwater catchment in the Jizera Mts. (Czech Republic), 1982-2015.

## Material and methods

### Study area

The study was performed in the upper plain of the Jizera Mts. (Fig. 1): the Jizerka experimental catchment (50°48'21" - 50°48'59"N, 15°19'34" - 15°20'48" E, Elbe river district 1-05-01-004) operating since 1981.

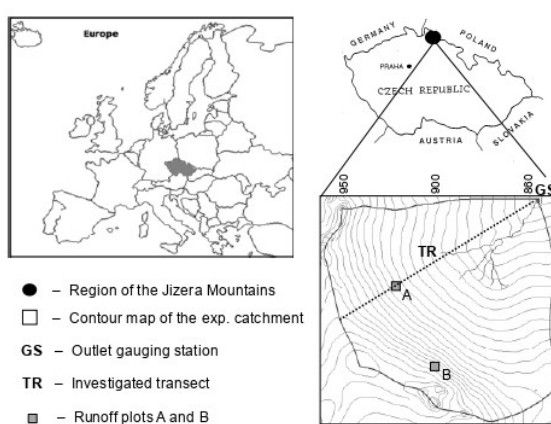


**Figure 1**  
*Jizera Mts. Region and the Jizerka experimental catchment.*

This area belongs to the North temperate climate zone (Köppen Dfc - sub-arctic region) with mean annual precipitation 1,400 mm, and mean annual air temperature 4°C (Tolasz, 2007). Low-base-status soils (sandy-loamy Podzols) developed on porphyritic granite achieves the depth from 0.5 to 1.2 m. Native forests include namely Norway spruce (*Picea abies*) and Common beech (*Fagus sylvatica*), but spruce plantations dominate since the second half of the 18<sup>th</sup> century. In the 1980s, the acid atmospheric deposition, followed by insect epidemics, defoliation and large-scale die-back of spruce plantations led to a forest calamity. After the clear-cut (1984–1988), grass communities *Junco effusi-Calamagrostietum villosae* became dominant, and has prolonged the forest regrowth (Křeček et al., 2010).

### Catchment monitoring

In 1982, the Jizerka catchment was instrumented by the sharp-crested V-notch weir with the automatic water level recorder at the stream-outlet. The volume of sediment has been estimated annually by changing bathymetry of the sedimentation pond (Fig. 2): the depth was measured manually in one-meter step using rubber boat moving in fixed cross sections. Along the basin transect TR standard meteorological observations were carried out in elevations 875 and 975 m.

Two elementary runoff plots (not affected by skid-trails), 30x30 m area, homogeneous slopes of approx. 10° (Plot A) and 20° (Plot B) were established to collect soil loss by 30 m long trenches covered with geotextile filter fabric (Fig. 1). Within the catchment area, inventory of erosion rills in skid trails was

accomplished in summer months of 1983 (before the harvest), 1985, 1990, 1995, 2003 and 2015.

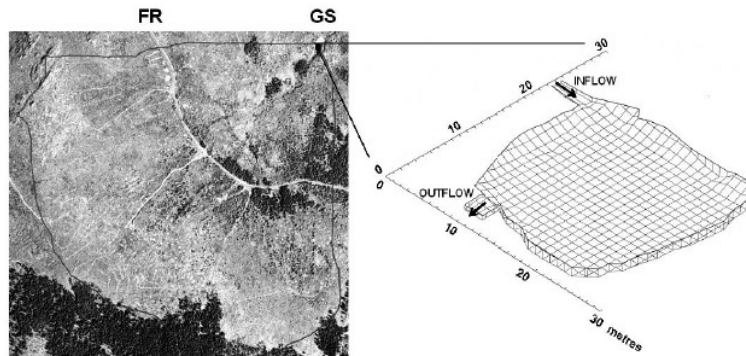


**Figure 2**  
*The Jizerka catchment after the forest harvest (1999).*

**FR** – Forest timber truck road  
**GS** – Outlet gauging station with sedimentation pond

The volume of erosion rills  $V$  (m<sup>3</sup>) was calculated by the volumetric equation [1]

$$V = \sum 0.5 (A_{i-1} + A_i) D \quad [1]$$

where:  $A_i$  – area of crosssection  $i$  (m<sup>2</sup>),  $A_{i-1}$  – area of crosssection  $i-1$  (m<sup>2</sup>),  $D$  – distance between crosssections (m).

Renard et al. (1997) proposed the empirical concept of revised universal soil loss equation (RUSLE) to predict the loss of soil by water erosion [2]

$$A = E I30 K (L/72.6)^m (a \sin \Theta + b) C P \quad [2]$$

where:  $A$  – average annual soil loss (tons acre<sup>-1</sup> year<sup>-1</sup>),  $E$  – storm rainfall energy (102 foot-tons acre<sup>-1</sup>),  $I30$  – maximum rainfall intensity in a 30 minute period within a storm (inch hour<sup>-1</sup>),  $K$  – soil erodibility factor (-),  $L$  – slope length (feet),  $m$  – slope length exponent,  $\Theta$  – slope angle (degrees),  $a$ ,  $b$  – coefficients in function making up slope term – values depend on slope (-),  $C$  – cropping management factor (-),  $P$  – conservation practice factor (-).

The size of eroded soil in the skidding lines was compared with the extent of harvested areas and volumes of harvested timber. On the whole, 156 phytosociological relevès (squares of 4 x 4metres) were investigated to analyse the herb layer development: this monitoring included 53 deep, 33 medium and 38 shallow rills, 15 plots with dead spruce stands, and 17 clear-cut spots. In the implemented phytosociological relevès, all species abundance was estimated, and the data transformed from Braun-Blanquet scale to 9-point scale of Van der Maarel (1979). Using the information on higher plants only, following characteristics were evaluated: percentage cover of herb layer; species richness (total species number

DOI: 10.6092/issn.2281-4485/8496

per relevè); life form categories of Raunkiaer (1934) according to Ellenberg et al. (1992). ANOVA statistics was used to test differences in the vegetation features among particular stands and age groups. The archive of LANDSAT imagery (NASA, 2014) was used to identify changes in the vegetative cover in the studied catchments (resolution of 30 m) in 1983–2016. Only clear-sky images collected in the high summer (June-August) were taken into account. From the multi-band raster images, five canopy classes were identified in the consecutive years 1983 – 2015 (Křeček and Krčmář, 2015). These classes (mature spruce forests, stands of the crown closure above 0.3, reforested plots with the crown closure below 0.3, areas covered only by grass communities, and clear-cut) correspond with the definition of “forest” used by the *United Nations Framework Convention on Climate Change*: crown closure > 0.3, and height >2–5 m at maturity), Sasaki and Putz (2009).

## Results

### Canopy changes

Initially, the Jizerka catchment was covered by mature spruce stands. In 1984, 62 % of the catchment area was harvested by clear-cutting, and about 88 % was harvested at the end of the 1980s. Canopy changes in 1982-2015 were reconstructed from the multi-band imagery (Fig. 3).

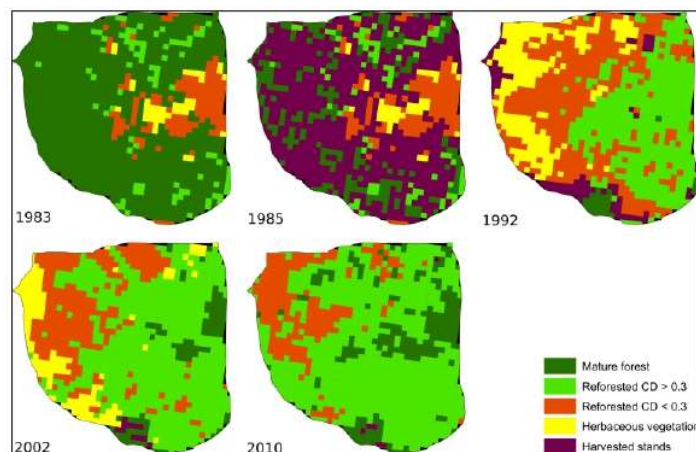


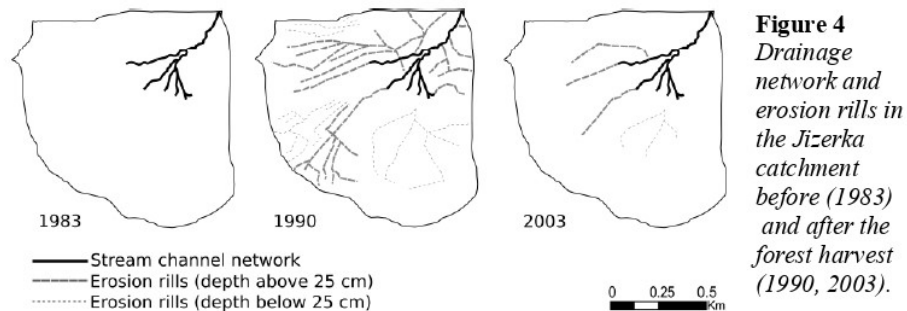
**Figure 3**  
Canopy in the Jizerka catchment, 1983-2010 (CD – crown closure of trees).

### Drainage network development

In the Jizerka catchment, before the forest harvest (Fig. 4), the drainage network was formed by 1,490 m of stream channels, the drainage density was  $1.45 \text{ km}^{-1}$  exceeding five times the value of  $0.26 \text{ km}^{-1}$  considered by Pallard et al. (2009) as critical for the risk of flooding. In 1984-1990, 10.3 km of skidding trails originated with the timber harvest; 6.1 km of rills deeper than 25 cm were directly connected with the existing drainage system. Thus, the drainage density increased from 1.45

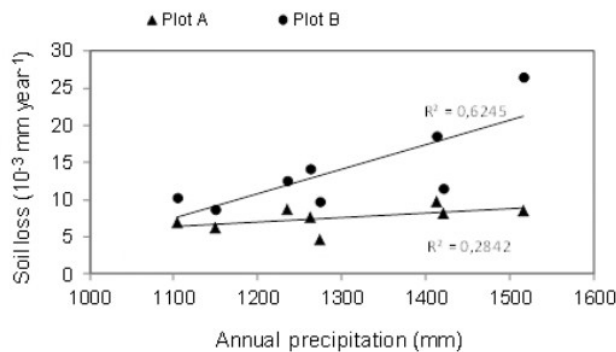


to  $7.55 \text{ km}^{-1}$ . With the natural regeneration, in 2003, only 1.5 km of active deeper rills (connected with the drainage network) and 1 km of shallow rills were identified (Fig. 4), and this situation did not change in 2015.



#### Soil erosion loss and sedimentation

Considering RUSLE parameters in the Jizerka catchment (Fig. 1), the maximum 30 minute rainstorm intensity  $I_{30} = 39 \text{ mm}$ , soil erodibility factor  $K = 0.26$ , and alternative values of the cropping management factor  $C$  (0.002 – coniferous forests, 0.09 – grassland, and, 0.325 - disturbed forest land, according to Panagos et al., 2015). The predicted loss of soil achieves maximum values  $0.0239 \text{ t ha}^{-1} \text{ year}^{-1}$  (spruce stands),  $1.38 \text{ t ha}^{-1} \text{ year}^{-1}$  (grassland) and  $5.01 \text{ t ha}^{-1} \text{ year}^{-1}$  (disturbed forest). Thus, for the scenario of clear-cut disturbances at Jizerka, predicted loss of soil might reach maximum 30 mm per year in extreme hill sites. Annual values of the soil loss observed in harvested runoff plots A and B are relatively small at both slopes ( $10^\circ$  and  $20^\circ$ ):  $0.007$  and  $0.014 \text{ mm year}^{-1}$  corresponding with those of undisturbed forests (Elliot et al., 1996). These plots were not damaged by skid trails, thus, the litter cover and herbaceous understory protected well the soil surface.



The washed soil included particles of raw humus (65%) and fine sand (35%). In the higher slope (plot B), there is a significant correlation of the annual loss of soil with annual precipitation ( $R = 0.79$ ,  $R_{crit} = 0.71$ ,  $p = 0.05$ ,  $n = 8$ ), contrary to the lower slope (plot A), Fig. 5.

The development of erosion rills and volume of eroded soil with the harvest of timber (and reduce in the area of mature stands) is given in Fig. 6. After the timber harvest, in 1990, the total length of 10.3 km significant skid trails represented volume of 8,122 m<sup>3</sup> erosion rills. From ten detailed skid trail profiles on slopes 5 – 15°, there was found in average 24% of that volume lost by crushing out and soil compaction.

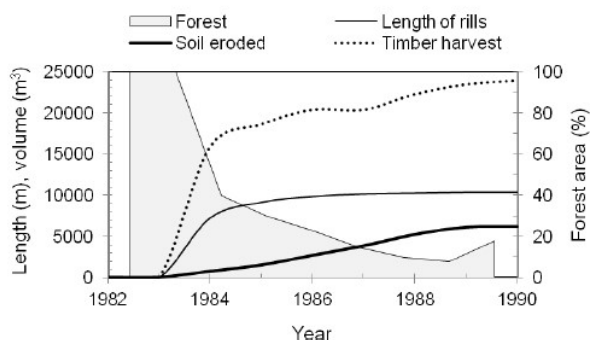


**Figure 6**  
Cumulative growth of rills and eroded volume of soil with forest harvest: the Jizerka catchment (1982-1990).

Therefore, in 1984 – 1990, the total transport of soil from the network of erosion rills was approx. 6,173 m<sup>3</sup> (i.e. 61.73 m<sup>3</sup> ha<sup>-1</sup>, or 6.17 mm). By the harvest of 23,882 m<sup>3</sup> of timber (i.e. 238.82 m<sup>3</sup> ha<sup>-1</sup>), the loss of soil was 0.25 m<sup>3</sup> per each 1 m<sup>3</sup> of harvested timber. Annual values of sediment yield observed at the catchment outlet are in Fig. 7.

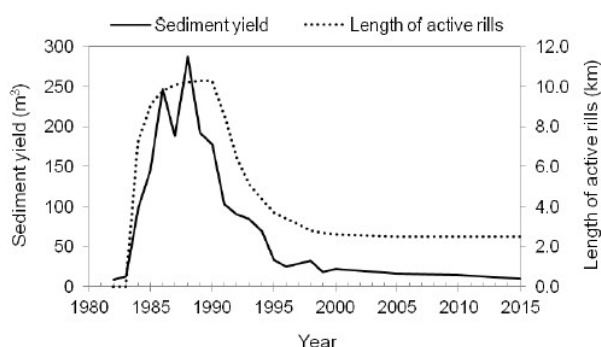


**Figure 7**  
Annual sediment yield and length of active erosion rills: the Jizerka catchment (1980-2015).

Before the harvest (1982-1983), the annual sediment yield was 0.01 mm year<sup>-1</sup>; while in the harvest period (1984-1990), the total yield of sediment was 1.34 mm

(i.e.  $0.19 \text{ mm year}^{-1}$ ). Thus, in the harvest period, sediment yield increased 19 times, and accomplished 22% of the volume of soil (6.17 mm) transported from the network of erosion rills (skid trails). In 1991-2015, the length of active erosion rills has decreased from 10.3 to 2.5 km by natural regeneration (Fig. 7); the total volume of sediment yield  $1,525 \text{ m}^3$  represents 25% of the eroded soil in the skid trails ( $6,156 \text{ m}^3$ ).

### **Natural recovery of skid-trails**

In the Jizerka catchment, a long-term defoliation of spruce stands and the extended clear-cut led to relatively low species richness in herb layers with dominating *Calamagrostis villosa*. In all investigated relevés, only 48 plant species were identified; the stand characterization included: dead forests with the herb layer covering 100% of the area and low number of species (maximum 6 per relevé), forest clearings with the herb cover 95-100% and number of species 5-10, middle erosion rills (between 25 and 50 cm) with plant cover 20-75%, and species richness 4-9, and deep erosion rills (depth above 50 cm) with plant cover only 1-30% and variable species richness (1-9). The species composition in forest clearings is associated with the harvested forest type and former composition of the herb layer (Nováková and Křeček, 2006). Plant cover was affected particularly by the depth of erosion rills ( $R^2 = 0.42$ ), few species were present noticeably rarely in the middle and deep rills in comparison with the other stands (e.g. *Calamagrostis villosa*, *Galium hircynicum*, *Vaccinium myrtillus*). Considering growth forms, the percentage of plants forming tillers decline gradually from clearings and dead forests (almost 40%) to shallow (33%) and deep rills (29%), in the same direction, the proportion of plants forming clusters increased from 60 to 71%. Within the life forms, hemicryptophytes dominate, they form 70-80% of species present in rills and dead forest stands against only 60% present in clear-cut areas. Only a weak positive correlation ( $R = 0.21$ ,  $p = 0.091$ ) was found between the species richness and slope. After the forest harvest, a relatively fast natural rehabilitation of shallow rills (depth below 25 cm) was observed: about 15% of their surface has been covered by grass (mainly hemicryptophytes) in 3 years, and 80% in 10 years after timber skidding. In deep rills, there is slightly higher proportion of stress-tolerant plants (45%) in comparison with shallow rills.

### **Discussion and conclusions**

Before the timber harvest, in the Jizerka catchment, the annual sediment yield ( $0.01 \text{ mm year}^{-1}$ ) is below the approximate annual soil genesis ( $0.036 \text{ mm year}^{-1}$ , given for a mountain environment in the humid temperate climate by Vladychenskiy, 2009); but, the clear-cut (1984-1990) led to exceeding the rate of soil genesis by four times in 12 consecutive years of 1984-1995. In 1996-2015, the sediment yield ( $0.021 \text{ mm year}^{-1}$ ) is back below the rate of soil formation. However, still in 1996-2015, the mean annual sediment yield ( $0.021 \text{ mm year}^{-1}$ ) is higher in comparison

with values ( $0.01 \text{ mm year}^{-1}$ ) before the harvest (1982-1984). After the forest harvest, a relatively fast natural rehabilitation of shallow rills (depth below 25 cm) was observed: about 15 % of their surface has been covered by grass (mainly hemicryptophytes) in 3 years, and 80 % in 10 years after timber skidding. The rate of erosion in skid trails is driven particularly by their depth and slope (Elliot et al., 1996); but, the depth of rills depends also on the frequency of timber skidding and hydrological conditions (Nearing et al., 1997). In deep rills at Jizerka was found a higher proportion of stress-tolerant plants (45%) in comparison with shallow rills; it confirms the low nutrient availability at the places where the top soil horizon was removed (Urbanska and Fattorini, 2000). In Central Europe, 250 years tradition of sustainable forest management has respected the ecosystem approach on multiple functions as well as conservation of soil and water (Spathelf, 2010). However, exogenic calamities (like the large scale acid rain impact) could affect this approach for a relatively longer period. In the Jizerka catchment, the signs of higher sediment runoff are remarkable from 1984 to 2015. There are several management practices used in forestry operations to mitigate the impact of logging, forest road and skid trail construction on stream water quality (Wallbrink and Croke, 2002, Spathelf, 2010): these practices are designed to control erosion and to minimize the delivery of sediments to drainage lines. Theoretically, with respect of those regulations in the forest clear-cut at Jizerka, it was possible to avoid the significant loss of soil by keeping the benefit of reducing the acid atmospheric load (Křeček et al., 2017).

### **Aknowledgements**

This research was supported by the Earthwatch Institute (Oxford, UK, Project on Mountain Waters of Bohemia, 1991–2012), the Czech Ministry of Education (INTER-EXCELLENCE: INTER-COST LTC 17006, 2017) and the Czech Technical University in Prague (SGS16/140/OHK1/2T/11, 2016-2017).

### **References**

- AKBARIMEHR M., NAGHDIR. (2012) Reducing erosion from forest roads and skid trails by management practices. *Journal of Forest Science*, 58:165–169.
- ELLENBERG H., WEBER H.E., DULL R., WIRTH V., WERNER W., PAULISSEN D. (1992) Zeigerwerte von Pflanzen in Mitteleuropa. *Scripta Geobotanica*, 18:1-258.
- FAO (2008) Forests and water, FAO Forestry paper 155, Food and Agriculture Organization of the United Nations, Rome, Italy, 78 p.
- FOREST EUROPE (2015) State of Europe's Forests 2015, Ministerial Conference on the Protection of Forests in Europe, FOREST EUROPE Liaison Unit Madrid, Spain, 312 p.
- FORMAN R.T.T. (1995) Land Mosaics. *The Ecology of Landscapes and Regions*, Cambridge University Press, Cambridge, 656 p.
- HILLEL D. 2008. *Soil in the Environment*, Academic Press, Cambridge, 320 p.
- KŘEČEK J., HOŘICKÁ Z. (2001) Degradation and recovery of mountain watersheds: the Jizera Mountains, Czech Republic. *Unasylva* 52:43-49.

- KŘEČEK, J., NOVÁKOVÁ J., HOŘICKÁ Z. (2010) Ellenberg's indicator in water resources control: the Jizera Mountains, Czech Republic. *Ecological Engineering*, 36:1112-1117.
- KŘEČEK J., KRČMÁŘ V. (2015) Landsat imagery applications to identify vegetation recovery from acidification in mountain catchments. *Hungarian Geographical Bulletin*, 64:121–126.
- KŘEČEK J., PALÁN L., STUHLÍK E. (2017) Acid atmospheric deposition in a forested mountain catchment. *iForest* 10:680-686.
- NASA (2014) Landsat science, <http://landsat.usgs.gov>, accessed on the 24th October 2016.
- NOVÁKOVÁ J., KŘEČEK J. (2006) Soil erosion and plant succession at clear-cut areas in the Jizera Mountains, Czech Republic. *Ecology (Bratislava)* 25:259-269.
- O'LOUGHLIN C.L., PEARCE A.J. (1984) *Symposium on Effects of Forest Land Use on Erosion and Slope Stability*, Environment and Policy Institute East-West Center, University of Hawaii, Honolulu, 310 p.
- PALLARD B., CASTELLARIN A., MONTANARI A. (2009) A look at the links between drainage density and flood statistics. *Hydrology and Earth System Sciences*, 13:1019–1029.
- PANAGOS, P., BORELLI, P., MEUSBURGER, K., ALEWELL C.; LUGATO E.; MONTANARELLA L. (2015) Estimating the soil erosion cover-management factor at the European scale. *Land Use Policy*, 48:38–50.
- RAUNKIAER C. (1934) *The Life Forms of Plants and Statistical Plant Geography*. Oxford University Press, Oxford, 632 p.
- RENARD K.G., FOSTER G.R., WEESIES G.A., McCOOL D.K., YODER D.C. (1997) *Predicting Soil Erosion by Water: A Guide to Conservation Planning with the Revised Universal Soil Loss Equation (RUSLE)*, USDA Agriculture Handbook 703, USDA-ARS, Tucson, Arizona, 404 p.
- SASAKI N., PUTZ F.E. (2009) Critical need for new definitions of “forest” and “forest degradation” in global climate change agreements. *Conservation Letters*, 2:1-7.
- SPATHELF P. (2010) *Sustainable Forest Management in a Changing World: A European Perspective*. Springer, Dordrecht (the Netherlands), 263 p.
- TOLASZ R. (2007) *Climate Atlas of the Czech Republic*, Czech Hydrometeorological Institute, Prague, Czech Republic, 256 p.
- URBANSKA K.M., FATTORINI M. (2000) Seed rain in high-altitude restoration plots in Switzerland. *Restoration Ecology*, 8:74-79.
- VAN DER MAAREL E. (1979) Transformation of cover-abundance values in phytosociology and its effect on community similarity. *Vegetatio*, 39:97-114.
- VLADYCHENSKIY A.S. (2009) Genesis of Soil and Factors of the Soil Formation, in Glazovsky, G.N., Zaitseva, N. (eds) *Environment Structure and Function: Earth System, Encyclopedia of Life Support Systems, EOLSS*, Oxford, United Kingdom, 95-107.
- WALLBRINK P.J., CROKE G. (2002) A combined rainfall simulator and tracer approach to assess the role of Best Management Practices in minimising sediment redistribution and loss in forests after harvesting. *Forest Ecology and Management*, 170:217–232.

## **CONSERVATION DES SOLS EN BASIN DE MONTAGNE FORESTIER**

### **Résumé**

De 1982 à 2015, les impacts environnementaux des pratiques forestières commerciales ont été analysés dans le bassin expérimental Jiserka situé dans les montagnes Jizera en République tchèque. Le débusquage d'arbres par les tracteurs à roues ont causé l'envasement des sentiers sur  $10.3 \text{ km}^{-1}$  et l'augmentation de la densité de drainage passant de  $1.45$  to  $7.55 \text{ km}^{-1}$ . Sur les parcelles de ruissellements récoltées non affecté par l'envasement des sentiers, la perte annuelle des sols de  $0.007$  à  $0.014 \text{ mm}$   $0.007 - 0.014 \text{ mm}^{-1}$  était comparable avec les forêts où il n'y a pas de pratiques forestières commerciales. Mais le sol érodé dans les sentiers envasés a atteint  $6.17 \text{ mm}$  ( $61.73 \text{ m}^3 \text{ ha}^{-1}$ ) par la récolte de  $23,882 \text{ m}^3$  de bois (c-à-d.  $0.25 \text{ m}^3$  par  $1 \text{ m}^3$  de bois récolté). À la sortie de captage, le rendement sédimentaire du sol érodé a atteint 25%. La régénération naturelle de l'érosion des ruissellements était compensée par la végétation herbacée. In 2003, douze années plus tard, seulement  $1.5 \text{ km}$  (15 %) des zones de ruissellements actifs étaient toujours repertoriées.

**Mots-clés:** *bassin de montagne; pluie acide; pratiques forestières; érosion du sol; récupération naturelle.*

## **CONSERVAZIONE DEL SUOLO IN UN BACINO MONTANO BOSCATO**

### **Riassunto**

Gli impatti ambientali delle utilizzazioni forestali sono stati studiati fra il 1982 ed il 2015 nel bacino sperimentale di Jizerka (Jizera Mountains, Repubblica Ceca). Il trascinamento dei tronchi per mezzo di trattori forestali ha causato la formazione di  $10.3 \text{ km}^{-1}$  di piste di esbosco ed un aumento della densità di drenaggio da  $1.45$  to  $7.55 \text{ km}^{-1}$ . In partelle sperimentali sottoposte a taglio ma non interessate da piste di esbosco la perdita di suolo variava fra  $0.007 - 0.014 \text{ mm year}^{-1}$ , risultando confrontabile con quella della foresta indisturbata. L'erosione del suolo lungo le piste di esbosco, al contrario, raggiungeva  $6.17 \text{ mm}$  ( $61.73 \text{ m}^3 \text{ ha}^{-1}$ ) rispetto all'asportazione di  $23,882 \text{ m}^3$  di legname ( $0.25 \text{ m}^3$  per  $1 \text{ m}^3$  of legname). Alla sezione di chiusura del bacino la produzione di sedimento risultava pari al 25% del suolo eroso. La rigenerazione naturale dei solchi di erosione è stata determinata principalmente dallo sviluppo di vegetazione erbacea. In 2003, dodici anni più tardi, solo  $1.5 \text{ km}$  (15 %) dei solchi di erosione attivi più profondi potevano ancora essere identificati.

**Parole chiave:** *bacino montano; piogge acide, pratiche forestali; erosione del suolo; ripristino naturale*

### 3.3. Vliv extrémních hydrologických jevů na bioindikaci kvality vody

V týdnu 3. - 9. srpna 2010 byla na povodí Holubího potoka zaznamenána extrémní suma srážkového úhrnu 434 mm, přičemž 313 mm/den spadlo při bouřkové události 7. srpna 2010. Na uzávěrovém profilu povodí je měrný objekt s kombinovaným přelivem – ostrohranný trojúhelníkový Thomson a obdelníkový Poncelet. Kapacita měrného objektu je 0.39 m<sup>3</sup>/s (odpovídá zhruba době opakování 12 let), povodně s vyšším průtokem musí být odhadovány z terénního šetření povodňových stop. Z povodňových stop byl odhadnut průtok srpnové události na 2.25 m<sup>3</sup>/s.

Tato událost byla modelována v programu HEC-HMS 4.4, kde byl modelován maximální průtok 2.38 m<sup>3</sup>/s. Hodnota takového průtoku je těsně pod dobou opakování 1 000 let ( $Q_{1000} = 2.46 \text{ m}^3/\text{s}$ , zjištěno interpolací ročním maxim Log-normálním rozdělením). Po tři hodiny intenzita deště překračovala infiltrační kapacitu půdy, takže dominoval povrchový odtok. Průměrné roční množství sedimentu pozorované v měrném objektu je 0.46 m<sup>3</sup>/rok, po této extrémní události bylo množství sedimentu v měrném objektu 2.7 m<sup>3</sup>. Ovšem zanedbatelná půdní eroze byla zjištěna na dvou experimentálních plochách (velikosti 30 x 30 m) pro zjištění geneze odtoku umístěných v mladém a vzrostlém bukovém porostu. Eroze tedy velkou měrou pocházela z toku, základní morfologie toku se nezměnil (tvořena velkými žulovými kameny), ale změnila se distribuce části dna z jemného na střední štěrk.

Během let 2010-2012 bylo v toku provedeno vzorkování makrozoobentosu před povodní i po ní v období jarního tání, v létě a na podzim. Vzorkování bylo provedeno standardní metodou kick-net sampling v úseku zhruba 100 m od uzávěrového profilu v 6 typech habitatů charakterizujících tok. Povodeň měla okamžitý devastující efekt na bentické organismy a negativně ovlivnila druhové i početní zastoupení na několik měsíců. Zhruba 9 měsíců po povodni byl zaznamenán vrchol v počtu zastoupených druhů a jedinců, způsobený neúspěšnou kolonizací cizích druhů, které nebyly pozorovány před povodní. Z šetření navíc vyplývá, že druhy, které ke svému životu potřebují jemný štěrk, mechový porost či měkký substrát (jenž podlehl erozi při povodni) nedosáhly počtu před povodni nebo zcela vymizely, z čehož můžeme usuzovat, že dno toku se stále nevrátilo do původní podoby. Ani dva roky po povodni nebyla pozorována celková obnova makrozoobentosu.

Podle měřených chemických veličin by se před povodní dalo vodní prostředí specifikovat jako mírně antropogenně okyselené. Po povodni byl pozorován statisticky významný pokles v měrné vodivosti, obsahu síranů, fluoridů, chloridů a hořčíku. Obsah vápníku a dusičnanů se rovněž snížily, zatímco hodnoty pH a alkalita se zvýšily, ale tyto změny nebyly statisticky významné. Zjištěné hodnoty i jejich vývoj naznačují dlouhodobé zotavování toku z acidifikace, tento trend lze vidět i na zvyšující se hodnotě pH srážek i vody v toku pozorovaný v letech 1995-2015. Povodeň částečně přispěla k zotavení toku z antropogenní acidifikace poklesem obsahu síranů (vyčerpání zásob síranů v půdě), v dlouhodobém hledisku však celkový průběh zotavení prostředí neovlivnila.

Blíže je celá problematika popsána v níže přiloženém článku: Impact of an extreme flood on the ecosystem of a headwater stream.



## Impacts of an extreme flood on the ecosystem of a headwater stream

Eva Pažourková,<sup>1</sup> Josef Křeček,<sup>1\*</sup> Peter Bitušík,<sup>2</sup> Pavel Chvojka,<sup>3</sup> Lenka Kamasová,<sup>4</sup> Takaaki Senoo,<sup>4</sup> Jan Špaček,<sup>5</sup> Evžen Stuchlík<sup>4</sup>

<sup>1</sup>Department of Hydrology, Czech Technical University in Prague, Thakurova 7, CZ-16629 Prague 6, Czech Republic; <sup>2</sup>Department of Biology and Ecology, Matej Bel University, Tajovského 40, SK-97401 Banská Bystrica, Slovakia; <sup>3</sup>Department of Entomology, National Museum, Cirkusová 1740, CZ-19300 Prague 9, Czech Republic; <sup>4</sup>Institute of Hydrobiology, Biology Centre, Czech Academy of Sciences, Na Sádkách 7, 370 05 České Budějovice, Czech Republic; <sup>5</sup>Povodí Labe, s.p., Vita Nejedlého 951, CZ-50003 Hradec Králové, Czech Republic

### ABSTRACT

Headwater streams are the smallest parts of rivers but make up the majority of river miles. The chemistry and macroinvertebrate composition of such streams are among the most important indicators of their environmental health. Macroinvertebrates are affected namely by runoff genesis and, in many regions of the world, also by acid atmospheric deposition and its consequences. The aim of this paper is to evaluate the impacts of an extreme summer flash flood on the physical environment, chemistry and macroinvertebrates in a small headwater stream located in the Beech-woods National Nature Reserve of the Jizera Mts. (Northern Bohemia, Czech Republic). The studied stream is characterized by a pluvial hydrologic regime with perennial streamflow uniformly distributed within the year, with peak-flows originating mainly from summer rainstorms, and moderate current anthropogenic acidification. During the observed summer flash flood of the return period near 1,000 years, high currents ( $1\text{--}2.5\text{ m s}^{-1}$ ) flushed out  $2.7\text{ m}^3$  of sand and gravel from the streambed, resulting in a devastating effect on macroinvertebrates. Both number of species/taxa and diversity were reduced by about 50% while the abundance of surviving taxa was reduced to about 10% compared with before the flood. The following spring after the event, both number of species/taxa, diversity and abundance increased, partially due to the temporary unsuccessful colonization of the site by several alien species creating a peak of biological diversity, but complete recovery of the original macroinvertebrate assemblages was not observed even during the subsequent two years. On the other hand, a significant drop in sulphate contents and rising alkalinity observed in stream waters during base flow conditions after the flood indicate positive effects on recovery of the aquatic environment by depleting the catchment sulphur pool. Thus, the flood did not significantly alter the long-term recovery of the studied headwater stream from acidification.

### INTRODUCTION

Headwater streams are the smallest part of rivers but make up the majority of river miles, providing habitats that are unique compared to other freshwater environments and used by a specialized subset of aquatic species (Richardson, 2019). Chemistry and macroinvertebrates are among the most important indicators of the environ-

mental health of headwater streams (Fritz *et al.*, 2013), while floods (overflows of stream water beyond normal limits) are among the most important natural hazards (Hickey and Salas, 1995). Extreme floods, defined by a return period exceeding 50 years (i.e. a 2% chance of incidence (Davis, 2007)), have huge destructive power, devastating landscapes and settlements but also aquatic environments (Knox and Kundzewicz, 1997). Macroinvertebrate assemblages of stream bottoms respond to the structure and functions of fluvial ecosystems (Allan and Castillo, 2007), and benthic macroinvertebrates are considered a very effective indicator of environmental health because of their limited mobility, relatively long life cycles and varied sensitivity to different types of pollution (Rashid and Pandit, 2014). Therefore, macroinvertebrate studies have been used for water quality assessments by several environmental monitoring programmes (Rosenberg and Resh, 1993; Dar and Ganai, 2017). While biological diversity in rivers is usually influenced by a combination of pressures from various anthropogenic impacts (Adámek *et al.*, 2010), communities in headwater streams are affected namely by water velocity and associated physical forces (Allan and Castillo, 2007). Thus, in mountain streams an adequate dynamic approach reflecting rapidly changing currents and discharge needs to be considered in analysing their water environment. Most

Corresponding author: josef.kreck@fsv.cvut.cz

Key words: Headwater catchment; acidification and recovery; flash flood; macroinvertebrates; species diversity.

Edited by: Francesca Bona, Dept. of Life Sciences and Systems Biology, University of Turin, Italy.

Received: 1 December 2020.  
Accepted: 30 March 2021.

This work is licensed under a Creative Commons Attribution Non-Commercial 4.0 License (CC BY-NC 4.0).

© Copyright: the Author(s), 2021  
Licensee PAGEPress, Italy  
*J. Limnol.*, 2021; 80(2):1998  
DOI: 10.4081/jlimnol.2021.1998

studies, however, concentrate primarily on base-flow conditions (Falkenmark and Allard, 2015).

In Central Europe, the biota in many mountain streams has been affected by acid atmospheric deposition and its consequences (Horecký *et al.*, 2013). Anthropogenic emissions of acidic precursors (sulphur and nitrogen oxides, and ammonia) increased from the industrial revolution of the 19th century and culminated in the late 1980s (Schöpp *et al.*, 2003). In the Czech Republic, mountain waters of low mineralization (and acid-neutralizing capacity) were stressed by strong acidification, with natural acidity (based on humic substances) overwhelmed by anthropogenic acidity (Veselý and Majer, 1996; Stuchlík *et al.*, 2006). This resulted in the rapidly decreasing pH of mountain streams and a dramatic decline in water quality including increased contents of heavy metals and toxic forms of aluminium (Křeček and Hořícká, 2001; Křeček *et al.*, 2019).

Since the early 1990s, with international cooperation to reduce atmospheric emissions (namely, the 1985 Helsinki Protocol on the Reduction of Sulphur Emissions or their Transboundary Fluxes by at least 30 percent; Holen *et al.*, 2013), signs of recovery in acidified headwater catchments were seen in Central Europe (Stuchlík *et al.*, 1997; Křeček and Hořícká, 2006), as well as in other parts of Europe and North America (Godbold and Hüttermann, 1994). However, ongoing recovery could be affected by changing physical forces. The aim of this paper is to evaluate the impacts of an extreme summer flash flood on the physical environment, chemistry and benthic macroinvertebrates in a small mountain stream in the context of atmospheric acid loads and recovery from acidification.

## METHODS

This study was performed in the Jizera Mountains (Northern Bohemia, Czech Republic): in the experimental catchment of the Holubí Potok stream, near the Oldřichov settlement (HPO catchment, 50°52'14"– 50°52'30"N, 15°6'11"– 15°6'21"E, Odra river district 2-04-10-014, Fig. 1, Tab. 1). The site is located in the National Nature Reserve "Beech-woods of the Jizera Mts." covered by semi-native forest stands with Common beech (*Fagus sylvatica*) dominating. This area has a humid continental climate (Köppen's Dfb) with mean annual precipitation 940 mm, mean air temperature 8.3°C, and an average of 86 days with snow cover (Tolasz *et al.*, 2007). Low-base-status soils (sand-loamy brown forest soils) developed on porphyritic granite reach depths of 0.7–1.3 m. The stream channel is characterized by steep gradients with step-pools (Palucis and Lamb, 2017) and a water depth below 0.5 m at bankfull discharge. The bed is covered by non-uniform sediments (sand, gravel and boulders) with a predominantly gravel substrate. Mean annual water

temperature is 9.3°C with a monthly minimum of 1.6°C in January and maximum of 16.4°C in July.

In the 1980s, the Jizera Mts. region (part of the so-called Black Triangle) was strongly affected by acid atmospheric loads. Plantations of Norway spruce (*Picea abies*) in the upper mountain ridges were heavily damaged and subsequently harvested by clearcutting, but only moderate defoliation (up to 20%) was observed in beech stands of the investigated catchment (Křeček and Hořícká, 2006), reflecting the fact that common beech trees show an intermediate tolerance to atmospheric emissions (Vacek *et al.*, 2007).

The experimental catchment was instrumented in 1982 (and re-instrumented in 1995). The outlet is equipped with a composite sharp-crested weir (Thomson V-notch and Poncelet weirs) and water level is measured by an ALA 4020 compound water pressure and temperature recorder, logging every ten minutes. The capacity of the gauging station (0.39 m<sup>3</sup> s<sup>-1</sup>) corresponds to a 12 years return period (see Tab. 4 in the results section). Thus, peak discharges above this limit were estimated by terrain footprints (Herget *et al.*, 2014), with the empirical Manning

**Tab. 1.** Morphology of the HPO catchment (for elevation and slope, arithmetic means with range values are given).

Parameter	Unit	Value
Area	(km <sup>2</sup> )	0.23
Elevation	(m)	518 (409 – 620)
Slope	(%)	34.5 (0.1 – 83.2)
Shape index	(–)	1.56
Length of streams	(m)	405
Drainage density	(km <sup>-1</sup> )	1.76
Slope of the stream	(%)	11.2 (10.1 – 15.3)
Strahler stream order	(–)	1

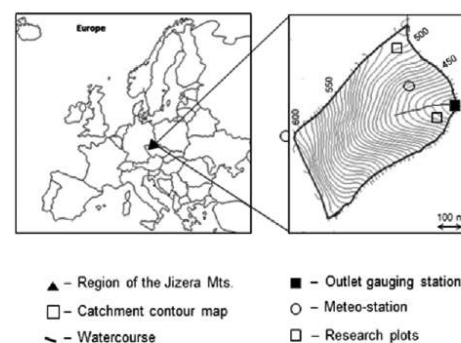


**Fig. 1.** The HPO experimental catchment.

equation (Venutelli, 2005) for mean flow velocity  $v$  into the continuity equation describing discharge  $Q$  as a product of cross-section area  $A$  and flow velocity  $v$ :

$$Q = A R^{2/3} S^{1/2} n^{-1} \quad (\text{eq. 1})$$

where:  $Q$  - the discharge ( $\text{m}^3 \text{s}^{-1}$ ),  $A$  - the cross-section area ( $\text{m}^2$ ) for the specific flood level,  $R$  - the hydraulic radius (m) for the flood level determined as a quotient of the cross-section area  $A$  ( $\text{m}^2$ ) and the wetted perimeter  $P$  (m),  $S$  - the energy line slope ( $\text{m m}^{-1}$ ), and  $n$  - the hydraulic roughness coefficient (-).

Flood waves were constructed by HEC – HMS 4.4 (USACE, 2000). The HEC – RAS 5.0.3 package (USACE, 2016) was used to simulate flow velocities and water depth in the HPO stream channel during the extreme event, with two dimensional unsteady flow calculations performed using the observed discharge at the catchment outlet as boundary conditions. The cross section geometry was measured along the stream channel every 10 m from the gauging station to the channel head, and the values of Manning's roughness coefficient  $n$  were estimated from the channel configuration using Cowan's composite approach (Wibowo *et al.*, 2015):

$$n = (n_0 + n_1 + n_2 + n_3 + n_4) m \quad (\text{eq. 2})$$

where:  $n_0$  represents surface roughness (caused by larger or smaller grain size of the sediments at the channel bottom up to minor submerged obstacles);  $n_1$  is the value including the effect of surface irregularities;  $n_2$  represents variations in the shape and size of the channel cross-section;  $n_3$ , for barriers;  $n_4$ , for vegetation; and  $m$  is a correction factor for channel meandering.

A digital terrain model of the catchment was created in ArcGIS 10.2 from the contour lines of 5 m resolution and the stream channel layers.

Standard meteorological observations (precipitation, solar radiation, air temperature and moisture, wind speed, soil moisture, registered every hour by the ALA monitoring system) were carried out in a forest opening (relatively well-sheltered from wind effects; Shaw, 2011), located in the centre of the catchment (elevation of 498 m, Fig. 1). Additional observations in two forest plots (30 x 30 m area, elevations of 409 and 507 m) addressed runoff genesis in young and mature beech stands.

Although stream water chemistry at HPO is the subject of long-term monitoring (Křeček and Hořická, 2001), this study of the extreme flood is based on ten samplings of stream water for detailed chemical analyses from 2009–2012 and eight samplings of macroinvertebrates over three years (2010–2012) during comparable base-flow regimes (Tab. 2). Stream water was sampled by a plastic jar near the catchment outlet, filtered through 40- $\mu\text{m}$  polyamide

mesh in site, kept in prewashed 0.5 L PET bottle, stored in the refrigerator, and analysed in the laboratory of the Hydrobiological Station Velký Pálenec (Charles University, Prague), which regularly participated in the UNECE ICP Waters international chemical and biological inter-comparisons. Concentrations of major ions were identified by ion chromatography with conductometric detection, pH measured with combination electrodes at the beginning of the determination of alkalinity by Gran titration on a TIM 900 automatic titrator (Radiometer Analytical), and specific conductivity was identified by a conductometric sensor (Radiometer Analytical) at the reference temperature 25°C (Stuchlík *et al.*, 2006). Benthic macroinvertebrates were sampled by a kick net, mesh-size 500  $\mu\text{m}$  (Rosenberg and Resh, 1993) at 6 different microhabitats reflecting the range of stream bed types along a 100 m stretch near the catchment outlet. The sampling dates included periods of snowmelt (March–May), summer (July–August), and the relatively dry autumn period (September–October). Quantification of samples was achieved by using a standard sampling time of 3 min at each microhabitat. Collected animals were preserved in 80% ethanol; determination of organisms and enumeration of each taxon were performed by specialists in the co-authors' team (usually to species level when allowed by the developmental stage). Evaluations of macroinvertebrate assemblages were based on the number of individuals and the number of species/taxa; biological diversity was characterised by indexes of Shannon entropy  $D_{SH}$  and Simpson concentration  $D_{SC}$ , equations (3) and (4), as they translate indexes of species diversity into effective numbers of species (Jost, 2006; Velle *et al.*, 2013).

$$D_{SH} = \exp(-\sum_1^S p_i \ln p_i) \quad (\text{eq. 3})$$

$$D_{SC} = 1 / \sum_1^S p_i^2 \quad (\text{eq. 4})$$

where:  $S$ , total number of taxa;  $p_i$ , relative number of individuals of taxon  $i$ ;  $\ln$ , natural logarithm;  $\exp$ , based on the Euler number (2.718).

**Tab. 2.** Macroinvertebrate sampling dates and physical properties of the stream water.

Sampling day	Discharge $Q_i$ ( $10^{-3} \text{ m}^3 \text{ s}^{-1}$ )	Water temperature $T$ ( $^{\circ}\text{C}$ )
18-Mar-10	1.72	4.9
27-Apr-10	0.73	8.2
28-Jul-10	1.68	12.6
5-Sep-10	2.04	9.7
16-Oct-10	1.65	7.5
4-May-11	0.62	6.2
13-Oct-11	1.73	7.1
21-Oct-12	2.11	5.9

GraphPad InStat 3.1 (Motulski, 2007) was employed to analyse basic statistics of the collected data; the non-parametric Mann Whitney two-tailed test was used to identify the statistical significance of changes in both means and standard deviations for chemical and biological characteristics before and after the flood, and trends in time series were tested by Spearman's correlation coefficient. Statistical significance was considered at the 0.05 probability level.

## RESULTS

### Stream flow dynamics

The studied HPO catchment is characterized by a pluvial hydrologic regime (Shaw, 2011) with perennial streamflow uniformly distributed within the year, and peak-flows originating mainly from summer rainstorms. Based on daily flow frequencies observed at the outlet from 1982-2018, the 90% frequency discharge ( $Q_{330} = 0.53 \cdot 10^{-3} \text{ m}^3 \text{ s}^{-1}$ , reached or exceeded for 330 days a year) is the 'minimum residual discharge' needed to protect the aquatic environment, as interpreted by the Water Act 254/2001 Coll. (Tureček, 2002). Peak flow and return periods, interpolated by the Log-normal distribution of the annual discharge maxima (Shaw, 2011), are presented in Tab. 3.

The mean annual discharge was  $Q_a = 2.5 \cdot 10^{-3} \text{ m}^3 \text{ s}^{-1}$ , and the bank-full discharge of  $Q_b = 0.1 \text{ m}^3 \text{ s}^{-1}$  corresponded to a return period between one and two years. In the investigated stream transect (Fig. 1), the bed particle distribution ( $d_{10} = 4.5$ ,  $d_{50} = 9$  and  $d_{90} = 18 \text{ mm}$ ) was fine gravel, and the threshold discharge (Olsen, 1993) to initiate transport of the 16th percentile particle diameter ( $d_{16} = 5 \text{ mm}$ ) at an 11% stream gradient was  $Q_c = 5.4 \cdot 10^{-3} \text{ m}^3 \text{ s}^{-1}$ . However, in non-uniform stream channels such as at HPO, smaller particles are sheltered behind larger grains and stones and require a higher flow to set them into motion (Palucis and Lamb, 2017). Considering the empirical channel stability approach (Olsen, 1993), the critical bottom velocity for fine gravel deposits was  $v_{crit} = 0.85 \text{ m s}^{-1}$  (i.e. mean cross-section velocity  $v = 1.2 \text{ m s}^{-1}$ ); and, the corresponding discharge  $Q_{crit} = 0.76 \text{ m}^3 \text{ s}^{-1}$  (close to the 50 years return period, Tab. 3). Thus, the relative bed stability of  $RBS = Q_{crit}/Q_5 = 3.3$  can be considered 'highly stable' (USDA, 2007) ( $Q_5$  is the peak flow with five-year return probability).

### Flash flood of 7 August 2010: Physical environment

During the week 3-9 August 2010, a total precipitation amount of 434 mm was recorded in the HPO catchment, with a particularly heavy rainstorm ( $313 \text{ mm day}^{-1}$ ) on 7 August (Fig. 2). This daily rainfall did not exceed the regional historical record ( $345 \text{ mm day}^{-1}$ ) of 29 July 1897 (Munzar and Ondráček, 2010), but that record was ob-

served in the upper plain of the Jizera Mts. that has 1.5 times higher annual precipitation on average.

The HEC- HMS 4.4 catchment modelling system reconstructed the flood wave (Fig. 3) with a peak discharge of  $Q_{max} = 2.38 \text{ m}^3 \text{ s}^{-1}$ , verified by flood footprints ( $2.25 \text{ m}^3$

Tab. 3. Peak discharge frequency at the HPO outlet.

Return period N (years)	Peak discharge $Q_N$ ( $\text{m}^3 \text{ s}^{-1}$ )
1	0.08
2	0.13
5	0.23
10	0.34
20	0.49
50	0.65
100	1.02
1000	2.46

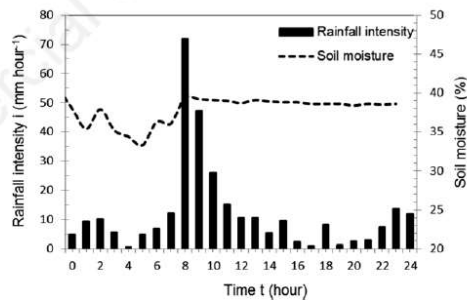


Fig. 2. Rainfall intensity ( $\text{mm hour}^{-1}$ ) and soil moisture (%) at the 15 cm depth on 7 August 2010.

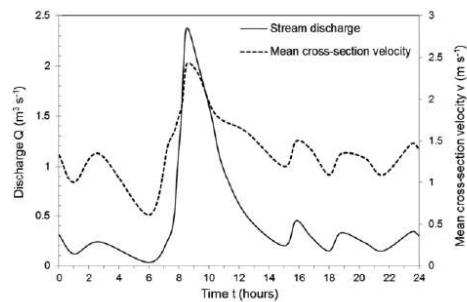


Fig. 3. Stream discharge  $Q$  ( $\text{m}^3 \text{ s}^{-1}$ ) and mean cross-section velocity  $v$  ( $\text{m s}^{-1}$ ) near the catchment outlet on 7 August 2010.

$s^{-1}$  with a Manning's roughness coefficient  $n = 0.065$ ). The return period of this event is close to 1,000 years (Tab. 3), though the unit peak discharge ( $10.35 \text{ m}^3 \text{ s}^{-1} \text{ km}^{-2}$ ) is below the European probable maximum given for the EuroMed-eFF database (Amponsah *et al.*, 2020). For three hours, rainfall intensities (culminating at  $72 \text{ mm hour}^{-1}$ ) exceeded the soil infiltration capacity of  $12 \text{ mm hour}^{-1}$  (measured by a double ring infiltrometer) and surface flow dominated (documented by the relatively low increase in soil moisture, Fig. 2). The lag time of discharge to rainfall was about 30 minutes (Figs. 2 and 3), and the event runoff coefficient was 0.77. During this flood, the drainage network expanded into two additional ephemeral branches and moved the channel head 30 meters higher. As simulated by HEC-RAS 5.0.3, during the peak flow ( $2.38 \text{ m}^3 \text{ s}^{-1}$ ) the discharge travel time in the main channel was 2.8 minutes; detailed currents and depth are given in Fig. 4. After the flood, the basic step-pool morphology (created by big granite blocks) did not change, but, the bed particle distribution in the investigated stream transect was altered from fine to medium gravel.

On 7 August 2010, the HPO stream had discharge above the threshold of stream bed stability ( $Q_{crit} = 0.76 \text{ m}^3 \text{ s}^{-1}$ ) for approximately two hours (Fig. 3). While the average annual volume of sediment collected at the HPO gauging station from 1996-2009 was  $0.46 \text{ m}^3 \text{ year}^{-1}$ , this extreme event resulted in  $2.7 \text{ m}^3$  of sand and gravel being eroded in the stream channel. There was negligible soil erosion at the two forest plots sheltered by the forest canopy and litter.

Annual streamflow extremes of the HPO outlet from 2002-2012 are given in Tab. 4. The observed minima are consistent with only a limited impact on stream biota, and except for the 2010 event, the maxima reached return periods of only 1-8 years.

#### Changes in stream water chemistry and macroinvertebrate assemblages

Basic characteristics of the HPO stream during a macroinvertebrate survey from 2010 up to 2012 are given in Tab. 2; sampling was performed during base-flow conditions, with discharges of mean daily duration between 150 and 330 days. Values of specific conductivity ( $71.6\text{--}80.3 \text{ }\mu\text{S cm}^{-1}$ ) and calcium content ( $5.4\text{--}7.2 \text{ mg L}^{-1}$ ) reflect low mineral contents; pH values (around 6), relatively high contents of sulphate ( $19.1\text{--}25.3 \text{ mg L}^{-1}$ ) and nitrate ( $1.9\text{--}3.7 \text{ mg L}^{-1}$ ) and depleted alkalinity ( $18.2\text{--}55.9 \text{ }\mu\text{eq L}^{-1}$ )

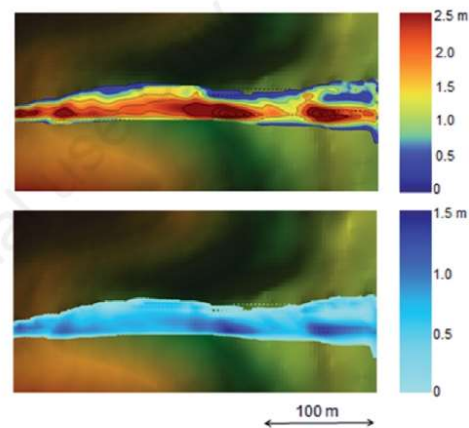


Fig. 4. Currents and depth in the schematized stream channel, from the branch junction (left) to the gauging station (right) during the peak discharge on 7 August 2010.

Tab. 4. Annual streamflow extremes in the HPO basin, 2002-2012.

Year	$Q_{min}$ ( $10^{-3} \text{ m}^3 \text{ s}^{-1}$ )	$Q_{max}$ ( $10^{-3} \text{ m}^3 \text{ s}^{-1}$ )	Flood origin (-)	Return period (years)
2002	0.42	285	summer rain	7 – 8
2003	0.35	43	snowmelt	<1
2004	0.33	124	summer rain	2
2005	0.44	145	summer rain	2 – 3
2006	0.51	272	summer rain	6 – 7
2007	0.33	100	snowmelt	1 – 2
2008	0.32	125	snowmelt	2
2009	0.38	78	snowmelt	<1
2010	0.35	2280	summer rain	900 – 1000
2011	0.36	141	summer rain	2 – 3
2012	0.34	120	snowmelt	1 – 2

Flood impacts on a headwater stream

(Tab. 5, Fig. 5) are consistent with a moderately anthropogenically-acidified aquatic environment (Veselý and Majer, 1996, Horecký *et al.*, 2013).

Changes in stream water chemistry after the flash flood of 7 August 2010 are given in Tab. 5. There were statistically significant declines in specific conductivity (4.8  $\mu\text{S cm}^{-1}$ , 6%) and contents of sulphate (3.9  $\text{mg L}^{-1}$ ,

16%), fluoride (0.1  $\text{mg L}^{-1}$ , 33%), chloride (0.3  $\text{mg L}^{-1}$ , 19%) and magnesium (0.2  $\text{mg L}^{-1}$ , 13%). Contents of calcium and nitrate also decreased, while values of pH and alkalinity increased, but these changes were not statistically significant. Consequently, there was an increasing trend in alkalinity and decreasing trend in conductivity in 2009-2012 (Fig. 5); these trends were statistically signifi-

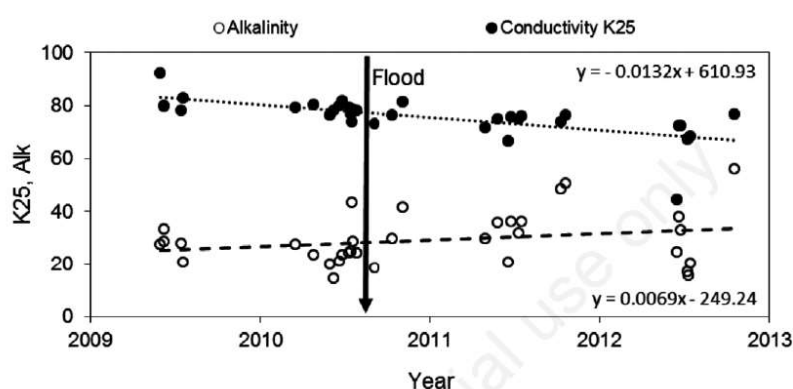


Fig. 5. Stream water conductivity (K25,  $\mu\text{S cm}^{-1}$ ) and alkalinity (Alk,  $\mu\text{eq L}^{-1}$ ), (HPO catchment, 2009-2012).

Tab. 5. Changes of chemical elements in the stream water during comparable base flow at the HPO outlet, before and after the flood.

Date	K <sub>25</sub>	pH	Alk	Na <sup>+</sup>	K <sup>+</sup>	Mg <sup>2+</sup>	Ca <sup>2+</sup>	F <sup>-</sup>	Cl <sup>-</sup>	NO <sub>3</sub> <sup>-</sup>	SO <sub>4</sub> <sup>2-</sup>
	$\mu\text{S cm}^{-1}$	-	$\mu\text{eq L}^{-1}$	$\text{mgL}^{-1}$	$\text{mgL}^{-1}$	$\text{mgL}^{-1}$	$\text{mgL}^{-1}$	$\text{mgL}^{-1}$	$\text{mgL}^{-1}$	$\text{mgL}^{-1}$	$\text{mgL}^{-1}$
10-Jun-09	79.4	6.0	28.6	2.7	0.4	1.5	7.0	0.3	1.7	2.4	24.7
17-Jul-09	78.0	6.0	27.9	2.7	0.4	1.5	7.1	0.3	1.7	2.5	25.0
18-Mar-10	79.3	5.9	27.6	2.6	0.5	1.5	7.2	0.3	1.6	3.0	25.3
27-Apr-10	80.3	5.9	23.4	2.4	0.5	1.6	6.7	0.3	1.6	3.7	24.3
28-Jul-10	77.9	6.0	24.3	2.5	0.4	1.3	5.7	0.3	1.6	3.1	23.0
5-Sep-10	73.0	5.9	18.2	2.3	0.5	1.3	5.6	0.3	1.4	3.7	20.9
16-Oct-10	76.1	6.1	29.4	2.3	0.5	1.3	6.8	0.3	1.4	3.1	22.1
4-May-11	71.6	6.2	29.6	2.3	0.5	1.2	5.4	0.2	1.2	2.7	20.0
13-Oct-11	73.8	6.4	48.5	2.6	0.7	1.3	5.8	0.2	1.3	1.9	20.5
21-Oct-12	76.5	6.0	55.9	3.0	0.6	1.4	6.9	0.2	1.2	2.5	19.1
<b>Before</b>											
Mean	79.0	6.0	26.4	2.6	0.4	1.5	6.7	0.3	1.6	3.0	24.4
SD	0.91	0.05	2.08	0.12	0.05	0.08	0.55	0.01	0.04	0.47	0.79
<b>After</b>											
Mean	74.2	6.2	36.3	2.5	0.6	1.3	6.1	0.2	1.3	2.8	20.5
SD	1.86	0.17	13.80	0.30	0.08	0.08	0.60	0.02	0.11	0.62	0.99
Means diff.	-4.8	0.2	9.9	-0.1	0.2	-0.2	-0.6	-0.1	-0.3	-0.2	-3.9
(%)	-6	3	38	-4	50	-13	-9	-33	-19	-7	-16
P	0,01	0,21	0,25	0,72	0,06	0,01	0,19	0,02	0,01	0,72	0,01
Significant	Yes	-	-	-	-	Yes	-	Yes	Yes	-	Yes

SD, standard deviation; P, Mann Whitney two-tailed P-value.

icant, with Spearman's correlation coefficient  $R_s$  values of 0.62 and 0.51, respectively, exceeding the critical value  $R_{Scrit} = 0.35$  at the 0.05 probability level. These results correspond with the long-term recovery of stream water from acidification, as reflected by the statistically significant rising trend in annual pH values of both precipitation and stream water from 1995-2015 (Fig. 6; Spearman's correlation coefficient  $R_s$  of 0.82 and 0.84, respectively, exceeding the critical value  $R_{Scrit} = 0.41$  at the 0.05 probability level).

Macroinvertebrate assemblages of the HPO stream were composed of 82 taxa (distinct taxonomical units) that belong to 7 orders of aquatic insects (included larvae, pupae and adults) and the subclass Oligochaeta. A complete list of taxa collected in eight sampling dates from 18 March 2010 to 29 October 2012 along with numbers of individuals of each taxon is given in Appendix 1. Plecoptera was the most abundant group (17 taxa and a maximum number of individuals of 743 on 27 April 2010) followed by Diptera (36 taxa and max. 507 individuals on 28 July 2010) dominated by families Simuliidae and Chironomidae. Trichoptera (14 species and max 229 individuals on 13 October 2011) and Coleoptera (9 species and max. 43 individuals on 28 July 2010) were also abundant, while Ephemeroptera were very rare (4 species, max 11 individuals on 29 October 2012). Oligochaetes were not determined to species level, and their numbers reached a maximum of 10 individuals on 13 October 2011. Heteroptera and Odonata were only found a total of three times, and we identified only a single taxon in each of these orders (Appendix 1, Tab. 6, Fig. 7).

The flood had an immediate devastating effect on macroinvertebrate assemblages and negatively influenced both the number of species/taxa and the number of indi-

viduals of each taxonomical group as well as their total values (Tab. 6, Fig. 7). For the whole period following this event changes in individual groups were statistically significant only for "other Diptera", the total number of individuals (N) and taxa (S) that declined significantly after the flood (Tab. 6). On the other hand, there was a long-term drop in the number of taxa in all groups except Oligochaetes and particularly mayflies, where the number of taxa temporarily increased. Both calculated indexes of diversity followed the same trend, as they reached the highest value ever 9 months after the flood; this resulted in a statistically nonsignificant effect of the flood on their values (Tab. 6).

The dominant species (occurring on all eight sampling dates) were *Leuctra nigra* with mean number of individuals (mni) 96, *Plectrocnemia conspersa* (mni 17), and *Nemurella pictetii* (mni 11). Slightly less dominant species (present on seven sampling dates but in relatively low numbers) were *Heterotanytarsus apicalis* (mni. 6), *Dicranota* sp. (mni. 5), *Agabus* sp. (mni 3), and *Odeles marginata* (mni 3). All those species were also present on at least one sampling date after the flood (7 August 2010) when the macroinvertebrate assemblages were significantly reduced (Tab. 6, Fig. 7), indicating their resistance to extraordinary high currents and streambed changes. Further frequent species were found in six samples: *Siphonoperla torrentium* (mni 22), *Leuctra pseudosignifera* (mni 26), *Protonemura auberti* (mni 43), *Sericostoma* cf. *personatum* (mni. 6), *Trissopelopia longimana* (m.n.i. 90, the second most numerous species), and *Eloeophila* sp. (mni 1). After the flood, the abundance of all these species gradually returned to their original numbers (Appendix 1). Two wider taxonomical groups in this category were not identified to species level: family

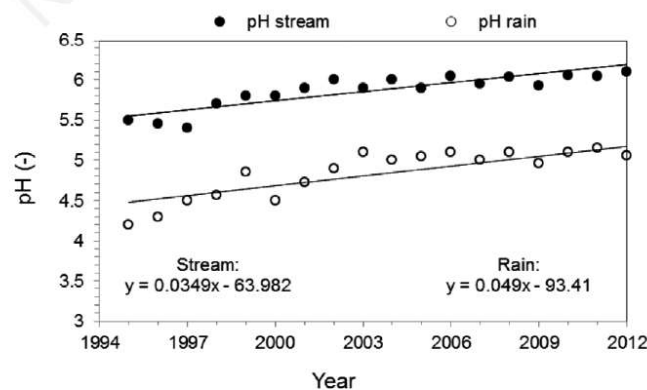


Fig. 6. Mean annual pH values of rain and stream water (HPO catchment, 1995-2012).

Flood impacts on a headwater stream

Simuliidae (mni 119), one of the most numerous organisms in the study that did not re-establish their original abundance after the flood, and the rare but regularly present Oligochaetes (mni. 3). There were also high numbers of individuals belonging to taxa with multiple early instars

like *Protonemura* sp. juv. (mni. 144) and *Plectrocnemia* sp. juv. (mni. 29), but the lack of precise identification makes this information difficult to interpret.

In addition, there was a group of species that occurred only one to three times but reached noticeable numbers

**Tab. 6.** Number of species/taxa in all collected groups of macroinvertebrates and population characteristics before and after the flood.

	OLI	ODO	EPH	PLE	TRI	CHR	ODI	COL	HET	N	S	D <sub>SE</sub>	D <sub>SC</sub>
18-Mar-10	1	0	1	13	7	13	9	2	0	1048	46	13	7
27-Apr-10	1	0	0	11	10	13	6	6	0	1327	47	10	5
28-Jul-10	0	0	0	7	7	12	8	4	1	891	39	11	7
5-Sep-10	1	0	0	5	3	3	3	3	0	86	18	6	3
16-Oct-10	1	0	0	7	3	2	3	1	1	128	18	8	6
4-May-11	1	0	2	8	6	17	6	1	0	563	41	17	11
13-Oct-11	1	1	2	8	8	10	5	3	0	830	38	11	8
29-Oct-12	0	0	1	6	5	12	3	3	0	839	30	8	5
<b>Before</b>													
Mean	0.7	0	0.3	10.3	8.0	12.7	7.7	4.0	0.3	1089	44	11.3	6.3
SD	0.58	0	0.58	3.06	1.73	0.58	1.53	2.00	0.58	221	4.36	1.53	1.15
<b>After</b>													
Mean	0.8	0.2	1.0	6.8	5.0	8.8	4.0	2.2	0.2	489	29.0	10.0	6.6
SD	0.45	0.45	1.00	1.30	2.12	6.30	1.41	1.10	0.45	366	10.82	4.30	3.05
Means diff.	0.1	0.2	0.7	-3.5	-3.0	-3.9	-3.7	-1.8	-0.1	-600	-15.0	-1.3	0.3
(%)	14	-	233	-34	-37	-31	-48	-45	-33	-55	-34	-12	5
P	0.82	0.41	0.34	0.20	0.13	0.29	0.04	0.29	0.81	0.03	0.04	0.45	0.88
Significant	-	-	-	-	-	-	Yes	-	-	Yes	Yes	-	-

OLI, Oligochaeta; ODO, Odonata; EPH, Ephemeroptera; PLE, Plecoptera; TRI, Trichoptera; CHR, Chironomidae; ODI, other Diptera; COL, Coleoptera; HET, Heteroptera; N, total number of individuals; S, total number of taxa; D<sub>SE</sub>, Shannon entropy; D<sub>SC</sub>, Simpson concentration; SD, standard deviation; P, Mann-Whitney two-tailed P-value.

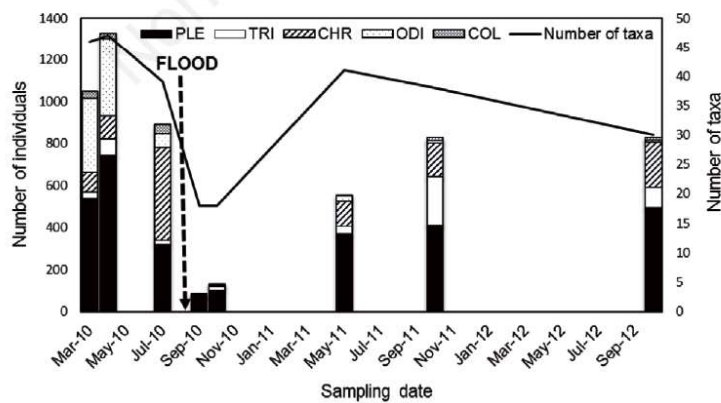


**Fig. 7.** Number of individuals in the most abundant groups of macroinvertebrates (stacked-bars) and the total number of taxa in all present taxonomical groups (line) in the HPO stream, 2010-2012. PLE, Plecoptera; TRI, Trichoptera; CHR, Chironomidae; ODI, other Diptera; COL, Coleoptera.



per sample. Some of them were present before the flood only, such as *Leuctra aurita* (mni 64), *Leuctra prima* (mni 12), *Leuctra major* (mni 6), *Diura bicaudata* (mni 2), *Crunoecia irrorata* (mni 2), *Philopotamus ludificatus* (mni 2), *Potamophylax cf. cingulatus* (mni 6), *Ibisia marginata* (mni 3) and *Limnius* sp. (mni 9). Other species appeared only after the flood, such as *Baetis rhodani*, *Siphonurus aestivalis*, *Nemoura cinerea* (mni 110), *Pseudodiamesa branickii* (mni 24), and *Chaetocladius piger* group (mni 10) - all found on 4 May 2011, the third sampling after the flood and the first with significant signs of recovery (Tab. 6, Fig. 7). There were also chironomid species that did not belong to any of the above categories: *Micropsectra cf. aristata* (mni 34) and *Heterotrissocladus marcidus* (mni 25) that were abundant before the flood but did not reach their original numbers after the flood. Other species were present at too low abundances to support any conclusions. Notable, however, was the finding of the very rare *Geothocladus* sp. (mni 1) that was present only during two samplings following the flood, when all macroinvertebrate assemblages were significantly reduced.

## DISCUSSION

Annual peak flows in the HPO are generated mainly by summer rainstorms, producing flash floods of relatively short duration (Tab. 4, Fig. 2, Fig. 3). The peak discharge of  $2.38 \text{ m}^3 \text{ s}^{-1}$  observed on 7 August 2010 was estimated to have a return period of 1,000 years (Tab. 4). This extreme event eroded and transported  $2.7 \text{ m}^3$  of sand and gravel (6 times more than the mean annual sediment outflow) from this relatively short first order headwater stream, while negligible soil erosion was found on slopes covered by beech forests, likely reflecting their canopy interception, leaf litter deposits and deep rooting (Chang, 2012).

For several decades, water chemistry in the HPO stream has been influenced by the acid atmospheric deposition of sulphur and nitrogen compounds (Křeček and Hořícká, 2001). In comparison with the upper plain of the Jizera Mts., acidification of the HPO catchment was limited by the lower (65%) annual precipitation and the stands of semi-native beech (*Fagus sylvatica*), which have lower winter deposition and leaf litter decomposition (Godbold and Hüttermann, 1994). Thus, since 1994, pH values in HPO stream waters did not decrease below 5.3, despite precipitation having a much lower pH (Fig. 6), and consequently reactive aluminium and its labile (toxic) forms were not found.

The chemical impacts of the extreme summer flood of 2010 include statistically significant declines in specific conductivity and contents of sulphate, fluoride, chloride and magnesium. Together with decreased concentrations of other chemical compounds (except nitrate, which in-

creased), this was evidently the result of the dilution of stream discharge by the high volume of rain (Fig. 2, Tab. 5). Accompanied by rising values of pH and alkalinity, this indicates a depletion of the sulphur pool in soils related to catchment runoff genesis. During intense rainstorms, streamflow in forested catchments is generated primarily through the organic and upper mineral soil horizons along streams (Chang, 2012), and these areas simultaneously contribute the majority of storm-associated sulphate to streams. Thus, after the August 2010 flood, the contents of sulphate in the HPO stream decreased by 16% (Tab. 5). However, changes in stream water chemistry during the following two years after the flood (Tab. 5, Fig. 5, Fig. 6) reflect the continued recovery of the HPO basin from acidification, evidenced also by the long-term trend in pH values in both precipitation and stream waters (Fig. 6). Thus, it is clear that the recorded flood did not significantly alter the recovery of the HPO surface waters from acidification.

The macroinvertebrate composition in HPO is consistent with a small headwater mountain stream with a heterogeneous bed, relatively low regular flow (mean annual discharge of  $2.5 \cdot 10^{-3} \text{ m}^3 \text{ s}^{-1}$ ) and slightly decreased pH values due to anthropogenic acidification (Tabs. 3 and 5; Fig. 6), being similar to other first-order headwater streams of the European Black Triangle as well as other mountain streams affected by anthropogenic acidification (Horecký *et al.*, 2013; Stockdale *et al.*, 2014). While such streams are very susceptible to hydrological extremes (floods and droughts), the most dominant species, such as the omnivorous stoneflies *Leuctra nigra* and *Nemurella pictetii* and the predatory caddisfly *Plectrocnemia conspersa*, are well adapted to such conditions (Horecký *et al.*, 2006, 2013) and so survived the flood of 2010 (Appendix 1).

Before the flood, the water chemistry of HPO (characterized by moderate acidity) was not limiting for the presence of even less acid-tolerant species such as the mayfly *Leptophlebia marginata*, stoneflies *Siphonoperla torrentium* and *Diura bicaudata*, caddisfly *Rhyacophila cf. polonica*, Simuliidae and many species of the family Chironomidae. These species do not inhabit strongly acidified streams with pH below 5 (Horecký *et al.* 2006; Hardekopf *et al.*, 2008). Continuing recovery from acidification during the two years after the flood brought a further improvement in water chemistry (Fig. 5), and the abundance of both dominant and less acid-tolerant species increased, as reported also from other acidified headwater catchments in the Czech Republic (Horecký *et al.* 2013; Beneš *et al.*, 2017) and abroad (Edwards, 1998; Garmo *et al.*, 2014; Stockdale *et al.*, 2014).

The flood had a devastating effect on the stream macroinvertebrates that was particularly pronounced for several months afterwards. Total number of species/taxa

(S), Shannon entropy ( $D_{SE}$ ) and Simpson concentration ( $D_{SC}$ ) were reduced by about 50%, while the abundance of taxa was reduced by about 10% compared with before the flood (Tab. 6, Fig. 7). These changes cannot be explained by natural seasonal variability that for dominant taxonomical groups (stoneflies, true flies, caddisflies and beetles) is much lower according to Beneš *et al.* (2017).

Moreover, because of the larger regional extent of the flood, there were likely limited local resources of adult insects for stream recolonization. By the end of the first year after the flood, both the number of taxa and number of individuals increased, but they remained significantly lower (Tab. 6). Complete recovery of macroinvertebrate assemblages was still not observed even two years after the flood, similarly as found by Smith *et al.* (2019). Simuliidae and other filter feeding taxa such as *Micropsectra aristata* and *Philopotamus ludificatus*, but also species inhabiting moss-grown or soft substratum such as *Trissopelopia longimana* and *Ibisia marginata*, did not reach their numbers before the flood or even totally disappeared. This may indicate a continued lack of fine particulate organic matter or organic substratum. Interestingly, sampling in May 2011 demonstrated an unsuccessful colonization of the HPO stream by alien species that had not been present before the flood (*Baetis rhodani*, *Siphonurus aestivalis*, *Nemoura cinerea*, *Diamasa dampfi* / *permacra*, *Chaetocladius piger* group, *Pseudodiamesa branickii*). These species temporarily inhabited the stream but then later disappeared, resulting in a distinct but ephemeral peak of biological diversity (Tab. 6, Appendix 1). Similar results were found by Stubbington *et al.* (2009), who described declines in invertebrate abundance as an impact of flooding in perennial streams, as well as Snyder and Johnson (2006), who reported prolonged such effects over several consecutive years.

## CONCLUSIONS

The extreme summer flash flood (with a return period close to 1,000 years) resulted in a devastating effect on stream macroinvertebrates in the studied catchment. Both the number of species/taxa and the total number of individuals were significantly reduced for the two years following the flood. A temporary peak in the total number of species/taxa and species diversity nine months after the flood was the result of unsuccessful colonization by alien species. On the other hand, the flood event partly contributed to the recovery of the stream from anthropogenic acidification, particularly through a decline in sulphur contents in the stream water (associated with a depletion of the sulphur pool of soils). The overall course of long-term recovery was not altered, however.

## ACKNOWLEDGMENTS

This research was funded by the Ministry of Education (INTER-EXCELLENCE: INTER-COST LTC 17006, 2017-2020), linked to activities conducted within the COST (European Cooperation in Science and Technology) Action CLIMO (Climate-Smart Forestry in Mountain Regions - CA15226) financially supported by the EU Framework Programme for Research and Innovation HORIZON 2020; Czech Technical University in Prague (Project SGS20/110IOHR112T/11, 2020-2021); Austrian-Czech Lead Agency project - Austrian Science Fund FWF No. 19770 / Czech Science Foundation No. 20-00892L and by the Ministry of Culture of the Czech Republic (DKRVO 2019-2023/5.I.b, National Museum, 00023272). Our thanks are also due to Zuzana Hořická for analyses of background data of water chemistry, to Martin Fikáček and Jiří Hájek for their help in the species identification of the beetles, and to David Hardekopf for language corrections.

## REFERENCES

- Adámek Z, Orendt C, Wolfram G, Sychra J, 2010. Macrozoobenthos response to environmental degradation in a heavily modified stream: Case study the Upper Elbe River, Czech Republic. *Biologia* 65:527-536.
- Allan JD, Castillo MM, 2007. Stream ecology: structure and function of running waters. Chapman and Hall, New York: 372 pp.
- Amponsah W, Marra F, Marchi L, Roux H, Braud I, Borga M, 2020. Objective analysis of envelope curves for peak floods of European and Mediterranean flash floods, p. 267-276. In: Leal Filho, W, Nagy, G, Borga, M, Chávez Muñoz, P, Mag-nuszewski, A. (eds), *Climate Change, Hazards and Adaptation Options*. Springer, Cham: 1084 pp.
- Beneš F, Horecký J, Senoo T, Kamasová L, Lamačová A, Tá-tosová J, Hardekopf DW, Stuchlík E, 2017. Evidence for responses in water chemistry and macroinvertebrates in a strongly acidified mountain stream. *Biologia* 72:1049-1058.
- Chang M, 2012. Forest hydrology: an introduction to water and forests. CRC Press, Boca Raton: 598 pp.
- Dar S, Ganai BA, 2017. Macroinvertebrates as bioindicators of water pollution. *J. Res. Dev.* 17:86-94.
- Davis DW, 2007. Is the current approach to managing flood threats in the United States sustainable? In: *Water Resources Engineering, EWRI Conference Proceedings*. Am. Soc. Civil Engin., Tampa: 638 pp.
- Edwards PJ, 1998. Sulfur cycling, retention, and mobility in soils: a review. General Technical Report NE-250. Delaware: USDA Forest Service, Northeastern Research Station: 18 pp.
- Falkenmark M, Allard B, 2015. Water quality genesis and disturbances of natural freshwaters. *Water Pollution* 5:45-78.
- Fritz KM, Hagenbuch E, D'Amico E, Reif M, Wigington PJ, Leibowitz JrSG, Comeleo RL, Ebersole JL, 2013. Comparing the extent and permanence of headwater streams from

- two field surveys to values from hydrologic databases and maps. *J. Am. Water Resour. Assoc.* 49: 867-882.
- Garmo ØA, Skjelkvåle BL, de Wit HA, Colombo L, Curtis Ch, Fölster J, Hoffmann A, Hruška J, Högåsen T, Jeffries DS, Keller WB, Krám P, Majer V, Monteith DT, Paterson AM, Rogora M, Rzychon D, Steingruber S, Stoddard JL, Vuorenmaa J, Worsztynowicz A. 2014. Trends in surface water chemistry in acidified areas in Europe and North America from 1990 to 2008. *Water Air Soil Poll.* 225:1880.
- Godbold DL, Hüttermann A. 1994. Effects of acid rain on forest processes. John Wiley & Sons, New York: 432 pp.
- Hardekopf DW, Horecký J, Kopáček J, Stuchlík E. 2008. Predicting long-term recovery of a strongly acidified stream using MAGIC and climate models (Litavka, Czech Republic). *Hydrol. Earth Syst. Sc.* 12:479-490.
- Herget J, Roggenkamp T, Krell M. 2014. Estimation of peak discharges of historical floods. *Hydrol. Earth Syst. Sc.* 18:4029-4037.
- Hickey JT, Salas JD. 1995. Environmental effects of extreme floods. *Hydrometeorology, Impacts, and Management of Extreme Floods. Proceedings of US-Italy Research Workshop, Perugia, Italy*, p. 1-22.
- Holen S, Wright R, Seifert I. 2013. Effects of long range transported air pollution (LRTAP) on freshwater ecosystem services. ICP-Waters report 115/2013. Norwegian Institute for Water Research, Oslo: 49 pp.
- Horecký J, Stuchlík E, Chvojka P, Hardekopf, D.W, Mihaljevič, M, Špaček, J. 2006. Macroinvertebrate community and chemistry of the most atmospherically acidified streams in the Czech Republic. *Water Air Soil Poll.* 173:261-272.
- Horecký J, Rucki J, Krám P, Křeček J, Bitušík J, Stuchlík E. 2013. Benthic macroinvertebrates of headwater streams with extreme hydrochemistry. *Biologia* 68:1-11.
- Jost L. 2006. Entropy and diversity. *Oikos* 113:363-375.
- Knox JC, Kundzewicz ZW. 1997. Extreme hydrological events, palaeo-information and climate change. *Hydrolog. Sci. J.* 42:765-779.
- Křeček J, Hořická Z. 2001. Degradation and recovery of mountain watersheds: the Jizera Mountains, Czech Republic. *Unasylva* 52:3-49.
- Křeček J, Hořická Z. 2006. Forests, air pollution and water quality: influencing health in the headwaters of Central Europe's "Black Triangle". *Unasylva* 57:46-49.
- Křeček J, Palán L, Pažourková E, Stuchlík E. 2019. Water-quality genesis in a mountain catchment affected by acidification and forestry practices. *Freshwater Sci.* 38:257-269.
- Motulski HW. 2007. Prism 5 Statistics Guide. GraphPad Software Inc., San Diego: 285 pp.
- Munzar J, Ondráček S. 2010. The historical precipitation record from the Jizera Mts. still unbroken. *Acta Musei Bohemiae Borealis Scientiae Naturales* 28:3-15.
- Palucis MC, Lamb MP. 2017. What controls channel form in steep mountain streams? *Geophys. Res. Lett.* 44:7245-7255.
- Olsen DS. 1993. Assessing stream channel stability thresholds. Graduate Student Theses 7470. University of Montana, Missoula: 76 pp.
- Rashid RA, Pandit AK. 2014. Macroinvertebrates (oligochaetes) as indicators of pollution: A review. *J. Ecol. Nat. Environ.* 6:140-144.
- Richardson JS. 2019. Biological diversity in headwater streams. *Water* 11:1-19.
- Rosenberg DM, Resh VH. 1993. Freshwater biomonitoring and benthic macroinvertebrates. Chapman and Hall, New York: 488 pp.
- Schöpp W, Posch M, Mylona S, Johansson M. 2003. Long-term development of acid deposition (1880-2030) in sensitive freshwater regions in Europe. *Hydrol. Earth Syst. Sc.* 7:436-446.
- Shaw EM. 2011. *Hydrology in practice*. 4th edition, Span Press, London: 546 pp.
- Smith AJ, Baldigob BP, Duffya BT, Georgeb SD, Dressera B. 2019. Resilience of benthic macroinvertebrates to extreme floods in a Catskill Mountain river, New York, USA: Implications for water quality monitoring and assessment. *Ecol. Indic.* 104:107-115.
- Snyder CD, Johnson ZB. 2006. Macroinvertebrate assemblage recovery following a catastrophic flood and debris flows in an Appalachian mountain stream. *J. N. Am. Benthol. Soc.* 25:825-840.
- Stockdale A, Tipping E, Fjellheim A, Garmo ØA, Hildrew AD, Lofis S, Monteith DT, Ormerod SI, Shilland EM. 2014. Recovery of macroinvertebrate species richness in acidified upland waters assessed with a field toxicity model. *Ecol. Indic.* 37:341-350.
- Stubbington R, Greenwood AM, Wood PJ, Armitage PD, Gunn J, Robertson AL. 2009. The response of perennial and temporary headwater stream invertebrate communities to hydrological extremes. *Hydrobiologia* 630:299-312.
- Stuchlík E, Hořická Z, Prchalová M, Křeček J, Barica J. 1997. Hydrobiological investigation of three acidified reservoirs in the Jizera Mountains, the Czech Republic, during the summer stratification. *Can. Tech. Rep. Fish. Aquat. Sci.* 2155:56-64.
- Stuchlík E, Kopáček J, Fott J, Hořická Z. 2006. Chemical composition of the Tatra Mountain lakes: response to acidification. *Biologia* 61:S11-S20.
- Tolász R, Míková T, Valeriánová A, Voženílek V. 2007. Climate atlas of Czechia. Czech Hydrometeorological Institute, Prague: 254 pp.
- Tureček K. 2002. [The water act]. [Book in Czech]. SONDY, Prague: 114 pp.
- USACE. 2000. HEC-HMS technical reference manual. US Army Corps of Engineers, Hydrologic Engineering Center, Davis: 148 pp.
- USACE. 2016. HEC-RAS river analysis system. Hydraulic Reference Manual, Version 5.0, US Army Corps of Engineers, Institute for Water Resources, Davis: 538 pp.
- USDA. 2007. Stream restoration design. National Engineering Handbook 654. Natural Resources Conservation Service, USDA, Washington: 54 pp.
- Váček S, Matějka M, Simon J, Malík V, Schwarz O, Mikeska M. 2007. [Health status and dynamics of forest ecosystems under air pollution stress in the Giant Mts.]. [Article In Czech]. *Folia Forestalia Bohemica* 6:216.
- Velle G, Telford RJ, Curtis C, Eriksson L, Fjellheim A, Frolova M, Fölster J, Grudule N, Halvorsen GA, Hildrew A, Hoffmann A, Indriksone I, Kamasová L, Kopáček J, Orton S, Krám P, Monteith DT, Senoo T, Shilland EM, Stuchlík E, Wiklund ML, de Wit H, Skjelkvåle BL. 2013. Biodiversity

Flood impacts on a headwater stream

- in freshwaters. Temporal trends and response to waterchemistry. ICP Waters Report 114/Biodiversity in freshwaters: temporal trends and response to water chemistry. ICP Waters report 114, NIVA, Oslo: 65 pp.
- Venutelli M, 2005. A constitutive explanation of Manning's formula. *Meccanica* 40:281-289.
- Vesely J, Majer V, 1996. The effect of pH and atmospheric deposition on concentrations of trace elements in acidified freshwaters: A statistical approach. *Water Air Soil Poll.* 88:227-246.
- Wibowo H, Suripin RK, Isdiyana RB, 2015. Comparing the calculation method of the Manning roughness coefficient in open channels. *Int. J. Engin. Res. Technol.* 4:1278-1285.

Non-commercial use only

**Impacts of an extreme flood on the ecosystem of a headwater stream**

**Eva Pažourková<sup>a</sup>, Josef Křeček<sup>a,\*</sup>, Peter Bitušík<sup>b</sup>, Pavel Chvojka<sup>c</sup>, Lenka Kamasová<sup>d</sup>,  
Takaaki Senoo<sup>d</sup>, Jan Špaček<sup>e</sup>, Evžen Stuchlík<sup>d</sup>**

<sup>a</sup> Department of Hydrology, Czech Technical University in Prague, Thakurova 7, CZ-16629 Prague 6, Czech Republic

<sup>b</sup> Department of Biology and Ecology, Matej Bel University, Tajovského 40, SK-97401 Banská Bystrica, Slovakia

<sup>c</sup> Department of Entomology, National Museum, Cirkusová 1740, CZ-19300 Prague 9, Czech Republic

<sup>d</sup> Institute of Hydrobiology, Biology Centre, Czech Academy of Sciences, Na Sádkách 7, 370 05 České Budějovice, Czech Republic

<sup>e</sup> Povodí Labe, s.p., Víta Nejedlého 951, CZ-50003 Hradec Králové, Czech Republic

\*Corresponding author: [josef.krecek@fsv.cvut.cz](mailto:josef.krecek@fsv.cvut.cz)

---

A complete list of macroinvertebrate data from 8 samples from the HPO stream, 2010 – 2012 (the double line splits the sampling to the period before and after the studied flood, numbers indicate total number of individuals in each species/taxon: OLI – Oligochaeta, ODO – Odonata, EPH – Ephemeroptera, PLE – Plecoptera, TRI – Trichoptera, DIP – Diptera, families Athericidae, Cecidomyiidae, Ceratopogonidae, Chironomidae, Dixidae, Empididae, Limoniidae, Pedicidae, Simuliidae, COL – Coleoptera, HET – Heteroptera, families and species are sorted in alphabetic order, N – total number of individuals, S – total number of taxa,  $D_{SE}$  – Shannon entropy,  $D_{SC}$  – Simpson concentration).

Group	Family	Species/Taxon	Sampling date											
			18-Mar-10	27-Apr-10	28-Jul-10	5-Sep-10	16-Oct-10	4-May-11	13-Oct-11	29-Oct-12				
OLI			3	1										
ODO		<i>R.sp.juv.</i>											1	
EPH	Baetidae	<i>Baetis rhodani</i>							2					
EPH	Leptophlebiidae	<i>Leptophlebia marginata</i>	2									1	11	
EPH	Siphonuridae	<i>Siphonurus aestivus</i>							8			1		
EPH	Siphonuridae	<i>Siphonurus sp.juv.</i>												
PLE	Chloroperlidae	<i>Siphonoperla torrentium</i>	30	28					1	9	47	17		
PLE	Leuctridae	<i>Leuctra nigra</i>	36	53	201		46	35	24	73	299			
PLE	Leuctridae	<i>Leuctra pseudosignifera</i>	8	6			2	10		3	125			
PLE	Leuctridae	<i>Leuctra major</i>	6											
PLE	Leuctridae	<i>Leuctra prima</i>	12											
PLE	Leuctridae	<i>Leuctra aurita</i>			64									
PLE	Leuctridae	<i>Leuctra autumnalis</i>												
PLE	Leuctridae	<i>Leuctra sp.</i>	13	59				15	57	74	1			
PLE	Nemouridae	<i>Nemoura pictetii</i>	9	4	5		3	9	37	20	3			
PLE	Nemouridae	<i>Nemoura uncinata</i>	45	12										
PLE	Nemouridae	<i>Nemoura marginata</i>	30	8					1					
PLE	Nemouridae	<i>Nemoura cambrica</i>	75	20										
PLE	Nemouridae	<i>Nemoura cinerea</i>							110					
PLE	Nemouridae	<i>Protonemura auberti</i>	85	105	10			1	58	1				
PLE	Nemouridae	<i>Protonemura sp.juv.</i>	180	439	28				71					
PLE	Nemouridae	<i>g.sp.juv.</i>	8	9	8		12	30			191	48		
PLE	Perlidae	<i>Diura bicaudata</i>			2									
TRI	Lepidostomatidae	<i>Crinoecia trionita</i>	2	1										
TRI	Limnephilidae	<i>Chaetopteryx villosa</i>			1									
TRI	Limnephilidae	<i>Drusus amulatus</i>									3			
TRI	Limnephilidae	<i>Potamophylax cf. cingulatus</i>	8	4										
TRI	Limnephilidae	<i>Potamophylax nigricornis</i>									10	1		
TRI	Limnephilidae	<i>Limnephilinae g.sp.juv.</i>	4	32	6		1	14	19	21	2			
TRI	Odontoceridae	<i>Odontocerum albicorne</i>	1	1										
TRI	Phlebotomidae	<i>Phlebotomus ludiatus</i>	2	1										
TRI	Polycentropodidae	<i>Plectrocnemia dispersa</i>	7	12	5		2	1	17	20	70			
TRI	Polycentropodidae	<i>Plectrocnemia cf. goniculata</i>							1	2				
TRI	Polycentropodidae	<i>Plectrocnemia sp.juv.</i>		10	4		3	4	1	170	9			
TRI	Rhyacophilidae	<i>Rhyacophila cf. polonica</i>		2					1	1				
TRI	Rhyacophilidae	<i>Rhyacophila sp.juv.</i>		6	2									
TRI	Sericostomatidae	<i>Sericostoma cf. personatum</i>	7	7	2				1	2	15			
DIP	Athericidae	<i>Ibata marginata</i>	4	5	1									
DIP	Cecidomyiidae		1											
DIP	Ceratopogonidae		10	8	14								2	
DIP	Chironomidae	<i>Britia bifida</i>	5	2					1					
DIP	Chironomidae	<i>Corynoneura cf. lobata</i>	3	4							2	3		
DIP	Chironomidae	<i>Corynoneura scutellata</i> group			4									
DIP	Chironomidae	<i>Diamesa damyfi / permara</i>							5	1				
DIP	Chironomidae	<i>Diamesa cernyi</i> group		1					8					
DIP	Chironomidae	<i>Endochironomus sp.</i>									1	1		
DIP	Chironomidae	<i>Eviaeffersella cf. brevicolar</i>	2	9					1	1				
DIP	Chironomidae	<i>Georhynchus sp.</i>												
DIP	Chironomidae	<i>Helaniella sp.</i>			2									
DIP	Chironomidae	<i>Heterotanytarsus apicalis</i>	10	11	1		4		11	2	2			
DIP	Chironomidae	<i>Heterotanytarsus marcidus</i>	2	1	96				2					
DIP	Chironomidae	<i>Hydrobaenus lugubris</i> group	1	6					2					
DIP	Chironomidae	<i>Chaetocladius piger</i> group							10					
DIP	Chironomidae	<i>Limnophyes sp.</i>			1									
DIP	Chironomidae	<i>Macropelopia sp.</i>			5									1
DIP	Chironomidae	<i>Metrocnemus sp.</i>	1											
DIP	Chironomidae	<i>Micropsectra cf. aristata</i>	46	7	103				6			6		
DIP	Chironomidae	<i>Micropsectra sp.</i>										1		
DIP	Chironomidae	<i>Paratrichocladius skirvathensis</i>	1	6						1				
DIP	Chironomidae	<i>Polypedium sp. A</i>			2				1			1		
DIP	Chironomidae	<i>Polypedium sp. B</i>										1		1
DIP	Chironomidae	<i>Prodiamesa olivacea</i>			11							1		3
DIP	Chironomidae	<i>Pseudocladus limbatellus</i> group	1				3	2	2					
DIP	Chironomidae	<i>Pseudodiamesa brancicki</i>							24					
DIP	Chironomidae	<i>Stempellmella sp.</i>		7					1		1		1	
DIP	Chironomidae	<i>Thomommina cf. partita</i>	12	5										
DIP	Chironomidae	<i>Trisoptelopia longimana</i>	11	54	206				21	89	156			
DIP	Chironomidae	<i>Tvetenia bovarica</i> group	1	1						1				
DIP	Chironomidae	<i>Zavelymya sp.</i>			6				20	62	40			
DIP	Dixidae		1		1									
DIP	Empididae	<i>Chelyfera sp.</i>		6	1				1	1	2			
DIP	Limoniidae	<i>Elyphidorea sp.+Phitidorea sp.</i>							1	1				
DIP	Limoniidae	<i>Elaeophila sp.</i>	1	2	1		1	1			2			
DIP	Limoniidae	<i>Rhypholobus sp.</i>	2											
DIP	Pedicidae	<i>Pedicia (P) sp.</i>	2		2						3	6		
DIP	Pedicidae	<i>Dicranota sp.</i>	1	2	23		1	1	2	2				

Group	Family	Species/Taxon	Sampling date							
			18-Mar-10	27-Aug-10	28-Jul-10	5-Sep-10	16-Oct-10	4-May-11	13-Oct-11	29-Oct-12
DIP	pupae							9		
DIP	Simuliidae		330	347	25	1		10	3	
COL	Dytiscidae	<i>Agabus</i> sp. (larva)	1	1	7	1		4	2	5
COL	Dytiscidae	<i>Agabus</i> sp. (imago)		1					4	
COL	Dytiscidae	<i>Hydroporus</i> sp. (larva)								1
COL	Elmidae	<i>Limnius</i> sp. (larva)		9						
COL	Elmidae	<i>Limnius perrisi</i> (imago)		1						
COL	Elmidae	<i>Limnius volchnari</i> (imago)		1						
COL	Hydraenidae	<i>Hydraena cf. gracilis</i> (imago)			2					
COL	Hydrophilidae	<i>Limnebius</i> sp. (imago)			1	1				
COL	Scirtidae	<i>Odeletis marginata</i> (larva)	29	12	33	3	1		10	6
HET	Velidae	<i>Velta caprai</i>			2			1		
N			1048	1327	891	86	128	563	830	839
S			46	47	38	18	17	41	38	30
Dse			13	10	11	6	8	17	11	8
Dsc			7	5	7	3	6	11	8	5

Non-commercial use only

### 3.4. Vliv změn klimatu na bioindikaci hydrologických procesů v horském povodí

Funkce lesa jsou různé (produkční, rekreační, krajinnou, půdo ochranou, atd.) a v průběhu času se i jejich chápání mění. Dříve převládalo chápání funkce lesa pouze jako produkční a bohužel tento názor někdy stále přetrvává. V minulosti však byly pozorovány problémy spojené se špatným stavem lesa, které vedly k zákonům a deklarácím na ochranu lesa (Pillí & Pase 2018; Magnein 1937). Zejména v horských povodích by měla lesnická praxe respektovat vodní režim území, ochranu kvality vod a půdy včetně bioty (Willis 2002). Vzhledem k měnícím se podmínkám způsobených klimatickou změnou se i horská zalesněná povodí mohou potýkat například se změnou hydrologického režimu (Kohler & Maselli 2009), proto FAO (2007) volá po včasných adaptivních praktikách v lesnické praxi, jelikož vliv zásahů a rozhodnutí v lesnictví se projeví až po dlouhé době.

Data denní průměrné teploty vzduchu a srážek byly staženy z mezinárodního projektu PRUDENCE (<http://prudence.dmi.dk>, Christensen & Christensen, 2007) pro období 1961-1990 (kontrolní období) a 2071-2100 (budoucí výhled). Data byla generována regionálním klimatickým modelem RegCM pro výstupy z globálních klimatických modelů HadAM3H A2 a HadAM2H B2 - jsou uvažovány dva scénáře IPCC: A2 (trvalý růst emisí) a B2 (kontrolovaný nárůst emisí během tohoto století). Srážkové úhrny byly staženy z databází s názvy precip.ICTP.A2.nc a precip.ICTP.B2.nc, uvedené jednotky (kg/m<sup>2</sup>\*den) odpovídají (mm/den). Teplotní data byla stažena z databází s názvy t2m.ICTP.A2.nc a t2m.ICTP.B2.nc (teplota vzduchu ve 2 m nad povrchem), teplotní data v databázi jsou v jednotkách absolutní teploty (K). Vlastní analýza dat byla provedena pomocí programu Intel® Array Viewer Version 3.3 s následným zpracováním v programu Microsoft Excel.

Stažená data průměrných denních teplot a srážkových úhrnů odpovídají průměrným nadmořským výškám rozlišovacích čtverců (50x50 km). Pro stanovení vstupních dat do modelu HBV (denních teplot a srážek) byl pro studovaná povodí proveden přepočít pomocí teplotního (-0,6°C/100m) a srážkového gradientu (+50mm/100m). Průměrný denní průtok byl stanoven hydrologickým modelem HBV pro období kalibrace (1991-2010), validace (2011-2016) a simulace (2071-2100).



Budoucí vývoj předpokládá nárůst teploty vzduchu v rozmezí 2.2-4.5°C, přičemž vyšší nárůst se předpokládá v období léta 4-8.3°C. Celkové množství srážek by se změnit nemělo, ale mělo by dojít k redistribuci s větším podílem v zimních měsících a se snížením srážkových úhrnů v letních měsících. Modelovaný odtok z povodí by měl klesnout o 123-65 mm (respektive o 14% pro scénář A2 a o 7% pro scénář B2) v porovnání s obdobím 1991-2006. Také by mělo dojít ke změně odtoku během roku, v letních měsících k poklesu z 47% na 29-33% a v období od října do dubna by mělo dojít k nárůstu z 53% na 70-67%. Období jarního tání by se mělo posunout z období dubna na březen. Hodnota evapotranspirace by se měla zvýšit z nynějších 434 mm na 557-499 mm. Ovšem velikost výparu je ovlivněna i vegetací, takže může být v budoucnu modifikována druhem vegetace. Dá se očekávat i změna ve frekvenci extrémů, u povodňových průtoků je modelována změna pro 10-ti letý průtok ze současných 2.5 m<sup>3</sup>/s/km<sup>2</sup> na 3.3-3.0 m<sup>3</sup>/s/km<sup>2</sup> a pro 100 letý průtok z 5.2 m<sup>3</sup>/s/km<sup>2</sup> na 6.8-6.3 m<sup>3</sup>/s/km<sup>2</sup>. U minimálního zůstatkového průtoků je předpokládán pokles o 61% ze současné hodnoty 7.52 l/s na 2.9 l/s.

Vývoj kyselé atmosférické depozice není snadné předvídat, jelikož z minulých let je patrné, že zatížení sírany je do jisté míry ovlivněno i vegetací. Na povodí Jizerky je patrné, že po smýcení lesa došlo ke snížení depozice sírany, ovšem pro sloučeniny dusíky tento trend není patrný. Poměr zatížení dusíku a síry se změnil z 0.35 (1982-1988) na 2 (po roce 2011) a tento trend je předpovídán i v tomto století (IPCC, 2013a, 2013b). Ve vodním prostředí vzhledem ke snížení vodnosti se dají předpokládat vyšší průměrné roční koncentrace síranů v rozmezí 3.4-3.1 mg/l u dusíku 2.2-2.0 mg/l a u hliníků 0.12-0.11 mg/l. Tato změna by však neměla mít významný vliv na biotu, ovšem nárůst teploty vody by mohl umožnit kolonizaci toku i jinými druhy. Pro vodní biotu bude pravděpodobně největší výzvou snížení minimálních průtoků (u Q<sub>90%</sub> ze současné hodnoty 7.52 l/s na 2.9 l/s) a předpovídaná vyšší frekvence povodňových průtoků, které mohou erozivní činností ovlivnit složení dna toku a tím i vyskytující bentické organismy. Doering & Robinson (2010) uvádí, že při povodni v roce 2002 v alpských vodních tocích došlo k redukci bentických organismů až na čtvrtinu původního zastoupení.

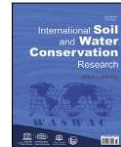
Podrobněji je tato problematika popsána v níže přiloženém článku: Role of forest in headwater control with changing enviromental and society.

Obdobné změny v povodňovém režimu vlivem klimatické změny se dají očekávat i v ostatních pramenných oblastech ČR, blíže popsáno v níže přiloženém článku [Assessing Insurance Flood Losses Using a Catastrophe Model and Climate Change Scenarios](#).



Contents lists available at ScienceDirect

International Soil and Water Conservation Research

journal homepage: [www.elsevier.com/locate/iswcr](http://www.elsevier.com/locate/iswcr)

Original Research Article

## Role of forests in headwater control with changing environment and society

Josef Křeček<sup>a,\*</sup>, Jana Nováková<sup>b</sup>, Ladislav Palán<sup>c</sup>, Eva Pažourková<sup>a</sup>, Evžen Stuchlík<sup>d</sup><sup>a</sup> Department of Hydrology, Czech Technical University in Prague, Thákurova 7, CZ-16629, Prague 6, Czech Republic<sup>b</sup> Independent Botanist, Na Vrchole 4, CZ-130 00, Prague, Czech Republic<sup>c</sup> AON Impact Forecasting, Václavské náměstí 19, CZ-110 00, Prague, Czech Republic<sup>d</sup> Institute of Hydrobiology, Biology Centre, Czech Academy of Sciences, Na Sádkách 7, CZ-370 05, České Budějovice, Czech Republic

## ARTICLE INFO

## Article history:

Received 9 July 2020

Received in revised form

3 November 2020

Accepted 4 November 2020

Available online 10 November 2020

## Keywords:

Headwater catchment

Forest functions

Water resource recharge

Acid atmospheric deposition

Climate change

## ABSTRACT

Forest practices in headwater catchments are related to environmental and social contexts. The aim of this study is to analyse the changing protective functions of forests in the upper plain of the Jizera Mts. (North Bohemia, Czech Republic) since the second half of the 19th century. With time, forests have gradually changed from native stands to spruce plantations (*Picea abies*), introducing exotic conifers (more resistant to air pollution), and, recently, back to more diverse mixed stands. The priority in protective forest functions there shifted from flood protection to integrated control of water resources (quantity and quality). In the 1980s, forest – water interactions were degraded by consequences of extreme acid atmospheric deposition, forest die-back, and extensive clear-cut. In the Jizerka catchment, first signs of recovery were observed in the early 1990s, but, stream waters there are still affected by prolonged acidification. While reconstruction of stream water chemistry at Jizerka follows the drop of the acid deposition in some 5 years, the revival of stream biota takes 10–15 years. In 2071–2100, the projected climate change shows rising annual air temperatures by 3.0–4.6 °C, decreasing water yield by 65–123 mm, 60% drop in 'minimum residual discharge', and 20–30% rise in peak-flows. However, these projected environmental changes cannot substantially decline the high potential in water resource recharge, or, start reverse processes in recent recovery from acidification and radically affect the existence of planned mixed forests in the upper plain of the Jizera Mts.

© 2020 International Research and Training Center on Erosion and Sedimentation, China Water & Power Press. Publishing services by Elsevier B.V. on behalf of KeAi Communications Co. Ltd. This is an open access article under the CC BY-NC-ND license (<http://creativecommons.org/licenses/by-nc-nd/4.0/>).

## 1. Introduction

Forest functions are strictly related to environmental and social contexts, reflecting knowledge, technical capabilities, economic interests, levels of human pressure, and also human emotions (for example fear from forest wildlife and environment), Corbin (1998), Klvač (2006), Woitsch (2006), Leggewie and Mauelshagen (2018). Three groups of forest functions have generally been considered (Krott, 2005): (i) the productive function (focusing on the economic utilization of timber), (ii) the protective function (including physical, chemical, and biological effects within the scope of the natural environment), and (iii) the recreation function (focusing on the

effects of the forest on human health and wellbeing).

In the history of the human civilisation, deforestation was one of the key processes in the decline of soil and water environments: already in 1530, a specific law of the Venetian Senate limited the harvest of forests to prevent possible landslides and water erosion phenomena in the Pre-Alpine territory (Pilli & Pase, 2018). The poor state of mountain forests in Europe by the end of the 19th century was given to the context of catastrophic floods frequency (Magnein, 1937), and initiated declarations of the soil improvement and the safe diversion of mountain waters. From that time, the steady growth in timber demand and the spread of new silvicultural practices resulted in the sustainable timber production and gradually reduced deforestation in Europe. Later, due to the increasing complexity of the social needs, the forest functions have been related with more recent environmental services and resulted in the multiresource forestry; particularly, in the headwater catchments, forestry practices should respect possible regulations of

\* Corresponding author.

E-mail addresses: [josef.kreckek@fsv.cvut.cz](mailto:josef.kreckek@fsv.cvut.cz) (J. Křeček), [navrcholu@gmail.com](mailto:navrcholu@gmail.com) (J. Nováková), [ladislav.palan@gmail.com](mailto:ladislav.palan@gmail.com) (L. Palán), [eva.pazourkova@fsv.cvut.cz](mailto:eva.pazourkova@fsv.cvut.cz) (E. Pažourková), [evzen.stuchlik@yandex.com](mailto:evzen.stuchlik@yandex.com) (E. Stuchlík).

<https://doi.org/10.1016/j.iswcr.2020.11.002>

2095-6339/© 2020 International Research and Training Center on Erosion and Sedimentation, China Water & Power Press. Publishing services by Elsevier B.V. on behalf of KeAi Communications Co. Ltd. This is an open access article under the CC BY-NC-ND license (<http://creativecommons.org/licenses/by-nc-nd/4.0/>).

water yield, runoff timing, frequency of extreme events, and water quality including the biota (Willis, 2002). Agnoletti et al. (2002) claim the importance of rising science in 'modern forestry', to emphasize ecological and social sustainability.

After the UN (1992) statement, particularly, the vital role of forest in biodiversity protection and carbon storage gained attention. Land cover changes (deforestation mainly) in the past have contributed almost 20 ppm to today's elevated atmosphere CO<sub>2</sub> concentrations (McGrath et al., 2015). In Europe, headwater catchments are mostly forested, thus, forestry strategies and practices are among the most important factors of their environmental services (FAO, 2008). At present, the share of untouched forest or forest with minimal human intervention is probably below 5% only (Schnitzler, 2014, in McGrath et al., 2015).

Considering water security in the future, the participation of water users in the management of headwaters should be practiced (Trotter & Slack, 2004), and a multi-functional view of forests respected due to the competitive interaction between forest services. Viviroli et al. (2007) considers the headwater catchments of mountain regions as 'water towers' with high potential by supplying lowland users. Priorities of forest protective functions in headwater ecosystem services are recently claimed by Křeček et al. (2017). Their importance for human society is rising with the population pressure (UNEP, 2007) and the global climate change (IPCC, 2015); the elevation-rising sensitivity to warming (Kohler & Maselli, 2009) can even accelerate changes in mountain forests and affect the hydrological cycle of headwater catchments. FAO (2007) calls particularly for timely adaptive practices, because, decisions on the forest management might remain irreversible for decades or even centuries.

The aim of this paper is to evaluate impacts of changing environment and society on the forest functions in a headwater catchment of the Jizera Mts. (Czech Republic) during the period 1850–2100.

## 2. Material and methods

### 2.1. Study site

The study was performed in the Jizerka experimental catchment (50°48'21" – 50°48'59"N, 15°19'34" – 15°20'48"E) located in the upper plain of the Jizera Mountains (Northern Bohemia, Czech Republic, Fig. 1), morphological characteristics are in Table 1. This catchment belongs to the Elbe river district 1-05-01-004 and to the 'high contributing potential to water resources' (relative water

**Table 1**  
Geomorphology of the Jizerka catchment.

Area	(km <sup>2</sup> )	1.03
Elevation	(m)	927 (862–994)
Slope	(%)	7.52 (0.02–24.33)
Shape index	(–)	0.69
Length of streams	(m)	1,490
Drainage density	(km/km <sup>2</sup> )	1.45
Length of the mainstream	(m)	657
Slope of the mainstream	(%)	5.98
Strahler stream order	(–)	2

yield RWY = 4.69 exceeds the critical value 1.25, according to Viviroli et al., 2007).

Climate characteristics of that unit are assigned from Tolasz et al. (2007): North temperate zone, Köppen Dfc sub-arctic region, mean annual precipitation 1,400 mm, mean annual air temperature 4 °C, and the average maximum snowpack of 120 cm (snow cover usually lasts from the beginning of November to the end of April). Sandy-loamy podsols developed on porphyritic granite show the depth between 0.7 and 1.2 m. The root system dominates in the topsoil occurring up to the depth of 15 cm. The topsoil is created by litter (O<sub>i</sub>, depth of 0–2 cm), humus layer (O<sub>f</sub> + O<sub>h</sub>, 2–10 cm), and leached horizon (A<sub>h</sub>, 10–15 cm); mor is the most common humus (2–5 cm) there. In the runoff genesis, surface and fast subsurface forms (direct runoff) dominate, and, groundwater bodies occur in the shallow subsurface layer only; the soil-bedrock complex shows a relatively low buffering capacity to acidification (Křeček & Hořícká, 2006).

According to the classification of Zlatník (1976), the climax forest there belongs to the belts of "Picea abies" and "Picea abies - Fagus sylvatica". By the end of the 19th century, the native forests were harvested (timber for constructions, charcoal, and, namely, for the nearby Jizerka glass manufacture) and converted to even-aged plantations of Norway spruce (*Picea abies*). In the 1970s and 1980s, these stands were defoliated by the 'acid rain' impact, and in 1984–1988 harvested by clear-cutting. The subsequent reforestation (mainly Norway spruce and introduced exotic conifers) was complicated by the acid environment, a relatively large open space, and competition of the herbaceous vegetation (namely, *Calamagrostis* sp.), Fig. 2.

### 2.2. Field observations

The experimental catchment (Fig. 1) was instrumented in 1982. The outlet is equipped by the sharp-crested V-notch weir with the automatic water pressure and temperature recorder ALA 4020

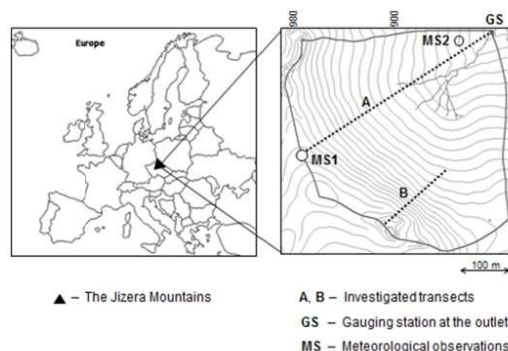


Fig. 1. The Jizerka experimental catchment.



Fig. 2. Forest regrowth of the Jizerka catchment in 2008 (20 years after the clear-cut).

(ALA, Bučovice, Czech Republic) operating in ten minutes. *In situ* monitoring of stream waters included temperature, pH and conductivity measured by the portable sensor WTW-350i (WTW, Weilheim, Germany). Standard meteorological observations (air temperature and humidity, global radiation, wind speed, atmospheric precipitation, soil moisture) were carried out in elevations of 875 and 975 m. Additionally, twelve passive fog collectors were installed along the catchment transect between elevations 862 and 994 m: At each collector, fog drip is generated by 400 m of Teflon line (diameter = 0.25 mm, surface area index SAI = 5) exposed at the height of 1.7 m above the ground. Detailed under-canopy observations were accomplished in the stand of mature spruce (area of 30 × 30 m, 975 m a.s.l., 80–100 years old): the canopy through-fall sampled by ten bulk collectors (200 cm<sup>2</sup> area), randomly distributed, and stemflow collected at two average trees. Next three observed forest plots are located outside from the catchment; including a comparable mature spruce stand in lower elevation (745 m a.s.l.) and two beech stands (*Fagus sylvatica*, 160 and 40 years old) in elevations of 420 and 690 m.

Collected rain/fog waters were sampled in monthly intervals and stream waters weekly; chemical analyses were performed in the laboratory of the Hydrobiological Station Velký Pálenec (Charles University in Prague) by the standard techniques developed for soft water studies in mountain environment (Stuchlík et al., 2006), concerned on pH, conductivity, and acidifying substances (SO<sub>4</sub><sup>2-</sup>, NO<sub>3</sub><sup>-</sup> and NH<sub>4</sub><sup>+</sup>). The potential growth of algae in rain/fog collectors was reduced by the dark sampling bottles and installed shelters, also, the bacterial activity in our field is controlled by relatively cold mountain climate (and also by relatively high concentrations of nitrogen, low pH values and dissolved organic carbon), Cape et al. (2001). Benthic macroinvertebrates were sampled in the stream channel near the catchment outlet in May (after snowmelt), July/August (high summer period), and in September/October (relatively dry period) in 1994, 2004–2005 (by the Czech regional campaign, Horecký et al., 2013) and 2015. The kick-net sampling technique (Rosenberg & Resh, 1993) with a hand net (500 μm) was used, the collected material sieved by a 300 μm net, and, counting of each taxa performed in the laboratory (by eye and under a binocular microscope at 12–16× power).

Detailed botanical investigations were carried out in vegetation seasons of 1991, 2002, 2005, 2008 and 2018. Phytosociological relevés (4 × 4 m) were taken at each of the twelve-point transect along the main slope of the catchment, and eight-point transect of the fragmented mature spruce stand. For each botanical relevé, the Ellenberg's indicator of soil moisture was calculated as the weighted average of all recognized species (Ellenberg, 1974). To include the impact of all species abundance, the data were transformed from the Braun-Blanquet's scale to a nine-point scale according to the approach of Van der Maarel (1979). The monitoring of forest stands corresponds to standard forest inventory techniques (Köhl et al., 2006); tree species, age, basal area, height, timber volume, horizontal canopy density, vitality of trees, and leaf area, were estimated. For the aerial extrapolation of ground observations, the free available satellite imagery of Landsat (4,5) and Sentinel (2) was employed (Palán et al., 2018).

Standard methods of historical research (Gunn, 2011) were used to identify the relationship between landscape and the built environment in the Jizera Mts. region with particular attention to the experimental catchment area. This activity included both the documentary evidence of archives and related historical writings.

### 2.3. Theory and calculations

In hydrological years (1st November – 31st October), the annual water budget of the investigated catchment can be considered by

equation (1), Shaw (2011).

$$ET = P - R \tag{1}$$

Where, *ET* is the evapotranspiration loss, *P* precipitation input, and *R* runoff observed at the catchment outlet (water yield), [mm].

According to Arora (2001), components of potential evaporation (available energy) and precipitation determine annual runoff regime in a region. Grismer et al. (2002) reported about fifty empirical methods to estimate potential evapotranspiration; their worth depend namely on quality and extent of meteorological inputs. Based on the Penman – Monteith combination approach (Dingman, 2002), Allen et al. (1998) suggested the reference crop evapotranspiration *RET* (FAO-56) representing a hypothetical grass reference cover with specific characteristics (cool-season grass, height of 0.12 m, albedo 0.23, surface resistance 70 s m<sup>-1</sup>, not short of water) calculated in daily steps by the equation (2).

$$RET = \frac{0.408 \times \Delta \times R + \gamma \times \frac{900}{T+273} \times u \times (e_{sat} - e_{act})}{\Delta + \gamma(1 + 0.34 \times u)} \tag{2}$$

Where, *RET* is the reference evapotranspiration [mm day<sup>-1</sup>], *R<sub>n</sub>* net radiation [MJ m<sup>-2</sup> day<sup>-1</sup>], *T* air temperature at 2 m height [°C], *u* wind speed at 2 m height [m s<sup>-1</sup>], *e<sub>sat</sub>* saturation vapour pressure [kPa], *e<sub>a</sub>* actual vapour pressure [kPa], *Δ* slope vapour pressure curve [kPa °C<sup>-1</sup>], *γ* psychrometric constant [kPa °C<sup>-1</sup>].

In mountain coniferous forests, canopy interception is considered as the dominant component of the total evapotranspiration loss (FAO, 2008; Palán & Křeček, 2018; Ringgaard et al., 2014). Interception loss (*I*) from tall canopies has been estimated by observing the net precipitation (*P'*) reaching the soil surface under the canopy, and the gross precipitation in an adjacent 'open field' (*P<sub>G</sub>*), equation (3):

$$I = P_G + P_F - P' = P_G + P_F - (P_T + P_S) \tag{3}$$

Where, *P'* is the net precipitation, *P<sub>G</sub>* open field (gross) precipitation, *P<sub>F</sub>* fog drip, *P<sub>T</sub>* throughfall under the canopy, and *P<sub>S</sub>* stemflow (in spruce stands supposed to be negligible), [mm].

The analytical model of Gash is the storm-based approach using the mean evaporation and rainfall rates, and the detailed rainfall pattern (Gash et al. (1995). This model considers rainfall to occur as a series of discrete events, each comprising a period of wetting, when the rainfall (*P<sub>G</sub>*), is less than the threshold value necessary to saturate the canopy (*P<sub>C</sub>*), a period of saturation, and a period of drying out after rainfall ceases. The forest structure is described in terms of a canopy storage capacity (*S*), which is defined as the amount of water left on the canopy in zero evaporation conditions when rainfall and throughfall have ceased, a free throughfall coefficient (*p*), which determines the amount of rain which falls directly to the forest floor without touching the canopy, and the proportion of rainfall diverted to stemflow (*p<sub>S</sub>*). The mean evaporation rate during rainfall (*E*) and the mean rainfall rate (*R*) are required to evaluate the loss from a saturated canopy until rainfall ceases. The separate components of the interception loss (*I<sub>1</sub>*, *I<sub>2</sub>*, *I<sub>3</sub>*, *I<sub>4</sub>*) are calculated as the interception of *m* relatively small storm insufficient to saturate the canopy (*I<sub>1</sub>*):

$$I_1 = (1 - p - p_S) \sum_{i=1}^m P_{G_i} \tag{4}$$

The loss (*I<sub>2</sub>*) by wetting the canopy, for *n* storms that saturate the canopy (*P<sub>G</sub>* > *P<sub>C</sub>*):

$$I_2 = n(1 - p - p_s)P_G - nS \quad (5)$$

Evaporation from saturation until rainfall ceases ( $I_2$ ):

$$I_3 = \frac{E}{R} \sum_{i=1}^n (P_{G_i} - P_G) \quad (6)$$

And, evaporation after rainfall ceases ( $I_4$ ):

$$I_4 = nS \quad (7)$$

Then, the total amount of intercepted rainwater ( $I$ ) in a certain period is:

$$I = I_1 + I_2 + I_3 + I_4 \quad (8)$$

Atmospheric precipitation inputs are affected by both elevation and vegetative canopy (Gash et al., 1995; Palán & Kreček, 2018). Thus, the hypsometric method was used to extrapolate point observations of gross precipitation and canopy throughfall, as well as the deposition of sulphate, nitrate and ammonia. Seasonal atmospheric loads of studied elements were estimated by equation (9):

$$m = (bE + b_0) A_{gr}^{-1} F_c \quad (9)$$

Where,  $m$  is the seasonal load (summer and winter) [ $\text{kg km}^{-2}$ ],  $b$ ,  $b_0$  empirical hypsometric coefficients [–],  $E$  elevation [m],  $A_{gr}$  effective receptor area [ $\text{m}^{-2}$ ], and  $F_c$  is the fog drip coefficient [–].

Methods of spatial interpolation (ArcGIS 10.2) were used to approximate the catchment deposition of water and acidifying substances ( $\text{SO}_4^{2-}$ ,  $\text{NO}_3^-$  and  $\text{NH}_4^+$ ); and their runoff was estimated from concentrations and discharge measured at the catchment outlet. Mean annual concentrations were calculated by weighted averages, and mean pH values recalculated by converted values of hydrogen ions. The method of local minima in the hydrograph separation (Sloto and Crouse 1996) was used to detect fast (direct) runoff forms.

Meteorological observations at Jizerka (1982–2016) were extrapolated with the data of two neighbouring climatological stations operated by the Czech Hydrometeorological Institute (Desná-Souš, P2DESN01, 772 m a.s.l., 1951–2016, and, Jablonec n.N., U2JANIOJ, 495 m a.s.l., rainfall registered since 1898), and trends in the time series detected according to WMO (2001). Concerning the future climate projection, simulated air temperatures (at 2 m height) and precipitation amounts were downloaded from the PRUDENCE archive (<http://prudence.dmi.dk>, Christensen & Christensen, 2007). These data are generated by the regional climate model RegCM driven for outputs of two global climate models HadAM3H A2 and HadAM2H B2 respect two emission scenarios (IPCC, 2013a, 2013b): a permanent growth of emissions (A2) and an effective emission control during this century (B2). Downloaded files of daily precipitation (precip.ICTP.A2.nc, precip.ICTP.B2.nc) and mean daily temperatures (t2m.ICTP.A2.nc, t2m.ICTP.B2.nc) were transformed with Intel® Array Viewer Version 3.3 to standard MS Excel base; these data are available for periods 1961–1990 (control) and 2071–2100 (forecast). The elevation gradients ( $-0.6 \text{ }^\circ\text{C per 100 m}$ ) for temperature and ( $+50 \text{ mm per 100 m}$ ) for precipitation (Kreček and Puncochár 2012) were used to transform the downloaded data (corresponding with the average elevation of the  $50 \times 50 \text{ km square}$ ) to the catchment elevation. Daily catchment runoff was calculated by HBV conceptual model (Seibert, 2005) respecting periods of calibration (1991–2010), validation (2011–2016) and simulation (2071–2100).

The standard descriptive statistics and one-way ANOVA were

applied to analyse the collected data sets and to identify relationships between the groups of data (Motulski & Searle, 1998). Trends in the time series were detected by the CTPA programme (WMO, 2001).

### 3. Results

#### 3.1. Changes in the vegetative canopy

According to the 2016 inventory in the Jizerka catchment, four recognized canopy groups (mature spruce stands, middle age stands, young stands with grass, and areas with dominating grass) are introduced in Table 2; and, the canopy structure reconstructed back to 1880 and projected to 2100 is given in Fig. 4. By the end of the 19th century, forests of the studied area were harvested (mainly providing the timber for local glassworks, Fig. 3) and converted to even-age plantations of Norway spruce (Rabštejnek, 1969). In the period 1983–2016, these stands were damaged by the acid rain impact and harvested, the clear-cut and forest regeneration were documented by the supervised classification of multiband raster images (Landsat 4,5, Sentinel 2).

Nowadays, coniferous stands (*P. abies* and introduced exotic species, *P. pungens* mainly) still dominate in the studied catchment with 90%; while deciduous species, mountain-ash (*Sorbus aucuparia*) and silver birch (*Betula pendula*) represent only 10%. It is evident, that the regrowth of forests was complicated by the extended clear-cut, acid environment and grass competition. Future forest projections respect the recommended adaptation strategies of IPCC (2015) and MZP (2017). Thus, by the end of the 21st century, the forest cover of the upper plain of the Jizera Mts. considers both existing stands of Norway spruce and deciduous species (*Fagus sylvatica*, *Sorbus aucuparia*, *Betula pendula*) replacing the recently introduced exotic confers.

#### 3.2. Changing climate

##### 3.2.1. Trends in air temperature and precipitation

Relatively high correlations between annual air temperatures and precipitation sums observed at Jizerka and neighbouring stations Desná – Souš and Jablonec n.N. ( $R = 0.96$  and  $0.83$ , respectively, by  $R_{crit} = 0.33$ ,  $n = 34$ ,  $p = 0.05$ ) allowed to extrapolate/interpolate data representing the studied catchment (Fig. 5, Fig. 6).

Both time series correspond to normal distribution and show an increasing tendency ( $2.2 \text{ }^\circ\text{C}$  and  $90 \text{ mm per 100 years}$ ), but, the statistically significant linear trend was found only for temperatures: correlation coefficient  $R = 0.54$  ( $R_{crit} = 0.24$ ,  $n = 66$ ,  $p = 0.05$ ), the two-tailed P value is below 0.0001 (extremely significant correlation), and not a significant departure from linearity (P value 0.09). The most intensive warming per a decade was identified in the winter season (months XII, I and II)  $0.26 \text{ }^\circ\text{C}$  ( $R = 0.36$ ) and lowest in the autumn (IX, X and XI)  $0.09 \text{ }^\circ\text{C}$  ( $R = 0.22$ , not a significant trend at  $p = 0.05$ ). Statistically significant was found the rising trend of annual extreme values: daily temperature maxima by  $0.22 \text{ }^\circ\text{C}$  ( $R = 0.37$ ) and annual daily rainfall maxima by  $4.5 \text{ mm}$  ( $R = 0.25$ ) per decade, Fig. 7 and Fig. 8.

##### 3.2.2. Warming projections in 2071–2100

In the climate normal period 1961–1990, there was found a relatively strong correlation between the simulated and observed mean monthly temperatures ( $R = 0.86$ ,  $R_{crit} = 0.19$ ,  $p = 0.05$ ), but not significant for precipitation data ( $R = 0.11$ ). In 2071–2100, the model shows an increase in the mean annual temperature of  $2.2 \text{ }^\circ\text{C}$  (B2 scenario) to  $4.5 \text{ }^\circ\text{C}$  (A2 scenario). Seasonal distribution of mean monthly temperatures (Fig. 9) shows higher increases in the high summer: maxima  $4 \text{ }^\circ\text{C}$  (B2) and  $8.3 \text{ }^\circ\text{C}$  (A2), in July–August. We can

**Table 2**  
Vegetative canopy in the Jizerka catchment, 2016.

Group	Canopy	Area		Mean height (m)	Leaf area index (–)
		(10 <sup>3</sup> m <sup>2</sup> )	(%)		
1	Mature spruce stands	45	4	23	6.8
2	Middle age stands	150	15	17	4.7
3	Young stands with grass	484	48	3.9	3.5
4	Grass dominating	332	33	0.5	2.2



**Fig. 3.** Forest harvest in the Jizerka Mts. by the end of the 19th century.  
Source: Museum of glass production, Kristiánov, Czech Republic

expect minor changes in annual amounts of precipitation, but, higher precipitation income during the winter (December–March) and lower in the summer (June–September), by 20–35%. These changes might lead to the shift in climax forest zones with the dominance of beech (*Fagus sylvatica*).

Generally, predictions of air temperatures and precipitation sums by global and regional climate models show a relatively high uncertainty, concerned particularly in the precipitation data, Prein and Gobiet (2017), Rajczak and Schär (2017). In mountain regions, these uncertainties accelerate namely with a lack of observation points (Křeček and Punčochář, 2012) and complicated orography in mountain catchments (Ban et al., 2015). However, the climate

projections in the Jizerka catchment correspond with outcomes of the recent world climate studies (IPCC, 2015).

### 3.3. Water budget

#### 3.3.1. Application of the conceptual catchment model

The HBV hydrological model was calibrated for the period 1991–2010, and simulated daily runoff showed a good agreement with the observed data in the validation period of 2011–2016 (Nash-Sutcliffe efficiency NSE = 0.82, Nash & Sutcliffe, 1970). In 2071–2100, water yield (mean annual outflow from the Jizerka catchment) decreases by 123 mm (i.e. 14%, A2) and 65 mm (7%, B2) in comparison with the period 1991–2016, Table 3. By comparable precipitation inputs, the annual water loss by evapotranspiration increases from 434 mm (recent) to 557 mm (A2) or 499 mm (B2).

Seasonal runoff in 2071–2100 (Fig. 10) has significantly shifted against 1991–2100: during four summer months (VI – IX), the runoff percentage (to the annual outflow) decreases from 47% to 29% (A2) and 33% (B2), while in the dormant season (X–IV), that percentage increases from 53% to 70% (A2) and 67% (B2). While in 1991–2016, the monthly runoff volume culminated by melting snowpack in April (14% of the annual flow), in 2071–2100, with the reduced snow pack volume and duration, that culmination is expected already in March.

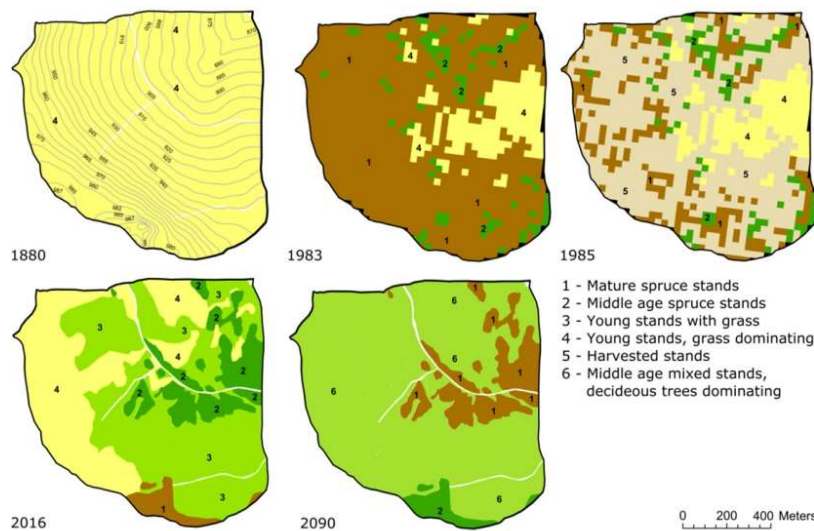


**Fig. 4.** Changing canopy in the Jizerka catchment: 1880–2090.

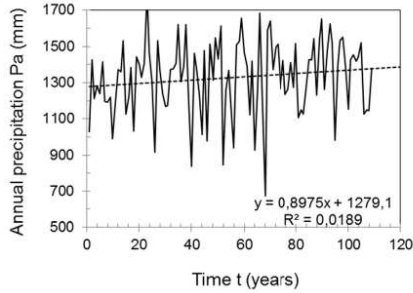


Fig. 5. Annual precipitation at Jizerka: 1900–2016.

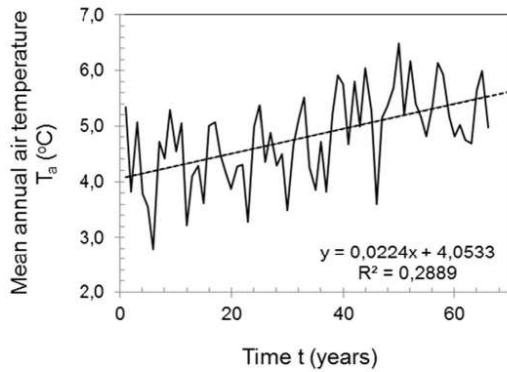


Fig. 6. Mean annual temperature at Jizerka: 1950–2016.

3.3.2. Evapotranspiration potential

Mean annual sums of reference evapotranspiration RET (FAO-56) calculated in daily steps (eq. (2), (Allen et al., 1998)) are

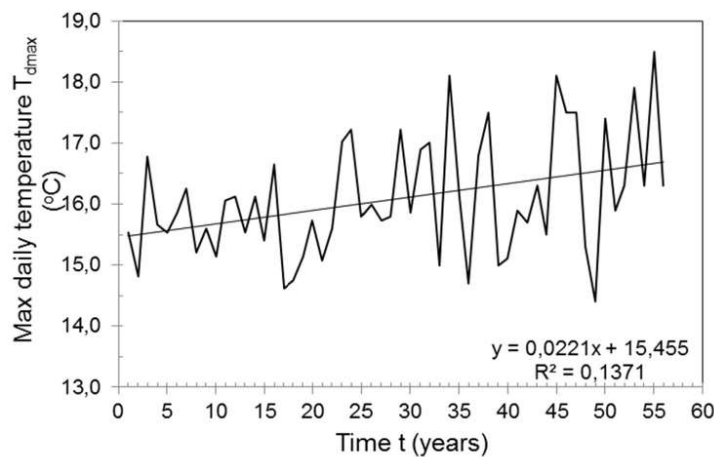


Fig. 7. Maximum daily temperature at Jizerka: 1960–2016.

presented in Table 4. For the period 2071–2100, increases of RET by 128 mm (A2) and 65 mm (B2), correspond with results of the HBV catchment model: drop in water yield by 117 mm (A2) and 65 mm (B2).

Forest canopy can intensify evaporation loss by the interception process (eqs. (4)–(8)). In the warm season of 2016, interception loss observed in the mature stand of Norway spruce is given in Table 5. With climate change, in 2071–2100, can be expected rising values of wet canopy vaporization ( $E$  from 0.21 to 0.26 mm hour<sup>-1</sup>), but, on the other hand, with predicted forest cover (Fig. 4), changing values of the canopy storage capacity  $S$  (from 1.7 to 1.4 mm), the threshold rainfall saturating the canopy  $P'$  (from 2.8 to 2.0 mm), throughfall coefficient  $p$  (from 0.22 to 0.3), and stemflow coefficient  $p_s$  evidence at deciduous trees (from 0 to 0.24). Thus, the rising potential of evaporation can be still modified by changes in forest canopy: by identical rainfall patterns (Table 5), in 2071–2100, the interception loss can change from 271 mm (current state) to 292 mm (A2) and 246 mm (B2).

However, relatively higher evapotranspiration of spruce stands in the investigated catchment has been affected by an additional precipitation income by the canopy fog drip. For the recent canopy structure (Fig. 4, Table 2), the annual income from fog drip is 81 mm (i.e., 10–12% of the annual runoff). In 2071–2100, by comparable atmospheric patterns and expected changes in forest stands (Fig. 2), the fog drip income might decrease to 61 mm (i.e. 75 % of the recent fog drip).

3.3.3. Moisture status

Perhumid environment of the Jizerka catchment is identified by the relatively high value of Lang's moisture factor, ratio between mean annual precipitation and mean average air temperature (Shaw, 2011)  $LMF = 350$ . Correspondingly, the moisture status of the Jizerka catchment is characterized by high values of Ellenberg's soil moisture index  $IF$  (Fig. 11) and relatively small differences between potential and actual evapotranspiration. However, after clear-cut of mature spruce stands (1984–1990), the average  $IF$  value has increased from original 5.76 (identified before the forest harvest in 1982) to 6.45 (1991), reaching maximum 6.97 (2005), and, decreasing back to 6.33 (2018) with forest regrowth. These changes are related to a temporary lower evapotranspiration after the forest



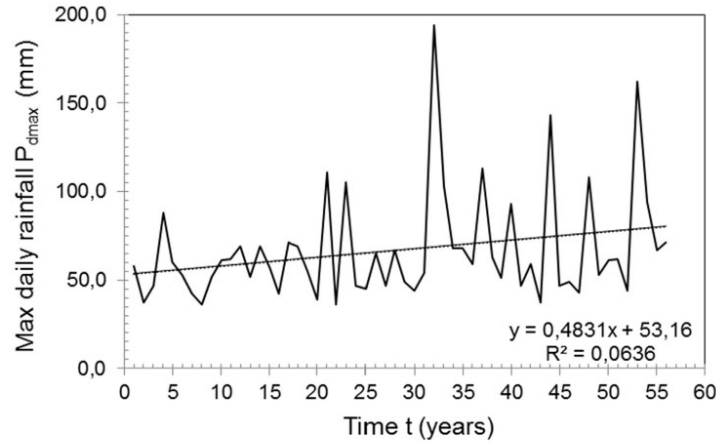


Fig. 8. Maximum daily rainfall at Jizerka: 1960–2016.

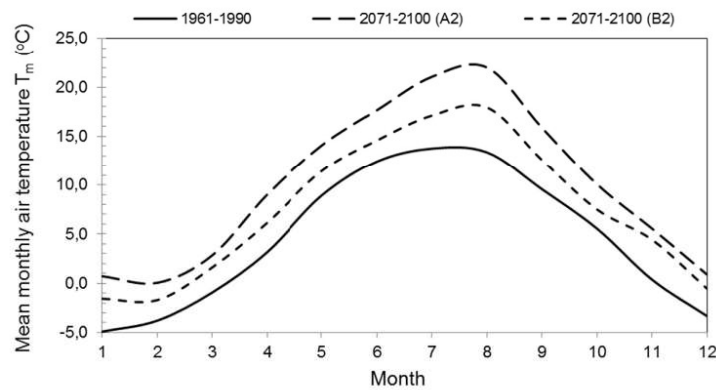


Fig. 9. Projected mean monthly temperatures at Jizerka (873 m a.s.l.): 2071–100.

**Table 3**  
Monthly ( $R_m$ ) and annual ( $R_a$ ) runoff at the outflow of the Jizerka catchment in a 'normal year' of periods 1991–2016 and 2071–2100.

Month	Monthly runoff $R_m$ (mm)		
	1991–2016	2071–2100	
		A2	B2
1	50	75	68
2	46	93	86
3	95	107	105
4	125	48	66
5	78	49	60
6	79	49	52
7	88	50	57
8	96	39	48
9	73	36	54
10	61	59	72
11	62	72	76
12	34	86	77
<b><math>R_a</math> (mm)</b>	<b>886</b>	<b>763</b>	<b>821</b>

harvest with the delay of a couple of years.

3.4. Floods and draughts

Frequency of peak flows in the Jizerka catchment is driven namely by probability of summer rainstorms causing flash floods. Annual maxima of daily rainfalls for the continuous observation period (1961–2019) show an extreme asymmetry (asymmetry coefficient  $C_s = 1.92$  by variation  $C_v = 0.45$ ). Using the Type 1 Gumbel extreme value distribution (Shaw, 2011), maxima of daily rainfall  $P_{dmax}$  (mm day<sup>-1</sup>) of return period 1, 10, 20, 50, 100 and 1000 years re given in Table 6.

Historical records in the Jizera Mts (Munzar & Ondráček, 2010), identified the maximum daily rainfall of 300 mm observed at Jizerka (and 345 mm at the nearby Nová Louka station) on the 29<sup>th</sup> July 1897. According to the frequency distribution (Table 5), this rainstorm (and related flood) might return in 600–700 years. During such an extreme event the role of forests (with retention capacity in an order of magnitude lower) is restricted only to a

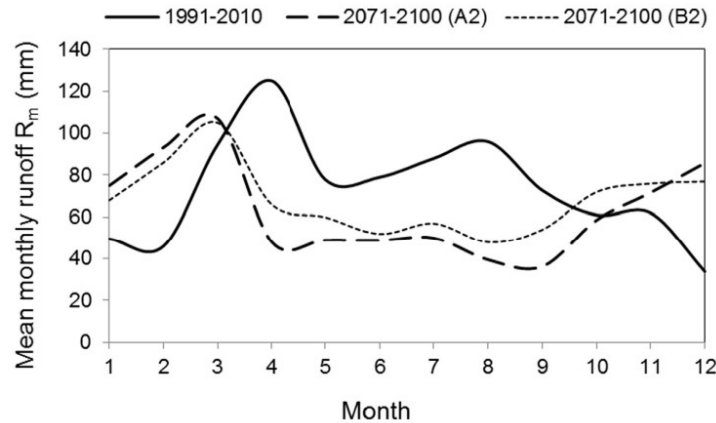


Fig. 10. Projected changes in mean monthly runoff  $R_m$  (mm per month), at the outlet of the Jizerka catchment.

**Table 4**  
Mean annual reference evapotranspiration RET at Jizerka (873 m a.s.l.) by the climate change scenarios A2 and B2.

RET (mm year <sup>-1</sup> )		
1991–2016	2071 -	2100
–	A2	B2
397	509	462

**Table 5**  
Results of the Gash storm-based interception model applied in the mature spruce stand at the Jizerka catchment, 2016.  $I_1, I_2, I_3, I_4$  – interception components (eqs. (4)–(8)),  $m, n$  – number of rainfalls (not enough, and saturating the canopy, respectively).

Month	V	VI	VII	VIII	IX	X	Sum
$m$	22	27	26	6	19	21	121
$n$	6	20	24	8	11	11	80
$I_1$	15.9	16.1	31.3	3.4	12.3	15.1	94
$I_2$	2.9	9.7	11.6	3.8	5.3	5.2	38
$I_3$	0.2	0.5	0.7	0.6	0.4	1	3
$I_4$	10.2	34.0	40.8	13.6	18.7	18.7	136
$I$	29.2	60.3	84.4	21.4	36.7	40	271

slope stabilisation and runoff retardation.

The set of annual peak flows observed at the Jizerka outlet (1982–2019) was extrapolated with the Log-Pearson Type III distribution (Shaw, 2011), Table 7. Discharge values with return periods of 10 and 100 years are  $Q_{10} = 2.5$  and  $Q_{100} = 5.2 \text{ m}^3 \text{ s}^{-1} \text{ km}^{-2}$ . With rising temperatures, according to the climate change scenarios A2 and B2, these values might increase up to  $Q_{10} = 3.3$  (3.0) and  $Q_{100} = 6.8$  (6.3)  $\text{m}^3 \text{ s}^{-1} \text{ km}^{-2}$  respectively; based on the hypothesis of intensifying rainstorm intensities by ca 7% per °K (Knist et al., 2018).

Frequencies of observed daily flows at the Jizerka outlet in 1982–2019 and modelled in 2071–2100 are given in Table 8. The 90% frequency discharge (value reached or exceeded during 330 days a year) is interpreted by the Water Act 254/2001 Coll (Tureček, 2002), as the ‘minimum residual discharge’ necessary to preserve the aquatic environment; in 2071–2100, there is the significant change in  $Q_{90\%}$  from 7.52 to 2.9  $\text{l s}^{-1}$  (decreasing to 39% of its original value).

During 1982–2019, there were not registered any hydrological draught (manifesting an abnormally low streamflow according to Van Loon, 2015). Significant summer drops (ca 50%) were identified in the soil moisture record (Fig. 12) at the top of the Jizerka catchment in years 2017–2019 with the lack of precipitation (reaching only 72% of the normal year), but not registered in lower parts of the catchment.

### 3.5. Acid atmospheric deposition

During the period of integrated environmental monitoring in the Jizerka catchment (since 1982), mean annual pH of precipitation moved up from 4.2 to 5.3, and a pH-adequate annual open field flux of  $\text{H}^+$  in precipitation decreased from 90 to 5  $\text{mg m}^{-2} \text{ year}^{-1}$ . The annual open field flux of buffering basic cations ( $\text{Ca}^{2+}, \text{Mg}^{2+}, \text{K}^+$  and  $\text{Na}^+$ ) fluctuates between 1.67 and 3.35 (mean 2.86)  $\text{g m}^{-2} \text{ year}^{-1}$ , not showing a significant trend in the investigated period. Based on the observed data (1982–2019), historical approximates (Kopáček et al., 2016) and future projections of IPCC (2013a, 2013b), the course of ‘open field’ acid load of  $\text{S-SO}_4^{2-}, \text{N-NO}_3^-$  and  $\text{N-NH}_4^+$  at Jizerka during 1850–2090 is given in Fig. 13.

Considering the effect of vegetative canopy, the atmospheric load of acidifying substances ( $\text{SO}_4^{2-}, \text{NO}_3^-$  and  $\text{NH}_4^+$ ) in the investigated catchment (Figs. 14–16) was estimated by the spatial interpolation according to the canopy classes and elevation (eq. (9)) for observed data in twelve stands of the catchment transect (from 862 to 975 m a.s.l.). Then, the total catchment deposition of sulphur ( $\text{S-SO}_4^{2-}$ ) and nitrogen ( $\text{N-NO}_3^-$  and  $\text{N-NH}_4^+$ ) in the period of 1850–2090 is shown in Fig. 17. Considering the periods of 1982–1984 (before the forest clear-cut) and 2001–15 (drop in emissions and forest regrowth), the mean total annual deposition of sulphur has decreased from 8.7 to 1.6  $\text{g m}^{-2} \text{ year}^{-1}$  (an extra load

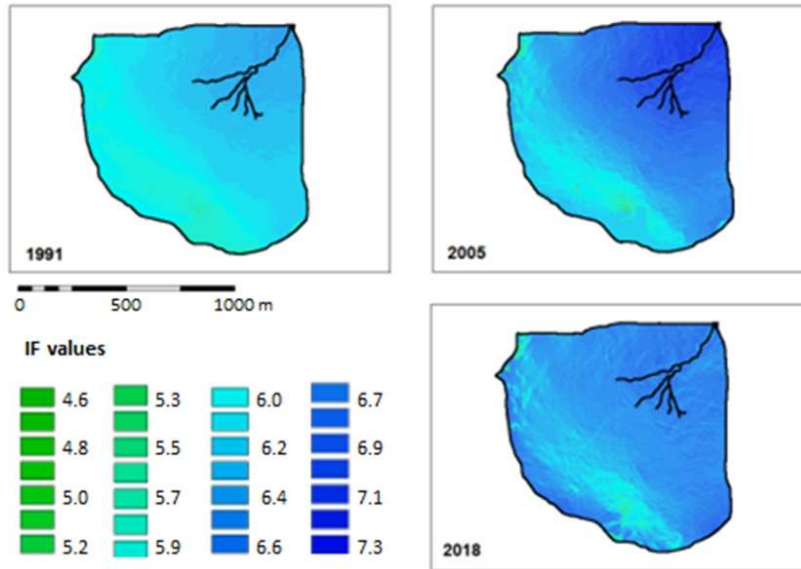


Fig. 11. Ellenberg's soil moisture indicator IF in the Jizerka catchment: 1991, 2005 and 2018.

**Table 6**  
Frequency of maximum daily rainfall at Jizerka, 1961–2010.

Return period N (years)	Rainfall maximum $P_{\text{dmax}}$ ( $\text{mm day}^{-1}$ )
1	56
10	115
20	158
50	201
100	262
1000	604

**Table 7**  
Peak discharge  $Q_N$  (N is return period in years) at the Jizerka outlet, 1982–2016 and 2071–2100.

Period	$Q_N$ ( $\text{l s}^{-1}$ )			
	$Q_1$	$Q_{10}$	$Q_{50}$	$Q_{100}$
1982–2016	0.9	2.5	4.3	5.2
2071–2100 (A2)	1.2	3.3	5.6	6.8
2071–2100 (B2)	1.1	3.0	5.2	6.3

**Table 8**  
Daily discharge frequencies at the outlet of the Jizerka catchment in periods 1982–2019 and 2071–2100 ( $Q_x$  is mean annual discharge).

Period	Discharge ( $\text{l s}^{-1}$ )				
	$Q_x$	$Q_{90\%}$	$Q_{95\%}$	$Q_{97\%}$	$Q_{99\%}$
1991–2010	28	7.52	6.10	5.04	3.13
2071–2100 (A2)	24	2.90	2.06	1.50	0.58
2071–2100 (B2)	26	2.94	2.18	1.55	0.59

of the canopy decreased from 60 to 40%) while nitrogen did not change significantly (from 2.62 to 2.74  $\text{g m}^{-2} \text{ year}^{-1}$  with decreasing canopy effect from 45 to 27%).

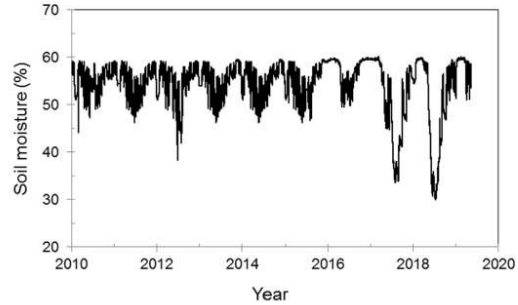


Fig. 12. Volumetric soil moisture at the top of the Jizerka catchment, 2010–2019.

In the period of observation (1982–2019), the ratio between the total load of nitrogen and sulphur in the Jizerka catchment has increased from 0.35 (1982–1988) to 2.0 (after 2011), and this trend is predicted also for the end of the 21st century (IPCC, 2013a, 2013b).

### 3.6. Water quality and biota

In the Jizerka catchment, stream water acidification culminated in the 1980s with the peak in atmospheric deposition of sulphur and nitrogen (Fig. 17), Table 9. In the 1990s, the recovery resulted from a synergy of the drop in  $\text{SO}_2$  emissions (following the 1985 Sulphur protocol, Holen et al., 2013) and the decline of the forest canopy (reducing the surface area as well as the air mass turbulence above the canopy). Later, open field deposition of sulphur and nitrogen have been stabilised, and stream water chemistry became

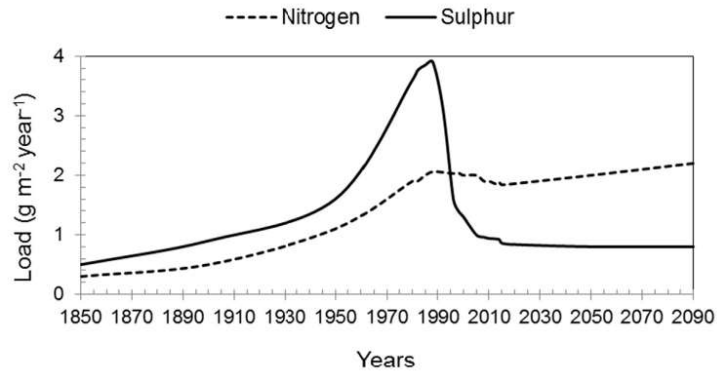


Fig. 13. The approximated bulk deposition of sulphur ( $S-SO_4$ ), and nitrogen ( $N-NO_3$  and  $N-NH_4$ ) at Jizerka, 1850–2090.

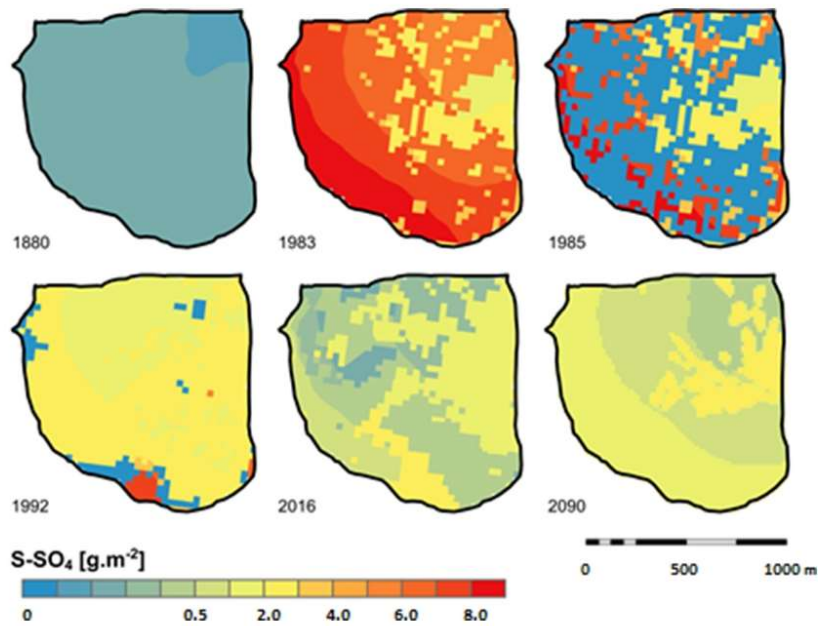


Fig. 14. The atmospheric load of sulphur ( $S-SO_4$ ) estimated under the canopy, in the Jizerka experimental catchment, 1880–2090.

controlled mainly by the regrowth of forest stands (Fig. 4).

Considering water resources recharge, no health-based guideline value has been proposed for the pH of water, but, WHO (2004) suggest that optimum pH for drinking water quality between 6.5 and 8.5. Low pH values observed in the Jizerka stream indicate also low hardness (up to 10 mg of calcium and magnesium per litre) and particularly higher contents of aluminium (Table 9). The limit of aluminium in drinking-water is 0.1 mg l<sup>-1</sup> for large treatment facilities, and 0.2 mg l<sup>-1</sup> for small facilities (WHO, 2004). In 2071–2100, the expected drop in annual catchment outflow (Table 3) can cause higher mean annual concentrations of sulphate:

3.4 mg l<sup>-1</sup> (A2 scenario) and 3.1 mg l<sup>-1</sup> (B2 scenario), nitrate: 2.2 mg l<sup>-1</sup> (A2) and 2.0 mg l<sup>-1</sup> (B2) and aluminium: 0.12 mg l<sup>-1</sup> (A2) and 0.11 mg l<sup>-1</sup> (B2).

The investigated stream at Jizerka was found fishless in the 1980s, and remained without any fish evidence also in 1990–2016. In 1994 (six years after the peak in acid load), the number of identified benthic taxa (36) there still indicated a 'strongly acidified environment', and, in 2005, the number of taxa increased to 68 detecting a 'moderately acidified environment' (with pH between 5.0 and 6.3), Table 9.

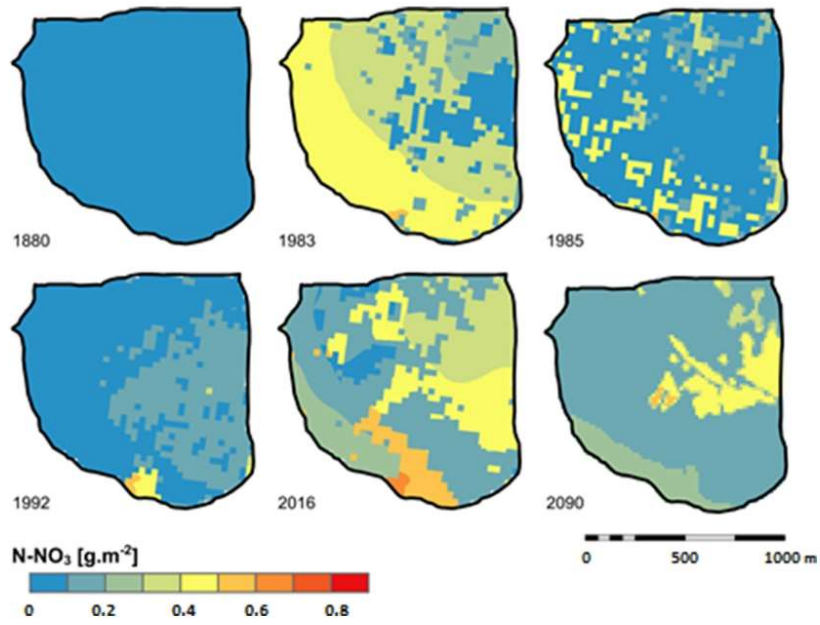


Fig. 15. The atmospheric load of nitrogen ( $N-NO_3$ ) estimated under the canopy in the Jizerka experimental catchment, 1880–2090.

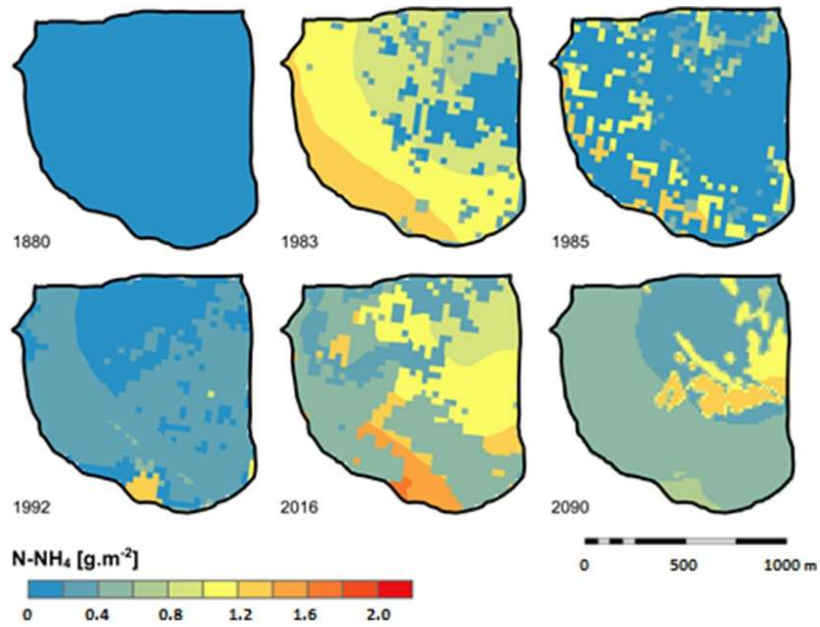


Fig. 16. The atmospheric load of nitrogen ( $N-NH_4$ ) estimated under the canopy in the Jizerka experimental catchment, 1880–2090.

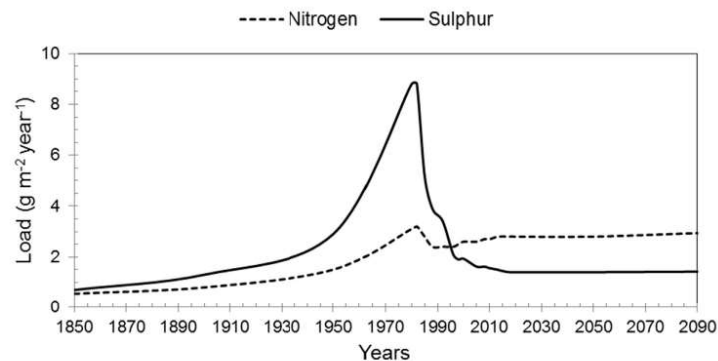


Fig. 17. The total atmospheric load of sulphur ( $S-SO_4^{2-}$ ) and nitrogen ( $N-NO_3$  and  $N-NH_4$ ) in the Jizerka catchment (estimated under the canopy), 1880–2090.

Table 9

Timber harvest and selected parameters of stream water quality at the outlet of the Jizerka catchment, 1982–2016.

	1982	1994	2005	2016
Mature spruce stands (%)	76.3	4.5	4.5	4.5
Mean annual pH (–)	4.1	5.2	5.8	6.0
Sulphate content ( $mg\ l^{-1}$ )	12.1	7.8	4.4	2.9
Nitrate content ( $mg\ l^{-1}$ )	5.0	3.9	2.5	1.9
Aluminium content ( $mg\ l^{-1}$ )	1.2	0.5	0.1	0.1
Benthic taxa (–)	–	36	68	–
Environmental status (–)	“strongly acidified”	“moderately acidified”	“moderately acidified”	“moderately acidified”

### 3.7. Historical context of forest functions in the Jizerka Mts

Since the first human interventions, priorities of forest management in the Jizerka Mts. have gradually changed from early protection of forests (to secure the state border and big game hunting), to sustainable timber harvesting and recent multi-resource forestry (Rabštejnek, 1969; Krečmer & Kreček, 1986). Particularly, with industrialisation in the 19th century, the occurrence of more frequent floods with intensive timber harvest in the Jizerka Mts (Fig. 3), was documented by Blask in Kutnar (1941). This situation initiated the declaration of soil and water protection (Austro-Hungarian Acts 116 and 117/1884 Coll.). Particularly, the catastrophic flood of 1897 commenced there the complex of protection activities including construction of retention dams, torrent control works, and reforestation activities, based on Surell's principle (1841, in Magnein, 1937): “The presence of forest prevents the formation of torrents”. Anyway, by the relatively fast reforestation, the original forests of native tree species (*Fagus sylvatica* L., *Picea abies*, and *Abies alba* Mill.) were converted to the plantations of Norway spruce (*Picea abies*) with lower ecological stability, mentioned already by Gayer (1886).

In 1956, the Protected Landscape Region of the Jizerka Mts. was claimed by the Czech government to preserve the unique natural elements of the region (Nature Protection Act 40/1956 Coll.); and, after the UN (1992) statement, the vital role of forest there was supported by Nature and Landscape Protection Act 114/1992 Coll. Later, with rising demand on drinking water supply, the Protected Headwater Area of the Jizerka Mts. was declared by the Decree 40/1978 of the Czech government (according to the Water Act 138/1973, 254/2001 Coll.) to support the regional recharge of water resources (quantity and quality) by controlling the reduction of forests and drainage development.

However, the traditional forest benefits in protecting water quality were declined by the acid rain phenomena, when the acid atmospheric deposition (namely by the airborne emissions of sulphur and nitrogen) was rising with the canopy area and roughness (Kreček & Hořická, 2006). Acid rain affects the ecosystems of the Jizerka Mts. (part of the European ‘Black Triangle’) since the 1850s (Figs. 13 and 17); culminating in the 1980s when the widespread acidification of freshwaters with damage to drinking water quality and populations of fish and other aquatic organisms became critical (Table 9). First signs of recovery occurred in early 1990s with both, the 1985 Helsinki Protocol on the Reduction of Sulphur Emissions or their Transboundary Fluxes (with loads of sulphur decreased to approx. 40% of those in 1987, Holen et al., 2013, Fig. 13), and the extensive dieback and clear-cut of spruce plantations (Figs. 4 and 17).

By reforestation, in the 1990s, several exotic species (blue spruce – *Picea pungens*, black spruce – *Picea mariana*, etc.) were introduced to produce stands more resistant to air pollution (Špulák et al., 2019). These exotic conifers show comparable performance (nutrient pools, topsoil chemistry, and growth) with stands of Norway spruce in the Jizerka Mts. Nowadays, conversion projects to produce forests near the native composition are motivated by the need for higher ecosystem stability, the danger of biotic agents (e.g. high damage caused by cloven-hoofed game to stands of *P. pungens*) and global climate change. While impacts of air pollution and acidification on forest functions was the most discussed topic in Central Europe in the 1980s and 1990s, nowadays, the global climate change and weather extremes are considered as the most important driving factor of mountain forests (Braun et al., 2015).

## 4. Discussion

While at the end of the 19th century, the protective role of forests in the Jizerka Mts. concentrated on flood control, nowadays, water resources recharge and biodiversity became the focus. With the expected status of society, climate, and water resources by the end of the 21st century (FAO, 2008; IPCC, 2015), these priorities in headwater catchments might be still emphasized.

By the end of the 20th century, in the Jizerka Mts., widespread acidification, forest dieback, and extensive clear-cut changed priorities in forestry for environmental reconstruction and assisted regeneration (Perrow & Davy, 2002). While emissions of sulphur are controlled effectively since the end of the 1980s (Protocol on the Reduction of Sulphur Emissions, Holen et al., 2013), nitrogen is still

considered as a future problem. Hůnová et al. (2020) reported a significant trend in reducing emissions of  $\text{NO}_x$  in big industrial cities of the Czech Republic since 1994, but not in mountain regions. Since 1982, the ratio between the total load of nitrogen and sulphur in the Jizerka catchment has gradually increased from 0.35 to 2.0. Contrary to the statement of UNEP (2007) that the historical decline in temperate forests has been reversed between 1990 and 2005, forest ecosystems in the Jizera Mts. are still threatened by acidification.

Besides atmospheric emissions, the acid atmospheric load in the studied catchment is controlled also by the vegetative canopy (Figs. 13 and 17). Contrary to conclusions of Neary et al. (2009) that the most sustainable and best quality freshwater sources in the world originate in forest ecosystems, in sensitive headwater catchment, forest regrowth leads to decreasing the base status of the soil and rendering soils and surface waters more sensitive to acid deposition (Jenkins et al., 1990). The critical loads of sulphur and nitrogen (75 and 55  $\text{meq m}^{-2} \text{ year}^{-1}$ , respectively; Schwarz, 2009) in the Jizerka catchment are still exceeded by the load of sulphur in forest stands (79–553  $\text{meq m}^{-2} \text{ year}^{-1}$ ) and nitrogen in both 'open field' (99–149  $\text{meq m}^{-2} \text{ year}^{-1}$ ) and forest stands (142–206  $\text{meq m}^{-2} \text{ year}^{-1}$ ). During the whole observation period (1982–2019) deposition of nitrogen exceeds by 2–3 times the empirical threshold  $1 \text{ g m}^{-2} \text{ year}^{-1}$  (i.e.  $71 \text{ meq m}^{-2} \text{ year}^{-1}$ ) suggested for forests of central Europe by Bobbink and Roelofs (1995); the load of  $\text{N-NH}_4^+$  presented 72% and  $\text{N-NO}_3^-$  28% of the atmospheric nitrogen deposition. Fangmeier et al. (1994) warned namely of the atmospheric ammonia impact on large scale nitrogen eutrophication and acidification of ecosystems, and, thus, higher susceptibility to abiotic (drought, frost) and biotic (pests) stress in mountain environments. The atmospheric input of nitrogen, together with rising air temperatures, is associated with increasing radial growth and the total number of cells in the tree rings by ca 10% detected in mature spruce trees at Jizerka by Vrtiška et al. (2018).

First signs of stream water recovery from acidification were observed at Jizerka in the early 1990s as results of both the 1985 Helsinki Protocol on the Reduction of Sulphur Emissions (Holen et al., 2013) and reduced canopy area by forest clear-cut (Figs. 4 and 17, Table 9). Thirty years after, forest – water interactions in the Jizerka catchment are still affected by the prolonged acid atmospheric deposition and lack of environmental forestry practices. Without acid rain impact, streams in the Jizera Mts. would show a mean pH level close to 6.5 (Křeček & Hořícká, 2006). According to Jenkins et al. (1990), besides the significant reduction in atmospheric emissions, stream water recovery requires also the control of forest canopy and treatment of forest soils by the addition of base cations; forests contribute to historical acidification of soils and surface waters by the nutrient demand. Thus, regrowth of coniferous stands can still slow down the recovery of surface waters in the Jizerka catchment (Křeček et al., 2019). Invertebrate communities are considered the best indicator to assess the environmental impact of stream water acidification (Guerold et al., 2000), strongly correlated with water pH (Horecký et al., 2006). During the investigated period 1982–2019, the number of identified benthic taxa at Jizerka (Table 9) manifested the change from 'strongly acidified' to 'moderately acidified' environment. While recovery of stream water chemistry there follows the drop of the atmospheric load in some five years, the revival of stream biota takes evidently a longer lag period (about ten to fifteen years).

The analysed instrumental time-series at Jizerka show a significantly rising trend in both annual mean air temperatures and annual maxima of daily temperatures (0.22 °C per decade) with more intensive warming in the winter (December–February, 0.26 °C per decade), and in annual daily rainfall maxima (4.5 mm per decade), but elevated annual precipitation (9 mm per decade)

was recognized as not statistically significant. In comparison with 1961–1990, the projected mean annual temperature for 2071–2100 rises by 4.6 °C (A2 scenario) and 3.0 °C (B2 scenario); mean monthly temperatures rise particularly in the high summer by 9 °C (A2) and 4 °C (B2). Generally, climate change predictions are linked to relatively high uncertainties (an IPCC outcome refers to the likelihood greater than 66% probable, Latif, 2011). In mountain regions, particularly, uncertainties in precipitation accelerate namely with the lack in observation points (Křeček and Puncochář, 2012, Prein & Gobiet, 2017) and complicated orography (Ban et al., 2015). However, the climate projections in the Jizerka catchment correspond well with recent trends in instrumental data. The projected warming can lead to the shift in climax zones to those with dominating beech forests, more diverse mixed stands with higher ecological stability, and lower acceleration of the acid atmospheric load. However, the projection of future forests considers the survival of existing spruce stands and conversion of recently introduced exotic conifers to deciduous species. Such a scenario corresponds with the findings of Vacek and Balcar (2004) and Špulák et al. (2019). The survival of native spruce (*Picea abies*) in the changing mountain environment can be still supported by planting its more resistant forms (Frýdl et al., 2011).

In 2071–2100, annual water yield of the Jizerka catchment is expected to decrease by 123 mm (i.e. 14%, A2) and 65 mm (i.e. 7%, B2), Table 3, with the seasonal shift from April to March (according to changes in snow accumulation and melting). The increase in vaporizing intensity (Table 4) can be still modified by forest canopy: the annual canopy interception can change from recent 271 mm to 292 mm (A2) or 246 mm (B2), Table 5. Moreover, the annual fog drip income might decrease from the recent 81 mm (ca. 10% of the annual runoff) to 61 mm (i.e. 75% of the recent fog drip). Despite these changes in water balance, the water supply potential of this headwater catchment will not be significantly declined: the contemporary high 'relative water yield'  $\text{RWY} = 4.69$  (long-term runoff ratio between the catchment cell and the whole lowland area, Viviroli et al., 2007) might still rise with expected more rapid drops in lowland mean annual discharge (reported by Trnka et al., 2016). The study of IPCC (2013a, 2013b) highlighted namely the problem of increasing draught episodes as a serious limiting factor of water supply facilities and biodiversity conservation. During 1982–2019, there were still not registered hydrological draughts at the outlet of the Jizerka catchment. Similarly, Hisdal et al. (2001) reported that it is still not possible to conclude when hydrological draughts in Europe at the end of the 19th century have become more severe or frequent. In 2071–2100, the 90% - frequency discharge  $Q_{90\%}$  ('minimum residual flow' to preserve aquatic life) is considered to drop from  $7.52 \text{ to } 2.91 \text{ s}^{-1}$  (i.e. to 39% of recent value), Table 8, while the peak flow of 100 year return period  $Q_{100}$  could increase from original  $Q_{100} = 5.2 \text{ m}^3 \text{ s}^{-1}$  to  $6.8 (6.3) \text{ m}^3 \text{ s}^{-1}$  for A2 (B2) scenarios, respectively, Table 7. This shift in peak flow frequencies can significantly affect the flood control design, for example, the design flow of  $Q_{100}$  will shift to  $Q_{50}$  (B2) or  $Q_{40}$  (A2).

The expected drop in annual runoff can cause higher mean annual concentrations of sulphate:  $3.4 \text{ mg l}^{-1}$  (A2) and  $3.1 \text{ mg l}^{-1}$  (B2); nitrate:  $2.2 \text{ mg l}^{-1}$  (A2) and  $2.0 \text{ mg l}^{-1}$  (B2), and, aluminium:  $0.12 \text{ mg l}^{-1}$  (A2) and  $0.11 \text{ mg l}^{-1}$  (B2), Table 9. These values might still rise by episodic runoff events (Křeček & Hořícká, 2006), but, they cannot affect the drinking water standard or the biodiversity conservation. Generally, the decline of stream water quality is associated with lower stream flows and higher contents of nutrients (Strayer & Dudgeon, 2010). On the other hand, climate warming can positively influence biogeochemical weathering associated with higher alkalinity of mountain waters (Catalan et al., 2014), and, thus, stimulate their chemical and biological recovery from acidification (Kopáček et al., 2019). In addition, rising water temperature

might allow colonization of stream waters by less stenothermic species from lower parts of the watercourse, and, thus to avoid a sharp change of the original (pre-acidification) biodiversity of the aquatic environment. Stream biota reflects also the stream bed structure (Rosenberg & Resh, 1993), thus, a higher frequency of peak-flows (Table 7) might intensify changes in stream bed with a higher potential for colonization by alien species. The drop in minimum flows (Table 8) is still not causing an intermittent flow regime, but, decreasing Q90% can significantly affect stream water biota.

## 5. Conclusions

During the last two hundred years, forests in the Jizera Mts. gradually changed from native stands to spruce plantations, introducing exotic conifers resistant to the air pollution, and back to the preference of stands near the native composition. While at the end of the 19th century, the protective role of forests concentrated mainly on flood control, nowadays, protection of water resources and biodiversity became the focus.

The study in the Jizerka experimental catchment, 1982–2019, shows that the acid atmospheric deposition (and stream water quality) can be modified by forestry practices, and, the recent recovery from acidification there is the result of both the drop in sulphur emissions and the clear-cut of mature spruce stands.

The projected environmental changes in 2071–2100 will not substantially decline the high potential in water resource recharge, water quality and aquatic biodiversity, or, start reverse processes in recent recovery from acidification in the upper plain of the Jizera Mts.

## Declaration of competing interest

None.

## Acknowledgement

This research was supported by the Ministry of Education, Youth and Sports (Czech Republic, INTER-EXCELLENCE LTC 17006), European Cooperation in Science and Technology (COST Action CLIMO CA15226), Czech Technical University in Prague (Czech Republic, Project SGS20/1101OHR112T/11), and Czech Science Foundation (Czech Republic, PROGRESS: 20-08294S).

## References

- Agnoletti, M., Dargavel, J., & Johann, E. (2002). History of forestry. In V. R. Squires (Ed.), *The role of food, agriculture, forestry and fisheries in human nutrition* (Vol. 2, pp. 1–29). Paris: UNESCO: EOLSS.
- Allen, R. G., Pereira, L. S., Raes, D., & Smith, M. (1998). *Crop evapotranspiration, guidelines for computing crop water requirements*. Rome: Food and Agriculture Organization of the United Nations. FAO Irrigation and Drainage Paper 56.
- Arora, V. K. (2001). The use of the aridity index to assess climate change effect on annual runoff. *Journal of Hydrology*, 265, 164–177.
- Ban, N., Schmidli, J., & Schär, C. (2015). Heavy precipitation in a changing climate: Does short-term summer precipitation increase faster? *Geophysical Research Letters*, 42, 1165–1172.
- Bobink, R., & Roelofs, J. G. M. (1995). Nitrogen critical loads for natural and semi-natural ecosystems: The empirical approach. *Water, Air, and Soil Pollution*, 85, 2413–2418.
- Braun, S., Remund, J., & Rihm, B. (2015). Indikatoren zur Schätzung des Trockenheits-risikos in Buchen- und Fichtenwäldern. *Schweizerische Zeitschrift für Forstwesen*, 6, 361–371.
- Cape, J. N., Kirika, A., Rowland, A. P., Wilson, D. R., Jickells, T. D., & Cornell, S. (2001). Organic nitrogen in precipitation: Real problem or sampling artefact? *Scientific World*, 1(52), 230–237.
- Catalan, J., Pla-Rabés, S., García, J., & Camarero, L. (2014). Air temperature-driven CO<sub>2</sub> consumption by rock weathering at short timescales: Evidence from a Holocene lake sediment record. *Geochimica et Cosmochimica Acta*, 136, 67–79.
- Christensen, J. H., & Christensen, O. B. (2007). A summary of the PRUDENCE model



- projections of changes in European climate by the end of this century. *Climate Change*, 81, 7–30.
- Corbin, A. (1998). *Le monde retrouvé de Louis-François Pinagot sur les traces d'un inconnu 1798-1876*. Paris: Flammarion.
- Dingman, S. L. (2002). *Physical hydrology* (2nd ed.). New York: McMillan.
- Ellenberg, H. (1974). Zeigerwerte der Gefäßpflanzen Mitteleuropas. *Scripta Geobotanica*, 9, 1–97.
- Fangmeier, A., Hadwiger-Fangmeier, A., Van der Eerden, L., & Jäger, H. J. (1994). Effects of atmospheric ammonia on vegetation - a review. *Environmental Pollution*, 86(1), 43–82.
- FAO. (2007). *Adaptation to climate change in agriculture, forestry and fisheries: Perspective, framework and priorities*. FAO Inter-departmental Working Group on Climate Change. Rome: Food and Agriculture Organization of the United Nations.
- FAO. (2008). *Forests and water*. FAO Forestry paper 155. Rome: Food and Agriculture Organization of the United Nations.
- Frydl, J., Novotný, P., Ivanek, O., Buriánek, V., & Čáp, J. (2011). Possibilities of silvicultural utilization of vegetatively maintained variants of resistant Norway spruce from the Ore Mountains (In Czech). *Methodological guide*. Jiloviste-Strnadý: VÚLHM.
- Gash, J. H. C., Lloyd, C. R., & Lachaud, G. (1995). Estimating sparse forest rainfall interception with an analytical model. *Journal of Hydrology*, 170, 79–86.
- Gayer, K. (1886). *Der gemischte Wald, seine Begründung und Pflege, insbe-sondere durch Horst- und Gruppenwirtschaft*. Berlin: Paul Parey Verlag.
- Grismer, M. E., Orang, M., Snyder, R., & Matyac, R. (2002). Pan evaporation and to reference evapotranspiration conversion methods. *Journal of Irrigation and Drainage Engineering*, 128(3), 180–184.
- Guerold, F., Boudot, J. P., Jacquemin, G., Vein, D., Merlet, D., & Rouiller, J. (2000). Macroinvertebrate community loss as a result of headwater stream acidification in the Vosges Mountains (N-E France). *Biodiversity & Conservation*, 9, 767–783.
- Gunn, S. (2011). *Research methods for history*. Edinburgh: Edinburgh University Press.
- Hisdal, H., Stahl, K., Tallaksen, L. M., & Demuth, S. (2001). Have streamflow droughts in Europe become more severe or frequent? *International Journal of Climatology*, 21, 317–333.
- Holen, S., Wright, R., & Seifert, I. (2013). *Effects of long range transported air pollution (LRTAP) on freshwater ecosystem services*. ICP-Waters report 115/2013. Oslo: Norwegian Institute for Water Research.
- Horecký, J., Rucki, J., Krám, P., Kreček, J., Bitušik, J., & Stuchlík, E. (2013). Benthic macroinvertebrates of headwater streams with extreme hydrochemistry. *Biologia*, 68, 1–11.
- Hunová, I., Baumelt, V., & Modlik, M. (2020). Long-term trends in nitrogen oxides at different types of monitoring stations in the Czech Republic. *The Science of the Total Environment*, 699(134378).
- IPCC. (2013a). *Climate change 2013: The physical science basis*. Cambridge: Cambridge University Press.
- IPCC. (2013b). *Climate change 2013: The physical science basis*. Cambridge: Cambridge University Press.
- IPCC. (2015). *Climate change 2014: Synthesis report*. Genève: World Meteorological Organization.
- Jenkins, A., Cosby, B. J., Ferrier, R. C., Walker, T. A. B., & Miller, J. D. (1990). Modelling stream acidification in afforested catchments: An assessment of the relative effects of acid deposition and afforestation. *Journal of Hydrology*, 120, 163–181.
- Klvac, P. (2006). *Man and forest*. Brno: Masarykova univerzita (In Czech).
- Knist, S., Goergen, K., & Simmer, C. (2018). Evaluation and projected changes of precipitation statistics in convection-permitting WRF climate simulations over Central Europe. *Climate Dynamics*. <https://doi.org/10.1007/s00382-018-4147-x>. Available from: . (Accessed 24 January 2020).
- Kohler, T., & Maselli, D. (2009). *Mountains and climate change – from understanding to action*. Bern: Geographica Bernensia, 978-3-905835-16-8.
- Köhl, M., Magnussen, S., & Marchetti, M. (2006). *Sampling methods, remote sensing and GIS multiresource forest inventory*. Berlin: Springer-Verlag.
- Kopáček, J., Hejzlar, J., Krám, P., Oulehle, F., & Posch, M. (2016). Effect of industrial dust on precipitation chemistry in the Czech Republic (Central Europe) from 1850 to 2013. *Water Research*, 103, 30–37.
- Kopáček, J., Kana, J., Bicărová, S., Brahmey, J., Navrátil, T., Norton, S., ... Stuchlík, E. (2019). Climate change accelerates recovery of the Tatra Mountain lakes from acidification and increases their nutrient and chlorophyll a concentrations. *Aquatic Sciences*, 81, 70.
- Krečmer, V., & Kreček, J. (1986). Forestry and water management – a brief history of ideas. *Ambio*, 15(5), 120–121.
- Krott, M. (2005). *Forests policy analysis*. Dordrecht: European Forest Institute (Springer).
- Kutnar, F. (1941). *Memories of farmer Josef Dlask*. Prague: Melantrich (In Czech).
- Kreček, J., Haigh, M., Hofer, T., Kubin, E., & Promper, C. (2017). *Ecosystem services of headwater catchments*. Cham: Springer.
- Kreček, J., & Horická, Z. (2006). Forests, air pollution and water quality: Influencing health in the headwaters of Central Europe's „Black Triangle“. *Unasylva*, 57(224), 46–49.
- Kreček, J., Palán, L., Pažourková, E., & Stuchlík, E. (2019). Water-quality genesis in a mountain catchment affected by acidification and forestry practices. *Freshwater Science*, 38(2), 257–269.
- Kreček, J., & Puničochář, P. (2012). Design of climate station network in mountain catchments. *Hungarian Geographical Bulletin*, 61(1), 19–29.
- Latif, M. (2011). Uncertainty in climate change projections. *Journal of Geochemical*



- Exploration, 110(1), 1–7.
- Leggewie, C., & Mauelshagen, F. (2018). *Climate change and cultural transition in Europe*. Leiden: Brill.
- Magnein, M. A. (1937). Control and use of little waters in France. In *Head was control and use* (pp. 227–232). Washington D.C.: United States Governmental Printing.
- McGrath, M. J., Luysaert, S., Meyfroidt, P., Kaplan, J. O., Bürgi, M., Chen, Y., ... Valade, A. (2015). Reconstructing European forest management from 1600 to 2010. *Biogeosciences*, 12, 4291–4316.
- Motulski, H. J., & Searle, P. (1998). *InStat guide to choosing and interpreting statistical tests*. San Diego, GraphPad Software, Inc.
- Munzar, J., & Ondráček, S. (2010). The historical precipitation record from the Jizera Mts. still unbroken. *Acta Musei Bohemiae Borealis, Scientiae Naturales*, 28, 3–15.
- MZP. (2017). *National action plan on adaptation to climate change*. Prague: Ministry of the Environment (MZE).
- Nash, J. E., & Sutcliffe, J. V. (1970). River flow forecasting through conceptual models part 1 – a discussion of principles. *Journal of Hydrology*, 10(3), 282–290.
- Neary, D. G., Ice, G. G., & Jackson, C. R. (2009). Linkages between forest soils and water quality and quantity. *Forest Ecology and Management*, 258, 2269–2281.
- Palán, L., & Kreček, J. (2018). Interception and fog drip estimates in fragmented mountain forests. *Environmental Processes*, 5, 727–742.
- Palán, L., Kreček, J., & Sato, Y. (2018). Leaf area index in a forested mountain catchment. *Hungarian Geographical Bulletin*, 67(1), 3–11.
- Perrow, M. R., & Davy, A. J. (2002). *Handbook of ecological restoration, ume I*. Cambridge: Cambridge University Press. Principles of restoration.
- Pilli, R., & Pase, A. (2018). Forest functions and space: A geohistorical perspective of European forests. *iForest*, 11(1), 79–89.
- Rabštejnec, O. (1969). Forests of the Jizera Mountains. *Nature Conservation (Ochrana Přírody)*, 24, 40–42 (In Czech).
- Ringgaard, R., Herbst, M., & Friberg, T. (2014). Partitioning forest evapotranspiration: Interception evaporation and the impact of canopy structure, local and regional advection. *Journal of Hydrology*, 517, 677–690.
- Rosenberg, D. M., & Resh, V. H. (1993). *Freshwater biomonitoring and benthic macroinvertebrates*. New York: Chapman and Hall.
- Schwarz, O. (2009). *Maps of critical atmospheric loads of sulphur and nitrogen in forest ecosystems of the Giant Mountains National Park and the Jizera Mountains (In Czech), Kostelec nad Černými lesy: Lesnická práce (CD-ROM)*.
- Seibert, J. (2005). *HBV Light version 2. User's manual*. Stockholm: Stockholm University.
- Shaw, E. M. (2011). *Hydrology in practice* (4th ed.). London: Span Press.
- Spulák, O., Kacálek, D., & Balcar, V. (2019). Seven spruce species on a mountain site – performance, foliar nutrients, and forest floor properties in stands 20 years old. *iForest*, 12, 106–113.
- Strayer, D. L., & Dudgeon, D. (2010). Freshwater biodiversity conservation: Recent progress and future challenges. *Freshwater Science*, 29, 344–358.
- Stuchlík, E., Kopáček, J., Fott, J., & Hořícká, Z. (2006). Chemical composition of the Tatra Mountain lakes: Response to acidification. *Biologia*, 61(Supplement 18), S11–S20.
- Tolacz, R., Míková, T., Valerianová, A., & Voženílek, V. (2007). *Climate atlas of Czechia*. Prague: Czech Hydrometeorological Institute.
- Tmka, M., Balek, J., Štěpánek, P., Zahradnický, P., Možný, M., Eitzinger, J., ... Brázdil, R. (2016). Drought trends over part of Central Europe between 1961 and 2014. *Climate Research*, 70, 143–160.
- Trotter, J., & Slack, P. (2004). *Managing water resources: Past and present. Linacre Lectures*. Oxford: Oxford University Press.
- Tureček, K. (2002). *The water act (In Czech)*. Prague: SONDY.
- UN. (1992). *Agenda 21. Rio de Janeiro: United Nations Conference on Environment and Development (Brazil) 3-14 Jun 1992*. Available from: <https://sustainabledevelopment.un.org/documents/Agenda21.pdf>. (Accessed May 2020).
- UNEP. (2007). *Global environmental outlook 4*. Valetta: United Nations Environmental Programme (Progress Press Ltd).
- Vacek, S., & Balcar, V. (2004). Sustainable management of mountain forests in the Czech Republic. *Journal of Forest Science*, 50(11), 526–532.
- Van der Maarel, E. (1979). Transformation of cover-abundance values in phytosociology and its effect on community similarity. *Vegetatio*, 97–114.
- Van Loon, A. F. (2015). Hydrological drought explained. *WIREs Water*, 2, 359–392.
- Viviroli, D., Dürr, H. H., Messerli, B., Meybeck, M., & Weingartner, R. (2007). Mountains of the world, water towers for humanity: typology, mapping, and global significance. *Water Resources Research*, 43, W07447.
- Vrtiška, J., Kreček, J., & Tognetti, R. (2018). Indication of environmental changes in mountain catchments by dendroclimatology. *Soil and Water Research*, 13(4), 208–217.
- WHO. (2004). *Guidelines for drinking water quality* (3rd ed.). Geneva: World Health Organization.
- Willis, K. G. (2002). *Benefits and costs of forests to water supply and water quality. Social and environmental benefits of forestry, report to forestry commission, phase 2*. Newcastle: Centre for Research, Centre for Research in Environmental Appraisal and Management, University of Newcastle.
- WMO. (2001). *Technology for detecting trends and changes in time series of hydrological and meteorological variables. Hydrological Operational Multipurpose System*. Geneva: World Meteorological Organization.
- Woitsch, J. (2006). Forest provider – man scared. Fear of forest in Middle Ages and early Modern History. *Dejiny a současnost (History and present)*, 28(11), 30–33 (In Czech).
- Zlatník, A. (1976). *Forest phytocenology*. Prague: SZN (In Czech).

Article

# Assessing Insurance Flood Losses Using a Catastrophe Model and Climate Change Scenarios

Ladislav Palán<sup>1,2,\*</sup> , Michal Matyáš<sup>1</sup>, Monika Váľková<sup>1</sup>, Vít Kovačka<sup>1,3</sup>, Eva Pažourková<sup>1,2</sup>  and Petr Punčochář<sup>1</sup>

- <sup>1</sup> Aon Impact Forecasting, Václavské náměstí 19, 110 00 Prague, Czech Republic; michal.matyas2@aon.com (M.M.); monika.valkova@aon.com (M.V.); vit.kovacka@aon.com (V.K.); eva.pazourkova@aon.com (E.P.); petr.puncochar@aon.com (P.P.)
- <sup>2</sup> Department of Hydraulics and Hydrology, Faculty of Civil Engineering, Czech Technical University in Prague, Thákurova 7, 166 29 Prague, Czech Republic
- <sup>3</sup> Department of Applied Geoinformatics and Cartography, Faculty of Science, Charles University, Albertov 6, 128 43 Prague, Czech Republic
- \* Correspondence: ladislav.palan@aon.com

**Abstract:** Impact Forecasting has developed a catastrophe flood model for Czechia to estimate insurance losses. The model is built on a dataset of 12,066 years of daily rainfall and temperature data for the European area, representing the current climate (LAERTES-EU). This dataset was used as input to the rainfall–runoff model, resulting in a series of daily river channel discharges. Using analyses of global and regional climate models dealing with the impacts of climate change, this dataset was adjusted for the individual RCP climate scenarios in Europe. The river channel discharges were then re-derived using the already calibrated rainfall–runoff models. Based on the changed discharges, alternative versions of the standard catastrophe flood model for the Czechia were created for the various climate scenarios. In outputs, differences in severity, intensity, and number of events might be observed, as well as the size of storms. The effect on the losses might be investigated by probable maximum losses (PML) curves and average annual loss (AAL) values. For return period 1 in 5 years for the worst-case scenario, the differences can be up to +125 percent increase in insurance losses, while for the return period 1 in 100 years it is a –40 percent decrease. There is no significant effect of adaptation measures for the return period 1 in 100 years, but there is a –20 percent decrease in the return period 1 in 5 years.

**Keywords:** catastrophe modelling in insurance; hydrological modelling; flood frequency under climate change; insurance losses; Czechia



**Citation:** Palán, L.; Matyáš, M.; Váľková, M.; Kovačka, V.; Pažourková, E.; Punčochář, P. Assessing Insurance Flood Losses Using a Catastrophe Model and Climate Change Scenarios. *Climate* **2022**, *10*, 67. <https://doi.org/10.3390/cli10050067>

Academic Editors: Ondřej Ledvinka, Josef Křeček, Anna Lamacova and Adam Kertesz

Received: 30 March 2022

Accepted: 6 May 2022

Published: 10 May 2022

**Publisher's Note:** MDPI stays neutral with regard to jurisdictional claims in published maps and institutional affiliations.



**Copyright:** © 2022 by the authors. Licensee MDPI, Basel, Switzerland. This article is an open access article distributed under the terms and conditions of the Creative Commons Attribution (CC BY) license (<https://creativecommons.org/licenses/by/4.0/>).

## 1. Introduction

Climate change is likely to be the most discussed factor in future risk due to its direct impacts on atmospheric perils and its indirect impacts on weather-driven perils, such as riverine and rainfall flooding. These trends were described by the IPCC in 2012 report [1]. Within Europe, climate change will alter the hydrologic cycle due to the expected shift in average temperatures and seasonal rainfall. This will lead to a change in flood frequencies; however, the frequency of specific flood events in different regions and year seasons might increase or decrease based on the related river segment locations and their specific climate regions in Europe. Although the main purpose of this article is to investigate changes in floods in terms of frequency and discharge, climate change should be taken to count as a whole process. As Sýs et al. [2] points out, change in the hydrological cycle is complex and will have consequences in water supply process, retention volume solutions, and in many other areas, such as integrated rescue system [3].

While predictions of the impacts of climate change on flood frequency are highly uncertain [4,5], we assume that it is possible to apply global and regional simulations

to catastrophic loss models to predict the possible impacts on modelled financial insurance loss. In the insurance sector, since the long-term observation and experience is not good enough to estimate possible insurance flood losses, catastrophe models have been developed. Catastrophe modelling allows insurers and reinsurers to evaluate and manage natural catastrophe risk and create financial preparation according to every regulatory demand. The main outputs of probabilistic catastrophe models are probable maximum losses (PML) curves and average annual loss (AAL) values. A different view on losses can be provided by two types of PML curves: Aggregate Exceedance Probability (AEP) and Occurrence Exceedance Probability (OEP).

The nature of climate change in European regions is captured by Global Climate Models (GCMs). As Kay et al. mentioned in his study [4], the GCM is the main source of uncertainty in future flood frequency estimation. GCM simulation is downscaled via Regional Climate Models (RCMs) based on designed scenarios referred to as Representative Concentration Pathways (RCPs). Its trajectory is adopted by the IPCC for its fifth Assessment Report (AR5) [6]. Four pathways have been selected for climate modelling and research. They describe different climate futures depending on how much greenhouse gases are emitted in future years. The four RCPs, namely RCP 2.6, RCP 4.5, RCP 6, and RCP 8.5, are labelled after a possible range of radiative forcing values in the year 2100 (2.6, 4.5, 6.0, and 8.5 W/m<sup>2</sup>, respectively). Those pathways are widely used in common studies [5,7–9]. The study by Rajczek et al. [9] examines the influence of future precipitation extremes. Based on their study, which investigates precipitation effected by RCP scenarios, changes in extremes do not scale proportionally to changes in mean. Basically, there is expected intensification of extrema and change in frequency of events. Single-day events intensify more than multiday precipitation. In the context of Czechia, recent changes are also examined in the research of the Czech Academy of Sciences in [10].

Floods across Europe are caused by numerous triggers. The largest and costliest floods have occurred during different seasons, in different regions, and in various regional patterns. In Czechia, flooding often occurs during the summer season, with most of the recent serious floods (e.g., 1997, 2002, and 2013) occurring during this time. Major flooding can also occur in the spring (e.g., 2006), which is induced by rain or by melting of the accumulated snowpack. There are several studies from Brázdil et al. which describe the synoptic causes of floods on the Morava River [11] and investigate past floods in Czechia [12]. The documentary evidence of past floods and their utility in flood frequency estimation is discussed in another article [13].

Considering the change in precipitation patterns during this region's annual cycle, a change can also be anticipated in the flood regime and flood magnitudes. As changes of flood frequency curves are a long-term reflection of atmosphere conditions and soil moisture together with snow, there is strong emphasis on regional climate and runoff generation processes. Blöschl et al. [14] mentioned that there is need for a large-scale continental study. Wider studies easily demonstrate the pattern of both increase and decrease of observed discharges. Based on his results, increasing autumn and winter rainfalls resulted in increasing floods in northwest Europe. On the other hand, decreasing precipitation and increasing evaporation caused a decrease of flood events in southern Europe. Additionally, decreasing snow cover and snowmelt results in decreased flooding in Eastern Europe. The redistribution must be considered from two connected perspectives: geographically and seasonally. Such redistribution will increase the number of flood events in winter and decrease the number of events in spring, mainly due to the changes in temperature and the amount of water accumulated in the snow cover.

There are many factors which modulate the flood response, so an increase in precipitation does not necessarily mean increasing floods. Trambley et al. [15] investigates Mediterranean basins, where decreasing soil moisture caused lower floods, even though rainfall increased. Initial saturation of the soil has a strong impact, together with future changes in evaporation caused by climate change.

The reduced precipitation amount (but with increased rainfall intensities) during the original flood season might cause a slight decrease in design flows. Still, causing an increase in the average temperature might induce floods during otherwise calm winters.

Snow storage and snowmelt are factors that modulate flood response. The effects of changing snowmelt process on flood frequency curves depend on flood-generating process in the region. For Central Europe, the most relevant process is rain-on-snow [16]. The shape of flood-frequency curve is likely to flatten out at large return periods [17]. This is caused by the reduction of lying snow cover and upper energy limit for melt.

The effect of changes in a hydrological regime that yields to the altered design flows might be incorporated directly into a catastrophic flood model. To evaluate the view of risk from the climate change scenarios, a view taken from those scenarios can be deployed in the current flood model by using the same vulnerability, exposure, and flood mitigation measures. Evaluation of the direct impacts on losses from future climate effects can be made for each scenario using the current socio-economic (and other) conditions.

Rädler [18] pointed that the reinsurance view of risk is not necessarily the same as the scientific view. The main aim is on the extrema, while the mean values of distribution play only a minor role in the risk. The Impact Forecasting Flood Model for Czechia [19] with climate change scenarios is designed to evaluate financial losses caused by riverine (fluvial) and rainfall-driven (pluvial) flooding, as well as any related groundwater (off-floodplain) flooding. This model, including climate change scenarios, is found to be well suited for investigating financial losses of the possible effects of the changed hydrological regime in Europe.

## 2. Materials and Methods

### 2.1. Meteorological Inputs

#### 2.1.1. Current Climate

The event set used for the current climate and for the development of the Impact Forecasting Flood Model for Czechia [19] is based on a long-term (12,066 years) time series of simulated daily precipitation and temperature fields over Europe. It was generated by Karlsruhe Institute of Technology [20] from the Max Planck Institute Earth System Model (MPI-ESM/ECHAMP6) global climate model (GCM) using a resolution of approximately 100 km. It was dynamically downscaled to approximately 25 km by use of a regional climate model (RCM) Consortium for Small Scale Modelling-Climate Limited-area Modelling Community (COSMO-CLM) CCLM5 [21].

The daily precipitation amount and daily mean temperature from two meters fields located above-ground are used as an input for the Impact Forecasting rainfall-runoff (IFRR) model (based on Hydrologiska Byråns Vattenbalansavdelning model-HBV [22]) to calculate the time series of discharges and identify flood events. Discharges from the COSMO-CLM precipitation datasets were calculated using the historical datasets (reanalysis) as the boundary condition, instead of the GCM. There are three different reanalyses used for the boundary data: ERA-Interim [23], ERA-20C [24], and NCEP 20CR [25].

The simulated precipitation and temperature fields are corrected for bias so that they statistically match with the observed values in the period of 1950 to 2016. We performed a thorough analysis of the various bias correction methods and their effect on simulated discharges. These were then compared to the observed discharges at gauging stations.

The final stochastic meteorological dataset, the LArge Ensemble of Regional climate model Simulations for EUrope (LARTES-EU) dataset [21,26], serves as a consistent source of precipitation for the entirety of Europe; however, the hydrological models require a higher resolution. The precipitation and temperature fields are interpolated to a higher resolution using various statistical or machine learning algorithms. The exact methods and final resolutions vary by basin. Bilinear interpolation was used in the Danube, for example, to produce a final resolution of up to 10 km. Machine learning was used in other basins, such as the Elbe and the Oder. For the machine learning method, we used adaptable random forests, as described in He et al. [27]. Prec-DWARF (Precipitation Downscaling

With Adaptable Random Forests) is a method which can outperform bilinear interpolation in precision of downscaled spatial and temporal patterns (tradeoff being significantly longer run time and the necessity to build and train the machine learning algorithm). As advised in He et al. [27], we used a double random forest approach to avoid underestimation of extreme rainfalls and also followed the advice to consider mainly adjacent cells and distance to dry cell as covariates in training the algorithm. Some other covariates (e.g., altitude, slope, temperature) were tested for significance, but did not improve the method significantly. The final algorithm trained to downscale 24.5 km grid to 6.125 km grid over the Czech basins used random forest with 10 trees to predict smaller (thus less influential) precipitation values and another independent random forest using 100 trees to predict more extreme precipitation values. The meteorological inputs with their higher resolutions provide the additional spatial variability (due to orographic effects) required for the detailed rainfall–runoff modelling.

### 2.1.2. Climate Scenarios

There are many climate simulations in the conditions outlined by the various time frames and scenarios [28]. To build a climate change version of the flood model, we extracted the differences between the current climate state and the temperature and precipitation in the scenarios. Those differences (on a monthly basis) were used to adjust the days in the 12,066 years of meteorological inputs for the IFRR model, which itself was used for the development of the Impact Forecasting Flood Model for Czechia [19].

The source of the key climate variables for scenarios and the reference period was chosen using [29]. The historical data covering the period of 1901 to 2020 in this dataset is based on the CRU-TS 4.05 dataset [30]. ClimateEU uses the climate data for the typical time period of 1961 to 1990 as a baseline (or reference) dataset. Preparing a complete dataset [29] included numerous sources and methods (including the PRISM methodology-Parameter-elevation Regressions on Independent Slopes Model) to cover the rain shadows and orographic precipitation in the mountainous terrain and to allow adjustments to any anomalies. The 1961 to 1990 time period represents the climate conditions at the start of the major anthropogenic changes in climate. Only a small anthropogenic warming signal, due to particulate and sulfur pollution, is seen in this period [31]. This period has been used as a reference period for long-term climate change assessments by the World Meteorological Organization.

Future climate projections consist of 15 representative GCMs (CanESM2, ACCESS1.0, IPSL-CM5A-MR, MIROC5, MPI-ESM-LR, CCSM4, HadGEM2-ES, CNRM-CM5, CSIRO Mk 3.6, GFDL-CM3, INM-CM4, MRI-CGCM3, MIROC-ESM, CESM1-CAM5, GISS-E2R) of the CMIP5 dataset corresponding to the IPCC Assessment Report 5 (IPCC 2014) [6]. Each of these models include two emissions scenarios (RCP 4.5 and RCP 8.5). Two time periods are considered: the 2050s (2041 to 2070) and the 2080s (2071 to 2100). In this study, due to combining various sources, we redefine the 2050s as (2050 to 2075) and the 2080s as (2075 to 2100). The average projected global warming increase for RCP 4.5 is +1.4 °C ( $\pm 0.5$ ) by the 2050s and +1.8 °C ( $\pm 0.7$ ) by the 2080s. For RCP 8.5, it is +2.0 °C ( $\pm 0.6$ ) by the 2050s and +3.7 °C ( $\pm 0.9$ ) by the 2080s.

The current LARTES-EU climate data in the Impact Forecasting dataset was shifted in daily steps that were in line with the scenario deltas of the temperature and precipitation variables. This was accomplished while keeping the differences between each scenario and the reference period in line with [29]. An example of an average change of seasonal precipitation over Europe for scenario RCP 8.5 in the 2080s (2075 to 2100) time period, in comparison with the reference period of 1961 to 1990, can be seen in Figure 1. Such an adjustment was made for all combinations of scenarios.

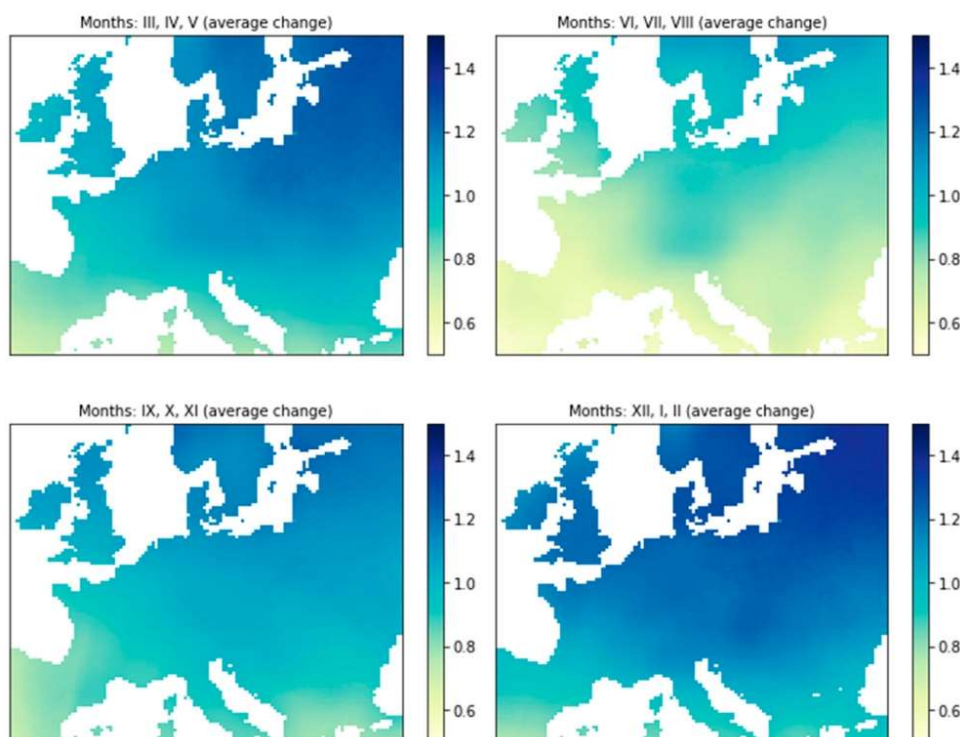


**Figure 1.** The derived average change of monthly precipitation (ratio) over Europe for scenario RCP.

There are a varying number of seasonal wet days in the scenario simulations. The number of wet days in each month was adjusted based on the information pertaining to the number of days that achieved the threshold of precipitation, and by changing the frequency of events available in [9,10]. For the purpose of the IFRR model, evapotranspiration was also recalculated.

Strong precipitation intensifications appear (in particular for extreme rainfall events) and most are consistent in cold seasons occurring in northern Europe, according to [9]. Decreases in the total precipitation amount and frequency appear in the summer season in some areas of Europe. The largest and most significant increases in extremes are projected for the autumn and winter seasons across all regions. Median estimates of precipitation increases are often larger than +20 percent. In summer, and to some extent in the transitional seasons of spring and autumn, changes in precipitation are more complex. Reductions in the event occurrences are opposed by a concurrent intensification of those events. For the changing frequency of wet days, we used [9] and the research of the Czech Academy of Sciences in [10]. The current climate development is so far most consistent with the RCP 8.5 emissions scenario, and in some parameters, this most dramatic scenario is already being exceeded, so this scenario was used by [10] for the assessment. However, they did work with other scenarios and state that until next turn of the century, the choice of an emission scenario does not play a significant role. Apart from winter, a decrease in precipitation can be expected, especially in spring and summer, and a decrease in precipitation combined with a higher air temperature (and thus higher evaporation) will lead to longer episodes of drought. The smallest increase or even decrease in precipitation will occur in southern Moravia, Czechia. However, in terms of flood genesis, the important

information is the number of days with precipitation (1, 10, 20, and 50 mm or more). These will increase as compared to the present, but the number of days with precipitation above 1 mm will not see a major change. The number of days with more than 10 and 20 mm of precipitation will continue to increase in the future, especially in winter. An increase in the number of days with greater than 50 mm of precipitation was already detected in the mid-twentieth century.

Since there are large differences between the models, we are considering the results from the medium model for the purpose of this study. The number of days with precipitation (1 mm or more) does not change much in the present or in the future, but the number of days with at least 10, 20, and 50 mm of precipitation is already changing. For the number of days with at least 10 mm in Czechia, the number increases for the near future (2021–2060) for RCP 8.5, especially in winter. Meanwhile, the number of wet days for summer months in all cases (1, 10, 20, 50 mm, and more) decreases. Overall, for the time period of 2021 to 2060, the consensus of the models is that the smallest increase in these days should occur in southern Moravia and western Bohemia, but there is a great dispersion in all model results. Alternatively, according to [10], most days with 10 mm or more of precipitation will occur in northern Moravia, the area including Prague, and southern Bohemia.

## 2.2. Rainfall Runoff Model

The hydrology mode in the IFRR model is a simulation used to analyze river discharge and is comprised of the following routines: a snow routine, a soil moisture routine, a response function, and a routing routine. Each of these routines needs several parameters in addition to input precipitation, temperature, and evapotranspiration. These parameters are estimated by calibration either directly, or by meta-parameters, which are the function of the various spatial datasets (soil types, altitude, and so on). Calibration of parameters is based first on the generation of 10,000 random combinations of all parameters and selection of the best option by referencing the Nash-Sutcliffe coefficient. However, this approach puts too much emphasis on the daily hydrological flows, while for IF models (or any reinsurance models) only the top flood events are important, and most daily flows are discarded. To improve the usefulness for event set preparation, different weights are introduced to prefer the match in flood events over the baseline flow. This can be further improved by additional changes in parameters to provide a better fit for the seasonality of floods, duration of flood events, and volume of the flood waves. The combination of all these calibration approaches usually leads to a good resimulation of historical discharges (Figure 2), with an example of the setting of one basin in Figure 3.

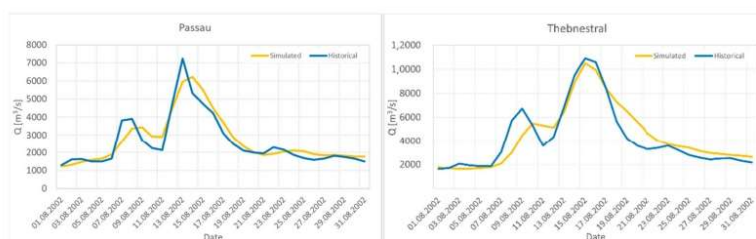
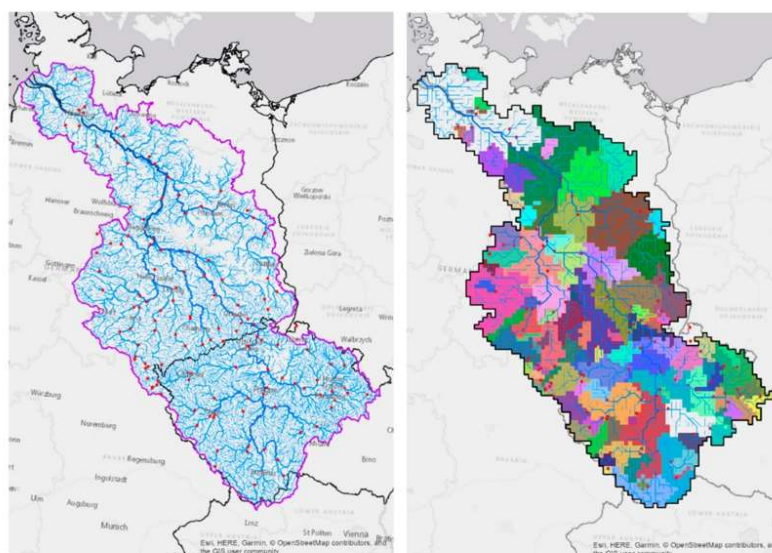


Figure 2. Example of the R-R model calibration–observation vs. model discharges.



**Figure 3.** Example of the settings of the hydrological model for Elbe basin. **Left**—river network identification, basin definition, collecting hydrological data for calibration; **Right**—model grid definition (consistent with climate model), river network schematization for discharge routing, definition of subbasements for calibration. Additional spatial datasets needed identified: field soil capacity, water capacity at wilting point, digital terrain model, flow direction raster, and soil type.

The daily time series of temperatures and precipitation was used as the input of the IFRR spatially distributed rainfall–runoff model based on the HBV model [22] and calibrated for individual catchments using historical discharge data in the frame of European basins (Figure 4). The calibrated rainfall–runoff model is then forced by precipitation and temperature fields from LAERTES-EU to simulate discharges in a daily time step. The uncertainties in the simulated discharges were analyzed by testing multiple sets of rainfall–runoff model parameters.

The output of the rainfall–runoff model serves as an input to the frequency analysis for each river segment. Output discharges are used for identifying the individual events in the frame of a processed country and producing an event set at completion. Despite careful calibration of the rainfall–runoff model, we do not directly use the values of simulated discharges, but instead convert them into a frequency domain. We then define the events as the maximum return period for those river segments within a specific time period (usually about 21 days due to the insurance practice). The final footprint of each event is the composition (patching) of flood extents for individual river segments. However, the partial flood extents for the selected predefined return periods are calculated using discharges from the design flow curves, which are usually derived from long term records or provided by the local authorities, and are considered more robust than the estimates from our rainfall–runoff model.

The calibrated model parameters and the model itself were used to calculate the magnitude of flows under the changing values of precipitation, temperature, and evaporation for each climate change scenario. In this case, the model output produces discharges comparable to the current climate.



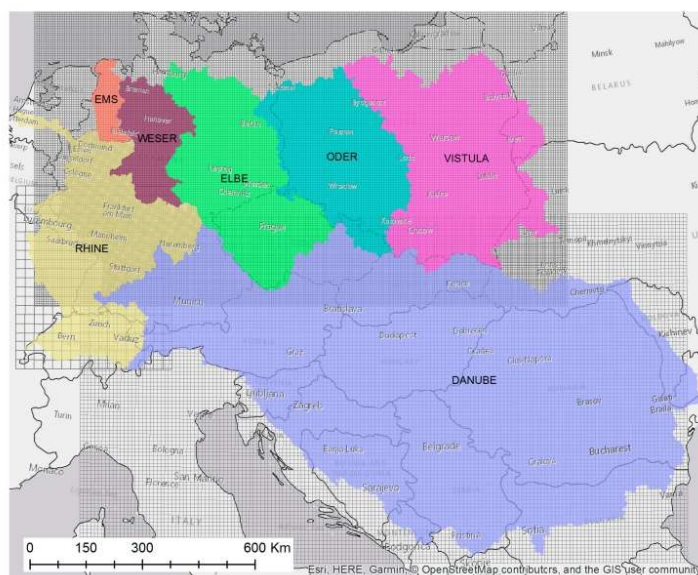


**Figure 4.** Impact Forecasting European Flood Model: the actual basin coverage delineation.

There is only one difference in using the rainfall–runoff model output for the current climate and climate scenarios. The resulting flows for the climate scenarios were labeled with the values of the return periods for individual river discharges from the frequency analysis performed on the current climate. Therefore, the return periods are produced using “current climate discharges and return periods”. This is due to the simulated flood maps being produced by deriving the design flows and 2D hydrodynamic modelling for the current climate, yet still using them for directly implementing the climate change scenarios and without the need to resimulate the flood maps.

### 2.3. Scenario Definition in the Loss Model

For the assessment of climate change impacts on floods in Czechia, two RCP scenarios (RCP 4.5 and RCP 8.5) and two time horizons, the 2050s (2050 to 2075) and the 2080s (2075 to 2100), were selected. These scenarios were used to evaluate the outcome when the climate conditions in the scenarios are transferred to the current world conditions. Everything is assumed to remain the same, including the level of flood protection, the type, composition and distribution of property, and loss ratio of flooded buildings, with only the events themselves behaving differently in terms of spatial extent and the intensity of the precipitation and discharges. It is important to note that this view calculates losses using the current price level and with no consideration of inflation. This pure hazard view allows for the identification of the flood types that are key in terms of the need to implement mitigation and adaptation measures. This view serves as a basis for stakeholders to initiate any necessary actions or even a chance for insurers to change their underwriting strategy.

Additionally, the four primary scenario models have been further adjusted for a basic assessment of the impact of adaptive measures. The baseline reference model within the 2D hydrodynamic simulations/flood maps already incorporates flood protection measures. However, each river segment keeps the information about the level of protection, right up to ‘no loss’ generated by the given peril. These protection levels can be adjusted to higher protection and additionally safeguard selected segments/locations. The assumptions about dike strengthening vary in the literature, for example, the EU Report Peseta V [32] works with the assumed levee strengthening for different climate scenarios by looking at a loss

reduction. It indicates up to 50 percent positive impact on losses by strengthening dikes. For the climate change scenarios with adaptation for the flood model for Czechia, the following assumptions were made. Flood barrier constructions (fixed dikes, mobile barriers, polders, dams, construction of a sewerage system, and other flood protection) are a function of time and are spatially highly variable. In light of this, a simplification is necessary for the flood protection implementation in the flood model for the purpose of estimating losses in climate change scenarios.

For the 2050s (2050 to 2075) and 2080s (2075 to 2100) time periods, we assume levee strengthening (relative to the return period of flood) for riverine floods of around +25 percent and +50 percent, respectively. For pluvial floods, we assume protection strengthening of around +10 percent and +20 percent, respectively. The assumption incorporates the individual house protection by using local mobile door barriers. The assumption is applicable for estimating losses on the whole portfolio but will not be valid for a local study on individual locations.

The event set with and without an adjusted level of flood protection can be further implemented using the same procedure as the default model for the current model. It can be used in the loss calculation platform ELEMENTS, to directly estimate the risk as a baseline reference for the Impact Forecasting Flood Model for Czechia [19]. This view, with the inclusion of adaptation changes, can serve as a basis for stakeholders to determine the effectiveness of measures against the flood types that drive the losses in the climate scenarios. It can help them decide whether to initiate other measures necessary for the landscape and society.

#### 2.4. Risk Analysis

##### 2.4.1. Event Identification and Event Set Generation

The event set developed for the baseline reference Impact Forecasting Flood Model for Czechia is defined using 12,066 years of daily discharges, originally defined on a grid. Each river segment is controlled by the corresponding European grid cell for Czechia. The discharges come from the IFRR model that works using meteorological inputs.

Here, a flood event is defined as an overflow or inundation that comes from a river or other body of water, whether caused by rainfall, waterway operation, dam break, water runoff or other means, that causes or threatens damage. In terms of the Impact Forecasting Flood model for the Czechia, there is a need to define the additional losses caused by rainfall that complements riverine flooding.

An event, in the framework of a catastrophic flood model, is a set of individual hydrological situations reaching a specified minimum return period and arriving at a given area in a river network (fluvial flood) or catchment (pluvial flood) at the specified window of time. It is then a prescription or list of segments and catchments and a prescription for the return period of discharges of the flood or rain in that location. The event set is a list of individual events; in the case of the reference baseline flood model for Czechia within the pan-European event set, having 63,888 events within 12,066 years. An example of one event can be a situation where half of Czechia is affected by some level of flood in a given time window, with the Vltava River in Prague reaching a return period of 1 in 300 years, the Elbe River in Děčín reaching 1 in 150 years, the Ohře River in Žatec reaching a return period of 1 in 30 years, and so on. Another event may only affect a few catchments in the Jizera Mountains where only a return period of 1 in 45 years is reached.

Each river segment of the river network of Czechia is controlled by the respective grid cell from which the rainfall–runoff model is calculated. The grid is a 3D matrix containing the daily step of the discharges, where the X and Y axes define the space while the Z axis defines the time (in days and years). Events are defined in a way that is consistent with re/insurance market conditions: anything falling within a predefined window of time is declared to be the event. The market uses the “hours clause” (HC) approach, where a window of three weeks (21 days) is used to identify the event. The discharges for each cell on each day are ranked and the return period of discharge is assigned.

Identification of events in a daily time step of 12,066 years is a non-trivial optimization problem where a maximum in time and space is sought. Events are identified by an iterative approach starting from the most severe event. Each event is assumed to last 21 days. The severity of events is measured by ground-up (GU) market losses, i.e., losses prior to the application of insurance terms and conditions, and thus includes not only the hydrological situation but also the exposure distribution and vulnerability. Measuring severity using only discharges would overestimate the importance of large, unexposed mountain and foothill areas and underestimate highly exposed urban areas.

As the intensity and distribution (both spatial and temporal) of the precipitation changes, there are also changes in climate scenarios and the temporal and spatial distribution of river channel discharges. Consequently, a different number of events can be expected in each climate scenario because each event will be unique to that specific scenario. As the heavy rains driving the most substantial flood events intensify, but become shorter, the climate change scenarios will tend towards a slightly larger number of events.

The identification of events is done using the same method as that of the reference model. The only difference is that the discharges on the grid from the rainfall–runoff model are labelled by the return period, based on the frequency analysis from the original model. This solution ensures that the modified scenario-based design flows can be translated directly into the modelled hazard language of the baseline reference model. Thus, there is no need to resimulate flood extents based on the new design flows. It is important to note that in the Impact Forecasting methodology, the river discharges are simulated for river segments at specified return periods of 1 in 5, 20, 50, 100, 200, 500, 1000, and 10,000 years. For the intermediate return periods, interpolation of depths is performed during the loss calculation in the ELEMENTS.

#### 2.4.2. Demand Surge

Demand surge is a phenomenon defined as “a sudden and usually temporary increase in the cost of materials, services, and labor due to the increased demand for them following a catastrophe” [33]. This usually occurs after exceedingly large disasters such as severe earthquakes, cyclones, or flooding. Some well-known examples of such events are the 2011 Christchurch earthquake in New Zealand, or Hurricane Katrina in the U.S.A. in 2005 [34]. A similarly strong effect was observed in the case of the 2002 floods in Czechia [35]. How and Hasson [35] noted that insurance companies incurred additional expenses to import claims adjusters because there was an insufficient number of local adjusters after each event.

There is a direct dependence of the intensity of the demand surge on the intensity of the natural disaster. Moreover, the disaster usually comes in a highly concentrated area. During reconstruction or even just removal of damaged constructions, the demand for labor and building materials, such as steel, cement, and timber, increases dramatically and quickly outstrips the supply, thereby pushing pricing increases. Oil and gas prices can also be affected. Demand surge can be quite substantial: commercial disaster modelers estimate a range of 20–50 percent, but it can be even greater [35,36].

The Impact Forecasting Flood model for Czechia incorporates the principle of demand surge. When sorting events by their size, the first event where there is some additional loss due to the demand surge starts to be applied for an event of return period 1 in 50-years loss (close to the 1997 historical event) calculated on the market portfolio. The maximum demand surge is considered +25 percent.

The application of demand surge is a simple operation. Losses per event are determined as if no material shortage has occurred. These losses are then multiplied by a coefficient derived from Czech historical claims and loss experience. At this point, the EP curve and the AAL value are calculated by standard formulas (the advantage is that it is possible to compare losses with and without the inclusion of demand surge).

For the purposes of implementing the demand surge concept in the climate scenarios, it is not possible to consider stronger demand increases in the future because such assumptions would be too uncertain. As the frequency and intensity of scenario events change

in comparison to the reference model, the same values of the increase in loss need to be applied by linking the absolute losses to the market portfolio. In practice, this means that in the reference model, the range of the individual demand surge values has been determined based on the GU loss. These absolute amounts are used to map the demand surge values in the scenario models (before the demand surge is applied). For example, the loss in the EP curve from a market portfolio of between €1.3 to €1.5 billion produces a demand surge of +20 percent, and any loss for a specific one-time event from the climate scenarios in the same market portfolio will have the same demand surge value. This is regardless of whether it is determined to be at a higher or lower return period of loss. Using this approach ensures full consistency with the reference model and the ability to compare the absolute loss among models. This mapping needs to be done for each individual scenario as listed in the previous section, because the events and the losses they produce are unique among the scenarios.

#### 2.4.3. Frequency Analysis

Due to changes of key meteorological variables in the climate scenarios that serve as the input to the rainfall–runoff model, changes can be expected in design flows in river channels and, by extension, changes in the direct flood risk in specific locations.

The major heavy rain events that generate large and severe floods are expected to become more intense, though they may occur for shorter periods of time or be more localized. This may result in moderate discharges on large rivers decreasing, but the largest discharges intensify on rivers with smaller catchment sizes.

In the reference event set, the largest floods that happen during the year usually occur (in Czechia's case) during the summer season. However, the data show that summer rainfall decreases on average in the climate scenarios, but the number of wet days varies. Additionally, much less water is stored in snow during the winter season in the climate scenarios, so there will be less flooding from snowmelt during the early spring season. The IFRR model includes a snow routine so that, based on a precipitation and temperature dataset, it can detect precipitation state of matter and calculate the correct amount of snowpack or snowmelt for a particular day according to the specific climate change scenario.

To explain the effects resulting from the different climate scenarios, a frequency analysis was performed on the discharges of selected large and small catchments to compare the reference model to the climate scenario models. A comparison was also made of the flood seasonality and wave duration. Additionally, the total number of events identified within the event set was compared between the reference model and the climate scenario models.

### 3. Results

Under the most pessimistic climate scenario, meteorological changes result in an increase in the number of small or moderate floods, in terms of the magnitude of financial losses. This is caused by either a relatively low flood intensity over a large area or a high flood intensity over a smaller area. However, the area of the largest intense floods decreases, as compared to the reference scenario. This observation may result in a different view of risk: lower return periods of losses on the EP curve and a sharp increase of the AAL, while the largest loss actually decreases due to the absence of the largest area-intensive events. Combined with the decrease in direct flood risk on large rivers, strengthening dikes on these rivers will not have a substantial effect on the loss. Alternatively, strengthening dikes on smaller rivers or building flood defenses where no flood protection measures currently exist (or building defenses against pluvial flooding) might have a more substantial effect. The effect of the increasing number of smaller events during the year can be observed from the difference between the aggregate exceedance probability (AEP) curve, which is based on the sum of losses within a year, and the occurrence exceedance probability (OEP) curve, which is based on the maximum of loss within a year.

### 3.1. Change in Discharges

Due to the increased temperature during the cold season in the climate scenario, more of the precipitation is expected to occur as rain, rather than snow, and less water is held in the snowpack. Thus, a different runoff within the catchment can be observed. In the reference model, when the warming happens, the runoff occurs both later and suddenly, as a flood wave. In the climate scenario, the warming runoff from the basin may occur gradually and in several lower waves.

Alternately, higher flows in small catchments are observed in the climate scenario during the summer months. Although less total precipitation occurs during the summer, relatively intense but short floods occur due to the high rainfall intensity or several intense events in a row.

An example of the changing rainfall–runoff relationship within a watershed is shown in Figure 5. These changes are driven by the changing meteorological conditions and spatiotemporal changes in the distribution of precipitation, combined with changes in the amount of water retained in the snowpack. In large catchments, decreasing design flows can be expected under the climate scenario. For smaller catchments, the trend is the opposite and there is an increased risk of more severe flooding. It can be expected that the risk of flooding, including the risk of flooding from heavy rainfall, will be significantly increased for small catchments. For small to medium sized catchments, the magnitude of design flows increases for lower return periods but decreases for higher return periods.

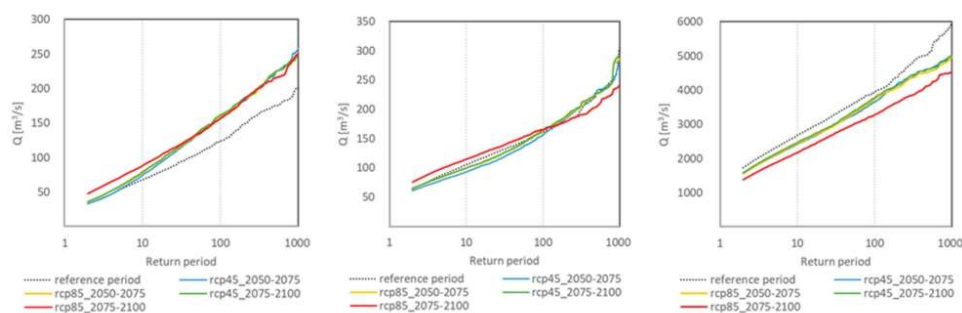


**Figure 5.** Example of the changed design flows per scenarios in comparison with the reference period for rivers within Elbe basin: Catchment size: **left**—451 km<sup>2</sup>, **middle**—1157 km<sup>2</sup>, **right**—41,831 km<sup>2</sup>.

The proportion of flood events for the Czech river basins in the reference period shows that most floods greater than the return period of 1 in 20 years occur in the spring months (due to snow melting and heavy rainfall), followed by summer floods. This is illustrated by the graph in Figure 6 for the three basin sizes that were demonstrated in Figure 5. However, the largest flood peaks in the reference period occur during the summer months when the most frequent and heaviest rainfall is observed. This is also due to the given climate scenario having less rain overall in the summer months (in Czechia/Central Europe), despite the fact that there is a redistribution of wet and dry days. This redistribution then has a major effect on flood peaks in small catchments.

The change in the proportion of floods greater than a return period of 1 in 20 years is shown for each climate scenario (Figure 7). Due to warming over Central Europe and less water being retained in snow, there is an increase in the number of winter flood events (which are generally less damaging, but more frequent), especially in the 2080s (2075 to 2100) period and in the most pessimistic emission scenario. The number of summer floods is decreasing, but their proportion and magnitude remain significant, especially for rivers with smaller catchments.

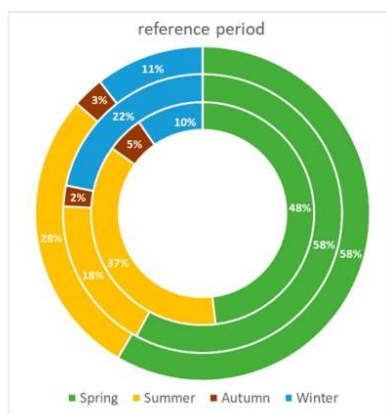


**Figure 6.** Example of number of peak months over return period 1 in 20 years per scenario—rivers within Elbe basin; catchment size: inner circle—451 km<sup>2</sup>, middle circle—1157 km<sup>2</sup>, outer circle—41,831 km<sup>2</sup>.



**Figure 7.** Example of the number of peak months over the return period 1 in 20 years per scenario—rivers within Elbe basin; catchment size: inner circle—451 km<sup>2</sup>, middle circle—1157 km<sup>2</sup>, outer circle—41,831 km<sup>2</sup>.

Considering the stronger but more localized storms and rainfall events, the impact of summer floods for large catchments is limited. This is due to the need to combine several events into one using a single window. In general, floods on large catchments are generated by long lasting precipitation over a substantial area of the catchment. Consequently, the overall decrease in rainfall during the wettest period (related to the reference period) leads to an overall decrease of maximum peaks in the large catchment. Conversely, increases in rainfall in drier periods have a substantial effect on the generation of floods in the small catchments.

### 3.2. Number of Events

Due to the changes in the spatial and temporal distribution of precipitation and temperature (shorter periods of more intense precipitation, more water in the springtime, and so on), the response in the river network changes, as does the definition of events according to Section 2.4 (where the HC component is used). Therefore, although the number of 12,066 years of daily precipitation and temperature is constant, there is still a change in the number of events within one year. Many smaller events break down into several independent events, with the overall effect of a different ranking of events in terms of frequency. This has consequences for the calculation of the OEP and AAP loss. The number of events per scenario before flood protection applications (i.e., events defined purely in hydrological terms) is listed in Table 1. The final number of events that drive the loss is smaller and depends both on the setting of local flood defenses, as well as the distribution of exposure within the portfolios.

**Table 1.** Number of events per scenario: two time periods and two scenarios.

Scenario	Number of Events
Reference period	63,888
RCP 4.5 2050–2075	69,116
RCP 4.5 2075–2100	73,811
RCP 8.5 2050–2075	72,243
RCP 8.5 2075–2100	77,883

### 3.3. Effect on Losses

#### 3.3.1. Loss Change in a Multiperil Perspective

Following the definition of events in previous sections, the impact of changing climatic conditions on losses in the different climate scenarios can be demonstrated in distinct ways. The largest events for the highest emission scenarios are spatially smaller and less intense, relevant to the reference period. This is the same for the 40th–42nd largest events (which affect the return period 1 in 250-year loss), 41st shown in Figure 8. In the following sections, the relative comparison of loss magnitudes between the scenarios and the reference period can be observed. Another perspective may be to compare the first few losses. A representation of the sum of the first five to fifty losses (on the market portfolio) is shown in Figure 9. One can see that the largest (spatially) fluvial flood events are less prone to loss in the individual scenarios. This is for the reasons previously discussed. Alternatively, there are an increasing number of smaller events (locally concentrated but intense, or events less intense but (spatially) larger. A limitation of the model is that it does not necessarily capture the impact of extremely short but intense rainfall events (within the pluvial component) that may be more dominant in losses when produced from a flood model considering climate scenarios.

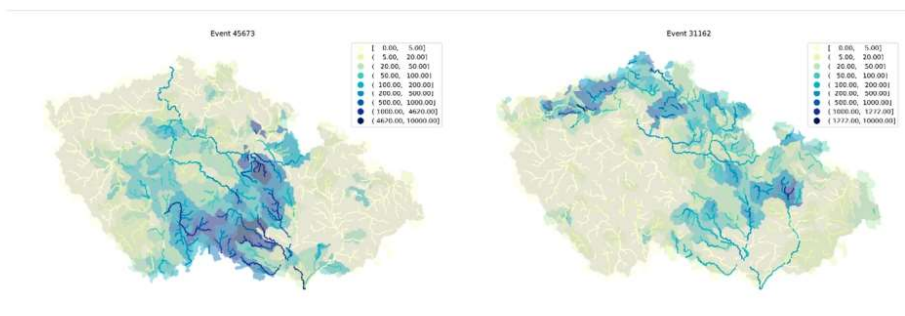


**Figure 8.** Example of the 41st largest market events: reference period, right—RCP 8.5 2075–2100 scenario without adaptation and expressed in the return period valid for reference period (lines—Figure 9). Relative comparison of the sum of the top losses on the market portfolio per climate scenario without adaptation, in comparison with the reference period: **left**—GU loss, **right**—Gross loss.



**Figure 9.** Relative comparison of the sum of the top losses on the market portfolio per climate scenario without adaptation, in comparison with the reference period: **left**—GU loss, **right**—Gross loss.

Loss analyses result not only in losses per event but also in an AAL and PML curve for each selected client portfolio. The analysis was performed using the portfolios of the seven largest Czech insurance companies and the Czech market portfolio. The PML was calculated for each scenario and period of interest for both the GU loss and the gross loss view (OEP and AEP).

By its very definition, an event set is a year-based model and the calculation of the PML is relatively straightforward. The comparison of the OEP (maximum) versus the AEP (sum of damages) is particularly interesting in terms of the frequency of the losses in the return period’s lower end of losses. The maximum return period shown on the graphs is 1 in 1000 years, but in terms of an even higher return period, the tail curve continues with an increasing trend. However, it has considerable uncertainty, and so it is not displayed.

A comparison of the PML values relative to the model results of the reference period for the variants with and without adaptation is shown in the graphs (Figures 10 and 11). There is a noticeable increase in the AAL values and in the lower return periods for all scenarios and a decrease in the tail losses, with this effect being more noticeable for AEP damages than for OEP losses. At the same time, this trend is stronger for the most pessimistic emissions scenario, and the smallest changes relative to the reference period are seen in the most optimistic emissions scenario. The impact of adaptation measures (by strengthening dikes) is mainly at the tail losses. The impact on lower return periods is relatively small and caused by losses that may occur more often as a result of heavy rainfall. This is mainly owing to locations where strong protection measures cannot be expected, or small rivers with flood discharges significantly amplified will not have access to the large flood protection measures (Figures 10 and 11).



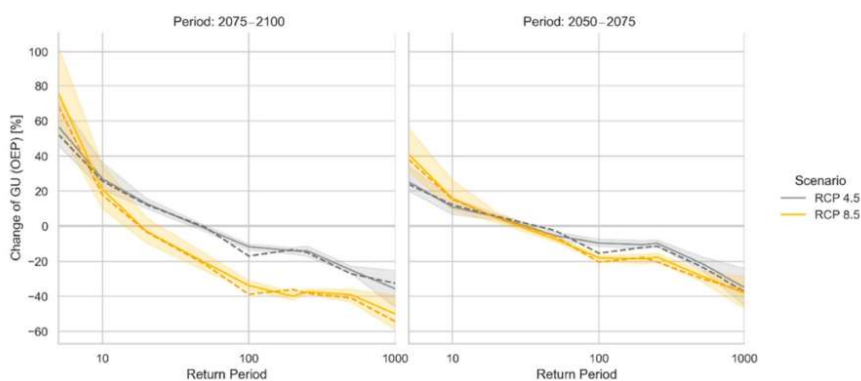


**Figure 10.** Percentual change of GU (OEP) for the two periods and RCP scenarios. The solid line with a filled area is the mean value with a 95 percent confidence interval based on the portfolios of the seven largest insurers. The dashed line indicates the aggregated market portfolio (postal code level only) comparison.

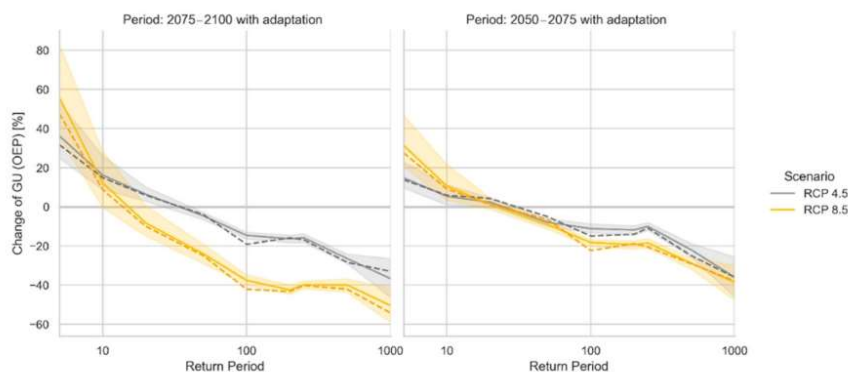


**Figure 11.** Percentual change of GU (OEP) for the two periods (including an adaptation) and RCP scenarios. The solid line with a filled area represents the mean value with a 95 percent confidence interval based on the portfolios of the seven largest insurers; the dashed line is the aggregated market portfolio (postal code level only) comparison.

### 3.3.2. Loss Change—Without Adaptation

This scenario assumed that key climate variables based on a specific scenario and time period are taken and transferred into the present-day climate condition. One can imagine it as if future conditions suddenly appeared in the present but everything else remained unchanged, such as the level of flood protection, spatial distribution of the exposure, loss ratio for buildings, and so on. Only the natural climate condition changed and only for the purposes of estimating the direct impact of the changes. This allows for the investigation of which hazard component and which condition will be more frequent or more important from the risk point of view. Stakeholders can then request greater details and at a more significant scale. They can also initiate real adaptation measures that are specifically targeted at the risk.

### 3.3.3. Loss Change—With Adaptation

As opposed to the model version, which considers climate change but from only the natural conditions, there was a developed version that includes a view of the partial adaptation measures. The original flood model for Czechia included a number of flood protections related to the river segment and the pluvial component.

Based on the table of projected strengthening of dikes in (Section 2.3), model versions with climate change scenarios and time periods have been updated with the projected levels of flood protection. The strengthening of dikes has been applied to all areas in the same ratio, so we can assume that the model can over/under-estimate the effect in more specific areas. However, other adaptation measures have not been taken into account, so we can assume that the uncertainty also covers other measures, such as the individual mobile flood barriers for doors or location-specific polders.

## 4. Discussion and Conclusions

This study assessed the change in risk under projected climate change scenarios, particularly in terms of their financial implications. This includes scenarios of simple climate change and scenarios with strengthened flood protection measures (to simplify, this also includes landscape measures). No additional financial implications arising from the need for levee construction or other adaptation measures are discussed in this study, nor is any loss from weather-driven perils such as windstorms, hail, or drought.

The pluvial component is considered in terms of a 24-h rainfall, for consistency with GCMs. Further research needs to be undertaken to better capture the impact of very intense but short duration torrential rainfall events on small areas and to account specifically for the impact of these storms. In terms of the rainfall–runoff model, there is a clear difference in the response of the landscape between a volume of rain that falls in six hours from a slow-moving cloud versus 24+ hours of precipitation.

Considerable uncertainty remains in the GCM outputs about changes in precipitation totals. RCMs agree with some GCM outputs, but there are other GCMs that show no change in precipitation. According to the RCMs, precipitation will increase by an average of 10 percent by the end of the century for RCP 4.5, and even by 13 percent under RCP 8.5, as compared to the reference period (in absolute terms, this means an increase in the annual average of 90 mm for RCP 8.5 and 60 mm for RCP 4.5 by the end of this century, while the national average in the reference period is 703 mm).

Decreasing precipitation amounts are expected in the northern regions and increasing amounts in the southern regions, with the transition located across Central Europe in the summer and the southern Mediterranean in the winter. A prominent intensification of precipitation extremes is present in all seasons and nearly all regions of Europe. In the continental and northern regions, the entire set of simulations shows an increase in total precipitation around +20 percent with the largest values in winter and autumn. In southern regions, changes are more complex and particularly uncertain in warmer seasons. In those regions, the significant reduction in the number of wet days might influence the occurrence of heavy flood events in summer. Knutti, Masson, and Gettelman 2013 [37] suggest this is in line with recent observations of the European precipitation regime, such as the intensification of heavy events that particularly appears in the winter season [38,39], which is projected to amplify in a future climate. It has been reported [40] that annual average precipitation will increase in northern and North-Central Europe, while it will decrease in Southern Europe.

In Central Europe, a smaller change in precipitation is expected. However, annual precipitation patterns will change. Southern Europe will experience lower rainfall year-round. There will be less precipitation during the summer season in Atlantic and continental Europe, but more winter precipitation. It has been reported [40] that decreases in annual average precipitation in Southern and Central Europe can be as high as 30–45 percent, and up to 70 percent in the summer in some regions. Due to this and warmer summer

temperatures, the risk of summer drought is likely to increase in Central Europe and in the Mediterranean area.

On the other hand, Kundzewicz et al. 2005 [41] suggested that the potential for intense precipitation is likely to increase in a warmer climate. According to the Clausius–Clapeyron Law, the atmosphere’s capacity to absorb moisture should increase with temperature. With a higher amount of precipitable water, the potential for intensive precipitation should increase. It seems likely that for broad parts of the investigation area the mean summer precipitation will decrease, corroborating the general projection of enhanced summer drying over continental interiors, while the amount of precipitation related to extreme events will increase [41]. However, the spatial size of extreme precipitation events will probably be reduced. We have observed intensification of extreme rainfall in our results, but with a reduced spatial size of storms.

Our study shows that there is very little change in total precipitation for Czechia, but the distribution of precipitation changes during the year and the number of wet and dry days also changes. This has a clear effect on runoff and flood genesis. Fewer floods are seen during spring seasons, due to the reduction of snowpack, which is consistent with predictions [9,10]. This led to a clear effect in our calibrated rainfall–runoff model for flood magnitude as well as on the superposition of flood waves. The amplification of less intense precipitation led to an amplification of flood waves on small and medium-sized catchments, while large catchments were affected by a decrease in design flows due to the stacking of flood waves. The distribution of events within the year is also changing, with an increasing number of winter floods.

Within the loss calculation where there is an increase in the loss of the lower part of the PML curve (more frequent small floods, or the splitting of a large event into several smaller ones) and a decrease in tail losses due to the reduction in the number of the largest flood events. In all climate scenarios considered, losses on the lower return periods increase and losses on the higher return periods decrease compared to the reference model. Only the magnitude of these changes differs.

The study contains several uncertainties: uncertainties in climate models, uncertainties in changing precipitation–runoff relationships in the landscape, and uncertainties in adaptation measures and in population development. To provide the most straightforward view of the estimation of the risk, the model is accordingly separated into two parts, with a portion using only the change in climate conditions for the current world and a portion using the assumption of adaptation.

This study is intended to highlight the possible trend in flood losses (without considering the price trends) and to provide a basis for further development and decision-making by the relevant institutions, the state or insurance companies. Floods over Europe are caused by various triggers. The largest and costliest floods happen in different seasons, in different regions and in different regional patterns. In Czechia, the majority of serious floods (e.g., 1997, 2002, 2013) currently happen during the summer season, but different types of flooding might dominate in the climate scenarios. Further work may target specific types of storms that do not occur in the current climate, which may play a significant role in climate scenarios. While the results of this study suggest this may be the case, the current model cannot capture this completely and without uncertainties. To evaluate the view of risk from climate change scenarios, it is possible to take a view of climate change scenarios and convey it to the current model. Using the same vulnerability, exposure, and flood mitigation measures, the evaluation of the direct impact on the losses can be achieved for each scenario of the future climate happening under current socio-economic and other conditions.

Subsequently, the effect of mankind’s efforts protecting themselves, reflected in flood mitigation, should be added to evaluate such effect. The third step in our future work is to evaluate the change in exposure (development of new residential, commercial, and industrial areas with different spatial distribution and sensitivity against flood losses) under current conditions of current costs associated with flooding.

One limitation of this study might be underestimation of the future frequency and magnitude of flash floods on small catchments due to the daily precipitation used for deriving event set and 24-h simulation of pluvial events. That might even intensify losses of lower return periods and AAL. However, hydrodynamic simulation based on derived design flows is based on a frequency analysis of extracted peaks directly from gauging stations. The output of the rainfall–runoff simulation is used only to evaluate the relative magnitude of discharge event and real flood hazard is modelled through 2-dimensional hydrodynamic simulation whose input parameters (hydrological data) are taken from intensity-duration-frequency (IDF) functions (for pluvial hazard simulations) and design flows, derived from daily maximum data. Therefore, the rainfall–runoff outputs are used only to describe the spatial patterns and relative severity magnitude of model’s stochastic events. That is why the described number of events in climate change scenarios might be considered to be comparable to the reference period.

In the studied climate scenario flood model for Czechia, for a return period 1 in 5 years for the worst-case scenario, the differences between scenario results and reference model can be up to +125 percent increase, while for the return period 1 in 100 years it is a –40 percent decrease. There is no significant effect of adaptation measures for the return period 1 in 100 years, but there is a –20 percent decrease in the return period 1 in 5 years. The study also considers exposure redistribution in addition to adaptation measures and brings attention to the significant risk of increasing tail loss in the PML curve when compared to the reference model (up to +30 percent). It also investigated pluvial flooding increases by about 10–20 percent (OEP) and 20–40 percent (AEP), respectively, in the model.

Another aim of this study was to provide a basis for the decision-making processes, which may lead to better targeting of adaptation measures in the landscape or construction of flood control measures, which may result in a significant reduction in losses from large floods of the “classic” type, as well as flood control measures in small catchments from heavy rainfall events. This may result in very different flood losses than the model projects. Stakeholders will likely wish to investigate this further, using this data to initiate processes of adaptation precisely targeted to their risk. While Impact Forecasting will continue to refine climate change scenarios in flood models to reflect new knowledge, the climate change scenarios for the Impact Forecasting Flood model for Czechia [19] considered here have been implemented into ELEMENTS so users can perform their own analyses using their portfolio data, and can make their own assumptions about exposure redistribution or price.

**Author Contributions:** Conceptualization, L.P. and P.P.; methodology, L.P., M.M., M.V.; software, L.P., M.V. and M.M.; validation, P.P.; formal analysis, L.P.; investigation, L.P., V.K. and E.P.; resources, L.P., M.V., M.M., V.K., E.P. and P.P.; data curation, M.M. and M.V.; writing—original draft preparation, L.P.; writing—review and editing, L.P., V.K. and P.P.; visualization, L.P.; supervision, P.P.; project administration, L.P.; funding acquisition, P.P. All authors have read and agreed to the published version of the manuscript.

**Funding:** This research received no external funding.

**Data Availability Statement:** Not applicable.

**Conflicts of Interest:** The authors declare no conflict of interest.

## References

1. IPCC. *Managing the Risks of Extreme Events and Disasters to Advance Climate Change Adaptation*; Cambridge University Press: Cambridge, UK, 2012.
2. Šýs, V.; Fošumpaur, P.; Kašpar, T. The Impact of Climate Change on the Reliability of Water Resources. *Climate* **2021**, *9*, 153. [[CrossRef](#)]
3. Yazdani, M.; Mojtahedi, M.; Loosemore, M.; Sanderson, D. A modelling framework to design an evacuation support system for healthcare infrastructures in response to major flood events. *Prog. Disaster Sci.* **2022**, *13*, 100218. [[CrossRef](#)]
4. Kay, A.L.; Davies, H.N.; Bell, V.A.; Jones, R.G. Comparison of uncertainty sources for climate change impacts: Flood frequency in England. *Clim. Chang.* **2009**, *92*, 41–63. [[CrossRef](#)]

5. Anaraki, M.V.; Farzin, S.; Mousavi, S.F.; Karami, H. Uncertainty Analysis of Climate Change Impact on Flood Frequency by Using Hybrid Machine Learning Methods. *Water Resour. Manag.* **2021**, *35*, 199–223. [CrossRef]
6. IPCC. Climate Change 2014: Synthesis Report. In *Contribution of Working Groups I, II and III to the Fifth Assessment Report of the Intergovernmental Panel on Climate Change*; Cambridge University Press: Cambridge, UK, 2014.
7. Donmez, C.; Berberoglu, S.; Cilek, A.; Krause, P. Basin-wide hydrological system assessment under climate change scenarios through conceptual modelling. *Int. J. Digit. Earth* **2020**, *13*, 915–938. [CrossRef]
8. Hengade, N.; Eldho, T.I.; Ghosh, S. Climate change impact assessment of a river basin using CMIP5 climate models and the VIC hydrological model. *Hydrol. Sci. J.* **2018**, *63*, 596–614. [CrossRef]
9. Rajczak, J.; Schär, C. Projections of Future Precipitation Extremes Over Europe: A Multimodel Assessment of Climate Simulations. *J. Geophys. Res. Atmos.* **2017**, *122*, 773–800. [CrossRef]
10. Štěpánek, P.; Trnka, M.; Jan, M.; Martin, D.; Pavel, Z.; Ondřej, L.; Petr, S.; Jan, K.; Aleš, F.; Daniela, S. *Expected Climatic Conditions in the Czech Republic: Part I. Change of Basic Parameters*, 1st ed.; Ústav Výzkumu Globální Změny Akademie věd České Republiky: Brno, Czech Republic, 2019; ISBN 978-8-879-2-28-8.
11. Brázdil, R.; Řezníčková, L.; Valášek, H.; Havlíček, M.; Dobrovolný, P.; Soukalová, E.; Rehánek, T.; Skokanová, H. Fluctuations of floods of the River Morava (Czech Republic) in the 1691–2009 period: Interactions of natural and anthropogenic factors. *Hydrol. Sci. J.* **2011**, *56*, 468–485. [CrossRef]
12. Brázdil, R.; Dobrovolný, P.; Elleder, L.; Kakos, V.; Kotyza, O.; Květoň, V.; Macková, J.; Müller, M.; Štekl, J.; Tolasz, R.; et al. *Historical and Recent Floods in the Czech Republic*; Masaryk University, Czech Hydrometeorological Institute: Prague, Czech Republic, 2005; p. 370.
13. Kjeldsena, T.T.; Macdonald, N.; Lang, M.; Mediero, L.; Albuquerque, T.; Bogdanowicz, E.; Brázdil, R.; Castellarin, A.; David, V.; Fleig, A.; et al. Documentary evidence of past floods in Europe and their utility in flood frequency estimation. *J. Hydrol.* **2014**, *517*, 963–973. [CrossRef]
14. Blöschl, G.; Hall, J.; Viglione, A.; Perdigão, R.A.P.; Parajka, J.; Merz, B.; Lun, D.; Arheimer, B.; Aronica, G.T.; Bilbashi, A.; et al. Changing climate both increases and decreases European river flood. *Nature* **2019**, *573*, 108–111. [CrossRef]
15. Tramblay, Y.; Mimeau, L.; Neppel, L.; Vinet, F.; Sauquet, E. Detection and attribution of flood trends in Mediterranean basins. *Hydrol. Earth Syst. Sci.* **2019**, *23*, 4419–4431. [CrossRef]
16. Kemter, M.; Merz, B.; Marwan, N.; Vorogushyn, S.; Blöschl, G. Joint Trends in Flood Magnitudes and Spatial Extents Across Europe. *Geophys. Res. Lett.* **2020**, *47*, 7. [CrossRef]
17. Bertola, M.; Viglione, A.; Vorogushyn, S.; Lun, D.; Merz, B.; Blöschl, G. Do small and large floods have the same drivers of change? A regional attribution analysis in Europe. *Hydrol. Earth Syst. Sci.* **2021**, *25*, 1347–1364. [CrossRef]
18. Rädler, A.T. Invited perspectives: How does climate change affect the risk of natural hazards? Challenges and step changes from the reinsurance perspective. *Nat. Hazards Earth Syst. Sci.* **2022**, *22*, 659–664. [CrossRef]
19. Aon—Impact Forecasting. *Impact Forecasting Flood Model for Czech Republic*; Aon UK. Limited Trading as Aon: Prague, Czech Republic, 2021; 197p.
20. Ehmele, F.; Kautz, L.-A.; Feldmann, H.; He, Y.; Kadlec, M.; Kelemen, F.D.; Lentink, Y.; Manful, D.; Ludwig, P.; Pinto, J.G. Adaptation and application of the large LAERTES-EU regional climate model ensemble for modeling hydrological extremes: A pilot study for the Rhine basin. *Nat. Hazards Earth Syst. Sci.* **2022**, *22*, 677–692. [CrossRef]
21. Rockel, B.; Will, A.; Hense, A. The Regional Climate Model COSMO-CLM (CCLM). *Meteorol. Z.* **2008**, *17*, 347–348. [CrossRef]
22. Bergström, S. The HBV model. In *Computer Models of Watershed Hydrology*; Singh, V.P., Ed.; Water Resources Publications: Highlands Ranch, CO, USA, 1995; pp. 443–476.
23. Berrisford, P.; Dee, D.P.; Poli, P.; Brugge, R.; Fielding, M.; Fuentes, M.; Källberg, P.W.; Kobayashi, S.; Uppala, S.; Simmons, A. The ERA-Interim Archive Version 2.0; Shinfield Park. Reading 1. 2011, p. 23. Available online: <https://www.ecmwf.int/en/elibrary/8174-era-interim-archive-version-20> (accessed on 20 July 2021).
24. Poli, P.; Hersbach, H.; Dee, D.P.; Berrisford, P.; Simmons, A.J.; Vitart, F.; Laloyaux, P.; Tan, D.G.H.; Peubey, C.; Thépaut, J.-N.; et al. ERA-20C: An Atmospheric Reanalysis of the Twentieth Century. *J. Clim.* **2016**, *29*, 4083–4097. [CrossRef]
25. NOAA: The Twentieth Century Reanalysis Project. 2022. Available online: [https://psl.noaa.gov/data/20thC\\_Rean/](https://psl.noaa.gov/data/20thC_Rean/) (accessed on 7 October 2021).
26. Ehmele, F.; Kautz, L.-A.; Feldmann, H.; Pinto, J.G. Long-term variance of heavy precipitation across central Europe using a large ensemble of regional climate model simulations. *Earth Syst. Dyn.* **2020**, *11*, 469–490. [CrossRef]
27. He, X.; Chaney, N.W.; Schleiss, M.; Sheffield, J. Spatial downscaling of precipitation using adaptable random forests. *Water Resour. Res.* **2016**, *52*, 8217–8237. [CrossRef]
28. IPCC. *Climate Change 2021: The Physical Science Basis. Contribution of Working Group I to the Sixth Assessment Report of the Intergovernmental Panel on Climate Change*, 1st ed.; Cambridge University Press: Cambridge, UK, 2021.
29. Marchi, M.; Castellanos-Acuña, D.; Hamann, A.; Wang, T.; Ray, D.; Menzel, A. ClimateEU, scale-free climate normals, historical time series, and future projections for Europe. *Sci. Data* **2020**, *7*, 428. [CrossRef]
30. Harris, I.; Jones, P.D.; Osborn, T.J.; Lister, D.H. Updated high-resolution grids of monthly climatic observations—The CRU TS3.10 Dataset. *Int. J. Climatol.* **2014**, *34*, 623–642. [CrossRef]
31. He, Y.; Wang, K.; Zhou, C.; Wild, M. A Revisit of Global Dimming and Brightening Based on the Sunshine Duration. *Geophys. Res. Lett.* **2018**, *45*, 4281–4289. [CrossRef]

32. Dottori, F.; Mentaschi, L.; Bianchi, A.; Alfieri, L.; Feyen, L. *Adapting to Rising River Flood Risk in the EU under Climate Change: EUR 29955 EN*; Publications Office of the European Union: Luxembourg, 2020; ISBN 978-92-76-12946-2.
33. Actuarial Standards Board. Actuarial Standard of Practice No. 39. 2000. Available online: <http://www.actuarialstandardsboard.org/asops/treatment-catastrophe-losses-property-casualty-insurance-ratemaking/#24-demand-surge> (accessed on 20 July 2021).
34. Döhrmann, D.; Gürtler, M.; Hibbeln, M. An econometric analysis of the demand surge effect. *Z. Gesamte Versicher.* **2013**, *102*, 537–553. [[CrossRef](#)]
35. How, S.; Hasson, I. Feeling the heat: Dealing with the impact of climate change. In *Insurance Digest, European Edition*; PricewaterhouseCoopers: London, UK, 2006; pp. 4–7.
36. Olsen, A.H.; Porter, K.A. What We Know about Demand Surge: Brief Summary. *Nat. Hazards Rev.* **2011**, *12*, 62–71. [[CrossRef](#)]
37. Knutti, R.; Masson, D.; Gettelman, A. Climate model genealogy: Generation CMIP5 and how we got there. *Geophys. Res. Lett.* **2013**, *40*, 1194–1199. [[CrossRef](#)]
38. Fischer, E.M.; Knutti, R. Observed heavy precipitation increase confirms theory and early models. *Nat. Clim. Chang.* **2016**, *6*, 986–991. [[CrossRef](#)]
39. Scherrer, S.C.; Fischer, E.M.; Posselt, R.; Liniger, M.A.; Croci-Maspoli, M.; Knutti, R. Emerging trends in heavy precipitation and hot temperature extremes in Switzerland. *J. Geophys. Res. Atmos.* **2016**, *121*, 2626–2637. [[CrossRef](#)]
40. The climate change challenge for european regions: Directorate general for regional policy. In *Background Document to Commission Staff Working Document Sec(2008) 2868 Final Regions 2020, an Assessment of Future Challenges for EU Regions*; European Commission: Brussels, Belgium, 2009.
41. Kundzewicz, Z.W.; Ulbrich, U.; Brücher, T.; Graczyk, D.; Krüger, A.; Leckebusch, G.C.; Menzel, L.; Pińskwar, I.; Radziejewski, M.; Szwed, M. Summer Floods in Central Europe—Climate Change Track? *Nat. Hazards* **2005**, *36*, 165–189. [[CrossRef](#)]

## Závěr

Ve sledovaném povodí Sklářského potoka (Jizerka, Jizerské hory) byla nejviditelnějším dopadem defoliace a poškození stávajícího smrkového porostu vedoucí k celkové holoseči. Následoval vývoj a dominance bylinné travní vegetace *Junco effusi-Calamagrostietum villosae* a obtížná obnova lesa. Na tyto změny vegetačního povrchu reagovaly významně testované Ellenbergovy indikátory prostředí (nejtěsnější korelace byla popsána indikátorem vlhkosti) a významně korespondovaly se změnami hydrologického režimu v uzávěrovém profilu povodí (jak kvantity, tak i kvality vody).

Naopak v povodí Holubího potoka s přirozeným bukovým porostem a nižší kyselou atmosférickou zátěží došlo pouze k mírným změnám (do 20% plochy vegetačního krytu), které nebylo možné postihnout významnou změnou Ellenbergových indexů; významné změny v makrozoobentosu uzávěrového profilu povodí byly vyvolány povodňovou situací a erozí koryta toku. Zvyšování povodňového rizika souvisí s globální klimatickou změnou, proto ve výhledovém období je nutno uvažovat rostoucí ovlivňování makrozoobentosu v horských povodích v závislosti na zvyšování emisí skleníkových plynů.

Indikační potenciál makrozoobentosu je schopen postihnout jevy sezónní a epizodní acidifikace v obou sledovaných povodích. V současné době došlo k poklesu emisí síry do atmosféry a poklesu celkové kyselé depozice, ale možný nárůst emisí dusíku může udržovat aktuálnost problému acidifikace vodního prostředí pramenných oblastí a zde se může projevit vliv klimatické změny na zesilování epizodní acidifikace vodního toku a složení makrozoobentosu.

## Seznam obrázků

Obr. 1: Experimentální povodí Sklářského potoka (Jizerka) .....	27
Obr. 2: Experimentální povodí Holubího potoka .....	29
Obr. 3: Širší okolí povodí Holubího potoka (zvýrazněno) s vyznačeným zkoumaným územím O1, O2 a O3. ....	30
Obr. 4: Ellenbergův index vlhkosti v povodí Sklářského potoka (Jizerka) pro roky 1991, 2005 a 2018. ....	32
Obr. 5: Evapotranspirace (červeně) a Ellenbergův index vlhkosti (modrá) v povodí Sklářského potoka v průběhu let 1982-2018.....	32
Obr. 6: Ellenbergův index přísunu světla v povodí Sklářského potoka (Jizerka) pro roky 1991 a 2018.....	42
Obr. 7: Ellenbergův index obsahu dusíku v povodí Sklářského potoka (Jizerka) pro roky 1991 a 2018.....	43

## Seznam tabulek

Tab. 1: Škála Ellenbergových indikačních hodnot pro světlo (Ellenberg, 1974, 1988).....	17
Tab. 2: Škála Ellenbergových indikačních hodnot pro teplotu (Zelený, 2012, Ellenberg, 1974, 1988).....	18
Tab. 3: Škála Ellenbergových indikačních hodnot pro vlhkost (Ellenberg, 1974, 1988).....	18
Tab. 4: Škála Ellenbergových indikačních hodnot pro reakci půdy (Ellenberg, 1974, 1988). ....	19
Tab. 5: Škála Ellenbergových indikačních hodnot pro obsah dusíku (Ellenberg, 1974, 1988). ....	19
Tab. 6: Morfologie povodí Sklářského potoka (Jizerka).....	26
Tab. 7: Morfologie povodí Holubího potoka (Oldřichov).....	28

## Seznam použitých zkratk

ČR ... Česká republika  
FAO ... Food and Agriculture Organization  
GCM ... Global Climate Model  
CHOPAV ... Chráněné oblasti přirozené akumulace vody  
RCM ... Regional Climate Model  
RCP ... Representative Concentration Pathways  
SRES ... Special report on emission scenarios  
WMO ... World Meteorological Organization

## Seznam literatury

- ANDĚL, P. (2011): Ekotoxikologie, bioindikace a biomonitoring, Evernia Liberec, ISBN 978 80-903787-9-7
- ARNELL, N. W. (1999): The effect of climate change on hydrological regimes in Europe: a continental perspective. *Global Environmental Change*, 9: 5-23.
- BACHE, B. W. (1985): Aluminium mobilization in soils and waters. *Journal of the Geological Society* 143:699–706.
- BLÖSCHL, G.; HALL, J.; VIGLIONE, A. et al. (2019): Changing climate both increases and decreases European river floods. *Nature* 573, pp. 108–111. <https://doi.org/10.1038/s41586-019-1495-6>
- BRITAIN, J. E. & EIKELAND, T. J. (1988): Invertebrate drift – A review, *Hydrobiologia* 166: pp. 77-93. <https://doi.org/10.1007/BF00017485>



- BROOKES, A. (1988): Channelized rivers: perspectives for environmental management. John Wiley & Sons, Inc., pp. 326
- CAPE, J. N.; KIRIKA, A.; ROWLAND, A. P.; WILSON, D. R.; JICKELLS, T. D.; CORNELL, S. (2001): Organic nitrogen in precipitation: real problem or sampling artefact? *The Scientific World*, 1(S2): 230–237.
- CHRISTENSEN, J. H., & CHRISTENSEN, O. B. (2007): A summary of the PRUDENCE model projections of changes in European climate by the end of this century. *Climate Change*, 81, 7-30.
- ČÍŽEK, L.; ROLEČEK, J.; DANIHELKA, J. (2007): Vliv plošné přípravy půdy na biodiverzitu, *Lesnická práce č. 08/07*, ročník 86.
- DOERING, M. & ROBINSON, C.T. (2010): Optimal ecological discharge. In: *Water Management Strategies against Water Scarcity in the Alps*, Report of the Interreg project IV B, Alpine Space Programme, 100 pp.
- ELLENBERG H. (1974): Zeigerwerte der Gefäßpflanzen Mitteleuropas. -*Scr. Geobot.* 9: 1-97
- ELLENBERG, H. (1988): *Vegetation Ecology of Central Europe*, fourth edition, Cambridge University Press, ISBN 978-0-521-11512-4.
- ELLENBERG, H.; WEBER, H. E.; DULL, R.; WIRTH, V.; WERNER, W.; PAULISSEN, D. (1992): Zeigerwerte von Pflanzen in Mitteleuropa. *Scripta Geobotanica*, vol. 18, pp 1-258.
- FALKENMARK, M. & ALLARD, B. (2015): *Water Quality Genesis and Disturbances of Natural Freshwaters*. *Water Pollution 5*: 45-78
- FAO (Food and Agriculture Organization, 2007): *Adaptation to climate change in agriculture, forestry and fisheries: Perspective, framework and priorities*. FAO Inter-departmental Working Group on Climate Change. Rome: Food and Agriculture Organization of the United Nations.
- FAO (Food and Agriculture Organization, 2008): *Forests and water*. FAO Forestry paper 155. Food and Agriculture Organization of the United Nations, Rome, Italy. (Available from: <http://www.fao.org/docrep/011/i0410e/i0410e01.pdf> )
- FAO (Food and Agricultural Organization, 2010): *Global Forest Resources Assessment 2010. Main report*. FAO Rome, 378 pp, ISBN 978-92-5-106654-6.
- FORMAN R. T. T. (1995): *Land Mosaics. The Ecology of Landscapes and Regions*, Cambridge University Press, Cambridge, 656 p.
- FRITZ, K. M.; HAGENBUCH, E.; D'AMICO, E.; REIF, M.; WIGINGTON, P. J.; LEIBOWITZ, Jr S. G.; COMELEO, R. L.; EBERSOLE, J. L. (2013): Comparing the extent and permanence of headwater streams from two field surveys to values from hydrologic databases and maps. *J. Am. Water Resour. Assoc.* 49: 867-882.
- GUEROLD, F.; BOUDOT, J. P.; JACQUEMIN, G.; VEIN, D.; MERLET, D.; ROUILLER, J. (2000): Macroinvertebrate community loss as a result of headwater stream acidification in the Vosges Mountains (NE France). *Biodiversity and Conservation* 9:767–783.

- HANEL, M.; KAŠPÁREK, L.; MRKVIČKOVÁ, M.; HORÁČEK, S.; VEZINA, A.; NOVICKÝ, O.; FRIDRICHOVÁ, R. (2011): Odhad dopadů klimatické změny na hydrologickou bilanci v ČR a možná adaptační opatření. Praha, Výzkumný ústav vodohospodářský TG Masaryka.
- HALL, R. J.; LIKENS, G. E.; HENDREY, G. R. (1980): Experimental acidification of a stream in the Hubbard Brook experimental forest, New Hampshire. *Ecology*, 61(4): 976-989.
- HÉDL, R.; SZABÓ, P.; RIEDL, V.; KOPECKÝ, M. (2011): Tradiční lesní hospodaření ve střední Evropě II. Lesy jako ekosystém, *Živa* 3/2011, s. 108-110, Akademie věd ČR.
- HOOVER, T. M. & RICHARDSON, J. S. (2010): Does water velocity influence optimal escape behaviors in stream insects?, *Behavioral Ecology*, Volume 21, Issue 2, March-April 2010, Pages 242–249, <https://doi.org/10.1093/beheco/arp182>
- HORECKÝ, J.; RUCKI, J.; KRÁM, P.; KŘEČEK, J.; BITUŠÍK, P.; ŠPAČEK, J.; STUHLÍK, E. (2013): Benthic macroinvertebrates of headwater streams with extreme hydrochemistry. *Biologia*, 68: 1-11.
- HORECKÝ, J.; STUHLÍK, E.; CHOJKA, P.; HARDEKOPF, W. D.; MIHALJEVIČ, M.; ŠPAČEK, J. (2005): Macroinvertebrate community and chemistry of the most atmospherically acidified streams in the Czech Republic. *Water Air Soil Pollut.* 173: 261-272.
- HRUŠKA, J. & KOPÁČEK, J. (2005): Kyselý déšť stále s námi – zdroje, mechanismy, účinky, minulost a budoucnost, edice PLANETA, odborný časopis, vydává MŽP, ročník XII, číslo 5/2005, 24 s.
- HRUŠKA, J. & KOPÁČEK, J. (2009): Účinky kyselého deště na lesní a vodní ekosystémy I. Emise a depozice okyselujících sloučenin, Akademie věd ČR, Nakladatelství Academia, *Živa* 2/2009, 93-96 s.
- IPCC (2013): Summary for Policymakers. In: *Climate Change 2013: The Physical Science Basis. Contribution of Working Group I to the Fifth Assessment Report of the Intergovernmental Panel on Climate Change* [Stocker, T.F., D. Qin, G.-K. Plattner, M. Tignor, S. K. Allen, J. Boschung, A. Nauels, Y. Xia, V. Bex and P.M. Midgley (eds.)]. Cambridge University Press, Cambridge, United Kingdom and New York, NY, USA
- IPCC (2013a): *Climate change 2013: The physical science basis*. Cambridge: Cambridge University Press.
- IPCC (2013b): *Climate change 2013: The physical science basis*. Cambridge: Cambridge University Press.
- IPCC (2014): *Climate Change 2014: Synthesis Report*. In *Contribution of Working Groups I, II and III to the Fifth Assessment Report of the Intergovernmental Panel on Climate Change*; Cambridge University Press.
- KNIST, S.; GOERGEN, K.; SIMMER, C. (2018): Evaluation and projected changes of precipitation statistics in convection-permitting WRF climate simulations over Central Europe, *Clim Dyn.* <https://doi.org/10.1007/s00382-018-4147-x>
- KOHLER, T.; MASELLI, D. (2009): *Mountains and climate change - from understanding to action*. Bern: Geographica Bernensia, 978-3-905835-16-8.
- KOKEŠ, J. & NĚMEJCOVÁ, D. (2006): Metodika odběru a zpracování vzorků makrozoobentosu tekoucích vod metodou PERLA, VÚV TGM.
- KOLKWITZ, R. & MARSSON, M. (1909): Ökologie der tierischen Saprobien. *Int. Revue ges. Hydrobiol.* 2: 126–152.

- KŘEČEK, J. & HOŘICKÁ, Z. (2006): Forests, air pollution and water quality: influencing health in the headwaters of Central Europe's "Black Triangle". *Unasylva* 57:46-49.
- KŘEČEK, J. & NOVÁKOVÁ, J. (2009): Soil water content and plant succession after the harvest of mature spruce stands in a mountain catchment. *Ekologia*, 28: 213-224.
- KŘEČEK, J.; NOVÁKOVÁ, J.; HOŘICKÁ, Z. (2010): Ellenberg's indicator in water resources control: the Jizera Mountains, Czech Republic. *Ecological Engineering*, 36: 1112-1117.
- KŘEČEK, J.; PALÁN, L.; STUHLÍK, E. (2019): Impact of land use policy on the recovery of mountain catchments from acidification. *Land Use Policy*, 80, 439-448.
- KŘEČEK, J. & PUNČOCHÁŘ, P. (2012): Design of climate station network in mountain catchments, *Hungarian Geographical Bulletin* 61 (1), p. 19-29.
- KULICH, J; FIGULA, T.; GUTZEROVÁ, N.; HRUBÝ, P. (2002): Bioindikace a biomonitoring, aneb, Jak poznat, v jakém prostředí žijeme. Horní Maršov: SEVER - Středisko ekologické výchovy a etiky Rýchory, 75 s. ISBN 80-902-9767-6.
- MAGNEIN, M. A. (1937): Control and use of little waters in France. In *Head was control and use* (pp. 227-232). Washington D.C.: United States Governmental Printing.
- MARGALEF, R. (1951): Diversidad de Especies en las Comunidades Naturales. *Publicaciones del Instituto de Biología Aplicada*, volume 6, pp. 59-72.
- MARKERT, B. A.; BREURE, A. M.; ZECHMEUSTER, H. G. (2003): *Bioindicators and Biomonitoring: Principles, Concepts and Applications*, Elsevier Science, ISBN 9780080441771
- MENHINICK, E. F. (1964): A comparison of some species-individual diversity indices applied to samples of field insects. *Ecology*, volume 45, pp. 859-861.
- MESSERLI, B.; VIVIROLI, D.; WEINGARTNER, R. (2004): Mountains of the world: Vulnerable water for the 21st century. *AMBIO Special Report* 13, 29-34.
- MOUCHA, P. & PELC, F. (2008): Současné lesnictví a ochrana přírody, *Ochrana přírody* č. 1/2008, s. 5-7.
- NIVA (2013): Effects of long range transported air pollution (LRTAP) on freshwater ecosystem services. *ICP-Waters report* 115/2013, Norwegian Institute for Water Research, Oslo, Norway.
- OPAŘILOVÁ, L. & HORKÝ, P.: Hydromorfologický stav toků a jeho odezvy v biologických společenstvech, *academia.edu*, s. 8.
- PANTLE, R. & BUCK, H. (1955): The biological monitoring of waters and the representation of results. (In German). *Gas-u. Wasser*. 96, 604.
- PILLÍ, R., & PASE, A. (2018): Forest functions and space: A geohistorical perspective of European forests. *iForest*, 11(1), 79-89.

PRECHTEL, A.; ALEWELL, C.; ARMBRUSTER, M.; et al. (2001): Response of sulphur dynamics in European catchments to decreasing sulphate deposition. *Hydrology and Earth System Sciences* 5: 311–325.

RAJCZAK, J. & SCHÄR, C. (2017): Projections of future precipitation extremes over Europe: A multimodel assessment of climate simulations. *Journal of Geophysical Research: Atmospheres*, 122, 10,773–10,800. <https://doi.org/10.1002/2017JD027176>

RASHID, R. A.; PANDIT, A. K. (2014): Macroinvertebrates (oligochaetes) as indicators of pollution: A review. *J. Ecol. Nat. Environ.* 6:140-144.

REUSS, J. O. & JOHNSON, D. W. (1986): Acid deposition and the acidification of soils and waters. *Ecological Studies*, 59, Springer, New York.

RÖDLOVÁ, S. (2012): Kvalita povrchových vod, biologické ukazatele znečištění, Přírodovědecká fakulta, UK.

ROSENBERG, D. M. & RESH, V. H. (1993): Introduction to freshwater biomonitoring and benthic macroinvertebrates. Pages 1-9 in D. M. Rosenberg and V. H. Resh (editors). *Freshwater biomonitoring and benthic macroinvertebrates*. Chapman and Hall, New York.

RŮŽIČKOVÁ, J.; HŘEBÍK, Š.; KODROVÁ, Z. (2004): Macroinvertebrate communities and water duality in episodically acidified lotic ecosystems in the mountains region affected by bark beetle calamity. Abstract. *Acta Universitatis Carolinae – Environmentalica* 18: 35-53.

SCHÖPP, W.; POSCH, M.; MYLONA, S.; JOHANSSON, M. (2003): Long-term development of acid deposition (1880-2030) in sensitive freshwater regions in Europe. *Hydrology and Earth System Sciences*, 7: 436-446.

SHAW, E. M. (1994): *Hydrology in Practice*. Third edition, ISBN 0 7487 4448 7, 628 p.

SLÁDEČEK, V. (1973): System of water quality from biological point of view. *Arch. Hydrobiol. Ergebn. Limnol.* 7: 1–218.

SCHMIDTLEIN, S. (2005): Imaging spectroscopy as a tool for mapping Ellenberg indicator values, *Journal of Applied Ecology*, volume 42, p. 966–974.

STATZNER, B. & HOLM, T. F. (1982): Morphological adaptations of benthic invertebrates to stream flow – An old question studied by means of a new technique (Laser Doppler Anemometry), *Oecologia*, volume 53, p. 290-292. <https://doi.org/10.1007/BF00389001>

STUHLÍK, E.; KOPÁČEK, J.; FOTT, J.; HOŘICKÁ, Z. (2006): Chemical composition of the Tatra Mountain lakes: response to acidification. *Biologia*, 61/Suppl. 18: S11–S20.

TAGLIAPIETRA, D.; SIGOVINI, M.; MAGNI, P. (2012): Saprobity: a unified view of benthic succession models for coastal lagoons, *Hydrobiologia* (2012), volume 686: p. 15-28. <https://doi.org/10.1007/s10750-012-1001-8>

TER BRAAK, C. J. F.; GREMMEN, N. J. M. (1987): Ecological amplitudes of plant species and the internal consistency of Ellenberg's indicator values for moisture. *Vegetatio*, vol. 69, pp 79-87.

TOLASZ, R. (2007): *Climate atlas of the Czech Republic*. Czech Hydrometeorological Institute, Prague, Czech Republic.

TRNKA, M.; ŽALUD, Z.; HLAVINKA, P.; BARTOŠOVÁ, L. a kol.: Očekávané dopady změn klimatu, Czech Globe, Akademie věd ČR.

TUREČEK, K. et al. (2002): Zákon o vodách 254/2001 s komentářem. SONDY

UNEP (United Nations Environmental Programme, 2007): Global environmental outlook 4. United Nations Environmental Programme, Progress Press, Valetta, Malta.

VESELÝ, J. & MAJER, V. (1996): The effect of pH and atmospheric deposition on concentrations of trace elements in acidified freshwaters: a statistical approach. *Water, Air, and Soil Pollution* 88:227–246.

VIVIROLI, D.; DÜRR H. H.; MESSERLI B.; MEYBECK M.; WEINGARTNER R. (2007): Mountains of the world, water towers for humanity: typology, mapping, and global significance. *Water Resources Research* 43:W07447.

VRTIŠKA, J.; KŘEČEK, J.; PAŽOURKOVÁ, E. (2016): Možnosti detekce povodňového průtoku v horském povodí pomocí dendrochronologie. In: Sborník příspěvků ze Semináře Adolfa Patery 2016. Praha: České vysoké učení technické v Praze, Fakulta stavební, pp. 188-193. ISBN 978-80-01-06048-3.

WILLIS, K. G. (2002): Benefits and costs of forests to water supply and water quality. Social and environmental benefits of forestry, report to forestry commission, phase 2. Newcastle: Centre for Research, Centre for Research in Environmental Appraisal and Management, University of Newcastle.

WMO (1994): Guide to Hydrometeorological practices: Data acquisition and processing, analysis, forecasting and other applications. Publication 168, Fifth edition, Geneva, p. 732.

Zákon o životním prostředí č. 17/1992 Sb. (1992).

ZELENÝ, D. (2012): Poznámky k používání průměrných Ellenbergových indikačních hodnot při analýze vegetačních dat, *Zprávy České Botanické Společnosti*, Praha 47: 159-178.

## Publikace autora

### Významné publikace relevantní k tématu

Palán, L.; Matyáš, M.; Váľková, M.; Kovačka, V.; Pažourková, E.; Punčochář, P. (2022): **Accessing Insurance Flood Losses Using a Catastrophe Model and Climate Change Scenarios**. *Climate*, 5(10), 1-21. ISSN 2225-1154. DOI 10.3390/cli10050067 <sup>1,2,4</sup>

Pažourková, E.; Křeček, J.; Bitušík, P.; Chvojka, P.; Kamasová, L.; Takaki, S.; Špaček, J.; Stuchlík, E. (2021): **Impacts of an extreme flood on the ecosystem of a headwater stream**. *Journal of Limnology*, 80(2), 1-12. ISSN 1723-8633. DOI 10.4081/jlimnol.2021.1998 <sup>1,2,3,4</sup>

Křeček, J.; Nováková, J.; Palán, L.; Pažourková, E.; Stuchlík, E. (2021): **Role of forests in headwater control with changing environment and society**. *International Soil and Water Conservation Research*, 9(1), 143-157. ISSN 2095-6339. DOI 10.1016/j.iswcr.2020.11.002 <sup>1,2,3,4</sup>

Pažourková, E.; Křeček, J.; Nováková, J. (2019): **Bioindication of water resources recharge in a small mountain catchment**. In: 19th International Multidisciplinary Scientific Geoconference SGEM 2019. Sofia: STEF92 Technology Ltd., p. 145-152. 19. vol. 1,4. ISSN 1314-2704. ISBN 978-619-7408-97-3. DOI 0.5593/sgem2019V/1.4 <sup>2</sup>

Křeček, J.; Palán, L.; Pažourková, E.; Stuchlík, E. (2019): **Water-quality genesis in a mountain catchment affected by acidification and forestry practices**. *Freshwater Science*, 38(2), 257-269. ISSN 2161-9549. DOI 10.1086/698533 <sup>1,2,3,4</sup>

Křeček, J.; Nováková, J.; Palán, L.; Pažourková, E. (2019): **Soil conservation in a forested mountain catchment**. *EQA-INTERNATIONAL JOURNAL OF ENVIRONMENTAL QUALITY*. 2019, 33(1), 27-36. ISSN 2039-9898. DOI 0.6092/issn.2281-4485/8496 <sup>1,4</sup>

### Ostatní významné publikace

Křeček, J.; Pažourková, E. (2017): **IMPACTS OF THE ACID ATMOSPHERIC DEPOSITION AND CLIMATE CHANGE ON WATER PHENOMENA IN A SMALL MOUNTAIN CATCHMENT**. In: *Hydrology and water resources, forest ecosystems*. SGEM WORLD SCIENCE, p. 211-218. Water Resources. Forest, Marine and Ocean Ecosystems. vol. 17. ISSN 1314-2704. ISBN 978-619-7408-27-0. DOI 10.5593/sgem2017H/33 <sup>2</sup>

Křeček, J.; Pažourková, E.; Punčochář, P. (2021): **Flood protection by managing mountain forests in the Czech Republic**. In: *Integral approach to the flood protection effect of the forest with special consideration of water and sediment retention*. Austrian Federal Ministry of Agriculture, Forest, p. 44-49. <sup>4,5</sup>

Křeček, J.; Pažourková, E.; Navrátil, P. (2021): **The Protective Functions of Forests in a Changing Climate: Czech Republic**. In: *The Protective Functions of Forests in a Changing Climate: European Experience*. Rome: Food and Agriculture Organization of United Nations, 2021. p. 33-40. Forestry Working Paper. vol. 20. ISSN 2664-1062. ISBN 978-92-5-133510-9. <sup>4,5</sup>

Křeček, J.; Pažourková, E. (2020): **Education Strategy Supporting Environmental Services of Mountain Forest Catchments**. In: Environmental Sustainability Education for a Changing World. Cham: Springer, 2020. p. 107-114. 1. vol. 1. ISBN 978-3-030-66383-4. <sup>4,5</sup>

Křeček, J.; Palán, L.; Pažourková, E. (2019): **Impact of acid rain and climate change on landscape processes in the Jizera Mountains (Czech Republic)**. In: Arte e ciencia: historia e resiliencia da paisagem. Rio de Janeiro: Rio Book's, 2019. p. 375-386. ISBN 978-85-9497-049-7. <sup>4,5</sup>

---

<sup>1</sup> indexováno v databázi WoS

<sup>2</sup> indexováno v databázi Scopus

<sup>3</sup> s IF

<sup>4</sup> recenzovaný

<sup>5</sup> kapitola v knize